

**SEMMELWEIS EGYETEM  
DOKTORI ISKOLA**

**Ph.D. értekezések**

**3121.**

**FELEGYI-TÓTH CSENGE ANNA**

**A gyógyszerészeti tudományok korszerű kutatási irányai  
című program**

Programvezető: Dr. Antal István, egyetemi tanár

Témavezető: Dr. Alberti Ágnes, egyetemi docens

**PHYTOCHEMICAL ANALYSIS OF  
*CARPINUS BETULUS* L. POLYPHENOLS WITH  
SPECIAL REGARD TO ITS DIARYLHEPTANOIDS**

**PhD thesis**

**Csenge Anna Felegyi-Tóth**

Doctoral School of Pharmaceutical Sciences  
Semmelweis University



Supervisor:            Ágnes Alberti, Ph.D.

Official reviewers:   Márta Mazákné Kraszni, Ph.D.  
                              Dezső Csupor, D.Sc.

Head of the Complex Examination Committee:  
                              István Antal, Ph.D.

Members of the Complex Examination Committee:  
                              Sándor Gonda, Ph.D.  
                              Gergő Tóth, Ph.D.

Budapest

2024

## Table of contents

List of abbreviations .....	5
<b>I. INTRODUCTION .....</b>	<b>8</b>
I.1. Characterization of <i>Carpinus betulus</i> and the <i>Carpinus</i> Genus.....	9
<i>I.1.1. Botanical Characterization of C. betulus</i> .....	10
<i>I.1.2. Chemical Characterization of C. betulus and Other Carpinus Species</i> .....	11
<i>I.1.3. Biological Activities of Carpinus Species</i> .....	13
I.2. Diarylheptanoids .....	15
<i>I.2.1. Classification of Diarylheptanoids</i> .....	16
<i>I.2.2. Occurrence of Diarylheptanoids in Plants</i> .....	21
<i>I.2.3. The Biological Effects of Cyclic Diarylheptanoids</i> .....	22
<b>II. OBJECTIVES.....</b>	<b>29</b>
<b>III. MATERIALS AND METHODS .....</b>	<b>30</b>
III.1. Plant Material .....	30
III.2. Solvents and Chemicals.....	30
III.3. Extraction and Sample Preparation .....	30
<i>III.3.1. Sample Preparation for the Qualitative HPLC-MS Analyses, the DPPH Assays, and the Quantitative UHPLC-DAD Determination</i> .....	30
<i>III.3.2. Sample Preparation for the Isolation of Constituents</i> .....	31
III.4. Chromatographic Analyses.....	31
<i>III.4.1. HPLC-DAD-ESI-MS/MS Conditions</i> .....	31
<i>III.4.2. Isolation Procedures</i> .....	32
<i>III.4.3. UHPLC-DAD-ESI-Orbitrap-MS/MS Conditions</i> .....	33
<i>III.4.4. UHPLC-DAD Conditions</i> .....	35
III.5. Method Validation.....	35
<i>III.5.1. Preparation of Standard Solutions, Linearity, and Selectivity</i> .....	35
<i>III.5.2. Precision, Accuracy, and Repeatability</i> .....	35
<i>III.5.3. Recovery</i> .....	36
III.6. NMR Conditions .....	36
III.7. Evaluation of the Antioxidant Activity .....	37
<i>III.7.1. DPPH Assay</i> .....	37
<i>III.7.2. DPPH-HPLC-DAD-MS Analysis</i> .....	37
III.8. Stability Studies.....	38

III.8.1. Aqueous Stability at Different pH Values.....	38
III.8.2. Evaluation of Storage Stability.....	39
III.9. Parallel Artificial Membrane Permeability Assay Studies.....	39
III.10. Evaluation of the <i>In Vitro</i> Cytotoxic Activity of the Main Diarylheptanoids.....	41
III.10.1. Cell Culturing and Media.....	41
III.10.2. Determination of the <i>In Vitro</i> Antiproliferative Activity.....	42
<b>IV. RESULTS.....</b>	<b>43</b>
IV.1. Qualitative Analyses of <i>Carpinus betulus</i> Polyphenols by HPLC-DAD-MS/MS	43
IV.2. Structural Elucidation of the Isolated Compounds.....	57
IV.2.1. Structural Elucidation of the Diarylheptanoid Compounds.....	57
IV.2.1. Structural Elucidation of Lignan and Flavonoid Compounds.....	60
IV.3. Evaluation of the Antioxidant Activity.....	61
IV.3.1. DPPH Assay.....	61
IV.3.2. DPPH-HPLC-DAD-MS Analysis.....	62
IV.4. Quantitative Analysis of the Main Diarylheptanoids in <i>Carpinus betulus</i> .....	65
IV.4.1. Method Validation.....	65
IV.4.2. Quantitative Results.....	67
IV.5. Stability Studies.....	67
IV.5.1. Evaluation of Aqueous Stability at Different pH Values.....	67
IV.5.2. Evaluation of Storage Stability.....	69
IV.5.3. Characterization of the Degradation Products by UHPLC-HR-MS/MS.....	70
IV.6. Parallel Artificial Membrane Permeability Assay Studies.....	71
IV.7. Evaluation of the Cytostatic Activity.....	71
<b>V. DISCUSSION.....</b>	<b>73</b>
V.1. Qualitative Analyses of <i>Carpinus betulus</i> Polyphenols by HPLC-DAD-MS/MS	73
V.2. Structural Elucidation of the Isolated Compounds.....	78
V.2.1. Structural Elucidation of the Isolated Diarylheptanoids.....	79
V.2.2. Structural Elucidation of the Isolated Flavonoids.....	83
V.2.2. Structural Elucidation of the Isolated Lignan.....	83
V.3. Evaluation of the Antioxidant Activity.....	84
V.3.1. DPPH Assay.....	84
V.3.2. DPPH-HPLC-DAD Analysis.....	85

V.4. Quantitative Analysis of the Main Diarylheptanoids in <i>Carpinus betulus</i> Bark ....	86
V.5. Stability Studies .....	86
V.5.1. Evaluation of Aqueous Stability at Different pH Values.....	86
V.5.2. Evaluation of Storage Stability .....	87
V.5.3. Characterization of the Degradation Products by UHPLC-HR-MS/MS.....	90
V.6. Parallel Artificial Membrane Permeability Assay (PAMPA) Studies.....	92
V.7. Evaluation of the Cytostatic Activity .....	93
<b>VI. CONCLUSIONS .....</b>	<b>95</b>
<b>VII. SUMMARY .....</b>	<b>97</b>
<b>VIII. ÖSSZEFOGLALÁS.....</b>	<b>98</b>
<b>REFERENCES .....</b>	<b>99</b>
<b>LIST OF PUBLICATIONS.....</b>	<b>114</b>
<b>ACKNOWLEDGEMENTS .....</b>	<b>116</b>
<b>APPENDIX .....</b>	<b>117</b>

## List of abbreviations

6-OHDA	6-hydroxydopamine
A	filter area (cm <sup>2</sup> )
ABTS	2,2'-azino-bis(3-ethylbenzothiazoline-6-sulphonic acid)
ACN	acetonitrile
Akt	protein kinase B
ANOVA	analysis of variance
AUC	area under the curve
B	hydroxybenzoic acid derivatives
Bax	Bcl-2-associated X protein
Bcl-2	B-cell lymphoma 2 protein
BE	bark ethyl acetate extract
BM	bark methanol extract
BMDCs	bone marrow-derived dendritic cells
BMDMs	bone marrow-derived macrophage cells
C	hydroxycinnamic acid derivatives
C/EBP $\alpha$	CCAAT/enhancer-binding protein alpha
$c_0$	initial concentration
$C_{\text{added}}$	concentration in the standard solution
$C_D(0)$	concentration of the compound in the donor phase at time 0
$C_D(t)$	concentration of the compound in the donor phase at time $t$
$C_{\text{found}}$	measured concentration
CID	collision-induced dissociation
$C_{\text{initial}}$	initial concentration
$C_{\text{log } P}$	calculated log P
CM	column compartment
$c_t$	concentration at time $t$
D	diarylheptanoids
DAD	diode-array detection
DAU	daunomycin
DHHDP	dehydrohexahydroxydiphenoyl
DMEM	Dulbecco's modified eagle medium
DMSO	dimethyl sulfoxide
DNA	deoxyribonucleic acid
DPPH	2,2-diphenyl-1-picrylhydrazyl
E	ellagitannins and ellagic acid derivatives
ED <sub>50</sub>	median effective dose
EE	hornbeam bark ethyl acetate extract
EM	hornbeam bark methanol extract
ERK	extracellular signal regulated kinase
ESI	electrospray ionization

F	flavonoids
FBS	fetal bovine serum
FE	female catkin ethyl acetate extract
FM	female catkin methanol extract
FRAP	ferric reducing ability of plasma
G	gallotannins and gallic acid derivatives
GC-MS	gas chromatography–mass spectrometry
GI <sub>50</sub>	half-maximal growth inhibitory concentration
HHDP	hexahydroxydiphenoyl
HIF-1 $\alpha$	hypoxia-inducible factor
HPLC	high-performance liquid chromatography
HPLC-DAD-ESI-MS/MS	high-performance liquid chromatography coupled with diode-array detection and electrospray ionization tandem mass spectrometry
HR-MS	high-resolution mass spectrometry
IC <sub>50</sub>	half-maximal inhibitory concentration
IFN	interferon
I $\kappa$ B $\alpha$	nuclear factor-kappa B inhibitor alpha
IL-6	interleukin-6
IL-12 p40	interleukin-12 subunit p40
iNOS	inducible nitric oxide synthase
<i>k</i>	reaction rate constant
L	lignans
LC	liquid chromatography
LE	leaf ethyl acetate extract
LM	leaf methanol extract
LOD	limit of detection
LOQ	limit of quantitation
LPS	lipopolysaccharide
MAPK	mitogen-activated protein kinase
MDC	macrophage-derived chemokine
ME	male catkin ethyl acetate extract
MEF2D	myocyte enhancer factor 2D
MeOH	methanol
MM	male catkin methanol extract
MR	membrane retention factor
mRNA	messenger ribonucleic acid
MS	mass spectrometry
MSH	melanocyte-stimulating hormone
NF- $\kappa$ B	nuclear factor-kappa B
NMR	nuclear magnetic resonance (spectroscopy)
NO	nitric oxide
OD <sub>control</sub>	optical densities of the control wells

OD <sub>treated</sub>	optical densities of the treated wells
PAMPA-BBB	parallel artificial membrane permeability assay for the blood-brain barrier
PAMPA-GI	parallel artificial membrane permeability assay for the gastrointestinal tract
PARP	poly-ADP ribose polymerase
PBLE	porcine polar brain lipid extract
PBS	phosphate-buffered saline
$P_e$	effective permeability (cm/s)
PPAR $\gamma$	peroxisome proliferator-activated receptor gamma
PTFE	polytetrafluoroethylene
QSM	quaternary solvent delivery pump
R	recovery
$r^2$	correlation coefficient
$r_a$	asymmetry ratio
ROS	reactive oxygen species
S/N	signal-to-noise ratio
SA	aqueous solution of the isolated compounds
SAR	structure-activity relationship
SFM	serum-free medium
SGLT	sodium-dependent glucose co-transporter
SM	methanol solution of the isolated compounds
SREBP1c	sterol regulatory element binding protein 1
STAT1	signal transducer and activator of transcription 1
$t$	treatment/incubation time
T	condensed tannins
$t_{1/2}$	half-life
TLR9	toll-like receptor 9
TNF- $\alpha$	tumor necrosis factor- $\alpha$
TPA	12- <i>O</i> -tetradecanoylphorbol-13-acetate
U	undefined
UHPLC	ultrahigh-performance liquid chromatography
QTOF	quadrupole time-of-flight mass spectrometry
$V_A$	volume in the acceptor phase (cm <sup>3</sup> )
$V_D$	volume in the donor phase (cm <sup>3</sup> )
VEGF	vascular endothelial growth factor
$\tau_{ss}$	time (s) to reach steady state

## I. Introduction

In recent years the demand of phytotherapeutics is growing continuously, more and more studies are focusing on plant species and their potentially bioactive constituents. However, the therapeutic use of phytochemical medicines is complicated by their complexity, i.e., the fact that they contain a plethora of different compounds. It is often very difficult to identify the active substance or substances which are responsible for the biological effect of the medicinal plant. For these examinations modern instrumental analytical methods such as ultrahigh- and high-performance liquid chromatography (UHPLC, HPLC) and mass spectrometry (MS) should be applied.

Diarylheptanoids are plant specialized (secondary) metabolites distinguished because of their antiproliferative, neuroprotective, and anti-inflammatory activities. In recent years several studies, examinations, and clinical trials were carried out investigating these molecules as isolated compounds or main components of herbal extracts. The most famous diarylheptanoid compound is curcumin; however, it should be noted that its poor pharmacokinetic properties and chemical stability can limit its pharmaceutical applications. Based on literature data, further promising diarylheptanoids were isolated from the Betulaceae family, although there also are yet ‘undiscovered’ species in this family such as the European hornbeam (*Carpinus betulus*). Although the hornbeam has been used for a long time in the wood industry, it was not widely used in the folk medicine. Its phytochemical and pharmacological characterization is insufficient, the published scientific works rather focus on other *Carpinus* species e.g., *C. turczaninowii*.

In the literature overview of this thesis, the first chapter summarizes the botanical features of the hornbeam, the chemical constituents of *Carpinus* species, and their biological effects. The next section describes the classification and occurrence of diarylheptanoids emphasizing the biological effects of cyclic diarylheptanoids.

The experimental part of the thesis gives a summary of our research, during which we aim to screen the phenolic profile of European hornbeam with special regard to cyclic diarylheptanoids and confirm their plausible presence in the species. To complete the chemical and pharmacokinetic characterization of the diarylheptanoids, we will investigate their aqueous stability at physiologically relevant pH values, determine their ability for transcellular passive diffusion across biological membranes, and their cytotoxic activity.

## I.1. Characterization of *Carpinus betulus* and the *Carpinus* Genus

More than 40 species belong to the *Carpinus* genus, thus it is one of the largest genera in the Betulaceae family (Fig. 1) [1]. The European hornbeam or *Carpinus betulus* L. is a characteristic tree species of the temperate zone in Europe. It has a wide geographical distribution extending to southern Europe, Central Europe, Scotland, the south of Sweden, the Caucasus, and northern Iran (Fig. 2). It occurs at elevations up to 700 m in Central Europe, 1000 m in the Western Alps, and 1800 m in Iran [2]. In Hungary, only European hornbeam and Oriental hornbeam (*Carpinus orientalis*) can be found [3].

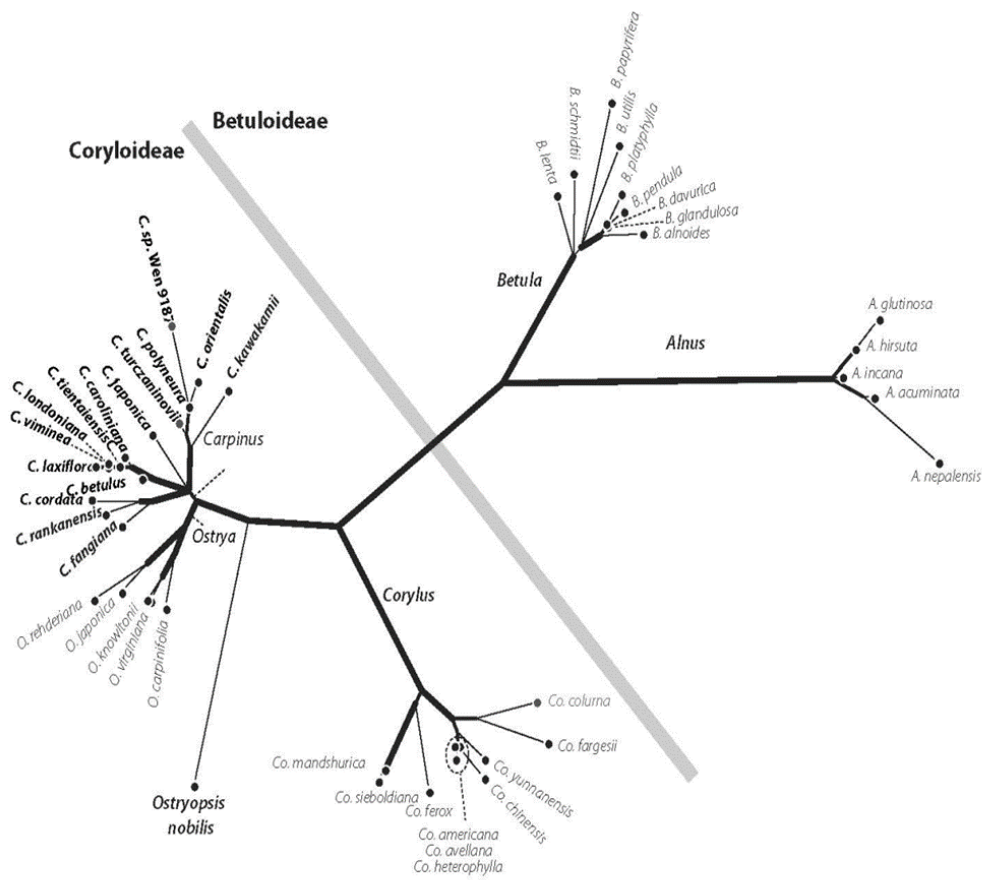


**Figure 1.** The genetic relationships among the genera of the Betulaceae family [1]

The name of hornbeam means ‘horn tree’ referring to its hardness. Its wood is inflexible and hard to work with, thus, its use in the timber industry is not widespread. Today it is applied to manufacture flooring panels, billiard cues, drumsticks, and piano

action mechanisms. Some varieties such as ‘Fastigiata’, ‘Columnaris’, and ‘Incisa’ are grown in parks and gardens [2].

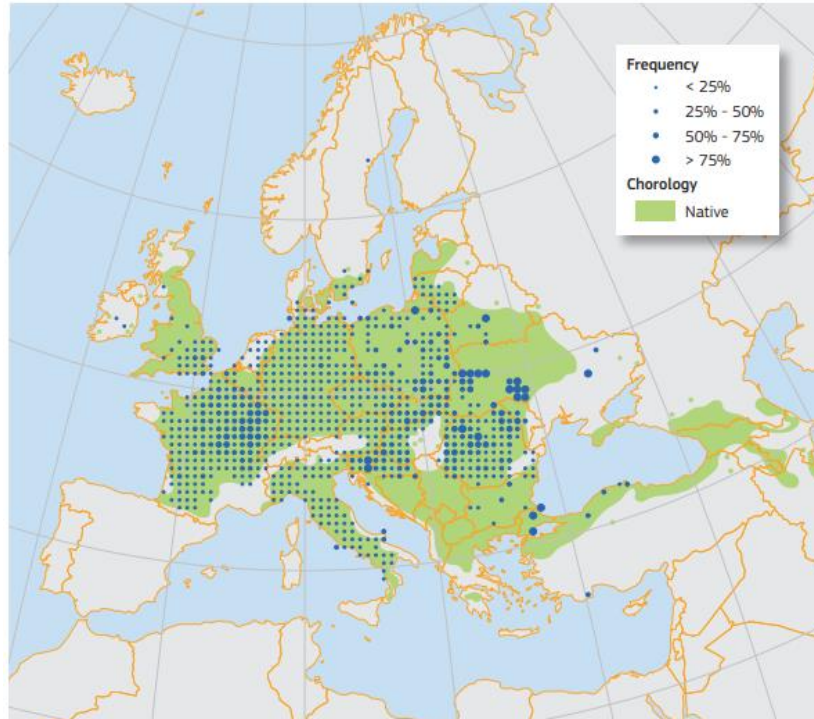


**Figure 2.** Distribution of *C. betulus* in Europe [2]

### ***1.1.1. Botanical Characterization of C. betulus***

The hornbeam is a medium sized deciduous tree, it grows up to 6-25 m height. The hornbeam can reach an age of over 120 years old, however, it already reaches its final height at the age of 50 years. Its crown is irregular, ovoid, or conic, becoming domed in old trees, the bark is smooth and steel-grey. The leaves are 6-12 cm long, simple, obovate, with serrated margins, and with prominent parallel veins. The dorsal side of the leaf is lighter, while the color of the ventral side is deep green. They can be confused with the leaves of the beech (*Fagus sylvatica*) but are less shiny and their edges are not wavy. The wind-pollinated, monoecious, unisexual flowers can be observed from March to April. The male catkins are loose, up to 6 cm long, while the female catkins are up to 15 cm long and to 6 cm broad. The fruits maturing in October are clustered in about 8 pairs of nutlets (achene), 6-8 mm, each pair at the base of a green leathery tri-lobate bract, 3.5 cm long (Fig. 3-4.) [4, 5].

The hornbeam prefers deep moist and well-drained soils. It favors full to partial sunny conditions; however, it is strongly shade tolerant. The hornbeam is a typical mesophilous species; therefore, it can be found on lowlands, hills and the low mountain belt. The common hornbeam grows in mixed stands with oaks (e.g., *Quercus robur*, *Quercus petraea*), forming oak-hornbeam forest communities representing the classic European temperate forest [2, 4, 5].

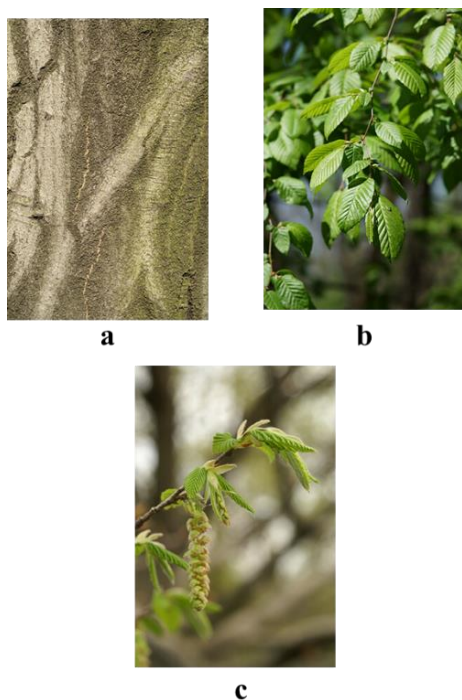


**Figure 3.** (a) Bark, (b) leaves, and (c) flower of *C. betulus* [6]



**Figure 4.** Illustration of *C. betulus* [7]

### ***1.1.2. Chemical Characterization of C. betulus and Other Carpinus Species***

Within the genus *Carpinus*, besides the universal metabolites, the secondary plant metabolites also show a diverse composition: chlorophyll derivatives, phenolics, and polyketides can be found in higher amount.

The hydrolysable and condensed (non-hydrolysable) tannins belonging to the phenolics, have been previously described in the genus *Carpinus*. Catechin isomers as building blocks of the non-hydrolysable tannins, and methyl gallate and its glycoside derivatives forming hydrolysable tannins were isolated from the methanol extract of *C. cordata* (heartleaf hornbeam) bark [8]. Hungarian researchers detected gallic acid

derivatives (mono-galloyl-hexosides) and tannins (e.g., galloyl-hexahydroxydiphenoyl-hexosides = galloyl-HHDP-hexosides, digalloyl-HHDP-hexosides, tri-, tetra-, and pentagalloylglucose) in high amount in the methanol extract of *C. betulus* leaf [3]. From another *Carpinus* species, *C. tschonoskii*, hydrolysable tannins such as casuarictin and casuarinin were isolated [9].

Several flavonoid compounds were detected in the genus, furthermore, the flavonoid profile was used to determine the degrees of kinship between the species. Besides the isoflavonoid genistein, flavonol (e.g., myricetin, quercetin, kaempferol) derivatives were described in *C. laxiflora* (Aka-shide hornbeam) and *C. caroliniana* (American hornbeam). The Hungarian *C. betulus* contained methoxylated flavonoids (isorhamnetin) [3], while flavones (e.g., apigenin, luteolin) were detected in the Chinese species *C. londoniana* and *C. tientaiensis* besides the European hornbeam [10].

Phenolic acids such as caffeic acid, methoxybenzoic acid, syringic acid, and protocatechuic acid derivatives were detected in the methanol leaf extract of *C. betulus*. These compounds can be found in glycosidic bond or conjugated to either shikimic acid or quinic acid [3].

Tálos-Nebahaj and colleagues conducted a comparative analysis, investigating the total phenol, flavonoid, and flavan-3-ol contents in methanolic extracts of leaves from 12 Hungarian forest tree species (European beech, European hornbeam, downy oak, sweet chestnut, black locust, Norway maple, Turkey oak, pedunculate oak, sessile oak, poplar, Scots pine, and black pine). They also assessed the antioxidant capacities of the leaf samples by the 2,2-diphenyl-1-picrylhydrazyl (DPPH), 2,2'-azino-bis(3-ethylbenzothiazoline-6-sulphonic acid) (ABTS), and ferric reducing ability of plasma (FRAP) assays throughout the vegetation period. The lowest flavan-3-ol content was observed in the methanolic leaf extracts of *C. betulus*, however, it emerged as one of the 'top-performing' species in this investigation, displaying high total flavonoid content with relatively low flavan-3-ol levels. Consequently, flavonoid-type compounds, along with other polyphenols lacking the flavan-3-ol structure (e.g., tannins, phenolic acids), were attributed to the exceptional antioxidant potency of European hornbeam leaves. Nonetheless, the antioxidant properties and phenolic concentrations exhibited diverse seasonal fluctuations, with the optimal antioxidant properties of *C. betulus* leaves presumed to occur between July and August [11, 12].

The essential oil of the leaves extracted by hydrodistillation was examined using gas chromatography-mass spectrometry (GC-MS). Terpenes, alkanes, and ester derivatives were detected. The main compounds were (*Z*)-3-hexen-1-ol, (*Z*)- $\beta$ -ocimene, caryophyllene, dodecane, hexyl acetate, and  $\alpha$ -terpinene, but also camphene, eucalyptol, hexanal, and hexanol compounds were described [13].

From some *Carpinus* species such as *C. cordata* and *C. turczaninowii* cyclic diarylheptanoids were isolated. These compounds were characterized as carpinontriols A and B, casuarinondiol, alnusdiol, and 11-oxo-3,7,12,13,17-tetrahydroxy-[7,0]-metacyclophane [8, 14, 15].

Fatty acids were also identified in the ethyl acetate extract of *C. betulus*, e.g., palmitic acid (C16:0), linoleic acid (C18:2), and  $\alpha$ -linolenic acid (C18:3). Pheophorbide A which is a product of chlorophyll breakdown was isolated from the same extract [16].

### ***1.1.3. Biological Activities of Carpinus Species***

The immunosuppressant effect of leaves and bark samples of *C. betulus* collected at different times during the vegetation period was investigated. The ethyl acetate and methanol extracts showed an *in vitro* immunosuppressant effect on T lymphocyte cell lines of Balb/c mice. The ethyl acetate extract of the leaf from May had the most potent activity due to the high pheophorbide A content. Furthermore, the leaf methanol extract from June also presented a strong immunosuppressant effect attributed to the high concentration of flavonoids [17].

In another examination, *C. betulus* leaves and stem bark collected in spring and autumn were tested *in vitro* on different cell lines. The spring ethyl acetate extract of the leaf presented significant growth inhibitory activity against U373 glioblastoma cells ( $IC_{50} = 23 \mu\text{g/mL}$ ), while the autumn samples were inactive. Based on previous phytochemical investigations, the active components were presumed to be terpene compounds [18]. Based on a bioguided isolation, Cieckiewicz and coworkers established that pheophorbide A was responsible for the effect [16]. The ethyl acetate and methanol extracts of the stem bark displayed cytotoxic activity against LoVo human colorectal cancer ( $IC_{50} = 24$  and  $18 \mu\text{g/mL}$ ), PC3 prostate cancer ( $IC_{50} = 38$  and  $38 \mu\text{g/mL}$ ), and U373 glioblastoma ( $IC_{50} = 55$  and  $22 \mu\text{g/mL}$ ) cell lines [18].

Thirteen hydrolysable tannins (e.g., carpinerin B, tetragalloylglucose, pentagalloylglucose, casuarictin, and casuarinin) were isolated from the methanol extract of *C. tschonoskii* galls growing on buds infected by *Eriophyes sp.* mites. These compounds could inhibit the antigen-induced activation of RBL2H3 rat basophilic leukaemia cells. The most potent tannin derivatives were tetragalloylglucose, pentagalloylglucose, casuarictin, and casuarinin without a cytotoxic effect after 24 h. Structure-activity relationships (SAR) could also be concluded: the compounds which contained a galloyl group at position 1 of the glucose molecule exhibited the strongest inhibitory activity (by almost 8-fold). The additional presence of the HHDP group at position 2 enhanced the activity, while the position of the hydroxyl group with a ring-opened glucose (e.g., in case of casuarinin) was also important [9].

The inhibitory effect of *C. tschonoskii* leaves methanol extract on pro-inflammatory cytokines and transcriptional factors was studied in TLR9 agonist-stimulated primary bone marrow-derived macrophage (BMDMs), and dendritic cells (BMDCs), and human embryonic kidney (HEK293T) cells. The extract showed a dose-dependent inhibitory effect on production of pro-inflammatory cytokines such as interleukin-12 subunit p40 (IL-12 p40), interleukin-6 (IL-6), and tumor necrosis factor- $\alpha$  (TNF- $\alpha$ ). However, the extract had no significant effect on mitogen-activated protein kinases (MAPKs) phosphorylation but inhibited nuclear factor-kappa B inhibitor alpha (I $\kappa$ B $\alpha$ ) degradation and the activity of the NF- $\kappa$ B [19].

The methanol extracts of *C. tschonoskii* leaves showed cytoprotective effect on H<sub>2</sub>O<sub>2</sub>-induced V79-4 Chinese hamster lung fibroblast cell lines. The extract enhanced the catalase activity and activated the phosphorylation of the extracellular signal regulated kinase (ERK), furthermore it prevented lipid peroxidation [20].

The *in vitro* neuroprotective effect of *C. tschonoskii* leaves ethanol extract was investigated on 6-hydroxydopamine- (6-OHDA-) induced oxidative damage in the PC12 rat pheochromocytoma cell line. The extract prevented the PC12 cell death in a dose-dependent manner, furthermore, it decreased the apoptotic events such as DNA fragmentation, chromatin condensation, caspase-3 activation, and poly-ADP ribose polymerase (PARP) cleavage. The extract may prevent PC12 cell apoptosis due to the up-regulation of myocyte enhancer factor 2D (MEF2D) and Akt kinase activity [21].

The ethanol extract of *C. tschonoskii* leaves was fractionated by solvent-solvent extraction (with hexane, chloroform, butanol, ethyl acetate, water) and the fractions were tested in HaCaT keratinocyte and RAW264.7 macrophage cell lines. In the case of HaCaT cells, the macrophage-derived chemokine (MDC) was inhibited by the ethanol, ethyl acetate, and butanol fractions, while the chloroform fraction significantly blocked the IFN- $\gamma$ -induced mRNA expression of MDC through inhibition of signal transducer and activator of transcription 1 (STAT1). In RAW264.7 macrophages, the chloroform extract showed anti-inflammatory effect due to the suppression of the mRNA expression of inducible nitric oxide synthase (iNOS) [22].

The leaf, branch, and trunk extracts of *C. turczaninowii* prepared with 70% ethanol were examined in human aortic smooth muscle cells against hyperglycemia-induced damage. During the study, the extract decreased the production of pro-inflammatory cytokines (such as TNF- $\alpha$  and IL-6) under high glucose conditions. Based on the ultrahigh-performance liquid chromatography-quadrupole time-of-flight mass spectrometry (UHPLC-QTOF) results, the main phenolics (e.g., galloylquinic acid and derivatives, gallo- and ellagitannins, and flavonoids) might be responsible for the effect, due to their antioxidant activity [23].

## **I.2. Diarylheptanoids**

Diarylheptanoids belong to the secondary plant metabolites making a subgroup of phenolics. The skeleton of the compounds contains a seven-carbon chain bearing two phenyl rings at positions 1 and 7. Diarylheptanoids can be categorized into two groups: acyclic or linear diarylheptanoids and cyclic diarylheptanoids [24]. The latter can be classified further in two types based on connection of the two aromatic rings: *meta,meta*-cyclophanes or biaryl-type compounds and *meta,para*-cyclophanes or diarylether-type derivatives (Fig. 5) [25, 26]. The most well-known diarylheptanoid is curcumin which was described by Trommsdorff in 1808 and was isolated by Vogel and Pelletier in 1815 [27]. Curcumin exhibits various biological activities in numerous tests, however, there are doubts regarding its application *in vivo* (due to pharmacokinetic and stability reasons). Nevertheless, there is a continued scientific interest towards curcumin and diarylheptanoids in general [24, 28]. Historically, *Zingiber* and *Curcuma* rhizomes,

containing numerous diarylheptanoids, have been widely employed as seasoning spices and components in folk remedies and traditional Asian medicinal preparations [29].

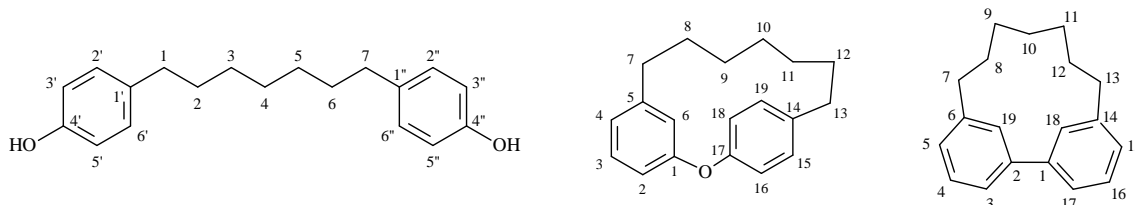


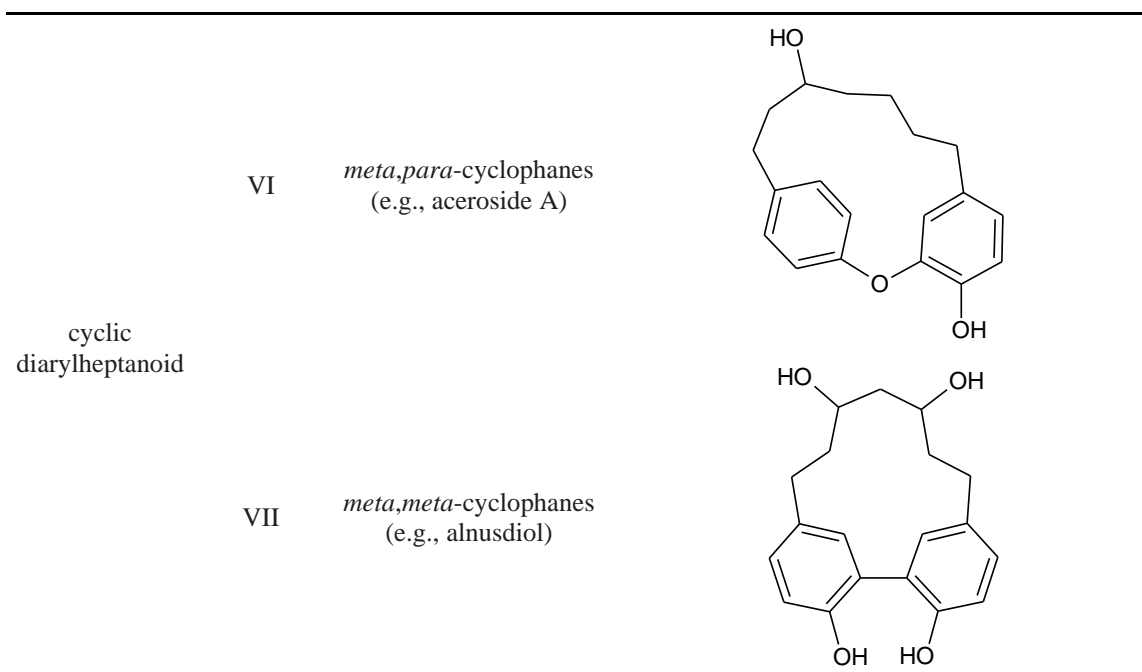
**Figure 5.** The general structures of linear, diarylether-type, and biaryl-type cyclic diarylheptanoids [24]

### ***1.2.1. Classification of Diarylheptanoids***

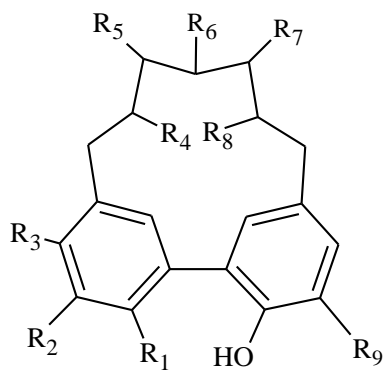
Due to the increasing number of identified diarylheptanoids, their structural categorization became necessary. Several classifications have been elaborated over the years. According to Cleason, diarylheptanoids could be classified into five groups: non-phenolic linear diarylheptanoids (Cleason Type I), phenolic linear diarylheptanoids (Cleason Type II), macrocyclic biarylheptanoids (Cleason Type III), macrocyclic diarylether-heptanoids (Cleason Type IV), and diarylheptanoids with a cyclized C<sub>7</sub>-chain (Cleason Type V) [30, 31]. However, with time further categorization was needed. The categorization of Lv and She takes into consideration additional substitutions of the compounds [15, 32]. Based on these, seven groups were established: linear diarylheptanoids with a saturated or an unsaturated heptane chain (Lv and She Type I), linear diarylheptanoids with a pyran or a furan ring (possessing a 1,5-oxy bridge or 3,6-oxy bridge) on the heptane chain (Lv and She Type II), linear diarylheptanoids with a flavonoid moiety on the heptane chain (Lv and She Type III), dimeric linear diarylheptanoids (Lv and She Type IV), unusual linear diarylheptanoid structures (Lv and She Type V), *meta,para*-cyclophanes (Lv and She Type VI), and *meta,meta*-cyclophanes (Lv and She Type VII). The last two groups are categorized further according to the number of olefinic bonds and/or carbonyl groups (Table 1.) [24].

**Table 1.** Structural characteristics of diarylheptanoids according to Lv and She [15, 24]

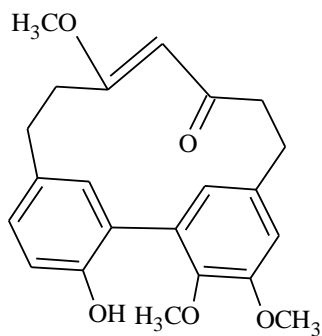
Type	Subtype	Skeleton	Examples
linear diarylheptanoid	I	heptane chain with or without olefinic bonds, carbonyl groups and/or a kavain side chain (e.g., curcumin)	
	II	pyran or furan ring in the carbon chain skeleton (e.g., rhoiptelol B)	
	III	a flavonoid type moiety attached to the carbon chain skeleton (e.g.; calyxin A with chalcone moiety)	
	IV	dimeric linear diarylheptanoids (e.g., blepharocalyxin D)	
	V	unusual structures (e.g., officinaruminane B)	



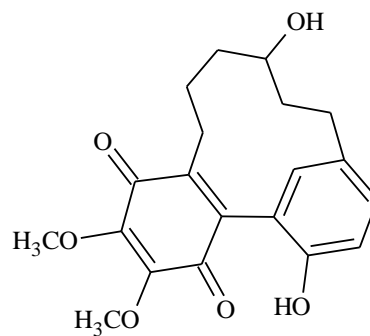
Jahng and Park focused on cyclic diarylheptanoids, when classifying the compounds [25]. They divided the biphenyl derivatives into four further categories based on their structural and chemotaxonomic properties: asadanin and related derivatives (Jahng and Park Type I), myricanone, myricanol, and related derivatives (Jahng and Park Type II), garuganins (Jahng and Park Type III), and miscellaneous compounds (Jahng and Park Type IV) (e.g., containing quinoidal structure) (Fig. 6).



	R <sub>1</sub>	R <sub>2</sub>	R <sub>3</sub>	R <sub>4</sub>	R <sub>5</sub>	R <sub>6</sub>	R <sub>7</sub>	R <sub>8</sub>	R <sub>9</sub>
<b>Type I</b>									
asadanin	OH	H	H	OH	H	=O	OH	OH	H
acerogenin K	OH	H	H	H	OH	H	H	H	H
acerogenin E	OH	H	H	H	=O	H	H	H	H
alnutsonol	OH	H	H	H	OH	H	=O	H	H
alnutdiol	OH	H	H	H	OH	H	OH	H	H
carpinontriol A	OH	H	H	OH	OH	H	=O	OH	H
carpinontriol B	OH	H	H	OH	OH	OH	=O	H	H
giffonin L	OH	H	H	OH	H	OH	OH	OH	H
giffonin M	OH	H	H	OH	H	OH	=O	H	H
giffonin N	OH	H	H	<i>O</i> -glc	H	OH	=O	H	H
giffonin O	OH	H	H	OH	OH	=O	H	OH	H
giffonin P	OH	H	H	OH	OH	OH	OH	OH	H
giffonin T	OH	H	H	OH	OH	OH	=O	H	<i>O</i> -glc
giffonin U	OH	H	H	OH	OH	OH	OH	=O	H
<b>Type II</b>									
myricanol	OCH <sub>3</sub>	OCH <sub>3</sub>	OH	H	H	H	OH	H	H
myricanone	OCH <sub>3</sub>	OCH <sub>3</sub>	OH	H	H	H	=O	H	H
juglanin B	OH	OCH <sub>3</sub>	H	H	H	H	OH	H	H



garuganin II (**Type III**)



actinidione (**Type IV**)

**Figure 6.** Classification of the main *meta,meta*-cyclophane diarylheptanoids according to Jahng and Park [25]

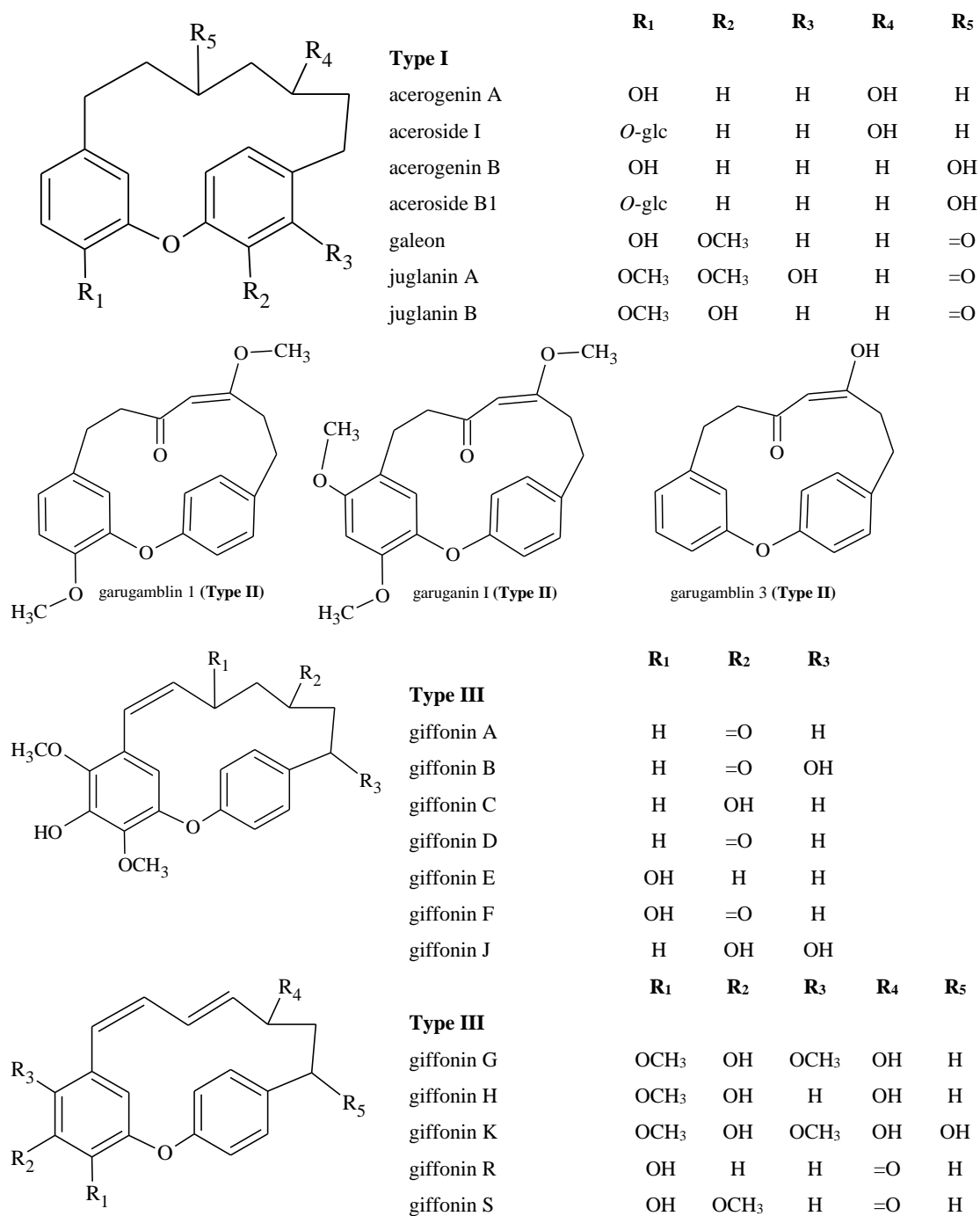


**Figure 7.** Classification of the main *meta,para*-cyclophane derivatives according to Jahng and Park [25]

The *meta,para*-cyclophane-type cyclic diarylheptanoids were classified into three primary groups according to their structural characteristics: acerogenins and acerosides (Jahng and Park Type I), garuganins and garugamblins (Jahng and Park Type II), and miscellaneous compounds (Jahng and Park Type IV) (Fig. 7) [25].

### 1.2.2. Occurrence of Diarylheptanoids in Plants

Over 400 diarylheptanoids had been described and isolated to date. The linear compounds occur mainly in the Zingiberaceae family (*Alpinia*, *Zingiber*, and *Curcuma* genera) and the Betulaceae family (*Alnus*, *Betula*, *Corylus*, and *Ostryopsis* genera) [33].

The cyclic diarylheptanoids are characteristic for the Betulaceae family (*Alnus*, *Betula*, *Corylus*, *Carpinus*, *Ostrya*, and *Ostryopsis* genera). The first ever *meta,meta*-cyclophane to be identified was asadanin from *Ostrya japonica*. Later, other related compounds such as deoxoasadanin, epiasadanol, isoasadanol, and di- and trideoxyasadanin-8-ene were also isolated [25, 34, 35]. The occurrence of diarylheptanoids in plants is summarized in Table 2.

**Table 2.** Occurrence of diarylheptanoids [15, 25]

Family	Genus	Diarylheptanoids		
		Linear diarylheptanoids	<i>Meta,meta</i> -cyclophanes	<i>Meta,para</i> -cyclophanes
Aceraceae	<i>Acer</i>	+	+	+
Actinidiaceae	<i>Clematoclethra</i>	-	-	+
Betulaceae	<i>Alnus</i>	+	+	+
	<i>Betula</i>	+	+	+
	<i>Carpinus</i>	-	+	-
	<i>Corylus</i>	+	+	-
	<i>Ostrya</i>	-	+	-
	<i>Ostryopsis</i>	+	+	+
Bursraceae	<i>Boswellia</i>	-	-	+
	<i>Garuga</i>	-	+	+
Casuarinaceae	<i>Casuarina</i>	-	+	-
Juglandaceae	<i>Engelhardia</i>	+	-	+
	<i>Juglans</i>	+	+	+
	<i>Platycarya</i>	-	+	+
	<i>Pterocarya</i>	-	-	+
	<i>Rhoiptelea</i>	+	+	+
Myricaceae	<i>Morella</i>	+	+	+
	<i>Myrica</i>	-	+	+
Rubiaceae	<i>Scyphiphora</i>	-	+	-
Zingiberaceae	<i>Alpinia</i>	+	-	-
	<i>Curcuma</i>	+	-	-

Asadanin was also described in common hazel (*Corylus avellana*) as the main contributor of the bitter off-taste [36]. Similar compounds were reported from Japanese alder (*Alnus japonica*) (e.g., alnusone, alnusonol, and alnusoxide), with alnusone and alnusonol being also isolated from Japanese hazel (*Corylus sieboldiana*). Leaves of

*C. avellana* contain giffonins A-P, T-U, X, and carpinontriol B, while the flowers comprise giffonins I, Q-S. Furthermore, giffonins I, T-U, and carpinontriol B were isolated from the green leafy covers, whilst giffonins P and V have been found in the shells [37]. From the ethyl acetate and methanol leaf extract of filbert (*Corylus maxima*), alnusonol-glucoside, alnusone, giffonin F, and carpinontriol B were described [38]. Acerogenin E and its derivatives were detected in different *Betula* species such as Dahurian birch (*B. dahurica*), Erman's birch (*B. ermanii*), monarch birch (*B. maximowicziana*), and Asian white birch (*B. platyphylla*) [39-43], while carpinontriol A and other cyclic diarylheptanoids were isolated from downy birch (*B. pubescens*) and silver birch (*B. pendula*) [44, 45].

The presence of cyclic diarylheptanoids is also characteristic for the Juglandaceae (*Engelhardia*, *Juglans*, *Platycarya*, *Pterocarya*, and *Rhoiptelea* genera) [46-50] and Myricaceae (*Myrica* and *Morella* genera) families [25, 51-53].

Diarylheptanoids are typically isolated from the inner stem and root bark of trees and shrubs as well as from the rhizomes of certain herbs [54-56]. They can also be extracted from the leaves and twigs of terrestrial plants [57, 58]. In an unusual discovery, cyclic diarylheptanoids like alnusone and related compounds have been found in the nest (*Nidus vespae*) of the paper wasp (*Polistes* spp.), while other diarylheptanoids were isolated from the marine sponge *Tedania ignis* [59, 60].

### ***1.2.3. The Biological Effects of Cyclic Diarylheptanoids***

Cyclic diarylheptanoid compounds have gained interest in different scientific fields. The following *in vitro* studies have verified antitumor, antibacterial, anti-inflammatory, antioxidant, neuroprotective, antiadipogenic, melanogenesis inhibitory,  $\alpha$ -glucosidase inhibitory, and sodium-dependent glucose cotransporters (SGLT) inhibitory effects of cyclic diarylheptanoids. These *in vitro* investigations of the compounds and extracts might guide future *in vivo* studies.

#### ***1.2.3.1. The In Vitro Biological Effects of Cyclic Diarylheptanoids***

The anti-inflammatory effect of the ethyl acetate extract of *C. turczaninowii* branches was investigated in the RAW 264.7 murine macrophage cell line. Using a bioassay-guided isolation, two active compounds, carpinontriols A and B were isolated

from the extract. The extract ( $IC_{50} = 57.5 \mu\text{g/mL}$ ), and carponontriols A and B ( $IC_{50} = 396.0$  and  $199.4 \mu\text{M}$ , respectively) decreased the release of NO without cytotoxic effect. Furthermore, the level of the pro-inflammatory cytokine IL-6 was also reduced in a dose-dependent manner [14].

Tedarene A, isolated from the marine sponge *T. ignis* (Tedaniidae), also exhibited a 68% inhibition of NO production at  $30 \mu\text{M}$  in LPS-activated J774.1 cells [60]. Furthermore, Maurent et al. confirmed its ability to inhibit 65% of NO release, along with 40% and 75% inhibition of IL-1 $\beta$  and IL-6 cytokine production, respectively, at the same concentration in LPS-stimulated RAW 264.1 macrophages. However, tedarene A displayed cytotoxicity, resulting in a cell viability of only 40% at  $30 \mu\text{M}$  concentration [61].

Acerogenins A, B, E, and K isolated from Nikko maple (*Acer nikoense*) inhibited the production of nitric oxide (NO) in lipopolysaccharide- (LPS-) induced mouse peritoneal macrophages. Acerogenins A and B belonging to the diarylether-type diarylheptanoids, presented  $IC_{50}$  values of 74 and  $88 \mu\text{M}$ , respectively. On the other hand, the biaryl-type compounds acerogenins E and K showed  $IC_{50}$  values of 24 and  $25 \mu\text{M}$ , respectively. These results suggest that *meta,meta*-cyclophanes demonstrate more potent inhibitory effect on NO production than *meta,para*-cyclophanes [62].

Acerogenins A and B also showed inhibitory effects on SGLTs. These compounds could inhibit SGLT-1 ( $IC_{50} = 20.0$  and  $26.0 \mu\text{M}$ , respectively), while the compounds showed an SGLT-2 inhibitory activity at higher concentrations ( $IC_{50} = 94.0$  and  $43.0 \mu\text{M}$ , respectively). Different derivatives of acerogenins were synthesized to get information on the structure-activity relationships. The glycosylated derivatives did not show inhibition and those with a hydroxyl group at C-9 or C-11 had no effect, either. However, constituents with oxo moieties had stronger effect, while derivatives with a benzoyl or a benzyl group on the heptane chain were less effective [63].

Furthermore, giffonins J, K, and P inhibited  $\alpha$ -glucosidase,  $IC_{50}$  values were 56.6, 70.0, and  $55.6 \mu\text{M}$ , respectively, while the positive control acarbose showed an  $IC_{50}$  value of  $115.1 \mu\text{M}$  [64]. Other cyclic diarylheptanoids such as alnusone, alnusonol, and 3,17-dihydroxy-tricyclo[12.3.1.1<sup>2,6</sup>]-nonadeca-1(18),2,4,6(19),14,16-hexaen-9,11-dione from *Alnus sieboldiana* also exhibited  $\alpha$ -glucosidase inhibitory effect ( $IC_{50} = 8.69$ , 2.34, and  $1.35 \mu\text{g/mL}$ , respectively, acarbose  $IC_{50} = 451 \mu\text{g/mL}$ ) [65].

4-hydroxy-almus-3,5-dione, dihydroalmusone, almusol, almusonone, and betulatetraol were isolated from the fruit of *A. japonica* and examined in the 3T3-L1 murine preadipocyte cell line. 4-hydroxy-almus-3,5-dione, dihydroalmusone, and betulatetraol exhibited significant inhibitory effects on adipocyte differentiation at 100  $\mu$ M. Among the compounds, 4-hydroxy-almus-3,5-dione was the most potent, it induced the down-regulation of the peroxisome proliferator-activated receptor  $\gamma$  (PPAR $\gamma$ ), the CAAT/enhancer binding protein  $\alpha$  (C/EBP $\alpha$ ), and the sterol regulatory element binding protein 1 (SREBP1c) [66].

The osteogenic activity of acerogenins A and B, and acerosides B1, I, and III was investigated in MC3T3-E1 mouse preosteoblastic cells. The compounds induced osteoblastic mineralization, and they significantly increased the level of alkaline phosphatase (30-100  $\mu$ M, except for acerogenin B: 10-100  $\mu$ M) and osteocalcin (except for aceroside III) in a dose-dependent manner. The presence of a hydroxyl group at C-9 or C-11 increased the activity, while compounds with glycosylated C-2 or C-11 hydroxyl groups were less effective due to their decreased membrane permeability. These observations suggested that hydroxyl groups at C-2, and C-9 or C-11 are essential for the osteogenic action of diarylether-type cyclic diarylheptanoids [67].

Nine cyclic diarylheptanoids were isolated from the ethyl acetate fraction of *A. nikoense* bark methanol extract. These compounds were examined on MSH-stimulated B16 melanoma cells as melanogenesis inhibitor agents. Aceroside I, aceroside III, aceroside VI, acerogenin B, aceroside B1, 9-oxoacerogenin A, and 9-*O*-glucosyl-acerogenin K exhibited melanogenesis inhibitory effects at concentration of 10  $\mu$ M with a higher activity than arbutin. The compounds were also examined in HL60 human leukaemia and CRL1579 human melanoma cell lines, where they showed no cytotoxic effect ( $IC_{50} > 100$   $\mu$ M) except aceroside B1 ( $IC_{50} = 25.1$   $\mu$ M) [68].

Ten cyclic diarylheptanoids were isolated from Chinese bayberry (*Myrica rubra*) bark. Among these compounds, myricanol-11-*O*-glucoside, myricanol-5-*O*-(6'-*O*-galloyl)-glucoside, myricanone-5-*O*-arabinosyl-(1 $\rightarrow$ 6)-glucoside, myricanone-17-*O*-(6'-*O*-galloyl)-glucoside, and 16-methoxy-acerogenin-9-*O*-apiosyl-(1 $\rightarrow$ 6)-glucoside showed melanogenesis inhibitory effects at 25  $\mu$ g/mL concentration, reducing the melanin content by 30-56% in B16 melanoma cells. The compounds were more effective than the control arbutin (at 25  $\mu$ g/mL concentration reduced by 77.4%). Additionally,

myricanol, myricanol-11-*O*-glucoside, myricanol-5-*O*-(6'-*O*-galloyl)-glucoside, myricanone, and myricanone-17-*O*-(6'-*O*-galloyl)-glucoside exhibited strong antioxidant activity against DPPH. Based on these results, glycosylation of the C-5 phenolic hydroxyl group decreased the activity, while the presence of a galloyl moiety increased the antioxidant effect [69].

Juglanins A, B, and C were isolated from *Juglans sinensis* (syn. *Juglans regia*) applying bioactivity-guided fractionation. The isolated compounds were investigated for their neuroprotective effect on glutamate-induced toxicity in HT22 mouse hippocampal cells. Juglanins A and C showed strong neuroprotective effect due to the reduction of the cellular peroxide overproduction, and by maintaining the glutathione reductase and glutathione peroxidase activity. ED<sub>50</sub> values were 3.92 and 2.29 μM for juglanins A and C, respectively (control was trolox ED<sub>50</sub> = 3.52 μM) [70]. In a similar study, the neuroprotective effect of myricanol was studied in H<sub>2</sub>O<sub>2</sub>-induced N2a mouse neuroblastoma cells. The compound neutralized the effect of H<sub>2</sub>O<sub>2</sub>, decreased the production of reactive oxygen species (ROS) and the changes in the concentration of Ca<sup>2+</sup> ions [71].

The inhibitory effects of giffonins A-I from *C. avellana* were investigated on human plasma lipid peroxidation induced by H<sub>2</sub>O<sub>2</sub> and H<sub>2</sub>O<sub>2</sub>/Fe<sup>2+</sup>. Giffonins D and H decreased lipid peroxidation at 10 μM concentration by more than 60% and 50%, respectively [72]. The antioxidant effect of giffonins C, D, F-H, J-P, V-X, alnusone, and carpinontriol B was evaluated by inhibition of human plasma lipid peroxidation. All compounds had protective effect except for alnusone and giffonin D. Giffonins K and G reduced the H<sub>2</sub>O<sub>2</sub>/Fe<sup>2+</sup>-induced protein carbonylation by 65% at 10 μM [73].

Carpinontriol B and giffonin U from *C. avellana* showed antibacterial effect against *Bacillus cereus*, *Staphylococcus aureus*, *Escherichia coli*, and *Pseudomonas aeruginosa* at 40 μg/disk, while giffonin T was less effective. The positive control was tetracycline at 7 μg/disk [74].

The cytotoxicity of cyclic diarylheptanoids was investigated in several studies. Myricanone had cytotoxic activity on A549 lung carcinoma, HeLa cervical cancer, and PC3 prostate cancer cell lines (IC<sub>50</sub> = 3.22, 29.6, and 18.4 μg/mL, respectively). The growth inhibitory effects of myricanone were significant and dose-dependent. A notable decrease in colony formation was observed, leading to the induction of cell apoptosis [75,

76]. Juglanins A and B from the pericarps of *J. regia* exhibited antitumor activity on Hep G2 human hepatoma cells ( $IC_{50} = 0.02$  and  $1.50 \mu\text{M}$ , respectively), the positive control was cisplatin ( $IC_{50} = 0.67 \mu\text{M}$ ) [77]. *Clematoclethra actinidioides* (syn. *Clematoclethra scandens* subsp. *actinidioides*), a climbing shrub native to China, contains actinidione, a cyclic diarylheptanoid with a special structure. This compound showed cytotoxicity on Lu06 (CaLu-06) human lung adenocarcinoma, Bre04 human breast cancer, and N04 human neuroma cells with half-maximal growth inhibitory concentration ( $GI_{50}$ ) values of 31.82, 15.02, and 26.67  $\mu\text{g/mL}$ , respectively ( $GI_{50}$  of irinotecan was 0.83  $\mu\text{g/mL}$ ) [78]. Cymodienol from the sea grass *Cymodocea nodosa* also had cytotoxic effect on SCL-N6 and A549 lung cancer cell lines ( $IC_{50} = 84.0$  and  $114.6 \mu\text{M}$ , respectively) [79]. Galeon and 4,17-dimethoxy-2-oxatricyclo[13.2.2.1<sup>3,7</sup>]eicosa-3,5,7(20),15,17,18-hexaene-10,16-diol from monkey nuts (*Juglans mandshurica*) were evaluated in human A549 lung carcinoma and HT-29 human colon carcinoma cells. Galeon exhibited potent cytotoxic activity both in A549 and HT-29 cells with  $IC_{50}$  values of 5.3 and 2.2  $\mu\text{g/mL}$ , respectively. The positive control was altromycin B ( $IC_{50} = 3.9$  and  $4.2 \mu\text{g/mL}$ ) [80]. On the other hand, carpinontriol B from *C. avellana* shells did not show antitumor activity in A375 and SK-Mel-28 melanoma, and HeLa cervical cancer cells [81].

#### 1.2.3.2. The *In Vivo* Biological Effects of Cyclic Diarylheptanoids

Ishida and coworkers investigated the antitumor-promoting effects of myricanone and 13-oxomyricanol in six-weeks-old female mice. The animals were pretreated with 7,12-dimethylbenz[a]anthracene, and after one week received tumor inducing 12-*O*-tetradecanoylphorbol-13-acetate (TPA) treatment. The mice were categorized into four groups: group 1 was the control group (only TPA was administered), group 2 received TPA and 13-oxomyricanol, group 3 was given TPA and myricanone, while group 4 got TPA and curcumin. The mean number of papillomas per mouse was 9.3 (Group 1), 6 (Group 2), 5.1 (Group 3), and 4.9 (Group 4) after 20 weeks. The studied compounds exhibited 33, 43, and 45% inhibition on the promotion of papillomas at 20 weeks. The investigation of structure-activity relationships revealed that the C-11 position of the cyclic structure was important, an oxo group increased the activity, while a hydroxyl group decreased it. Derivatives methylated and acetylated at both the C-5 and C-17 hydroxyl groups were less effective [82].

The anti-tumor activity of myricanol was investigated on lung adenocarcinoma A549 xenografts in nude mice. Myricanol treatment (40, 20, and 10 mg/kg body weight) significantly decreased the volume and the mass of the tumor (Fig. 8), furthermore, it delayed the progression. The myricanol therapy increased the mRNA expression of the Bax pro-apoptotic protein (Bcl-2-associated X protein) in a dose-dependent manner, and decreased the levels of Bcl-2 (B-cell lymphoma 2 protein), vascular endothelial growth factor (VEGF), hypoxia-inducible factor (HIF-1 $\alpha$ ), and survivin [83].

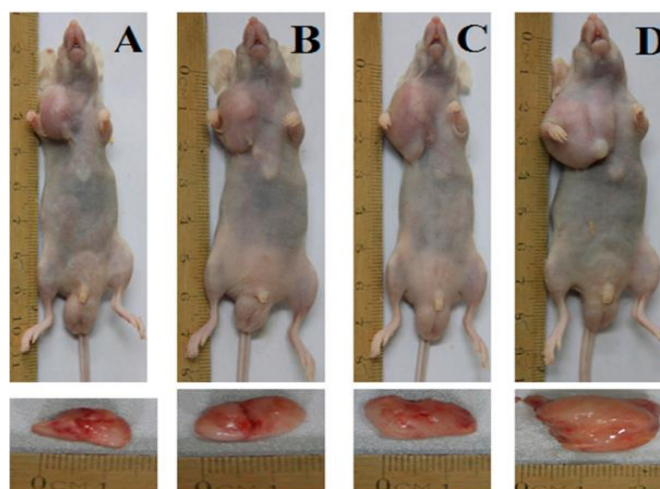


**Figure 8.** Antitumor effect of myricanol on lung adenocarcinoma A549 xenografts in nude mice. (A) Myricanol 40 mg/kg; (B) myricanol 20 mg/kg; (C) myricanol 10 mg/kg; (D) control group [83]

Myricanone, myricanol, myricanone-5-*O*-glucoside, and myricanol-*O*-glucoside from *A. japonica* were evaluated as anti-inflammatory agents, inflammation was induced by carrageenan in rat paw. The control group got indomethacin (10 mg/kg), while the treatment groups received the isolated compounds individually (10 mg/kg). The effect of myricanol was comparable to that of indomethacin, probably due to the inhibition of prostaglandins [84].

Anti-androgenic activity of *M. rubra* ethanol extract and myricanol was studied in Syrian hamsters. The castrated hamsters were divided into groups and were administered 5  $\mu$ L of the negative or positive control, or myricanol, or the *M. rubra* extract topically. Group 1 got 50% ethanol (as negative control), group 2 received 2% oxendolone (as positive control), group 3 was given myricanol (at two concentrations:

0.015  $\mu\text{mol}/5 \mu\text{L}$  50% ethanol and 0.05  $\mu\text{mol}/5 \mu\text{L}$  50% ethanol), while group 4 got 50% *M. rubra* extract. Oxendolone, the *M. rubra* extract, and myricanol at both concentrations showed a significant anti-androgenic effect due to the inhibition of  $5\alpha$ -reductase. The extract was more potent than the isolated myricanol. The ethanol extract of *M. rubra* was also examined in a hair regrowth assay in mice. The extract showed significant anti-androgenic effect similar to that of oxendolone [85].

In another study, mice received daily intraperitoneal injections of 3,5-dimethoxy-4-hydroxy-myricanol extracted from the leaves of *Micromelum integerrimum* for two weeks. This treatment aimed to assess the outer retinal function. The results indicated that the isolated compound significantly enhanced retinal function by amplifying electroretinography signals, preserving retinal morphology, reducing apoptosis of photoreceptor cells, alleviating inflammatory responses, and mitigating endoplasmic reticulum stress [86].

Although several examinations evaluating the biological effects of diarylheptanoids were carried out, most of these were *in vitro* experiments. Therefore, the results must be handled with caution. Our knowledge about the pharmacokinetics and toxicity of the compounds or extracts is limited. Furthermore, in some experiments, large doses were used, which are not feasible for human therapy. While the effects of some compounds are promising, further research is needed.

## II. Objectives

Literature data on the phenolic composition of *Carpinus betulus* is limited, the phenolic fingerprint of its different parts has not been studied and compared yet. Chemical, pharmacological, and pharmacokinetic characterization of its constituents have neither been performed. Based on this, our aims were to:

1. Carry out a detailed and extensive phytochemical characterization of European hornbeam by high-performance liquid chromatography coupled with diode-array detection and tandem mass spectrometry (HPLC-DAD-MS/MS).
2. Screen the phenolic profile of hornbeam samples (leaves, bark, male, and female catkins) with special regard to cyclic diarylheptanoids and confirm their plausible presence.
3. Develop suitable methods for the isolation of the cyclic diarylheptanoids and other characteristic constituents and reveal their structures.
4. Examine the mass spectrometric fragmentation of the cyclic diarylheptanoids and reveal the possible fragmentation pathways established on their structural features.
5. Determine the *in vitro* antioxidant activity of the extracts and the isolated compounds by employing the DPPH assay and assess the contribution of each individual constituent to the total radical scavenging activity of the extracts by an off-line DPPH-HPLC-DAD-MS method.
6. Develop and validate an UHPLC-DAD method for the quantitative determination of the main diarylheptanoid compounds.
7. Investigate the effects of ambient conditions, including storage time, temperature, and medium (pH, solvent, and accompanying constituents) on the stability of the main diarylheptanoids.
8. Determine the main diarylheptanoids' ability for transcellular passive diffusion across biological membranes by the parallel artificial membrane permeability assay for the gastrointestinal tract and for the blood–brain barrier (PAMPA-GI and PAMPA-BBB).
9. Determine the *in vitro* cytotoxic activity of the leading diarylheptanoids against different human cancer cell lines.

### **III. Materials and Methods**

#### **III.1. Plant Material**

For the qualitative HPLC-MS analyses, the DPPH assays, and the UHPLC-DAD quantitation, bark, leaf, female, and male catkin samples of *C. betulus* were collected in Hungary, in the Buda Hills (Budai-hegység, April 2015), Mátraháza (May 2016) and Visegrád Hills (Visegrádi-hegység, July 2018). For the isolation of the constituents, bark samples of *C. betulus* were collected in Hungary, in Mátraháza (May 2017) and Lajosháza (May 2019), while the stability tests were performed using bark samples collected in the Visegrád Hills (July 2018). Authenticated samples and herbarium specimens are deposited at the Herbarium of the Department of Pharmacognosy, Semmelweis University, Budapest, Hungary.

#### **III.2. Solvents and Chemicals**

Chloroform, ethyl acetate, methanol, and *n*-hexane of reagent grade as well as HPLC grade methanol and acetonitrile were acquired from Molar Chemicals Kft. (Halásztelek, Hungary). Acetic acid 100% for HPLC LiChropur™, DPPH, rutin, trolox (6-hydroxy-2,5,7,8-tetramethylchromane-2-carboxylic acid), PBS tablet (Phosphate Buffered Saline, pH 7.4), trifluoroacetic acid, methanol-*d*<sub>4</sub>, and dimethyl sulfoxide-*d*<sub>6</sub> (DMSO-*d*<sub>6</sub>) for NMR measurements were purchased from Sigma-Aldrich (Steinheim, Germany). DMSO, *n*-dodecane, sodium chloride (NaCl), hydrochloric acid (HCl), disodium hydrogen phosphate heptahydrate (Na<sub>2</sub>HPO<sub>4</sub> · 7H<sub>2</sub>O), and sodium dihydrogen phosphate monohydrate (NaH<sub>2</sub>PO<sub>4</sub> · H<sub>2</sub>O) were purchased from Reanal-Ker (Budapest, Hungary), while phosphatidylcholine, cholesterol, and the porcine polar brain lipid extract were obtained from Merck (Darmstadt, Germany). High-purity water was gained by a Millipore Direct Q5 Water Purification System (Billerica, MA, USA).

#### **III.3. Extraction and Sample Preparation**

##### ***III.3.1. Sample Preparation for the Qualitative HPLC-MS Analyses, the DPPH Assays, and the Quantitative UHPLC-DAD Determination***

Dried and milled bark, leaf, female, and male catkin samples (3.0 g each) were extracted by Soxhlet extraction (6 h) with ethyl acetate and methanol (250 mL each). The extracts were distilled to dryness under reduced pressure with a rotary evaporator (Büchi

Rotavapor R-200, Flawil, Switzerland) at 50 °C. The samples were redissolved in 4.0 mL methanol of HPLC gradient grade and filtered through Minisart RC 15 0.2 µm syringe filters (Sartorius AG, Goettingen, Germany). Prior to analysis, the purified samples were evaporated to dryness at 50 °C under reduced pressure and redissolved in 1.0 mL 70% (v/v) HPLC grade methanol.

### ***III.3.2. Sample Preparation for the Isolation of Constituents***

The combined and dried bark samples (500 g) were ground, then extracted at room temperature in an ultrasonic bath with chloroform (3 × 2 L, 2 h each). In the following, the residue was extracted consecutively with solvents of increasing polarity: ethyl-acetate and then methanol (3 × 2 L for both solvents, 2 h each). The ethyl acetate and methanol extracts were distilled to dryness under reduced pressure with a rotary evaporator at 50 °C. The residue was suspended in 70% (v/v) methanol (to get a concentration of 500 mg in 4 mL, and 1000 mg in 4 mL, respectively).

## **III.4. Chromatographic Analyses**

### ***III.4.1. HPLC-DAD-ESI-MS/MS Conditions***

Qualitative phytochemical screening of *Carpinus* extracts was performed with an Agilent 6410B triple quadrupole equipped with an electrospray ionization source (ESI) coupled to an Agilent 1100 HPLC system (G1379A degasser, G1312A binary gradient pump, G1329A autosampler, G1316A column thermostat, G1315C diode array detector) (Agilent Technologies, Santa Clara, CA, USA, and Waldbronn, Germany). The separation of the extracts was carried out on a Zorbax SB-C18 column (150 × 3.0 mm i.d., 3.5 µm; Agilent Technologies), the column temperature was 25 °C. Eluent A was 0.3% acetic acid in water, eluent B was methanol. A gradient elution was performed at a flow rate of 0.3 mL/min as follows: 10–40% B (0–35 min), 40–60% B (35–45 min), 60–100% B (45–47 min), 100% (47–50 min). The injection volume was 10 µL. The ionization source was operated in the negative ionization mode, the mass spectrometric parameters were as follows: Nitrogen was applied as drying gas (350 °C, 9 L/min), nebulizer pressure: 45 psi, fragmentor voltage: 120 V, capillary voltage: 3500 V. High purity nitrogen was used as collision gas, the collision energy varied between 10–40 eV. Full scan mass spectra were recorded in negative ionization mode in the range of  $m/z$  100

and 1000. The MassHunter B.01.03 software was used for data acquisition and qualitative analyses.

#### ***III.4.2. Isolation Procedures***

The bark ethyl acetate extract was fractionated using a CombiFlash NextGen 300 + (Teledyne Isco, Lincoln, NE, USA) flash chromatograph, applying a RediSep Rf Gold C18 column (100 g, Teledyne Isco) as stationary phase. Eluent A was 0.3% acetic acid in water, eluent B was methanol, and the following gradient elution was applied at a flow rate of 60 mL/min: 30% B (0–3 min), 30–100% B (3–33 min), 100% B (33–38 min). 144 fractions (of 16 mL each) were collected. Fractions 56–60 yielded compound **177** (23.5 mg). Chromatographic separations of additional fractions were performed by semi-preparative HPLC on a Waters 2690 HPLC system equipped with a Waters 996 diode array detector (Waters Corporation, Milford, MA, USA). As stationary phase, a Luna C18 (150 × 10 mm i.d., 5 µm; Phenomenex Inc; Torrance, CA, USA) column or a Kinetex C18 (150 × 10 mm i.d., 5 µm; Phenomenex Inc) column was used. Different gradient elution methods with 0.3% acetic acid in water as eluent A and methanol as eluent B were applied at a flow rate of 1 mL/min. Fractions 38–41 were separated to obtain **106** (3.5 mg,  $t_R = 22.3$  min), **114** (1.3 mg,  $t_R = 24.1$  min), and **154** (1.5 mg,  $t_R = 30.0$  min), using the gradient as follows: 33% B (0–20 min), 33–100% B (20–25 min), 100% B (25–33 min). Fractions 68–71 were chromatographed using the gradient 50% B (0–20 min), 50–100% B (20–23 min), 100% B (23–33 min), to yield compound **191** (2.2 mg,  $t_R = 24.1$  min). For the chromatographic separation of fractions 61–67 to purificate **164** (0.7 mg,  $t_R = 13.6$  min) and **187** (0.5 mg,  $t_R = 14.4$  min), we applied a different gradient elution system consisting of 0.3% acetic acid (eluent A) and acetonitrile (eluent B) at a flow rate of 1 mL/min: 40–64% B (0–16 min), 64–100% B (16–17 min).

The bark methanol extract was separated by flash chromatography as described for the ethyl acetate extract. Fractions were further separated by semi-preparative HPLC (using the same instrumentation and stationary phase as detailed above). Different gradient elutions were employed at a flow rate of 1 mL/min. Fractions 50–55 were purified with the gradient as follows (eluent A: 0.3% acetic acid in water, eluent B: methanol): 50% B (0–20 min), 50–100% B (20–22 min), 100% B (22–32 min), 6 fractions were collected. Fraction 2 ( $t_R = 12$  min) was further chromatographed applying

the following gradient elution (eluent A: 0.3% acetic acid, eluent B: acetonitrile): 22–24% B (0–22 min), to yield **148** (1.2 mg,  $t_R = 19.2$  min). Fractions 56–61 from flash chromatography were separated to collect 8 fractions, with the gradient (eluent A: 0.3% acetic acid, eluent B: methanol): 45–50% B (0–20 min), 50–100% B (20–22 min), 100% B (22–32 min). Fraction 8 ( $t_R = 23$  min) was chromatographed with the gradient elution (eluent A: 0.3% acetic acid, eluent B: acetonitrile) 35% B (0–16 min), 35–100% B (16–17 min), to yield **149** (1.7 mg,  $t_R = 13.7$  min), **157** (2.0 mg,  $t_R = 14.7$  min), and **161** (0.7 mg,  $t_R = 12.5$  min). Fractions 73–75 from flash chromatography were separated to yield **185** (3.3 mg,  $t_R = 17.1$  min), using the following gradient (eluent A: 0.3% acetic acid, eluent B: acetonitrile): 40–60% B (0–25 min). The isolation procedure is depicted in Fig. 9. Purity of the isolated substances was surveyed by HPLC-DAD-MS/MS.

#### ***III.4.3. UHPLC-DAD-ESI-Orbitrap-MS/MS Conditions***

High-resolution mass spectra of the isolated compounds were obtained using a Dionex Ultimate 3000 UHPLC system (3000RS diode array detector, TCC-3000RS column thermostat, HPG-3400RS pump, SRD-3400 solvent rack degasser, WPS-3000TRS autosampler), hyphenated with an Orbitrap Q Exactive Focus Mass Spectrometer equipped with electrospray ionization source (Thermo Fischer Scientific, Waltham, MA, USA). An Acquity UPLC BEH C18 column (30 × 2.1 mm i.d., 1.7 μm; Waters Corporation) was used (column temperature: 25 °C), the mobile phase consisted of 0.1% formic acid in water (eluent A) and a mixture of 0.1% formic acid in water and acetonitrile (20:80, v/v) (eluent B). The following gradient elution was applied at a flow rate of 0.3 mL/min: 10–60% B (0.0–3.5 min), 60–100% B (3.5–4.0 min), 100% B (4.0–4.5 min), 100–10% B (4.5–7.0 min). The injection volume was 1 μL. The ESI source was operated in the negative ionization mode, and operation parameters were optimized automatically using the built-in software. The working parameters were as follows: spray voltage 2500 V; capillary temperature 320 °C; sheath gas (N<sub>2</sub>), 47.5 °C; auxiliary gas (N<sub>2</sub>) 11.25 arbitrary units, and spare gas (N<sub>2</sub>) 2.25 arbitrary units. The resolution of the full scan was of 70000, and the scanning range was between  $m/z$  100–500 units. The most intense ions detected in full scan spectrum were selected for data-dependent MS/MS scan at a resolving power of 35000, in the range of  $m/z$  50–500. Parent ions were fragmented with normalized collision energy of 10%, 30%, and 45%.

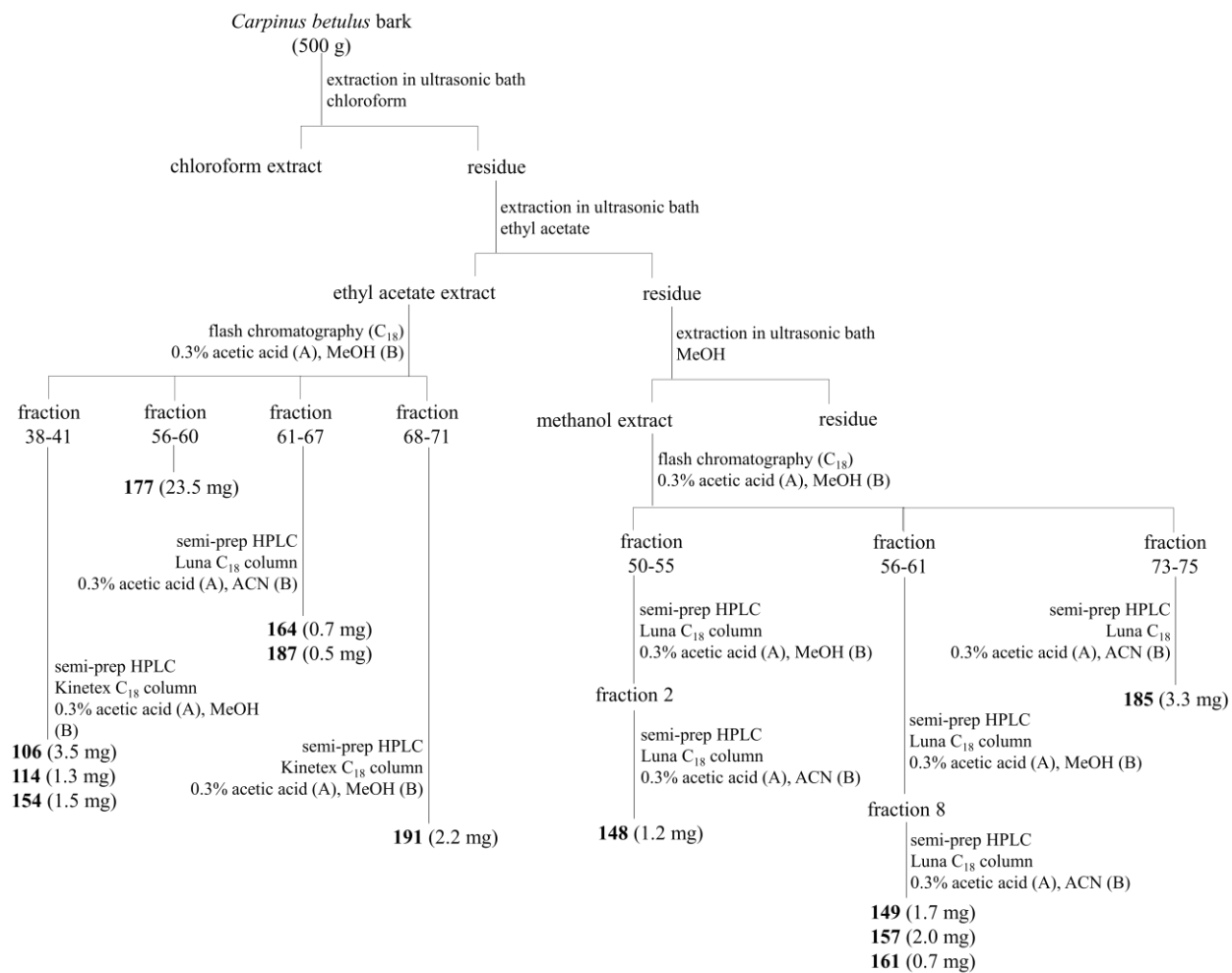


**Figure 9.** Extraction of *C. betulus* bark sample and isolation of diarylheptanoids. Abbreviations: MeOH: methanol, ACN: acetonitrile

#### ***III.4.4. UHPLC-DAD Conditions***

A validated UHPLC-DAD method was developed for the quantitative determination of the isolated diarylheptanoids (**106**, **149**, **154**, and **157**), as well as to analyze their chemical stability, and their ability for passive diffusion in the PAMPA method. The samples were analyzed by an ACQUITY UPLC H-Class PLUS System equipped with a quaternary solvent delivery pump (QSM), an auto-sampler manager (SM-FTN), a column compartment (CM), and a photodiode array (PDA) detector (Waters Corporation). An Acquity BEH C18 column (100 × 2.1 mm i.d., 1.7 μm; Waters Corporation) maintained at 30 °C was used as stationary phase. Eluent A was 0.3% acetic acid in water and eluent B was acetonitrile, the following gradient elution was applied (flow rate: 0.3 mL/min): 12.0–13.5% B (0.0–19.0 min), 13.5–75.0% B (19.0–25.5 min), 75.0–100.0% B (25.5–26.0 min), 100.0% B (26.0–28.0 min). The injection volume was 2 μL. Chromatograms were recorded at 295 nm.

### **III.5. Method Validation**

#### ***III.5.1. Preparation of Standard Solutions, Linearity, and Selectivity***

Quantitation was performed by the external standard method. Stock solutions containing 1 mg/mL of the isolated **106**, **149**, **154**, and **157** in HPLC grade methanol were prepared. For the preparation of the calibration curve, stock solutions were diluted with methanol of HPLC grade, to yield solutions with concentrations of 1, 2.5, 5, 25, 50, 100, and 250 μg/mL. Each standard solution was prepared in triplicate and injected once. Standard solutions were stored at 4 °C before injection. Linearity curves were constructed by plotting peak areas against corresponding concentrations. Slope, intercept, and correlation coefficient were determined by least squares polynomial regression analysis. Limits of detection (LOD) and quantitation (LOQ) were determined at signal-to-noise (S/N) ratios 3 and 10, respectively. The selectivity of the method was evaluated by analyzing blank samples (extracts obtained by extraction with *n*-hexane), and spiked samples (extracts fortified with standard solutions of the analytes).

#### ***III.5.2. Precision, Accuracy, and Repeatability***

Quality control samples were prepared at 5, 50, and 250 μg/mL nominal concentrations. All samples were prepared in triplicate and injected once on the same day

(intra-day precision and accuracy) or on three consecutive days (inter-day precision and accuracy). Retention time repeatability was assessed by injecting the standard solutions in six successive parallels.

### III.5.3. Recovery

Extraction recovery for giffonin X (**157**) was tested in a concentration range to match with that of the target analyte in the plant sample. 1.0–1.0 g dried *C. betulus* bark samples were spiked with 0.25 mL aliquots of a solution of **157** (1.0 mg/mL) and extracted at room temperature in an ultrasonic bath with ethyl acetate and methanol (3 × 10.0 mL, 30 min each), respectively. Samples were prepared in three parallels. Further sample preparation steps were the same as described in Section III.3.1. Recovery (*R*) was calculated as

$$R = 100 \times (C_{found} - C_{initial})/C_{added} \quad (1)$$

where  $C_{found}$  = measured concentration of the analyte of interest in the fortified sample,  $C_{initial}$  = initial concentration of the analyte of interest in the sample,  $C_{added}$  = concentration of the analyte of interest in the standard solution used.

### III.6. NMR Conditions

NMR spectra of the isolated compounds were recorded in methanol- $d_4$  on a Varian DDR 600 (600/150 MHz) instrument equipped with a 5-mm inverse-detection gradient probehead at 298 K or on a BRUKER AVANCE III HD 600 (600/150 MHz) instrument equipped with Prodigy cryo-probehead at 295 K. High temperature NMR experiments were conducted on a Bruker Avance III 400 (400/100 MHz) equipped with a PA BBO 400W1 BBF-H-D-05 Z (Billerica, MA, USA) probehead at 370 K in DMSO- $d_6$ . The pulse programs were taken from the vendor's software library (TopSpin 3.5 or VnmrJ 3.2).  $^{13}\text{C}$  and  $^1\text{H}$  chemical shifts ( $\delta$ ) are given in ppm relative to the NMR solvent or relative to tetramethylsilane, while coupling constants ( $J$ ) are given in ppm and in Hz, respectively. The complete  $^1\text{H}$  and  $^{13}\text{C}$  resonance assignments were achieved using 1D  $^1\text{H}$  NMR,  $^{13}\text{C}$  NMR, DeptQ, and homo- and heteronuclear 2D  $^1\text{H}$ - $^1\text{H}$  COSY,  $^1\text{H}$ - $^{13}\text{C}$  edHSQC,  $^1\text{H}$ - $^{13}\text{C}$  HMBC,  $^1\text{H}$ - $^1\text{H}$  NOESY, or  $^1\text{H}$ - $^1\text{H}$  ROESY, and  $^1\text{H}$ - $^1\text{H}$  TOCSY experiments.

### **III.7. Evaluation of the Antioxidant Activity**

#### **III.7.1. DPPH Assay**

Antioxidant activities of *C. betulus* extracts and the isolated compounds were determined by spectrophotometry in an *in vitro* decolorization assay using DPPH as free radical. For comparison, solutions of trolox and rutin were also studied. The following method was applied: 10 mg of DPPH was dissolved in 25.0 mL HPLC grade methanol, stock solutions were diluted with HPLC methanol just before measuring, so that the absorbance of the diluted free radical solution was approximately 0.90. Detection was carried out at 515 nm wavelength which is the characteristic absorption maximum of the DPPH• radical. Hornbeam extracts of 5 different concentrations were added to the free radical solutions (2.5 mL) in triplicate. After incubation for 6 min at room temperature in the dark, the decrease in absorbance was measured with a HITACHI U-2000 spectrophotometer (Hitachi Ltd., Tokyo, Japan). Half maximal inhibitory concentration value (IC<sub>50</sub>, µg/mL) was determined for each sample [87]. Comparison between hornbeam extracts prepared with ethyl acetate and methanol was performed by one-way analysis of variance (ANOVA), followed by Tukey's post hoc HSD test.

#### **III.7.2. DPPH-HPLC-DAD-MS Analysis**

An off-line DPPH-HPLC-DAD method was applied to compare the contribution of each compound to the total antioxidant effect against DPPH [88]. Hornbeam samples (0.5 mg/mL) were mixed with a DPPH solution (1.5 mg DPPH / 1 mL HPLC methanol, prepared right before the assays) at the ratio of 1:1 (v:v). The mixtures were incubated at room temperature for 30 min protected from light. The control samples were made by adding methanol instead of the DPPH solution to the samples in the same ratio. The DPPH-treated samples and control samples were evaluated in 3 parallels by HPLC-DAD-MS using the same method as detailed in Section III.4.1. Phenolics with antioxidant activities decompose while reacting with the DPPH• radicals, thus their AUC (area under the curve) values in HPLC-DAD-MS chromatograms decrease, as compared to control samples. We calculated the changes in AUC values using the following formula:

$$(\%) = (1 - \text{AUC}_{\text{DPPH}} / \text{AUC}_{\text{control}}) \times 100 \quad (2)$$

where  $AUC_{DPPH}$  = AUC value of an antioxidant compound in the sample containing DPPH,  $AUC_{control}$  = AUC value of an antioxidant compound in the sample not containing DPPH.

### III.8. Stability Studies

We studied the effects of different conditions, including storage time, storage temperature, and solvent, on the stability of the cyclic diarylheptanoids **106**, **149**, **154**, and **157**. Their chemical stability at different pH values was also investigated. Additionally, degradation kinetics of the compounds were examined, while degradation pathways and mechanisms were also explored.

#### III.8.1. Aqueous Stability at Different pH Values

The buffers modelling the gastric fluid (pH 1.2), the intestinal fluid (pH 6.8), and the blood and the tissues (pH 7.4) were prepared as follows. Buffer pH = 1.2: 1.0 g NaCl and 3.5 mL HCl dissolved in distilled water, final volume: 500.0 mL. Buffer pH = 6.8: 20.2 g  $Na_2HPO_4 \cdot 7H_2O$  and 3.4 g  $NaH_2PO_4 \cdot H_2O$  dissolved in distilled water, final volume: 1000.0 mL, pH adjustment with 0.5 M NaOH or 0.5 M HCl. Buffer pH = 7.4: one PBS tablet dissolved in 200.0 mL distilled water. The stock solutions of compounds **106**, **149**, **154**, **157** were prepared with DMSO at a concentration of 10.0 mM. The stock solutions were diluted 100-fold with each buffer separately to obtain the working solutions (297.0  $\mu$ L buffer + 3.0  $\mu$ L stock solution). All working solutions were filtered through Phenex-RC 15 mm, 0.2  $\mu$ m syringe filters (Gen-Lab Ltd., Budapest, Hungary). The samples were incubated for 81 h at 37 °C, aliquots were taken for analysis every 9 h in accordance with the time required to quantify the analytes of interest in one set of samples. The total incubation time of 81 h was applied to obtain data for ten measurement points. The previously described UHPLC-DAD method was used to examine the changes in compound concentrations (see Section III.4.4.).

For the determination of pH stability, the initial AUC values were compared with the data after 9 and 81 h using paired-sample *t* test; significant difference was reported at  $p < 0.05$ . The effects of the pH were analyzed through one-way analysis of variance (ANOVA) followed by Tukey's post hoc HSD test ( $p < 0.05$ ). All experiments were performed in triplicate ( $n = 3$ ).

We used the following equations to calculate the first-order reaction rate constant ( $k$ ) and the half-life ( $t_{1/2}$ ) indicating the time required to reduce the concentration of diarylheptanoids by 50% [89]:

$$\ln (c_t/c_0) = -k \times t \quad (3)$$

$$t_{1/2} = -\ln 0.5 \times k^{-1} \quad (4)$$

where  $c_t$  is the concentration of the diarylheptanoids at time  $t$ ,  $c_0$  is the initial concentration,  $k$  is the reaction rate constant,  $t$  is the treatment time.

### **III.8.2. Evaluation of Storage Stability**

The chemical stability of the isolated compounds in solutions was examined at a concentration of 50  $\mu\text{g/mL}$  in methanol and water (in the latter case using methanol as co-solvent, final composition: water-methanol 90:10,  $v/v$ ). Furthermore, the methanol and ethyl acetate extracts of *C. betulus* bark (concentration 4  $\text{mg/mL}$ ) were also studied, in order to assess the effects of the accompanying substances. The storage stability studies were performed at a neutral pH value. All solutions were filtered through Phenex-RC (15 mm, 0.2  $\mu\text{m}$ ) syringe filters (Gen-Lab Ltd.). The samples were prepared in triplicate and stored protected from light at  $22 \pm 2.0$   $^\circ\text{C}$ ,  $5 \pm 1.5$   $^\circ\text{C}$ , and  $-15 \pm 2.0$   $^\circ\text{C}$  for 23 weeks. Quantities of the analytes of interest were quantified at weeks 12 and 23 using the abovementioned UHPLC-DAD method (see Section III.4.4.).

For the determination of the stability, the initial AUC values were compared with the data of weeks 12 and 23 using paired-sample  $t$  test, significance was reported at  $p < 0.05$ . The effects of the temperature and the medium (i.e., solvent and accompanying substances) were analyzed through one-way ANOVA followed by Tukey's post hoc HSD test ( $p < 0.05$ ). To establish the kinetic parameters  $t_{1/2}$  and  $k$ , Equations (3) and (4) were applied, respectively.

### **III.9. Parallel Artificial Membrane Permeability Assay Studies**

A parallel artificial membrane permeability assay was used to determine the effective permeability ( $Pe$ ) for the *Carpinus* diarylheptanoids. Stock solutions of the isolated compounds (10 mM in DMSO) were diluted with the defined buffer (pH 7.4 for the PAMPA-BBB and pH 6.8 for the PAMPA-GI assays) to obtain the donor solutions

(composition: 297.0  $\mu\text{L}$  buffer + 3.0  $\mu\text{L}$  stock solution). Donor solutions were filtered through Phenex-RC (15 mm, 0.2  $\mu\text{m}$ ) syringe filters (Gen-Lab Ltd.).

For the PAMPA-BBB test, 5  $\mu\text{L}$  of porcine polar brain lipid extract (PBLE) solution (16.0 mg PBLE + 8.0 mg cholesterol dissolved in 600.0  $\mu\text{L}$  *n*-dodecane) was applied for each well of the 96-well polycarbonate-based filter donor plates (top plate) (Multiscreen<sup>TM</sup>-IP, MAIPN4510, pore size 0.45  $\mu\text{m}$ ; Merck). For the PAMPA-GI assay, the wells of the top plate were coated with 5  $\mu\text{L}$  of the mixture of 8.0 mg phosphatidylcholine + 4.0 mg cholesterol dissolved in 300.0  $\mu\text{L}$  *n*-dodecane. The 150.0  $\mu\text{L}$  aliquots of the filtrated donor solutions were placed on the membrane. The 96-well polytetrafluoroethylene (PTFE) acceptor plates (bottom plates) (Multiscreen Acceptor Plate, MSSACCEPTOR; Merck), were filled with 300.0  $\mu\text{L}$  buffer solution (0.01 M PBS buffer, pH 7.4). The donor plate was placed upon the acceptor plate, and both plates were incubated together at 37  $^{\circ}\text{C}$  for 4 h in a Heidolph Titramax 1000 Vibrating platform shaker (Heidolph, Schwabach, Germany).

After the incubation, the plates were separated and the compound concentrations in the donor ( $C_D(t)$ ) and acceptor ( $C_A(t)$ ) solutions were determined using the aforementioned UHPLC-DAD method (see Section III.4.4.). In advance, concentrations of the analytes of interest in the donor solutions at zero time point ( $C_D(0)$ ) were also established by UHPLC-DAD. The effective permeability and the membrane retention in the PAMPA-BBB and the PAMPA GI experiments were calculated by Equations (5) and (6), respectively [90]:

$$P_e = \frac{-2.303}{A(t - \tau_{SS})} \cdot \left( \frac{V_A \cdot V_D}{V_A + V_D} \right) \cdot \lg \left[ 1 - \left( \frac{V_A + V_D}{(1 - \text{MR}) \cdot V_D} \right) \times \left( \frac{C_A(t)}{C_D(0)} \right) \right] \quad (5)$$

$$P_e = \frac{-2.303}{A(t - \tau_{SS})} \cdot \left( \frac{1}{1 + r_a} \right) \cdot \lg \left[ -r_a + \left( \frac{1 + r_a}{1 - \text{MR}} \right) \times \left( \frac{C_D(t)}{C_D(0)} \right) \right] \quad (6)$$

where  $P_e$  is the effective permeability coefficient (cm/s),  $A$  is the filter area (0.24  $\text{cm}^2$ ),  $V_D$  and  $V_A$  are the volumes in the donor (0.15  $\text{cm}^3$ ) and acceptor phases (0.30  $\text{cm}^3$ ),  $t$  is the incubation time (s),  $\tau_{SS}$  is the time (s) to reach steady state (240 s),  $C_D(t)$  is the concentration (mol/ $\text{cm}^3$ ) of the compound in the donor phase at time  $t$ ,  $C_D(0)$  is the concentration (mol/ $\text{cm}^3$ ) of the compound in the donor phase at time 0, MR is the

estimated membrane retention factor (the estimated mole fraction of solute lost to the membrane), and  $r_a$  is the sink asymmetry ratio (gradient-pH-induced), defined as:

$$r_a = \frac{V_D}{V_A} \times \frac{P_e^{(A \rightarrow D)}}{P_e^{(D \rightarrow A)}} \quad (7)$$

$$\text{MR} = 1 - \frac{C_D(t)}{C_D(0)} - \frac{V_A}{V_D} \frac{C_A(t)}{C_D(0)} \quad (8)$$

All experiments were performed in triplicate on three consecutive days ( $n = 9$ ), caffeine was used as positive control, while rutin was used as negative control. Clog  $P$  values were calculated using ACD/ChemSketch (Freeware) 2 January 2020 (Advanced Chemistry Development, Inc., Toronto, ON, Canada).

### **III.10. Evaluation of the *In Vitro* Cytotoxic Activity of the Main Diarylheptanoids**

#### ***III.10.1. Cell Culturing and Media***

The evaluation of the *in vitro* antiproliferative activity of the compounds was carried out in cooperation with members of the HUN-REN-ELTE Research Group of Peptide Chemistry.

For the experiments, the following human cell lines were used: A2058 (melanoma, derived from metastatic site: lymph node), Hep G2 (hepatocellular carcinoma), U87 (glioblastoma), HT-29 (colorectal carcinoma), and HL-60 (acute promyelocytic leukaemia). Cell lines were gifts from Dr. József Tóvári (Department of Experimental Pharmacology, National Institute of Oncology, Budapest, Hungary).

For maintaining the U87 cell culture, Dulbecco's modified eagle medium (DMEM) supplemented with 10% fetal bovine serum (FBS), 2 mM L-glutamine, 100 µg/mL penicillin/streptomycin, 1 mM pyruvate and 1% non-essential amino acids (CM DMEM) were used. A2058, HT-29, Hep G2, and HL-60 cells were cultured in RPMI-1640 medium supplemented with 10% FBS, 2 mM L-glutamine, and a penicillin-streptomycin antibiotics mixture (50 IU/mL and 50 µg/mL, respectively). The cultures were maintained at 37 °C in a humidified atmosphere with 5% CO<sub>2</sub>.

### III.10.2. Determination of the In Vitro Antiproliferative Activity

The cells were grown to confluency and then divided into 96-well tissue culture plates (Sarstedt, Nümbrecht, Germany) with an initial cell number of 5000 cells/well. Cells were incubated at 37 °C in a 5% CO<sub>2</sub> humidified atmosphere overnight. Before the assay, 50 µL of the supernatant was removed and replaced with a 50 µL serum-free medium (SFM). The stock solutions of the compounds (c = 20 mM) were serially diluted with SFM and added to the cells in 100 µL volume. The final concentration of each compound in the cells was 0.16 µM, 0.8 µM, 4 µM, 20 µM, and 100 µM (each concentration has four parallels). The cells were treated for 24 h with the compounds, while negative control cells (no compound control) were treated with SFM only (incubated at 37 °C). As a positive control, we employed daunomycin (DAU) [91, 92] and etoposide [93, 94] as FDA-approved clinically used drugs as well as compound Sal (5-chloro-2-hydroxy-N-[4-(trifluoromethyl)phenyl]benzamide) as a cytostatic drug candidate [95]. After 24 h of incubation, cells were washed 3 times with SFM, and then the cells were further cultured in 10% FBS-containing complete medium. After three days, a 22 µL Alamar Blue (resazurin sodium salt, Merck) solution (0.15 mg/mL in PBS) was added to each well, and after 4 h of incubation, the fluorescence was measured at  $\lambda_{\text{Ex}} = 530/30$  and  $\lambda_{\text{Em}} = 610/10$  nm using a Synergy H4 multi-mode microplate reader (BioTek, Bad Friedrichshall, Germany). The percentage of cytostasis was calculated with the following equation:

$$\text{Cytostatic effect (\%)} = [1 - (\text{OD}_{\text{treated}}/\text{OD}_{\text{control}})] \times 100 \quad (9)$$

where the values OD<sub>treated</sub> and OD<sub>control</sub> correspond to the optical densities of the treated and the control wells, respectively.

Cytostasis (%) was plotted as a function of concentration, fitted to a dose–response curve and the 50% inhibitory concentration value was determined from these curves. Data were evaluated with Excel (version: 365; Microsoft, Redmond, WA, USA) and the curves were defined using Microcal OriginPro (version: 2018; OriginLab, Northampton, MA, USA) software. In each case, two independent experiments were carried out with four parallel measurements, and the mean IC<sub>50</sub> values together with ± SD were represented. The Excel (version: 365) (Microsoft) and Microcal OriginPro (version: 2018) (OriginLab) softwares were used for data evaluation.

## IV. Results

### IV.1. Qualitative Analyses of *Carpinus betulus* Polyphenols by HPLC-DAD-MS/MS

High-performance liquid chromatography coupled with diode-array detection and electrospray ionization tandem mass spectrometry (HPLC-DAD-ESI-MS/MS) in negative ionization mode was used to evaluate the phenolic profile of the extracts. In the ethyl acetate and methanol extracts of hornbeam bark, leaf, male, and female catkin samples, 194 compounds were tentatively characterized by comparing their retention times, UV spectra, and mass spectrometric fragmentation patterns with data from the literature. In the MS/MS experiments, different collision energy values were used in order to get mass spectra with various fragmentation degrees from the precursor ion, thus, obtain as much structural information as it was possible. UV chromatograms of the extracts detected at 290 nm are shown in Fig. 10 and Fig. S1-S7. Occurrence of the detected compounds, their chromatographic, and mass spectrometric properties are listed in Table 3.

Among the detected compounds, six main secondary metabolite groups could be distinguished such as gallotannins and gallic acid derivatives, ellagitannins and ellagic acid derivatives, hydroxybenzoic acid derivatives, hydroxycinnamic acid derivatives, flavonoids, and condensed tannins. Some compounds (e.g., **106**, **149**, **154**) could not be identified using mass spectrometry, therefore, after their isolation NMR techniques were applied for the structural elucidation.

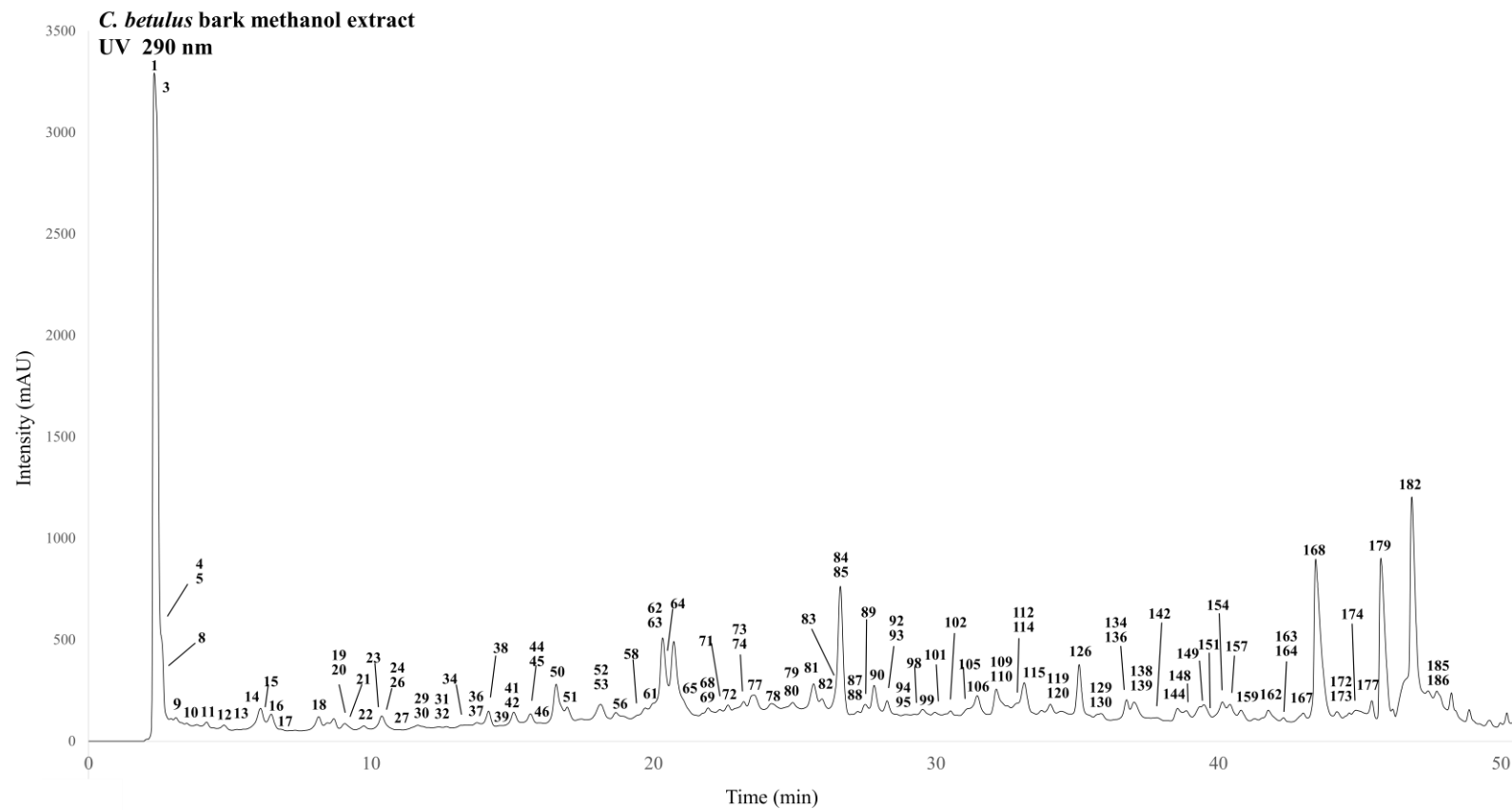


**Figure 10.** UV chromatogram of hornbeam bark extract prepared with methanol. Detection wavelength: 290 nm. Compound numbers refer to Table 3. For chromatographic conditions see Section III.4.1.

**Table 3.** HPLC-DAD-MS/MS data and tentative characterization of constituents from *Carpinus betulus* bark, leaf, female, and male catkin extracts

No.	Comp. type <sup>b</sup>	t <sub>R</sub> (min)	λ <sub>max</sub> (nm)	[M-H] <sup>-</sup> (m/z)	Fragment ions (m/z)	Tentative structural characterization	Presence of compounds in the extracts <sup>c</sup>								Ref.
							B E	B M	L E	L M	F E	F M	M E	M M	
1	C	2.3	305	341	377 [M+Cl] <sup>-</sup> , 215, 179, 161, 135	caffeoyl hexose	x	x	x	x	x	x	x	x	[96]
2	C	2.3	305	371	191, 173, 135	3- <i>O</i> -hydroxydihydrocaffeoyl quinic acid			x	x					[97]
3	C	2.3	305	533	371, 191	5- <i>O</i> -hydroxydihydrocaffeoyl-hexosyl quinic acid	x	x	x		x		x		[97]
4	G	2.4	275, 305sh	331	271, 241, 211, 169, 153, 151, 125, 123	monogalloyl hexose	x	x	x	x	x	x	x	x	[98]
5	E	2.4	275, 305sh	783	507, 439, 301, 275	bis-HHDP hexose		x							[99]
6	E	2.6	273	633	301	galloyl-HHDP hexose						x		x	[100]
7	G	2.6	273	325	651 [2M-H] <sup>-</sup> , 169, 137, 125, 111	galloylshikimic acid			x				x		[101]
8	G	2.7	273	343	687 [2M-H] <sup>-</sup> , 191, 169, 125	3- <i>O</i> -galloylquinic acid	x	x	x		x	x	x		[102]
9	G	3.0	270	331	169, 153, 125	monogalloyl hexose	x				x		x		[98]
10	E	3.2	275	481	301, 275	HHDP hexose	x				x				[103]
11	G	4.2	277	331	663 [2M-H] <sup>-</sup> , 311, 271, 241, 211, 183, 169, 125	monogalloyl hexose	x	x	x		x	x	x		[98]
12	E	4.9	270, 305sh	783	481, 437, 419, 341, 301, 300, 275	bis-HHDP hexose		x							[99]
13	G	5.5	270	331	271, 169, 125	monogalloyl hexose		x		x		x		x	[98]
14	G	6.1	268	169	125	gallic acid	x	x	x	x	x	x	x	x	[104]
15	E	6.1	268	783	481, 301, 275	bis-HHDP hexose		x							[99]

No.	Comp. type <sup>b</sup>	t <sub>R</sub> (min)	λ <sub>max</sub> (nm)	[M-H] <sup>-</sup> (m/z)	Fragment ions (m/z)	Tentative structural characterization	Presence of compounds in the extracts <sup>c</sup>								Ref.
							B E	B M	L E	L M	F E	F M	M E	M M	
16	G	6.5	272	343	687 [2M-H] <sup>-</sup> , 191, 169	5-O-galloylquinic acid	x					x	x	[102]	
17	G	6.8	275	331	169	monogalloyl hexose	x					x	x	[98]	
18	G	8.1	275	343	687 [2M-H] <sup>-</sup> , 191, 173, 169, 125	4-O-galloylquinic acid	x	x	x			x	x	x	[102]
19	G	9.0	270	483	331, 313, 271, 169	digalloyl hexose	x		x			x	x	x	[105]
20	E	9.1	270	633	481, 301, 275, 169	galloyl-HHDP hexose	x					x	x	[100]	
21	G	9.3	270	345	183, 169, 124	methylgalloyl hexose	x					x	x	[106]	
22	B	9.7	273	315	152, 108	dihydroxybenzoic acid hexoside	x							[107]	
23	E	10.0	260, 295sh	633	301	galloyl-HHDP hexose	x					x	x	[100]	
24	E	10.4	260, 295sh	783	481, 301, 275	bis-HHDP hexose	x					x	x	[99]	
25	E	10.4	258, 297	469	425, 365, 263, 219, 209, 193, 163	valoneic acid dilactone / sanguisorbic acid dilactone isomer						x		[108]	
26	G	10.4	260, 295	331	663 [2M-H] <sup>-</sup> , 169, 153, 125	monogalloyl hexose	x	x	x			x	x	x	[98]
27	G	11.4	263, 298	325	651 [2M-H] <sup>-</sup> , 169, 137, 125, 93	galloylshikimic acid	x	x	x	x	x	x	x	x	[101]
28	B	11.6	260, 294	153	123, 109, 107	dihydroxybenzoic acid			x			x	x	[99]	
29	G	11.6	270	483	313, 303, 271, 241, 211, 183, 169, 125	digalloyl hexose	x		x			x	x	x	[105]
30	E	11.7	260, 290sh	633	481, 301, 275	galloyl-HHDP hexose	x					x	x	[100]	
31	B	11.9	272	329	167, 152, 123, 108	hydroxy-methoxybenzoic acid hexoside	x							[99]	
32	G	12.0	260, 294	325	651 [2M-H] <sup>-</sup> , 169, 125	galloylshikimic acid	x	x	x			x	x	x	[101]
33	G	12.1	277	483	331, 313, 271, 211, 169	digalloyl hexose				x		x	x	[105]	
34	G	13.2	270	325	651 [2M-H] <sup>-</sup> , 169, 125	galloylshikimic acid	x	x	x	x	x	x	x	x	[101]

No.	Comp. type <sup>b</sup>	t <sub>R</sub> (min)	λ <sub>max</sub> (nm)	[M-H] <sup>-</sup> (m/z)	Fragment ions (m/z)	Tentative structural characterization	Presence of compounds in the extracts <sup>c</sup>								Ref.
							B E	B M	L E	L M	F E	F M	M E	M M	
35	T	13.6	275	577	407, 289, 245, 161, 125	procyanidin dimer type B						x	x		[109]
36	G	13.7	270, 300sh	345	183, 124	methylgalloyl hexose	x							x	[106]
37	E	13.8	268, 300sh	785	483, 392, 301, 275	digalloyl-HHDP hexose	x		x		x			x	[103]
38	E	14.2	269	633	331, 301, 275, 169	galloyl-HHDP hexose	x		x		x			x	[100]
39	B	14.5	271	359	197, 182, 167, 153, 138, 123	hydroxy-dimethoxybenzoic hexoside	x								[103]
40	E	14.5	272	935	169	galloyl-bis-HHDP hexose								x	[99]
41	G	14.9	272	635	483, 465, 313, 169	trigalloyl hexose	x					x		x	[99]
42	B	15.0	272	447	315, 207, 163, 152, 109	dihydroxybenzoic acid hexosyl-pentoside	x								[110]
43	E	15.3	276	633	463, 301, 275, 249, 169	galloyl-HHDP hexose				x		x			[100]
44	B	15.8	263, 305sh	285	152, 108	dihydroxybenzoic acid pentoside	x					x			[3]
45	B	15.8	265, 310	359	719 [2M-H] <sup>-</sup> , 197, 182, 167, 153, 138	hydroxy-dimethoxybenzoic hexoside	x	x							[103]
46	G	16.2	230, 270	345	183, 124	methylgalloyl hexose	x	x	x		x	x	x	x	[106]
47	G	16.4	276	483	271, 169	digalloyl hexose								x	[105]
48	T	16.5	245, 278	289	245, 205, 203, 161, 151, 123, 109	catechin/epicatechin								x	[111]
49	C	16.6	275	325	163, 119	coumaroyl hexose			x					x	[112]
50	E	16.7	273	935	467, 331, 313, 301, 275, 169, 125	galloyl-bis-HHDP hexose	x					x			[99]
51	E	17.0	273	633	463, 301, 275	galloyl-HHDP hexose	x					x		x	[100]
52	G	18.1	275	635	483, 465, 313, 169	trigalloyl hexose	x					x	x	x	[99]

No.	Comp. type <sup>b</sup>	t <sub>R</sub> (min)	λ <sub>max</sub> (nm)	[M-H] <sup>-</sup> (m/z)	Fragment ions (m/z)	Tentative structural characterization	Presence of compounds in the extracts <sup>c</sup>								Ref.
							B E	B M	L E	L M	F E	F M	M E	M M	
53	G	18.2	240, 278	183	168, 125, 124	methylgallic acid	x	x	x	x	x	x	x	x	[113]
54	T	18.4	240, 278	289	245, 221, 205, 203, 175, 187, 175, 161, 149, 125	catechin/epicatechin	x				x	x	x		[111]
55	G	18.7	278, 330	683	351, 231, 169	not identified gallotannin				x	x		x		[99]
56	U	19.0	273	383	767 [2M-H] <sup>-</sup> , 351, 263, 251, 231, 219, 203, 187, 175, 163	not identified	x		x		x		x		-
57	G	19.2	277	925	462, 331, 271, 211, 169	not identified gallotannin							x	x	[99]
58	G	19.7	272	495	343, 325, 191, 173, 169	3,4-di-O-galloylquinic acid	x		x		x	x	x		[102]
59	G	19.8	280	683	351, 331, 263, 251, 231, 219, 203, 169	not identified gallotannin				x	x		x		[99]
60	G	19.8	280	635	483, 465, 313, 169	trigalloyl hexose					x	x	x		[99]
61	E	20.2	271	785	633, 483, 301, 275	digalloyl-HHDP hexose	x		x		x		x		[103]
62	U	20.4	271	383	351, 251, 231, 203, 187, 177	not identified	x		x		x		x		-
63	U	20.4	271	351	291, 251, 231, 203, 175	not identified	x		x		x		x		-
64	G	20.5	271	483	967 [2M-H] <sup>-</sup> , 331, 313, 271, 241, 211, 169, 125	digalloyl hexose	x		x		x	x	x		[105]
65	C	21.1	301sh, 326	353	707 [2M-H] <sup>-</sup> , 191, 179, 161	<i>trans</i> -5-O-caffeoylquinic acid	x	x	x		x	x	x		[97]
66	E	21.2	277, 310sh	935	467, 301, 275, 196, 125	galloyl-bis-HHDP hexose								x	[99]
67	G	21.8	278	477	325, 183, 169	digalloylshikimic acid							x	x	[103]
68	G	22.0	280	453	327, 313, 285, 273, 247, 225, 183, 169, 151, 125	hydroxy-methoxyphenyl-galloyl hexose	x	x			x	x	x	x	[103]
69	G	22.2	276	483	271, 169, 967	digalloyl hexose	x		x		x		x		[105]
70	G	22.5	277, 305	683	351, 251, 231, 169	not identified gallotannin				x	x		x		[99]

No.	Comp. type <sup>b</sup>	t <sub>R</sub> (min)	λ <sub>max</sub> (nm)	[M-H] <sup>-</sup> (m/z)	Fragment ions (m/z)	Tentative structural characterization	Presence of compounds in the extracts <sup>c</sup>								Ref.
							B E	B M	L E	L M	F E	F M	M E	M M	
71	E	22.7	275	481	437, 313, 169, 151, 125, 123	HHDP hexose	x					x	x	x	[103]
72	G	23.0	280	453	327, 313, 291, 273, 247, 211, 169, 151, 139, 125	hydroxy-methoxyphenyl-galloyl hexose	x					x	x		[103]
73	G	23.2	276	477	325, 169	digalloylshikimic acid	x						x		[103]
74	D	23.2	275	507	327	linear diarylheptanoid hexoside	x	x							[24]
75	G	23.2	275	635	483, 465, 313, 169	trigalloyl hexose				x	x	x	x		[99]
76	E	23.3	278	951	933, 613, 463, 461, 445, 301	galloyl-HHDP-DHHDP hexose				x	x				[99]
77	E	23.5	272	935	-	galloyl-bis-HHDP hexose	x					x	x		[99]
78	G	24.3	275	483	439, 331, 313, 285, 255, 169, 125	digalloyl hexose	x								[105]
79	G	25.4	276, 360	291	247, 219, 191, 175	brevifolin carboxylate	x		x		x	x	x		[99]
80	G	25.4	276	247	219, 191, 173, 145	brevifolin	x		x		x	x	x		[114]
81	E	25.7	276	935	467, 423, 313, 169, 125	galloyl-bis-HHDP hexose	x								[99]
82	G	26.1	276	635	483, 465, 313, 221, 169, 125	trigalloyl hexose	x	x	x		x	x	x		[99]
83	C	26.5	300	353	707 [2M-H] <sup>-</sup> , 191, 161	<i>cis</i> -5- <i>O</i> -caffeoylquinic acid	x	x	x		x	x	x		[97]
84	E	26.8	276	633	463, 301, 275, 169	galloyl-HHDP hexose	x	x		x	x	x			[100]
85	G	26.8	275	635	465, 313, 169	trigalloyl hexose	x		x		x	x	x		[99]
86	E	27.1	275	951	933, 613, 463, 461, 445, 301	galloyl-HHDP-DHHDP hexose				x	x				[99]
87	G	27.3	277	477	325, 307, 289, 263, 219, 169, 151, 137, 125	digalloylshikimic acid	x	x	x		x	x	x		[103]
88	G	27.3	275	635	483, 465, 423, 313, 211, 193, 169	trigalloyl hexose	x				x				[99]
89	E	27.6	276	937	465, 301	trigalloyl-HHDP hexose	x		x		x		x		[103]

No.	Comp. type <sup>b</sup>	t <sub>R</sub> (min)	λ <sub>max</sub> (nm)	[M-H] <sup>-</sup> (m/z)	Fragment ions (m/z)	Tentative structural characterization	Presence of compounds in the extracts <sup>c</sup>								Ref.	
							B E	B M	L E	L M	F E	F M	M E	M M		
90	E	27.6	276	935	467, 449, 423, 315, 313, 169, 152, 125	galloyl-bis-HHDP hexose	x									[99]
91	C	27.7	292, 324sh	337	191, 163, 119	<i>trans</i> -5- <i>p</i> -O-coumaroylquinic acid			x	x		x				[97]
92	E	28.3	260, 280	481	437, 313, 241, 169, 151, 125	HHDP hexose	x	x								[103]
93	E	28.3	260, 280	857	825, 781, 589, 537, 505, 437, 419, 301, 275	not identified ellagitannin		x				x		x		[99]
94	D	28.8	275	359	329, 299, 269, 257, 240, 239, 227	cyclic diarylheptanoid	x	x								-
95	G	29.0	275	497	465, 345, 313, 183, 169	galloyl-methylgalloyl hexose	x				x	x	x	x	x	[103]
96	G	29.1	282	787	617, 449, 417	tetragalloyl hexose			x						x	[99]
97	G	29.2	282	197	169, 124	ethylgallic acid			x		x		x			[115]
98	C	29.3	275	335	179, 161, 135	caffeoylshikimic acid	x					x		x		[3]
99	G	29.6	282	477	307, 289, 263, 219, 169, 151, 137, 125	digalloylshikimic acid	x		x		x	x	x	x		[103]
100	C	30.0	294, 325	335	179, 161, 135	caffeoylshikimic acid			x	x	x	x	x	x	x	[3]
101	G	30.1	274	605	453, 393, 363, 333, 291, 273, 247	hydroxy-methoxyphenyl-digalloyl hexose	x			x		x		x		[103]
102	G	30.6	275	635	483, 465, 423, 313, 211, 169	trigalloyl hexose		x		x		x	x	x		[99]
103	D	30.7	252, 282	359	299, 269, 257, 240, 227	cyclic diarylheptanoid	x									-
104	E	31.4	277	965	933, 301, 275	not identified ellagitannin					x		x			[99]
105	G	31.6	279	787	635, 617, 465, 447, 443, 403, 313, 295, 277, 221, 169, 125	tetragalloyl hexose		x	x	x		x	x	x		[99]
106	D	31.7	245, 294	343	283, 269, 257, 239, 225, 211, 197, 193, 183	carpinontriol A	x	x							x	NMR

No.	Comp. type <sup>b</sup>	t <sub>R</sub> (min)	λ <sub>max</sub> (nm)	[M-H] <sup>-</sup> (m/z)	Fragment ions (m/z)	Tentative structural characterization	Presence of compounds in the extracts <sup>c</sup>								Ref.	
							B E	B M	L E	L M	F E	F M	M E	M M		
107	T	31.7	278	441	289, 245, 205, 203, 169, 125	catechin gallate/epicatechin gallate								x	[116]	
108	D	32.1	249, 286	341	313, 269, 267, 240, 239, 211	cyclic diarylheptanoid	x								-	
109	E	32.2	278	937	468, 445, 419, 370, 301, 275, 249, 169, 125	trigalloyl-HHDP hexose		x					x	x	x	[103]
110	G	32.3	278	787	635, 617, 465, 447, 313	tetragalloyl hexose		x		x			x	x	x	[99]
111	C	32.5	285, 310sh	337	191	<i>cis-5-p-O-coumaroylquinic acid</i>				x	x		x		[97]	
112	E	32.5	276	965	933, 301, 275	not identified ellagitannin		x		x			x	x	[99]	
113	G	32.5	280	387	183, 124	methylgallic acid derivative							x		[103]	
114	D	32.6	254, 279	359	719 [2M-H] <sup>-</sup> , 329, 299, 269, 257, 239, 211, 197, 193	giffonin U	x	x							NMR	
115	T	33.2	276, 355	305	611 [2M-H] <sup>-</sup> , 273, 245, 229, 217, 201, 189, 173, 161, 145	galocatechin/epigallocatechin	x	x	x	x	x	x	x	x	[99]	
116	C	33.7	295, 325	367	191	<i>trans-5-O-feruloylquinic acid</i>				x	x	x		x	[97]	
117	E	33.8	265, 290sh, 355	625	300, 271, 255, 243, 179, 151, 133	HHDP dihexose								x	x	[99]
118	G	34.1	280	939	469, 355, 295, 275, 241, 169, 125	pentagalloyl hexose							x		[99]	
119	D	34.1	252, 281	359	329, 299, 269, 240, 239, 211	cyclic diarylheptanoid	x	x							-	
120	G	34.2	280	787	617, 465, 449, 417, 169	tetragalloyl hexose		x	x	x			x	x	x	[99]
121	E	34.3	270, 285sh, 360	625	463, 445, 300, 179	HHDP dihexose								x	x	[99]
122	C	34.7	272, 290sh	335	179, 161, 135	caffeoylshikimic acid				x	x			x	x	[3]
123	G	34.8	278	939	469	pentagalloyl hexose								x	x	[99]
124	D	34.9	252, 280	343	269, 239, 211, 193	cyclic diarylheptanoid	x								-	

No.	Comp. type <sup>b</sup>	t <sub>R</sub> (min)	λ <sub>max</sub> (nm)	[M-H] <sup>-</sup> (m/z)	Fragment ions (m/z)	Tentative structural characterization	Presence of compounds in the extracts <sup>c</sup>								Ref.
							B E	B M	L E	L M	F E	F M	M E	M M	
125	E	35.0	278, 360sh	625	300	HHDP dihexose							x	x	[99]
126	E	35.2	280	857	825, 687, 655, 589, 463, 437, 419, 301, 275, 169	not identified ellagitannin	x		x		x			x	[99]
127	E	35.4	278	937	-	trigalloyl-HHDP hexose								x	[103]
128	G	35.5	277	939	-	pentagalloyl hexose							x	x	[99]
129	E	35.8	279	937	767, 468, 465, 301, 169, 125	trigalloyl-HHDP hexose	x		x		x	x	x		[103]
130	G	36.0	276	629	477, 289, 245, 201, 169, 137	trigalloylshikimic acid	x		x		x			x	[103]
131	E	36.1	284, 340sh	463	301, 300, 169	ellagic acid hexoside			x	x					[117]
132	C	36.3	284, 320sh	367	191	<i>cis</i> -5- <i>O</i> -feruloylquinic acid			x	x			x		[97]
133	T	36.7	278	575	423, 331, 271, 243, 211	procyanidin dimer type A	x								[99]
134	E	36.8	278	785	633, 301, 275	digalloyl-HHDP hexose	x								[103]
135	F	36.9	280, 365	479	317, 316, 287, 271, 179, 151	myricetin-3- <i>O</i> -hexoside			x	x	x	x	x	x	[118]
136	D	36.9	280	343	325, 269, 240, 239, 211	cyclic diarylheptanoid	x	x							-
137	E	37.1	270	997	633, 363, 301, 275	galloyl-HHDP hexose derivative	x		x		x			x	[99]
138	G	37.2	280	939	787, 769, 601, 465, 447, 431, 313, 301, 295, 277, 169, 125	pentagalloyl hexose	x	x	x		x	x	x		[99]
139	D	37.2	254, 283	505	325, 307, 239, 199, 227, 251, 211, 119, 113	linear diarylheptanoid hexoside	x	x							-
140	D	37.2	254, 283	329	311, 255, 211, 193	cyclic diarylheptanoid	x								-
141	E	37.5	278	951	933, 613, 301	galloyl-HHDP-DHHDP hexose							x		[99]
142	T	37.6	276	575	539, 423, 331, 271, 243	procyanidin dimer type A		x							[99]
143	D	38.3	250, 281	475	311, 211, 161,	cyclic diarylheptanoid	x	x							-

No.	Comp. type <sup>b</sup>	t <sub>R</sub> (min)	λ <sub>max</sub> (nm)	[M-H] <sup>-</sup> (m/z)	Fragment ions (m/z)	Tentative structural characterization	Presence of compounds in the extracts <sup>c</sup>								Ref.
							B E	B M	L E	L M	F E	F M	M E	M M	
144	E	38.6	278	937	767, 468, 465, 301, 300, 275, 249, 169, 125	trigalloyl-HHDP hexose	x	x	x		x	x	x	[103]	
145	D	38.9	280	477	327, 205, 121	oregonin	x	x			x	x		[24]	
146	E	39.0	280	997	961, 633, 363, 301, 275	galloyl-HHDP hexose derivative	x		x		x		x	[99]	
147	F	39.1	281, 325	609	429, 285, 284, 271, 257, 179	kaempferol derivative						x	x	[119]	
148	L	39.1	242, 283	505	527 [M+Na-2H] <sup>-</sup> , 359, 341, 326, 314, 313, 311, 299, 187	aviculin	x	x				x	x	NMR	
149	D	39.5	250, 297	343	687 [2M-H] <sup>-</sup> , 284, 283, 270, 269, 239, 211, 197, 193	carpinontriol B	x	x				x	x	NMR	
150	E	39.5	274	997	961, 633, 363, 301, 275	galloyl-HHDP hexose derivative					x		x	[99]	
151	E	39.7	250, 287sh, 366	477	955 [2M-H] <sup>-</sup> , 315, 300	methylellagic acid hexoside	x	x			x		x	[113]	
152	T	39.7	290	441	289, 245, 205, 169, 125	catechin gallate/epicatechin gallate							x	[116]	
153	F	39.9	264, 351	449	317, 316, 179	myricetin-3- <i>O</i> -pentoside				x	x	x	x	[120]	
154	D	40.2	245, 295	325	307, 269, 239, 211, 209, 197, 193, 183, 113	3,12,17-trihydroxytricyclo <sup>2,6</sup> [12.3.1.1]-nonadeca-1(18),2(19),3,5,14,16-hexaene-8,11-dione	x	x						NMR	
155	F	40.3	262, 352	463	927 [2M-H] <sup>-</sup> , 317, 316, 287, 271, 259, 242, 214, 179, 151	myricetin-3- <i>O</i> -deoxyhexoside	x	x	x	x	x	x	x	[121]	
156	F	40.4	266, 355	449	317, 316, 289, 271, 151	myricetin-3- <i>O</i> -pentoside				x	x	x	x	[120]	
157	D	40.6	248, 298	327	300, 269, 268, 267, 241, 239, 211, 197, 193, 183	giffonin X	x	x						NMR	
158	F	40.6	247, 359	541	461, 446, 328, 314	trihydroxy-dimethoxyflavone- <i>O</i> -pentoside- <i>O</i> -sulfate		x						[122]	

No.	Comp. type <sup>b</sup>	t <sub>R</sub> (min)	λ <sub>max</sub> (nm)	[M-H] <sup>-</sup> (m/z)	Fragment ions (m/z)	Tentative structural characterization	Presence of compounds in the extracts <sup>c</sup>								Ref.		
							B E	B M	L E	L M	F E	F M	M E	M M			
159	F	41.0	270, 352	491	476, 359, 328, 313, 298, 285	trihydroxy-dimethoxyflavone- <i>O</i> -hexoside	x	x									[123]
160	F	41.5	266, 349	447	895 [2M-H] <sup>-</sup> , 285, 284	kaempferol-3- <i>O</i> -hexoside		x	x	x	x	x	x	x			[124]
161	D	41.6	285	327	283, 269, 267, 253, 239, 225, 211, 197 193	casuarinondiol	x	x									NMR
162	E	41.9	255, 300sh, 360	433	301, 300	ellagic acid pentoside		x				x	x	x			[113]
163	F	42.1	263, 352	463	927 [2M-H] <sup>-</sup> , 301, 300, 271, 255, 179, 151	quercetin-3- <i>O</i> -hexoside	x	x	x	x	x	x	x	x			[119]
164	D	42.2	270	313	254, 251, 241, 239, 227, 211, 210, 207, 189, 163, 149	5-hydroxy-1,7-bis-(4'-hydroxyphenyl)-3-heptanone	x	x									NMR
165	F	42.6	270, 353	609	301, 300	quercetin-3- <i>O</i> -hexosyl-deoxyhexoside	x	x	x	x	x	x	x	x			[118]
166	G	42.9	277	507	446, 396, 344, 183, 115	caffeoyl-methylgalloyl hexose								x	x		[113]
167	G	43.1	268	555	345, 183	methylgallic acid derivative		x									[113]
168	E	43.7	254, 304sh, 368	301	300, 284, 269, 257, 245, 229, 201, 185, 173, 157, 145, 129	ellagic acid	x	x	x	x	x	x	x	x	x		[99]
169	F	44.0	255, 360	433	867 [2M-H] <sup>-</sup> , 301, 300, 271, 255, 151	quercetin-3- <i>O</i> -pentoside			x		x	x	x	x			[125]
170	T	44.2	270	591	523, 301, 289, 245, 109	catechin/epicatechin ellagic acid ester								x			[99]
171	D	44.7	252, 285	323	267, 237, 211, 193, 111	cyclic diarylheptanoid	x										-
172	E	44.7	260, 350	967	935, 917, 767, 633, 273	galloyl-HHDP hexose derivative		x		x		x	x	x			[99]
173	D	44.8	249, 288	341	283, 267, 239, 237, 211, 197, 129	cyclic diarylheptanoid	x	x									-
174	F	45.0	268, 360	409	329, 314, 299, 271	trihydroxy-dimethoxyflavone- <i>O</i> -sulfate	x					x		x			[122]

No.	Comp. type <sup>b</sup>	t <sub>R</sub> (min)	λ <sub>max</sub> (nm)	[M-H] <sup>-</sup> (m/z)	Fragment ions (m/z)	Tentative structural characterization	Presence of compounds in the extracts <sup>c</sup>								Ref.	
							B E	B M	L E	L M	F E	F M	M E	M M		
175	F	45.1	267, 338	431	863 [2M-H] <sup>-</sup> , 341, 323, 311, 269, 268	apigenin- <i>C</i> -hexoside			x	x	x					[126]
176	F	45.2	267, 338	433	867 [2M-H] <sup>-</sup> , 301, 300, 271, 255, 179, 151, 119	quercetin-3- <i>O</i> -pentoside	x		x		x	x	x	x		[125]
177	F	45.6	256, 351	447	895 [2M-H] <sup>-</sup> , 301, 300, 271, 255, 179, 151	quercetin-3- <i>O</i> -rhamnoside	x	x	x	x	x	x	x	x		NMR
178	G	45.9	251, 300sh	491	345, 183	coumaroyl-methylgalloyl hexose							x	x		[113]
179	F	46.0	250, 365	447	315, 300, 283, 271	tetrahydroxy-methoxyflavone- <i>O</i> -pentoside	x	x				x	x	x		[123]
180	G	46.3	265, 305sh	521	345, 183	feruloyl-methylgalloyl hexose							x	x		[113]
181	F	46.4	260, 350	491	329, 328, 313	trihydroxy-dimethoxyflavone- <i>O</i> -hexoside							x	x		[123]
182	F	46.8	265, 365	343	423 [M+HSO <sub>4</sub> ] <sup>-</sup> , 328, 313, 298, 285	dihydroxy-trimethoxyflavone			x							[127]
183	F	47.0	248, 362	461	446, 328, 313, 298	trihydroxy-dimethoxyflavone- <i>O</i> -pentoside	x	x								[123]
184	E	47.1	270, 365	461	315, 300	methyllellagic acid deoxyhexoside	x	x	x	x	x	x	x	x		[113]
185	F	47.4	267, 317sh, 345	577	431, 285, 169	kaempferol-3- <i>O</i> -(4''- <i>E</i> - <i>p</i> -coumaroyl)-rhamnopyranoside			x		x					NMR
186	F	47.4	267, 317sh, 345	577	431, 285, 169	kaempferol-3- <i>O</i> -(4''- <i>Z</i> - <i>p</i> -coumaroyl)-rhamnopyranoside			x		x					[128]
187	D	47.5	250, 296	311	286, 267, 253, 241, 211, 197	3,11,17-trihydroxytricyclo[12.3.1.1 <sup>2,6</sup> ]-nonadeca-1(18),2(19),3,5,14,16-hexaen-8-one	x									NMR
188	F	47.5	248, 362	343	423 [M+HSO <sub>4</sub> ] <sup>-</sup> , 328, 313, 298, 285	dihydroxy-trimethoxy flavone			x							[127]

No.	Comp. type <sup>b</sup>	t <sub>R</sub> (min)	λ <sub>max</sub> (nm)	[M-H] <sup>-</sup> (m/z)	Fragment ions (m/z)	Tentative structural characterization	Presence of compounds in the extracts <sup>c</sup>								Ref.
							B E	B M	L E	L M	F E	F M	M E	M M	
189	E	48.0	250, 370	315	300	methylelagic acid	x					x	x	x	[113]
190	F	48.5	244, 363	343	423 [M+HSO <sub>4</sub> ] <sup>-</sup> , 328, 313, 285	dihydroxy-trimethoxy flavone						x		x	[127]
191	F	48.5	264, 344	431	285, 284, 269, 255, 227, 151	kaempferol-3- <i>O</i> -rhamnoside	x		x	x	x	x	x	x	NMR
192	F	49.3	256, 370	301	255, 239, 229, 201, 179, 151, 149, 107	quercetin			x	x	x	x	x	x	[129]
193	F	50.6	265, 365	285	201, 175, 151, 133, 107	kaempferol	x		x	x	x		x	x	[130]
194	F	50.8	248, 375	329	314, 299, 271	dihydroxy-dimethoxy flavone	x								[127]

<sup>a</sup> Compound numbers and retention times (t<sub>R</sub>) refer to UV chromatograms shown in Figures 10 and S1–S7. <sup>b</sup> Abbreviations types of phenolic compounds: G: gallotannins and gallic acid derivatives, E: ellagitannins and ellagic acid derivatives, B: hydroxybenzoic acid derivatives, C: hydroxycinnamic acid derivatives, F: flavonoids, T: condensed tannins, L: lignans, D: diarylheptanoids, U: undefined. <sup>c</sup> Abbreviations extracts: BE: bark ethyl acetate extract, BM: bark methanol extract, LE: leaf ethyl acetate extract, LM: leaf methanol extract, FE: female catkin ethyl acetate extract, FM: female catkin methanol extract, ME: male catkin ethyl acetate extract, MM: male catkin methanol extract. Abbreviations compounds: HHDP: hexahydroxydiphenyl, DHHDP: dehydrohexahydroxydiphenyl.

## IV.2. Structural Elucidation of the Isolated Compounds

### IV.2.1. Structural Elucidation of the Diarylheptanoid Compounds

For the determination of the exact structures, UHPLC-Orbitrap® (Table 4) and NMR measurements were applied.

**Table 4.** HR-MS data of the isolated diarylheptanoid compounds

No.	[M-H] <sup>-</sup> ( <i>m/z</i> ) experimental	Error (ppm)	Fragment ions ( <i>m/z</i> )	Molecular formula	Structure
<b>106</b>	343.1184	2.23	283, 269, 257, 239, 225, 211, 197, 193, 183	C <sub>19</sub> H <sub>20</sub> O <sub>6</sub>	carpinontriol A
<b>114</b>	359.1134	2.42	329, 299, 269, 257, 239, 211, 197, 193	C <sub>19</sub> H <sub>20</sub> O <sub>7</sub>	giffonin U
<b>149</b>	343.1186	2.84	284, 283, 270, 269, 239, 211, 197, 193	C <sub>19</sub> H <sub>20</sub> O <sub>6</sub>	carpinontriol B
<b>154</b>	325.1079	2.46	307, 269, 239, 211, 209, 197, 193, 183, 113	C <sub>19</sub> H <sub>18</sub> O <sub>5</sub>	3,12,17-trihydroxytricyclo[12.3.1.1 <sup>2,6</sup> ]- nonadeca-1(18),2(19),3,5,14,16- hexaene-8,11-dione
<b>157</b>	327.1238	3.48	300, 269, 268, 267, 241, 239, 211, 197, 193, 183	C <sub>19</sub> H <sub>20</sub> O <sub>5</sub>	giffonin X
<b>161</b>	327.1235	-0.9	283, 269, 267, 253, 239, 225, 211, 197 193	C <sub>19</sub> H <sub>20</sub> O <sub>5</sub>	casuarinondiol
<b>164</b>	313.1437	0.78	254, 251, 241, 239, 227, 211, 210, 207, 189, 163, 149	C <sub>19</sub> H <sub>22</sub> O <sub>4</sub>	5-hydroxy-1,7-bis-(4'-hydroxyphenyl)- 3-heptanone
<b>187</b>	311.1287	3.00	286, 267, 253, 241, 211, 197	C <sub>19</sub> H <sub>20</sub> O <sub>4</sub>	3,11,17-trihydroxytricyclo[12.3.1.1 <sup>2,6</sup> ]- nonadeca-1(18),2(19),3,5,14,16- hexaen-8-one

The cyclic diarylheptanoid skeletons of compounds **106**, **114**, **149**, **154**, **157**, **161**, and **187** were the same based on the characteristic multiplicities and splitting patterns during the <sup>1</sup>H NMR and <sup>13</sup>C NMR data evaluation (Tables 5-6.). To determine the exact location of substituents such as carbonyl and hydroxyl groups of the cyclic diarylheptanoid structure, homo- and heteronuclear 2D experiments (<sup>1</sup>H-<sup>1</sup>H COSY, <sup>1</sup>H-<sup>13</sup>C edHSQC, <sup>1</sup>H-<sup>13</sup>C HMBC, <sup>1</sup>H-<sup>1</sup>H NOESY, or <sup>1</sup>H-<sup>1</sup>H ROESY, and <sup>1</sup>H-<sup>1</sup>H TOCSY) were executed. However, complete <sup>1</sup>H NMR and <sup>13</sup>C NMR resonance assignments could not be performed for **114** and **154** [131].

**Table 5.** Complete  $^1\text{H}$  and  $^{13}\text{C}$  NMR resonance assignments for compounds **157**, **106**, and **149** in methanol- $d_4$

	<b>157</b>		<b>106</b>		<b>149</b>	
No.	$\delta$ $^1\text{H}$ (multiplicity)	$\delta$ $^{13}\text{C}$	$\delta$ $^1\text{H}$ (multiplicity)	$\delta$ $^{13}\text{C}$	$\delta$ $^1\text{H}$ (multiplicity)	$\delta$ $^{13}\text{C}$
1	-	127.5	-	127.2	-	127.6
2	-	126.9	-	127.9	-	126.6
3	-	152.2	-	153.1	-	152.1
4	6.80 (d, $J=8.2$ Hz, 1H)	117.0	6.79 (d, $J=8.3$ Hz, 1H)	116.9	6.80 (d, $J=8.3$ Hz, 1H)	116.9
5	7.05 (dd, $J=8.2, 2.5$ Hz, 1H)	129.6	7.02 (dd, $J=8.3, 2.0$ Hz, 1H)	131.5	7.07 (dd, $J=8.3, 2.4$ Hz, 1H)	129.5
6	-	131.9	-	129.9	-	131.4
7	3.05 (m, 1H)	26.7	3.54 (d, $J=15.3$ Hz, 1H)	39.3	3.13 (m, 1H)	25.2
	2.90 (m, 1H)		2.89 (m, 1H)		2.84 (m, 1H)	
8	3.25 (m, 1H)	43.2	4.45 (dd, $J=6.5, 1.7$ Hz, 1H)	78.0	3.51 (m, 1H)	37.6
	2.91 (m, 1H)				2.93 (m, 1H)	
9	-	212.0	-	218.5	-	215.0
10	2.96 (m, 1H)	49.4	3.74 (dd, $J=19.0, 8.5$ Hz, 1H)	46.8	4.22 (d, $J=10.1$ Hz, 1H)	78.8
	2.88 (m, 1H)					
11	4.20 (m, 1H)	67.6	4.05 (m, 1H)	73.6	3.87 (d, $J=10.1$ Hz, 1H)	69.8
12	4.47 (dd, $J=11.4, 4.0$ Hz, 1H)	71.0	4.06 (m, 1H)	69.2	4.71 (dd, $J=11.9, 4.5$ Hz, 1H)	68.7
13	3.01 (m, 1H)	37.3	2.99 (m, 1H)	39.4	3.04 (m, 1H)	37.1
	2.89 (m, 1H)		2.89 (m, 1H)		2.89 (m, 1H)	
14	-	130.8	-	130.5	-	130.7
15	7.03 (dd, $J=8.2, 2.4$ Hz, 1H)	130.9	7.07 (dd, $J=8.3, 2.0$ Hz, 1H)	130.8	7.00 (dd, $J=8.3, 2.4$ Hz, 1H)	130.7
16	6.78 (d, $J=8.2$ Hz, 1H)	117.0	6.81 (d, $J=8.3$ Hz, 1H)	117.2	6.77 (d, $J=8.3$ Hz, 1H)	116.9
17	-	153.0	-	153.0	-	153.0
18	6.69 (d, $J=2.4$ Hz, 1H)	135.0	6.66 (d, $J=2.0$ Hz, 1H)	135.7	6.64 (d, $J=2.4$ Hz, 1H)	135.0
19	6.49 (d, $J=2.5$ Hz, 1H)	135.0	6.57 (d, $J=2.0$ Hz, 1H)	135.1	6.35 (d, $J=2.4$ Hz, 1H)	135.1

**Table 6.** Complete  $^1\text{H}$  and  $^{13}\text{C}$  NMR resonance assignments for compounds **187** and **161** in methanol- $d_4$

No.	<b>187</b>		<b>161</b>	
	$\delta$ $^1\text{H}$ (multiplicity)	$\delta$ $^{13}\text{C}$	$\delta$ $^1\text{H}$ (multiplicity)	$\delta$ $^{13}\text{C}$
1	-	127.3	-	127.2
2	-	127.2	-	128.4
3	-	152.4	-	153.5
4	6.80 (d, $J=8.3$ Hz, 1H)	117.1	6.78 (d, $J=8.3$ Hz, 1H)	117.1
5	7.05 (dd, $J=8.3, 2.5$ Hz, 1H)	129.6	7.00 (dd, $J=8.3, 2.3$ Hz, 1H)	131.7
6	-	132.2	-	129.6
7	2.99 (m, 2H)	27.3	3.47 (m, 1H) 2.87 (m, 1H)	40.3
8	-	212.0	4.39 (dd, $J=6.6, 2.0$ Hz, 1H)	78.1
9	3.19 (m, 1H) 2.90 (m, 1H)	43.0	-	220.1
10	3.02 (m, 1H) 2.68 (m, 1H)	54.1	3.52 (m, 1H) 2.89 (m, 1H)	39.6
11	4.20 (m, 1H)	67.4	1.87 (m, 2H)	32.2
12	2.46 (m, 1H) 1.80 (m, 1H)	35.6	4.04 (m, 1H)	73.2
13	2.88 (m, 2H)	29.0	3.03 (m, 1H) 2.80 (m, 1H)	42.0
14	-	132.4	-	130.2
15	7.04 (dd, $J=8.3, 2.5$ Hz, 1H)	130.7	7.04 (dd, $J=8.3, 2.3$ Hz, 1H)	130.5
16	6.78 (d, $J=8.3$ Hz, 1H)	117.0	6.80 (d, $J=8.3$ Hz, 1H)	116.9
17	-	152.7	-	153.1
18	6.79 (d, $J=2.3$ Hz, 1H)	134.6	6.74 (d, $J=2.3$ Hz, 1H)	135.6
19	6.60 (d, $J=2.3$ Hz, 1H)	134.6	6.52 (d, $J=2.3$ Hz, 1H)	134.7

Linear diarylheptanoid derivatives such as 5-hydroxy-3-platyphyllone (**164**) have not been reported before in *Carpinus* genus, the isolated compound was investigated using  $^1\text{H}$  NMR,  $^{13}\text{C}$  NMR,  $^1\text{H}$ - $^1\text{H}$  COSY,  $^1\text{H}$ - $^{13}\text{C}$  edHSQC,  $^1\text{H}$ - $^{13}\text{C}$  HMBC,  $^1\text{H}$ - $^1\text{H}$  NOESY, or  $^1\text{H}$ - $^1\text{H}$  ROESY, and  $^1\text{H}$ - $^1\text{H}$  TOCSY measurements (Table 7).

**Table 7.** Complete  $^1\text{H}$  and  $^{13}\text{C}$  NMR resonance assignments for compound **164** in methanol- $d_4$

<b>164</b>		
No.	$\delta$ $^1\text{H}$ (multiplicity)	$\delta$ $^{13}\text{C}$
1	2.74 (m, 2H)	29.8
2	2.73 (m, 2H)	46.4
3	-	211.9
4	2.56 (m, 1H)	51.3
	2.52 (m, 1H)	
5	4.00 (m, 1H)	68.2
6	1.65 (m, 2H)	40.5
7	2.63 (m, 1H)	32.0
	2.52 (m, 1H)	
1'	-	133.2
2', 6'	6.99 (m, 2H)	130.3
3', 5'	6.67 (m, 2H)	116.1/116.2
4'	-	156.6/156.4
1''	-	134.1
2'', 6''	6.99 (m, 2H)	130.3
3'', 5''	6.67 (m, 2H)	116.1/116.2
4''	-	156.6/156.4

#### IV.2.1. Structural Elucidation of Lignan and Flavonoid Compounds

For the structural elucidation of the lignan aviculin (**148**)  $^1\text{H}$ ,  $^{13}\text{C}$ , and additional 2D spectra were used, while for the flavonoid compounds (**177**, **185**, **191**)  $^1\text{H}$  and  $^{13}\text{C}$  NMR data were used, besides the LC-MS/MS data (Table 8, Supplementary Fig. S8-9) [132-135].

**Table 8.** MS/MS data of the isolated lignan and flavonoid compounds

No.	$[\text{M}-\text{H}]^-$ ( $m/z$ )	Fragment ions ( $m/z$ )	Molecular formula	Structure
<b>148</b>	505	527 $[\text{M}+\text{Na}-2\text{H}]^-$ , 359, 341, 326, 314, 313, 311, 299, 187	$\text{C}_{26}\text{H}_{34}\text{O}_{10}$	aviculin
<b>177</b>	447	895 $[2\text{M}-\text{H}]^-$ , 301, 300, 271, 255, 179, 151	$\text{C}_{21}\text{H}_{20}\text{O}_{11}$	quercetin-3- <i>O</i> -rhamnoside
<b>185</b>	577	431, 285, 169	$\text{C}_{30}\text{H}_{26}\text{O}_{12}$	kaempferol-3- <i>O</i> -(4''- <i>E</i> -p-coumaroyl)-rhamnopyranoside
<b>191</b>	431	285, 284, 269, 255, 227, 151	$\text{C}_{21}\text{H}_{20}\text{O}_{10}$	kaempferol-3- <i>O</i> -rhamnoside

### IV.3. Evaluation of the Antioxidant Activity

#### IV.3.1. DPPH Assay

Antioxidant capacities of hornbeam bark, leaf, male, and female catkin extracts prepared with methanol and ethyl acetate were compared. Table 9 summarizes the results of the DPPH scavenging assay; data are expressed as means  $\pm$  SD. We also investigated the antioxidant activities of the constituents isolated from *C. betulus* samples. For comparison, reference compounds with known radical scavenging activity were also studied, results are shown in Table 9 [131].

**Table 9.** DPPH scavenging activity of *C. betulus* extracts, constituents isolated from the bark, and reference compounds (Data are expressed as means  $\pm$  SD)

<b>Extracts</b>	<b>IC<sub>50</sub> <math>\pm</math> SD (<math>\mu</math>g/mL)</b>
Bark ethyl acetate extract ( <b>BE</b> )	9.0 $\pm$ 0.3
Bark methanol extract ( <b>BM</b> )	10.7 $\pm$ 0.3
Leaf ethyl acetate extract ( <b>LE</b> )	14.0 $\pm$ 0.4
Leaf methanol extract ( <b>LM</b> )	5.5 $\pm$ 0.2
Female catkin ethyl acetate extract ( <b>FE</b> )	9.4 $\pm$ 0.2
Female catkin methanol extract ( <b>FM</b> )	11.9 $\pm$ 0.7
Male catkin ethyl acetate extract ( <b>ME</b> )	13.3 $\pm$ 0.5
Male catkin methanol extract ( <b>MM</b> )	7.6 $\pm$ 0.3
<b>Isolated constituents</b>	
Carpinontriol A ( <b>106</b> )	77.2 $\pm$ 4.5
Carpinontriol B ( <b>149</b> )	123 $\pm$ 10
Giffonin X ( <b>157</b> )	138 $\pm$ 11
Casuarinondiol ( <b>161</b> )	> 250
5-Hydroxy-3-platyphyllone ( <b>164</b> )	121 $\pm$ 9
Aviculin ( <b>148</b> )	23.8 $\pm$ 0.9
Quercitrin ( <b>177</b> )	6.9 $\pm$ 0.5
Afzelin ( <b>191</b> )	> 250
Kaempferol-3- <i>O</i> -(4''- <i>E-p</i> -coumaroyl)rhamnopyranoside ( <b>185</b> )	> 250
<b>Reference compounds</b>	
Trolox	5.3 $\pm$ 0.2
Rutin	7.3 $\pm$ 0.3

### IV.3.2. DPPH-HPLC-DAD-MS Analysis

In order to assess the contribution of the individual antioxidant constituents to the total antioxidant activity of *C. betulus* extracts, an off-line DPPH-HPLC-DAD-MS method was applied. Upon reaction with DPPH, phenolics which can neutralize the free radical DPPH<sup>•</sup> by providing hydrogen atoms or by electron donation, will be oxidized to form free radicals, and subsequently stable quinoidal structures. As a consequence of this structural change, peak areas (peak intensities) of these antioxidants will decrease in the HPLC chromatogram [136]. Chromatograms of hornbeam samples were compared before and after reacting with DPPH. The antioxidant effect was characterized by the decrease of the intensity (area under the curve, AUC) values in percentage. The compounds which have intensities reduced by more than 20% were considered as potential antioxidants [88]. Values are means of intensity reductions determined for each extract containing the specific compound. Results are presented in Table 10. Representative HPLC-UV chromatograms demonstrating untreated and DPPH-treated bark methanolic samples are shown in Fig. 11 [131].

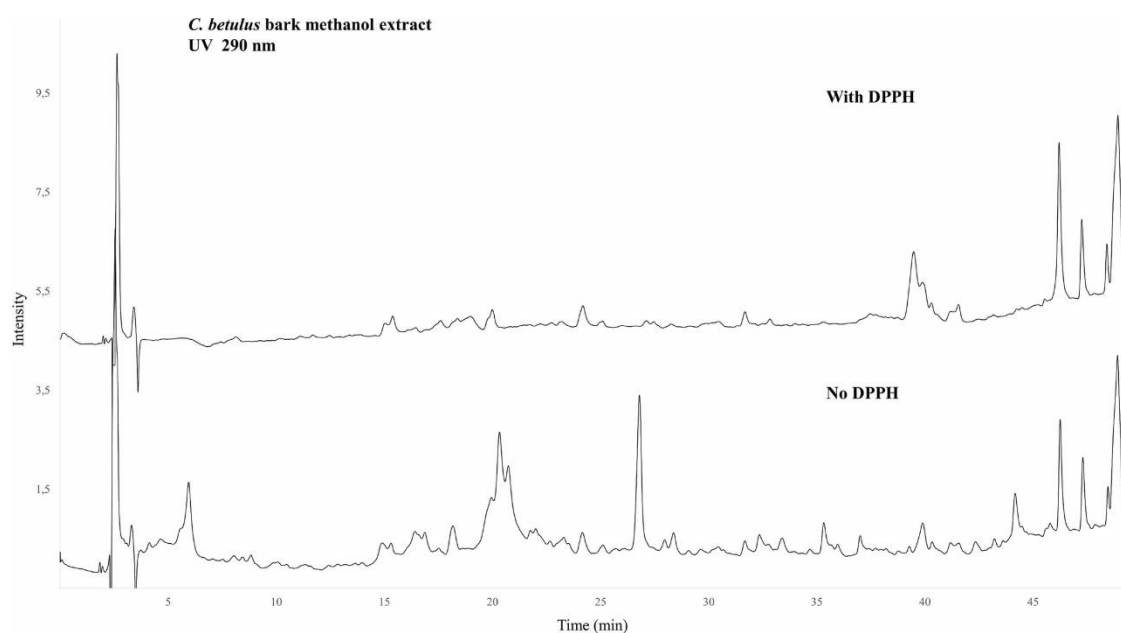


**Figure 11.** Chromatograms of untreated and DPPH-treated *C. betulus* bark methanolic extract samples. Detection wavelength: 290 nm. For chromatographic conditions see Section III.4.1.

**Table 10.** Potential antioxidants in *Carpinus betulus* extracts <sup>a,b</sup> [88]

No.	Compound	[M-H] (m/z)	Occurrence in the extracts <sup>c</sup>	Intensity reduced by (%) <sup>d</sup>
1	caffeoyl hexose	341	BE, BM, LM, FM	48.6
3	5- <i>O</i> -hydroxydihydrocaffeoyl-hexosyl quinic acid	533	BM, LM, FM	43.3
4	monogalloyl hexose	331	LE, TM, PM	69.6
11	monogalloyl hexose	331	LM	86.5
14	gallic acid	169	BE, BM, LE, LM, FE, FM, ME, MM	95.8
16	5- <i>O</i> -galloylquinic acid	343	BM	100.0
18	4- <i>O</i> -galloylquinic acid	343	BM, LE, LM, FM, PM	93.4
27	galloylshikimic acid	325	LE, LM, FE, FM, ME, MM	95.2
28	dihydroxybenzoic acid	153	LE	41.4
29	digalloyl hexose	483	LM	94.8
32	galloylshikimic acid	325	LE, LM, FM, ME, MM	92.4
34	galloylshikimic acid	325	LE, LM, FE, FM, ME, MM	95.2
38	galloyl-HHDP hexose	633	FM, MM	96.1
42	dihydroxybenzoic acid hexosyl-pentosided	447	BM	100.0
43	galloyl-HHDP hexose	633	LM	97.1
45	hydroxy-dimethoxybenzoic acid hexoside	359	BE, BM	53.7
46	methylgalloyl hexose	345	BE, ME, MM	86.4
51	galloyl-HHDP hexose	633	BM	100.0
53	methylgallic acid	183	BE, BM, LM, FE, FM, ME, MM	94.4
54	catechin/epicatechin	289	ME	88.5
56	not identified	383	LM	81.8
58	3,4-di- <i>O</i> -galloylquinic acid	495	FM	82.1
59	not identified gallotannin	683	LM	97.9
62	not identified	383	LM	87.8
63	not identified	351	LM	84.6
64	digalloyl hexose	483	FM, MM	90.7
65	<i>trans</i> -5- <i>O</i> -caffeoylquinic acid	353	LE, LM, FM	79.8
68	hydroxy-methoxyphenyl- <i>O</i> -galloyl hexose	453	BE, ME	100.0
70	not identified gallotannin	683	LM	96.8
75	trigalloyl hexose	635	LM, FM	86.6
78	digalloyl hexose	483	BM	100.0
79	brevifolin carboxylate	291	FM, MM	89.4
82	trigalloyl hexose	635	LM, FM, ME, MM	96.3
83	<i>cis</i> -5- <i>O</i> -caffeoylquinic acid	353	LE, LM, FM	80.6
84	galloyl-HHDP hexose	633	BE, BM, LM, FM, MM	99.9
85	trigalloyl hexose	635	MM	100.0
87	digalloylshikimic acid	477	LM, ME	88.5
88	trigalloyl hexose	635	FM	86.3
92	HHDP hexose	481	BE, BM	100.0
95	galloyl-methylgalloyl hexose	497	ME	100.0
97	ethylgallic acid	197	FE	97.3
99	digalloylshikimic acid	477	LM, FM, ME, MM	85.8

100	caffeoylshikimic acid	335	LE, FE, ME	76.0
102	trigalloyl hexose	635	MM	100.0
105	tetragalloyl hexose	787	FM	100.0
107	catechin gallate/epicatechin gallate	441	ME	76.3
111	<i>cis</i> -5- <i>p</i> - <i>O</i> -coumaroylquinic acid	337	LE, LM	28.1
113	methylgallic acid derivative	387	FE	62.2
114	giffonin U	359	BE	60.3
115	gallocatechin/epigallocatechin	305	BE, BM, LM, FM, MM	92.7
116	<i>trans</i> -5- <i>O</i> -feruloylquinic acid	367	LE, LM, FE	74.2
121	HHDP dihexose	625	MM	81.4
122	caffeoylshikimic acid	335	LM	92.7
126	not identified ellagitannin	857	LM	100.0
129	trigalloyl-HHDP hexose	937	LM, FM	98.0
132	<i>cis</i> -5- <i>O</i> -feruloylquinic acid	367	LE	76.2
135	myricetin-3- <i>O</i> -hexoside	479	LM, FE, FM, MM	90.4
137	galloyl-HHDP hexose derivative	997	LM	100.0
138	pentagalloyl hexose	939	LM	100.0
143	cyclic diarylheptanoid	475	BE	75.5
144	trigalloyl-HHDP hexose	937	LM	100.0
148	aviculin	505	BE, BM	67.7
149	carpinontriol B	343	BE, BM	66.3
151	methylgallic acid hexoside	477	BM	41.6
153	myricetin-3- <i>O</i> -pentoside	449	FM	86.3
155	myricetin-3- <i>O</i> -deoxyhexoside	463	BE, BM, LE, LM, FE, FM, ME, MM	97.7
159	trihydroxy-dimethoxyflavone- <i>O</i> -hexoside	491	BE, BM	54.4
160	kaempferol-3- <i>O</i> -hexoside	447	LE, LM, FE, FM	72.9
162	ellagic acid pentoside	433	MM	100.0
163	quercetin-3- <i>O</i> -hexoside	463	BE, LE, FE, FM, ME, MM	68.9
168	ellagic acid	301	BE, BM, LE, LM, FE, FM, ME, MM	94.9
169	quercetin-3- <i>O</i> -pentoside	433	FE	70.5
174	trihydroxy-dimethoxyflavone- <i>O</i> -sulfate	409	FM	48.2
176	quercetin-3- <i>O</i> -pentoside	433	BE, LE, FE, ME, MM	68.3
177	quercetin-3- <i>O</i> -rhamnoside	447	BE, BM, LE, LM, FE, FM, ME, MM	64.3
179	tetrahydroxy-methoxyflavone- <i>O</i> -pentoside	447	BE, BM, FM	39.5
183	trihydroxy-dimethoxy flavone- <i>O</i> -pentoside	461	BE	29.8
183	trihydroxy-dimethoxy flavone- <i>O</i> -pentoside	461	BM	30.8
184	methylgallic acid deoxyhexoside	461	FE	41.6
188	dihydroxy-trimethoxy flavone	343	BM	22.0
189	methylgallic acid	315	BE	88.3
191	kaempferol-3- <i>O</i> -rhamnoside	431	LE, FE, FM, ME	20.8
192	quercetin	301	FE	98.9
194	dihydroxy-dimethoxy flavone	329	BE	32.5

<sup>a</sup> Compounds with peak intensities reduced by more than 20%. <sup>b</sup> Compound numbers refer to Table 3. <sup>c</sup> Abbreviations extracts: BE: bark ethyl acetate extract, BM: bark methanol extract, LE: leaf ethyl acetate extract, LM: leaf methanol extract, FE: female catkin ethyl acetate extract, FM: female catkin methanol extract, ME: male catkin ethyl acetate extract, MM: male catkin methanol extract. <sup>d</sup> Values are means of intensity reductions determined for the extracts indicated for each constituent

#### IV.4. Quantitative Analysis of the Main Diarylheptanoids in *Carpinus betulus*

There are currently no literature data regarding the quantitative analysis of diarylheptanoids in *C. betulus*. Therefore, a UHPLC-DAD method was developed and validated for the quantitative determination of the four main diarylheptanoids in the bark, leaf, female, and male catkins extracts: carpinontriols A (**106**) and B (**149**), 3,12,17-trihydroxytricyclo[12.3.1.1<sup>2,6</sup>]nonadeca-1(18),2(19),3,5,14,16-hexaene-8,11-dione (**154**), and giffonin X (**157**). Using optimized conditions, the applied gradient solvent system enabled sufficient separation of the four analytes of interest in the ethyl-acetate and methanol extracts. (Fig. 12.).

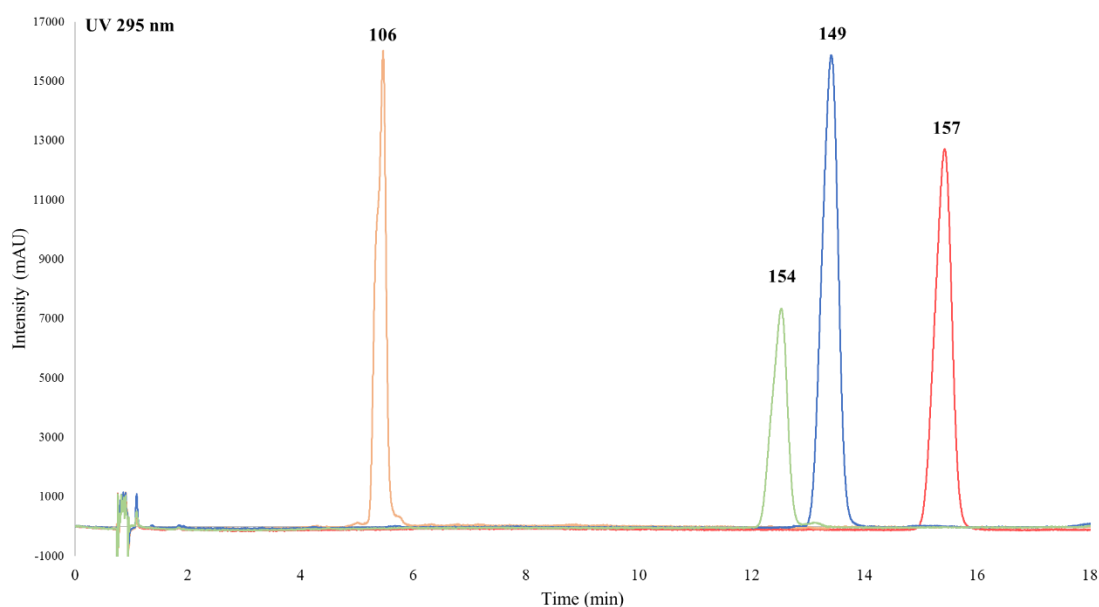


**Figure 12.** The chromatographic separation of compounds **106**, **149**, **154**, and **157**. For chromatographic conditions see Section III.4.4.

##### IV.4.1. Method Validation

The linearity regression equations, correlation coefficients ( $r^2$ ), linearity ranges, LOD, and LOQ values of the quantitative method are shown in Table 11. Excellent linearity was achieved ( $r^2 \geq 0.9995$ ) in the range of 1–250  $\mu\text{g/mL}$  for all analytes. The LOD and LOQ values were within the ranges of 0.1–0.2  $\mu\text{g/mL}$  and 0.3–0.6  $\mu\text{g/mL}$ , respectively.

**Table 11.** Method validation: regression, LOQ and LOD of the quantitative method

Compound	Regression equation	r <sup>2</sup>	Regression range (µg/mL)	LOD (µg/mL)	LOQ (µg/mL)
<b>106</b>	$y = 88.99x + 177.77$	0.9997	1-250	0.15	0.5
<b>149</b>	$y = 95.80x + 228.73$	0.9995	1-250	0.1	0.3
<b>154</b>	$y = 43.17x - 16.79$	0.9999	1-250	0.2	0.6
<b>157</b>	$y = 86.71x + 177.24$	0.9996	1-250	0.15	0.5

Intra-day and inter-day precision evaluated at low, mid, and high concentration ranges was also acceptable (0.16–3.33 RSD%), while intra- and inter-day accuracy results varied from 80.31% to 107.06% (Table 12.).

**Table 12.** Method validation: Precision and accuracy of the quantitative method

Nominal concentration (µg/mL)	Precision (RSD%)		Accuracy (%)	
	Intra-day	Inter-day	Intra-day	Inter-day
<b>Carpinontriol A (106)</b>				
5	0.53	0.75	80.95	81.69
50	1.81	1.48	105.22	106.54
250	0.16	0.24	99.62	99.63
<b>Carpinontriol B (149)</b>				
5	0.96	1.65	80.31	81.34
50	0.73	0.88	104.92	105.02
250	0.59	0.80	99.43	99.61
<b>3,12,17-Trihydroxytricyclo[12.3.1.1<sup>2,6</sup>]nonadeca-1(18),2(19),3,5,14,16-hexaene-8,11-dione (154)</b>				
5	0.76	2.38	107.68	107.38
50	1.37	2.06	97.27	98.43
250	0.43	3.33	100.14	103.74
<b>Giffonin X (157)</b>				
5	2.84	1.69	81.10	81.81
50	0.72	1.81	105.54	107.06
250	1.56	1.44	99.48	100.29

The extraction recovery rate of **157** was  $96.29 \pm 1.36\%$  for the ethyl acetate extract, and  $114.91 \pm 2.19\%$  in case of the methanol extract. Retention time repeatability was suitable for all four compounds, relative standard deviation ranged from 0.18% to 0.58% ( $n = 6$ ). In order to evaluate the selectivity of the method, blank samples (hexane extracts which do not contain the analytes of interest) were compared to extracts spiked

with **106**, **149**, **154**, and **157**. No co-elution was observed at the retention times of the analytes of interest, indicating that this method provides good selectivity. These results show that the method was reliable and repeatable [131].

#### IV.4.2. Quantitative Results

Ethyl acetate and methanol extracts of all samples (bark, leaf, female, and male catkins) were analyzed. In accordance with the results of the qualitative screening, the evaluated diarylheptanoids were not detected in leaf and female flower extracts. The calculated diarylheptanoid concentrations can be seen in Table 13.

**Table 13.** Quantitative determination of the main diarylheptanoids in *Carpinus betulus* extracts (data are expressed as mg/g dry extract) <sup>a</sup>

Compound	Quantity $\pm$ SD (mg/g dry extract)			
	BE	BM	ME	MM
<b>106</b>	19.13 $\pm$ 0.10	13.94 $\pm$ 0.26	n.d.	3.55 $\pm$ 0.05
<b>149</b>	6.44 $\pm$ 0.18	4.16 $\pm$ 0.15	7.60 $\pm$ 0.12	16.25 $\pm$ 0.19
<b>154</b>	16.04 $\pm$ 0.12	11.05 $\pm$ 0.02	n.d.	n.d.
<b>157</b>	18.07 $\pm$ 0.03	9.97 $\pm$ 0.10	n.d.	n.d.

<sup>a</sup> Data are expressed as mean values  $\pm$  SD ( $n = 3$ ). Abbreviations: BE: bark ethyl acetate extract, BM: bark methanol extract, ME: male catkin ethyl acetate extract, MM: male catkin methanol extract, n.d.: not detected.

#### IV.5. Stability Studies

##### IV.5.1. Evaluation of Aqueous Stability at Different pH Values

The stability of the main diarylheptanoids (**106**, **149**, **154**, and **157**) was evaluated in aqueous medium at 37 °C at three biorelevant pH values (pH 1.2 modelling the gastric fluid, pH 6.8 simulating the intestinal fluid, pH 7.4 mimicking the blood and the tissues).

Table 14 summarizes the results; compound concentrations are expressed as % values compared to the initial values. To calculate the kinetic parameters [degradation rate constant ( $k$ ) and half-life ( $t_{1/2}$ )], a linear regression model was used, which followed first-order kinetics in line with previous data for diarylheptanoids (Table 15) [137].

**Table 14.** Aqueous stability of the isolated diarylheptanoid compounds <sup>a,b</sup>

Incubation time	pH	Compound			
		106	149	157	154
9 h	pH 7.4	96.9 ± 1.2 <sup>a</sup>	102.0 ± 0.9 <sup>a</sup>	82.6 ± 7.7 <sup>#b</sup>	102.0 ± 3.7 <sup>a</sup>
	pH 6.8	97.4 ± 1.5 <sup>#a</sup>	105.2 ± 3.9 <sup>a</sup>	98.9 ± 0.8 <sup>a</sup>	105.8 ± 2.6 <sup>a</sup>
	pH 1.2	97.1 ± 8.9 <sup>a</sup>	101.7 ± 4.2 <sup>a</sup>	100.6 ± 6.9 <sup>a</sup>	68.5 ± 4.5 <sup>#</sup>
81 h	pH 7.4	71.5 ± 5.2 <sup>#b</sup>	101.5 ± 1.1 <sup>a</sup>	46.7 ± 4.7 <sup>#</sup>	103.1 ± 2.2 <sup>a</sup>
	pH 6.8	75.3 ± 3.0 <sup>#b</sup>	101.9 ± 6.4 <sup>a</sup>	93.2 ± 2.0 <sup>#ab</sup>	88.9 ± 2.0 <sup>#</sup>
	pH 1.2	70.5 ± 2.6 <sup>#b</sup>	100.7 ± 5.1 <sup>a</sup>	83.4 ± 5.3 <sup>#b</sup>	31.0 ± 7.0 <sup>#</sup>

<sup>a</sup> Data are expressed as relative concentrations (%) after 9 and 81 h compared to the initial value. <sup>b</sup> Data are expressed as mean values ± SD ( $n = 3$ ). Values with identical lower-case letters (a–b) in the same column are not significantly different (Tukey test,  $p < 0.05$ ); <sup>#</sup>  $p < 0.05$  compared with the initial concentration.

**Table 15.** Kinetic parameters of the investigated *Carpinus* diarylheptanoids following storage at 37 °C at different pH values

Compound	pH 7.4		pH 6.8		pH 1.2	
	$k$ (h <sup>-1</sup> )	$t_{1/2}$ (h)	$k$ (h <sup>-1</sup> )	$t_{1/2}$ (h)	$k$ (h <sup>-1</sup> )	$t_{1/2}$ (h)
106	$4.19 \times 10^{-3}$	165.6	$3.65 \times 10^{-3}$	189.6	$4.15 \times 10^{-3}$	167.1
149	-	-	-	-	-	-
157	$8.49 \times 10^{-3}$	81.6	$8.38 \times 10^{-4}$	826.8	$2.32 \times 10^{-3}$	298.4
154	-	-	$1.42 \times 10^{-3}$	487.7	$1.27 \times 10^{-2}$	54.4

#### IV.5.2. Evaluation of Storage Stability

A further aim of our work was to determine the mid-term (12 weeks) and long-term (23 weeks) stability of the four major diarylheptanoids by evaluating the effects of storage time, and temperature. The results of the chemical stability studies are summarized in Table 16.

**Table 16.** Chemical stability of *Carpinus* diarylheptanoids: Effects of storage time, temperature, and medium on the concentrations of compounds **106**, **149**, **154**, and **157** as compared to the initial value (%) <sup>a</sup>

Storage time (week)	Storage temperature (°C)	Medium	Compound				
			106	149	157	154	
12	22	SM	63.5 ± 8.7 <sup>#a</sup>	99.7 ± 0.4 <sup>a</sup>	84.5 ± 7.4 <sup>#a</sup>	100.1 ± 0.5 <sup>ab</sup>	
		SA	61.7 ± 5.7 <sup>#a</sup>	100.4 ± 1.1 <sup>a</sup>	96.2 ± 0.1 <sup>#bcd</sup>	100.8 ± 1.1 <sup>a</sup>	
		EE	110.9 ± 3.6 <sup>#bc</sup>	100.2 ± 0.7 <sup>a</sup>	101.6 ± 2.2 <sup>#bc</sup>	106.3 ± 2.6 <sup>#</sup>	
		EM	114.0 ± 2.2 <sup>#b</sup>	101.1 ± 1.1 <sup>a</sup>	102.7 ± 0.9 <sup>#bc</sup>	120.9 ± 2.6 <sup>#</sup>	
	5	22	SM	90.8 ± 2.3 <sup>#def</sup>	99.4 ± 0.6 <sup>a</sup>	99.0 ± 0.1 <sup>#bcd</sup>	100.1 ± 0.6 <sup>ab</sup>
			SA	91.4 ± 0.2 <sup>#def</sup>	99.9 ± 0.4 <sup>a</sup>	99.3 ± 0.1 <sup>#bcd</sup>	100.5 ± 0.7 <sup>ab</sup>
			EE	104.6 ± 1.0 <sup>#bcg</sup>	99.5 ± 0.4 <sup>#a</sup>	100.8 ± 0.5 <sup>#bcd</sup>	102.0 ± 1.7
			EM	110.1 ± 6.2 <sup>bc</sup>	99.9 ± 0.8 <sup>a</sup>	100.2 ± 1.1 <sup>bcd</sup>	105.5 ± 2.5
		-15	SM	94.0 ± 0.8 <sup>#efg</sup>	99.1 ± 1.3 <sup>a</sup>	100.4 ± 1.2 <sup>bcd</sup>	99.1 ± 0.7 <sup>ab</sup>
			SA	93.5 ± 0.4 <sup>#ef</sup>	99.1 ± 1.3 <sup>a</sup>	100.1 ± 0.6 <sup>bcd</sup>	98.6 ± 1.3 <sup>b</sup>
			EE	100.5 ± 0.5 <sup>ceg</sup>	100.1 ± 0.7 <sup>a</sup>	103.5 ± 0.2 <sup>b</sup>	103.5 ± 0.8
			EM	108.7 ± 1.5 <sup>#bc</sup>	99.8 ± 0.7 <sup>a</sup>	101.6 ± 3.1 <sup>#bc</sup>	102.8 ± 3.3 <sup>#</sup>
23	22	SM	32.3 ± 6.3 <sup>#h</sup>	99.9 ± 0.6 <sup>a</sup>	67.1 ± 7.5 <sup>#</sup>	100.2 ± 0.5 <sup>ab</sup>	
		SA	23.0 ± 0.5 <sup>#h</sup>	99.8 ± 0.9 <sup>a</sup>	87.6 ± 0.7 <sup>#ae</sup>	100.3 ± 0.6 <sup>ab</sup>	
		EE	81.5 ± 3.9 <sup>#di</sup>	99.7 ± 0.5 <sup>a</sup>	95.7 ± 0.5 <sup>#cd</sup>	108.5 ± 2.7 <sup>#</sup>	
		EM	77.7 ± 2.9 <sup>#ij</sup>	99.7 ± 0.3 <sup>#a</sup>	95.6 ± 2.4 <sup>#cd</sup>	135.7 ± 9.7 <sup>#</sup>	
	5	22	SM	67.1 ± 7.5 <sup>#aj</sup>	99.2 ± 0.5 <sup>a</sup>	81.9 ± 1.0 <sup>#a</sup>	100.3 ± 0.5 <sup>ab</sup>
			SA	87.2 ± 0.4 <sup>#dfi</sup>	99.9 ± 0.5 <sup>a</sup>	99.1 ± 0.1 <sup>#bcd</sup>	100.0 ± 0.5 <sup>ab</sup>
			EE	92.1 ± 1.3 <sup>#def</sup>	100.1 ± 0.4 <sup>a</sup>	100.9 ± 1.3 <sup>bcd</sup>	107.8 ± 2.6 <sup>#</sup>
			EM	84.1 ± 1.1 <sup>#dfi</sup>	99.2 ± 1.2 <sup>a</sup>	93.8 ± 1.3 <sup>#de</sup>	107.0 ± 4.1
		-15	SM	88.9 ± 3.1 <sup>#dfi</sup>	99.1 ± 1.2 <sup>a</sup>	95.8 ± 0.1 <sup>#cd</sup>	99.8 ± 1.2 <sup>ab</sup>
			SA	93.7 ± 0.3 <sup>#efg</sup>	99.1 ± 1.2 <sup>a</sup>	97.9 ± 2.9 <sup>bcd</sup>	99.9 ± 1.2 <sup>ab</sup>
			EE	91.3 ± 4.2 <sup>#def</sup>	99.8 ± 0.4 <sup>a</sup>	101.1 ± 2.7 <sup>#bcd</sup>	108.0 ± 2.2 <sup>#</sup>
			EM	88.3 ± 3.4 <sup>#dfi</sup>	99.6 ± 0.7 <sup>a</sup>	97.6 ± 3.2 <sup>bcd</sup>	103.6 ± 3.5

<sup>a</sup> Results are expressed as mean values ± SD ( $n = 3$ ). Values with identical lower-case letters (a–j) in the same column are not significantly different (Tukey test,  $p < 0.05$ ); <sup>#</sup>  $p < 0.05$  compared with the initial samples. Abbreviations: SM: methanol solution; SA: aqueous solution; EE: ethyl acetate extract; EM: methanol extract.

Influence of the medium, i.e., that of the solvent (in aqueous and methanol solutions) as well as that of other accompanying compounds (being present in methanol and ethyl acetate extracts of the hornbeam bark) was also investigated. Aqueous and methanol solutions of the isolated compounds together with hornbeam bark extracts prepared with ethyl acetate and methanol were stored at 22, 5, and  $-15$  °C. The storage temperatures were chosen to represent common storage conditions such storage at ambient temperature, in a refrigerator, or in a freezer, respectively. The degradation kinetic parameters of the pure diarylheptanoids are presented in Table 17 [131].

**Table 17.** Kinetic parameters of carpinontriol A (**106**) and giffonin X (**157**) in aqueous and methanolic solutions following storage at 22 °C, 5 °C, and  $-15$  °C for 23 weeks

Temperature (°C)	Medium	Carpinontriol A ( <b>106</b> )		Giffonin X ( <b>157</b> )	
		$k$ (week <sup>-1</sup> )	$t_{1/2}$ (week)	$k$ (week <sup>-1</sup> )	$t_{1/2}$ (week)
22	SA	$5.97 \times 10^{-2}$	11.61	$5.90 \times 10^{-3}$	117.48
	SM	$4.53 \times 10^{-2}$	15.30	$1.85 \times 10^{-2}$	37.47
5	SA	$4.47 \times 10^{-3}$	147.48	$5.0 \times 10^{-4}$	1386.29
	SM	$1.40 \times 10^{-2}$	50.23	$7.10 \times 10^{-3}$	97.63
$-15$	SA	$1.70 \times 10^{-3}$	407.73	-	-
	SM	$3.60 \times 10^{-3}$	192.54	$1.60 \times 10^{-3}$	433.22

Abbreviations: SA: aqueous solution; SM: methanol solution.

### V.5.3. Characterization of the Degradation Products by UHPLC-HR-MS/MS

The structural analysis of the degradation products formed in the storage and pH stability studies was performed by ultrahigh-performance liquid chromatography–high-resolution tandem mass spectrometry (UHPLC-HR-MS/MS) measurements. The chromatographic and mass spectrometric data of the original constituents and the degradation products are presented in Table 18.

**Table 18.** HR-MS data of the diarylheptanoids **106** and **157** and their degradation products

No.	[M-H] <sup>-</sup> (m/z) experimental	[M-H] <sup>-</sup> (m/z) calculated	Error (ppm)	Molecular formula	Fragment ions (m/z)
<b>106</b>	343.1199	343.1182	3.75	C <sub>19</sub> H <sub>19</sub> O <sub>6</sub>	283.0976 (C <sub>17</sub> H <sub>15</sub> O <sub>4</sub> ), 271.0977 (C <sub>16</sub> H <sub>15</sub> O <sub>4</sub> ), 269.0820 (C <sub>16</sub> H <sub>13</sub> O <sub>4</sub> ), 241.0869 (C <sub>15</sub> H <sub>13</sub> O <sub>3</sub> ), 211.0758 (C <sub>14</sub> H <sub>11</sub> O <sub>2</sub> )
<b>106a</b>	361.0927	361.0923	2.37	C <sub>18</sub> H <sub>17</sub> O <sub>8</sub>	343.0812 (C <sub>18</sub> H <sub>15</sub> O <sub>7</sub> ), 285.0769 (C <sub>16</sub> H <sub>13</sub> O <sub>5</sub> ), 258.0534 (C <sub>14</sub> H <sub>10</sub> O <sub>5</sub> ),
<b>106b</b>	345.0977	345.0974	2.25	C <sub>18</sub> H <sub>17</sub> O <sub>7</sub>	327.0872 (C <sub>18</sub> H <sub>15</sub> O <sub>6</sub> ), 309.0764 (C <sub>18</sub> H <sub>13</sub> O <sub>5</sub> ), 285.0767 (C <sub>16</sub> H <sub>13</sub> O <sub>5</sub> ), 258.0531 (C <sub>14</sub> H <sub>10</sub> O <sub>5</sub> ), 225.0549 (C <sub>14</sub> H <sub>9</sub> O <sub>3</sub> )
<b>106c</b>	325.1084	325.1076	4.06	C <sub>19</sub> H <sub>17</sub> O <sub>5</sub>	269.0820 (C <sub>16</sub> H <sub>13</sub> O <sub>4</sub> ), 253.0862 (C <sub>16</sub> H <sub>13</sub> O <sub>3</sub> ), 241.0865 (C <sub>15</sub> H <sub>13</sub> O <sub>3</sub> ), 239.0862 (C <sub>15</sub> H <sub>11</sub> O <sub>3</sub> ), 225.0910 (C <sub>15</sub> H <sub>13</sub> O <sub>2</sub> ), 211.0759 (C <sub>14</sub> H <sub>11</sub> O <sub>2</sub> )
<b>157</b>	327.1240	327.1233	4.05	C <sub>19</sub> H <sub>19</sub> O <sub>5</sub>	269.0821 (C <sub>16</sub> H <sub>13</sub> O <sub>4</sub> ), 267.1028 (C <sub>17</sub> H <sub>15</sub> O <sub>3</sub> ), 253.0866 (C <sub>16</sub> H <sub>13</sub> O <sub>3</sub> ), 239.0716 (C <sub>15</sub> H <sub>11</sub> O <sub>3</sub> ), 211.0758 (C <sub>14</sub> H <sub>11</sub> O <sub>2</sub> )
<b>157a</b>	309.1134	309.1127	4.10	C <sub>19</sub> H <sub>17</sub> O <sub>4</sub>	267.1020 (C <sub>17</sub> H <sub>15</sub> O <sub>3</sub> ), 253.0876 (C <sub>16</sub> H <sub>13</sub> O <sub>3</sub> ), 225.09131 (C <sub>15</sub> H <sub>13</sub> O <sub>2</sub> ), 211.0758 (C <sub>14</sub> H <sub>11</sub> O <sub>2</sub> )

#### IV.6. Parallel Artificial Membrane Permeability Assay Studies

The ability of the isolated cyclic diarylheptanoid compounds to cross biological membranes of the gastrointestinal tract and the blood–brain barrier by passive diffusion was investigated by the PAMPA model [138, 139]. Results are presented in Table 19.

**Table 19.** Results of the PAMPA experiments: log*P<sub>e</sub>* values (*n* = 9) and the calculated clog *P* values (Chemsketch Freeware)

Compound	log <i>P<sub>e</sub></i> PAMPA-BBB ( <i>n</i> = 9)	log <i>P<sub>e</sub></i> PAMPA-GI ( <i>n</i> = 9)	clog <i>P</i>
<b>106</b>	n.d.	-6.25 ± 0.04	0.93 ± 0.46
<b>149</b>	n.d.	-5.46 ± 0.06	1.92 ± 0.67
<b>157</b>	-5.92 ± 0.04	-5.22 ± 0.07	1.77 ± 0.41
<b>154</b>	n.d.	n.d.	0.94 ± 0.46

Abbreviations: n.d.: not detected in the acceptor phase

#### IV.7. Evaluation of the Cytostatic Activity

The *in vitro* antiproliferative activities of the isolated *Carpinus* diarylheptanoids were studied by the Alamar Blue assay in HT-29 (colorectal carcinoma), Hep G2 (hepatocellular carcinoma), HL-60 (acute promyelocytic leukaemia), U87

(glioblastoma), and A2058 (melanoma, derived from metastatic site: lymph node) human cancer cell lines for the first time (Table 20).

**Table 20.** Effect of *C. betulus* diarylheptanoids on human cancer cell lines <sup>a</sup>

Compound	Cell Line <sup>b</sup>				
	HT-29 IC <sub>50</sub> ± SD (µM) <sup>c</sup>	Hep G2 IC <sub>50</sub> ± SD (µM)	HL-60 IC <sub>50</sub> ± SD (µM)	U87 IC <sub>50</sub> ± SD (µM)	A2058 IC <sub>50</sub> ± SD (µM)
<b>106</b>	> 100	> 100	> 100	> 100	14.9 ± 2.3
<b>149</b>	> 100	> 100	> 100	> 100	> 100
<b>154</b>	> 100	> 100	> 100	> 100	> 100
<b>157</b>	> 100	> 100	> 100	> 100	> 100
<b>Reference compounds <sup>d</sup></b>					
<b>Etoposide</b>	18.5 ± 1.7	20.9 ± 1.2	no data	27.0 ± 2.3	8.9 ± 0.2
<b>Dau</b>	0.2 ± 0.01	1.2 ± 0.2	0.02 ± 0.01 <sup>30</sup>	0.4 ± 0.05	0.16 ± 0.1
<b>Sal</b>	no data	5.8 ± 0.7	4.5 ± 0.7	0.8 ± 0.3	6.8 ± 1.2

<sup>a</sup> Data are expressed as means ± SD ( $n = 2$ ). <sup>b</sup> HT-29 colorectal carcinoma cells, Hep G2 hepatocellular carcinoma cells, HL-60 acute promyelocytic leukaemia cells, U87 glioblastoma cells, A2058 metastatic melanoma cells. <sup>c</sup> IC<sub>50</sub>: required concentration of compounds to inhibit cell proliferation by 50% expressed as µM; <sup>d</sup> Experimental data in agreement with previous literature data [94, 140]. Abbreviations: Dau: Daunomycin; Sal: 5-chloro-2-hydroxy-*N*-[4-(trifluoromethyl)phenyl]benzamide, MW: 315.7 g/mol.

## V. Discussion

### V.1. Qualitative Analyses of *Carpinus betulus* Polyphenols by HPLC-DAD-MS/MS

In line with literature data, gallotannins and ellagitannins prevailed in hornbeam bark, leaf, female, and male catkins extracts [3]. Gallic acid (as a small polar compound) and its derivatives eluting at low retention times were distinguished by their characteristic fragment ions at  $m/z$  169 which is the deprotonated molecular ion of gallic acid, and  $m/z$  125 which is created by the cleavage of the carboxyl group from gallic acid [99, 103].

Compounds **8**, **16**, and **18**, tentatively identified as galloylquinic acid isomers, could be differentiated based on the relative intensities of their fragment ions [102]. In case of 5-*O*-galloylquinic acid (**16**), the fragment ion at  $m/z$  191 was dominating, while for compound **18**, the relative intensity of the fragment ion at  $m/z$  173 was the highest indicating the 4-*O*-galloylquinic acid structure. 3-*O*-galloylquinic acid (**8**) which showed the lowest retention time, yielded comparatively intense fragment ions both at  $m/z$  169 and 191.

Gallotannins (**G**, Table 3) contain a hexose core (mainly glucose) where the hydroxyl groups are partly or completely substituted via ester linkage with a varying number of galloyl moieties. These components presented the characteristic fragment ions of gallic acid at  $m/z$  169 and  $m/z$  125 as well as neutral losses of 170 Da (gallic acid), 152 Da (galloyl moiety), and 134 Da (galloyl moiety losing a water molecule) [99, 141]. Eight trigalloyl hexose isomers (**41**, **52**, **60**, **75**, **82**, **85**, **88**, **102**) were detected displaying the  $[M-H]^-$  ion at  $m/z$  635. The fragment ions  $[M-H-170]^-$  at  $m/z$  465 and  $[M-H-170-152]^-$  at  $m/z$  313 were generated by the cleavage of a gallic acid and a galloyl moiety, respectively. Compounds **96**, **105**, **110**, and **120** presented  $[M-H]^-$  ions at  $m/z$  787 and based on the literature, were characterized as tetragalloyl hexose isomers, while pentagalloyl hexose isomers (**118**, **123**, **128**, **138**) exhibited their  $[M-H]^-$  ion at  $m/z$  939 (Fig. 13). Gallotannins dominated in extracts of leaf, female, and male flower samples prepared with the (relatively) polar solvent methanol, due to them being polyhydroxylated.

Ellagitannins (**E**, Table 3) contain HHDP groups attached via ester linkage to a polyol core (e.g., glucose). These compounds were identified by the representative presence of the ellagic acid fragment ion at  $m/z$  301, the monogalloyl hexose fragment ion at  $m/z$  331, and the ellagic acid hexoside fragment ion at  $m/z$  463 [99, 103, 113].

Compounds **6**, **20**, **23**, **30**, **38**, **43**, **51**, and **84** with  $[M-H]^-$  ions at  $m/z$  633, identified as galloyl-HHDP hexose isomers, and galloyl-bis-HHDP hexoses (**40**, **50**, **66**, **77**, **81**, **90**) with  $[M-H]^-$  ions at  $m/z$  935 were found in the methanolic extracts of bark and flower samples. Three digalloyl-HHDP hexoses (**37**, **61**, **134**) exhibited the  $[M-H]^-$  ion at  $m/z$  785, and five trigalloyl-HHDP hexose isomers (**89**, **109**, **127**, **129**, **144**) with the  $[M-H]^-$  ion at  $m/z$  937 were identified [131].

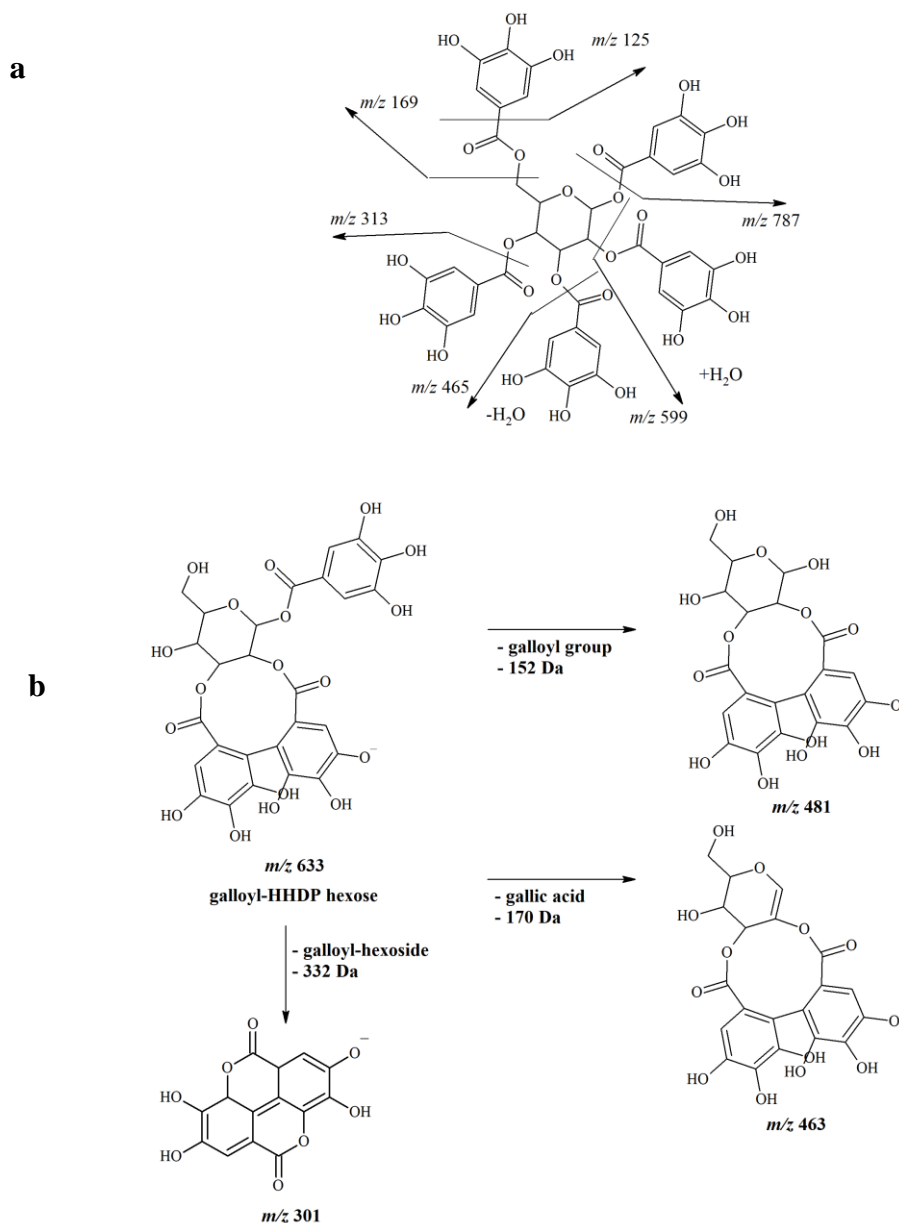


**Figure 13.** (–)-ESI-MS/MS-fragmentation of hydrolysable tannins: (a) fragmentation of pentagalloyl hexose (**118**, **123**, **128**, **138**), (b) fragmentation of galloyl-HHDP hexose (**6**, **20**, **23**, **30**, **38**, **43**, **51**, **84**) [141]

Glycosylated and methoxy-substituted hydroxybenzoic acid derivatives (**B**, Table 3) were present primarily in the methanolic extract of the bark sample. Their typical fragment ions included the dihydroxybenzoic acid moiety at  $m/z$  153 and its fragment ion at  $m/z$  109, yielded by the cleavage of the CO<sub>2</sub> group [99]. In contrast to hydroxybenzoic acids, hydroxycinnamic acid derivatives (**C**, Table 3) were representative of leaf, female, and male catkin samples. Similarly to the galloylquinic acids, the relative intensities of fragment ions in the mass spectra of the cinnamoylquinic acid isomers could facilitate their differentiation. Thus, the abundant fragment ion at  $m/z$  191 indicated the identification of **65** as 5-*O*-caffeoylquinic acid, **91** as 5-*p-O*-coumaroylquinic acid, and **116** as 5-*O*-feruloylquinic acid [97]. The minor components **83**, **111**, and **132** displayed identical fragmentation patterns. According to the results of Jaiswal et al. [97], these compounds eluting at higher retention times were assumed as the more hydrophobic *cis* isomers of the corresponding 5-*O*-caffeoyl-, 5-*O*-coumaroyl-, and 5-*O*-feruloylquinic acids, respectively [131].

In accordance with previous studies [3, 10], flavonol and flavone derivatives occurred in the flower and leaf extracts (**F**, Table 3) mainly in their glycosidic form. Cleavage of a hexose, a deoxyhexose, or a pentose sugar moiety during the collision-induced dissociation (CID) of flavonoid glycosides resulted in neutral losses of 162, 146, and 132 Da, respectively [119]. The glycosylation site of flavonol glycosides could also be deduced. Flavonol-3-*O*-glycosides favor the homolytic cleavage of the saccharide moiety during their CID in negative ionization mode. Thus, the relative abundance of the radical aglycone ion  $[Y_0-H]^{-\bullet}$  (deriving from a homolytic cleavage) was higher in their mass spectra than that of the aglycone anion  $[Y_0]^-$  [124]. Peak **155** presenting the  $[M-H]^-$  ion at  $m/z$  463 was identified as myricetin-3-*O*-deoxyhexoside, based on the relative abundance of its  $[M-H-147]^{-\bullet}$  ion at  $m/z$  316. Analogously, **135** and **153** displayed their  $[M-H]^-$  ions at  $m/z$  479 and 449, respectively, and the  $[M-H-163]^{-\bullet}$  and  $[M-H-133]^{-\bullet}$  ions at  $m/z$  316. Therefore, **135** and **153** were identified as myricetin-3-*O*-hexoside and myricetin-3-*O*-pentoside, respectively. Quercetin- and kaempferol-3-*O*-monoglycoside derivatives (**160**, **163**, **169**, **176**, **177**, **191**) were characterized similarly [118-121, 125, 129, 130].

Compounds **185** and **186** showed complex UV spectra with absorption maxima at 267, 317, and 345 nm. In their mass spectra, two successive losses of 146 Da and the

aglycone anion at  $m/z$  285 could be observed, thus, the constituents were supposed to be kaempferol-dideoxyhexoside isomers. However, as a result of a more rigorous analysis, one of the 146 Da losses was later characterized as a coumaroyl moiety (coumaric acid–H<sub>2</sub>O). This presumption was confirmed by the presence of the fragment ion at  $m/z$  163, which could be assigned to the [M–H]<sup>–</sup> ion of coumaric acid. Thus, **185** and **186** were established as kaempferol-deoxyhexoside coumaroyl ester isomers [128, 131].

Methoxylated flavones as well as their glycosylated and sulfated derivatives were detected in bark samples. Neutral losses of 15 Da referred to the cleavage of methyl radicals (–CH<sub>3</sub><sup>•</sup>) indicating the presence of methoxy groups in the molecule [127]. Accordingly, compound **179** exhibiting fragment ions at  $m/z$  315 and 300 was assumed as a methoxyflavone derivative. Constituents **159**, **181**, and **183** presented fragment ions at  $m/z$  328, 313, and 298 which denoted the cleavage of two methyl radicals, thus, these compounds were characterized as dimethoxyflavone derivatives. Similarly, compounds **188** and **190** with [M–H]<sup>–</sup> ions at  $m/z$  343 and fragment ions at  $m/z$  328, 313, 298 were identified as trimethoxyflavones. Both **174** and **158** displayed a neutral loss of 80 Da which indicated the cleavage of a SO<sub>3</sub> moiety [122], therefore, they were recorded as trihydroxy-dimethoxyflavone-*O*-sulfate and its pentoside, respectively [131].

Constituents **48** and **54** exhibiting [M–H]<sup>–</sup> ions at  $m/z$  289 were identified as flavan-3-ol derivatives catechin or epicatechin, due to their typical fragment ion [M–H–CO<sub>2</sub>]<sup>–</sup> at  $m/z$  245, deriving from the decarboxylation of catechin or epicatechin from the rearrangement of the A ring [11, 142]. Compound **115** with its pseudomolecular ion at  $m/z$  305 and [M–H–OH–CO<sub>2</sub>]<sup>–</sup> ion at  $m/z$  245 was referred to as galocatechin or epigallocatechin. Peaks **107** and **152** presenting their [M–H]<sup>–</sup> ions at  $m/z$  441 and fragment ions at  $m/z$  289, 245, 169, and 125 were tentatively characterized as catechin gallate or epicatechin gallate [99].

The UV spectra of several constituents (**D**, Table 3) were similar to those of gallic acid derivatives ( $\lambda_{\text{max}} = 280\text{--}290$  nm), however, their mass spectra did not display the characteristic fragment ions at  $m/z$  169 and 125. Although cyclic diarylheptanoids, also exhibiting intense UV absorption in this range, have not yet been detected in *C. betulus*, we hypothesized their presence due to their occurrence in other *Carpinus* species [8]. The mass spectra of compounds **106**, **114**, **149**, **154**, **157**, **161**, and **187** showed a fragmentation pattern analogous to that of other diarylheptanoids [128]: a base peak at

$m/z$  269 and a fragment ion at  $m/z$  211. Results from the structural elucidation of the isolated compounds by HR-MS and NMR later confirmed the presumed cyclic diarylheptanoid structures (see Section V.2.1.). In parallel to the isolated constituents, compounds **94**, **103**, **108**, **119**, **124**, **136**, **140**, **143**, **171**, and **173** also exhibited typical fragment ions at  $m/z$  269 and 211, thus, we assumed their structures as cyclic diarylheptanoids, too [131].

Furthermore, **74**, **139**, **145**, and **164** were characterized as linear diarylheptanoids, previously unprecedented in *Carpinus* species. The deprotonated molecular ion  $[M-H]^-$  of **164** was detected at  $m/z$  313 and its typical fragment ions at  $m/z$  207, 163, 149 (Fig. 14), thus the component was indicated as 5-hydroxy-1,7-bis-(4'-hydroxyphenyl)-3-heptanone (i.e., 5-hydroxy-3-platyphyllone).

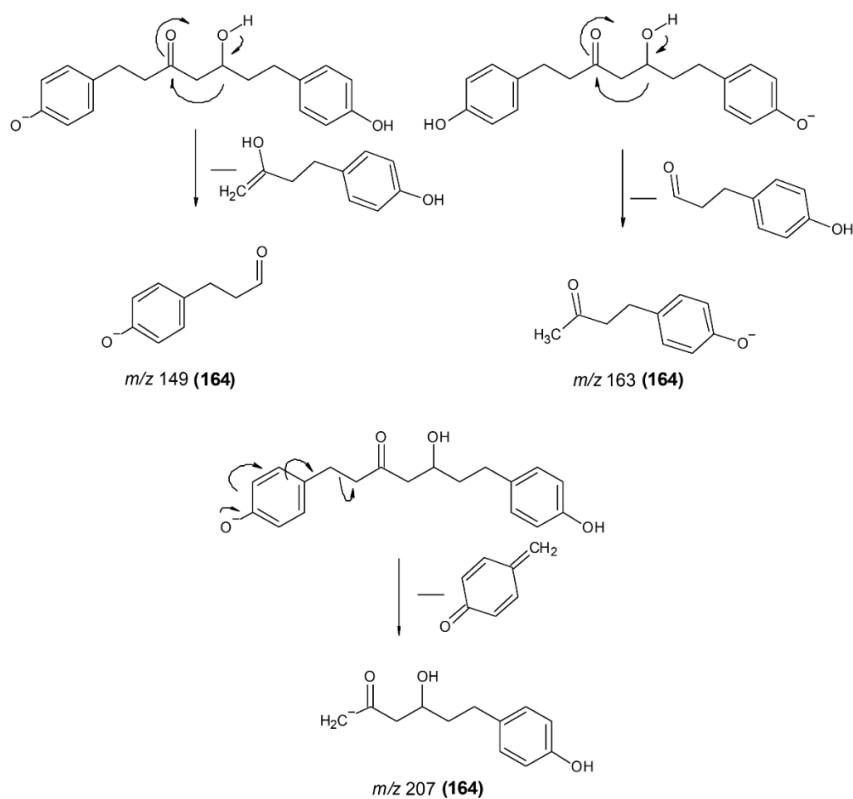


**Figure 14.** Proposed mass spectrometric fragmentation pathway of the linear diarylheptanoid 5-hydroxy-3-platyphyllone (**164**)

Compound **145** presented a neutral loss of 150 Da, while peaks **74** and **139** showed a neutral loss of 180 Da, indicating the cleavage of a pentose and a hexose moiety from the hydroxyl group on the linear  $C_7$ -chain, respectively [24]. Based on these data, **145**

was tentatively characterized as oregonin, while compounds **74** and **139** were denoted as linear diarylheptanoid hexosides [131].

The UV spectrum of **148** was similar to those of diarylheptanoids or gallic acid derivatives, however, their characteristic fragment ions at  $m/z$  211 or 169 were not presented in the mass spectrum of **148**. According to the neutral losses observed during the CID of **148**, the presence of a deoxyhexose moiety  $[M-H-146]^-$ , a hydroxyl group connected to a saturated chain  $[M-H-146-18]^-$ , and two methoxy groups  $[M-H-146-18-15-15]^-$  could be deduced. However, further conclusions could not be drawn, therefore, NMR analysis was necessary to determine the structure of **148** (see Section V.2.2.).

## V.2. Structural Elucidation of the Isolated Compounds

In order to unambiguously identify their structures, eight diarylheptanoids (**106**, **114**, **149**, **154**, **157**, **161**, **164**, **187**), three flavonoids (**177**, **185**, **191**), and one lignan (**148**) were isolated by C<sub>18</sub> flash chromatography followed by multiple successive C<sub>18</sub> semi-preparative HPLC separations from the bark extracts. Their structures were established by 1D and 2D NMR experiments as well as HR-ESI-MS (Orbitrap MS) analyses. Fig. 15 presents the structures of the isolated constituents, Table 4 summarizes the high-resolution mass spectrometric data of the diarylheptanoid-type compounds, while their <sup>1</sup>H NMR and <sup>13</sup>C NMR data are shown in Tables 5-7 [131].

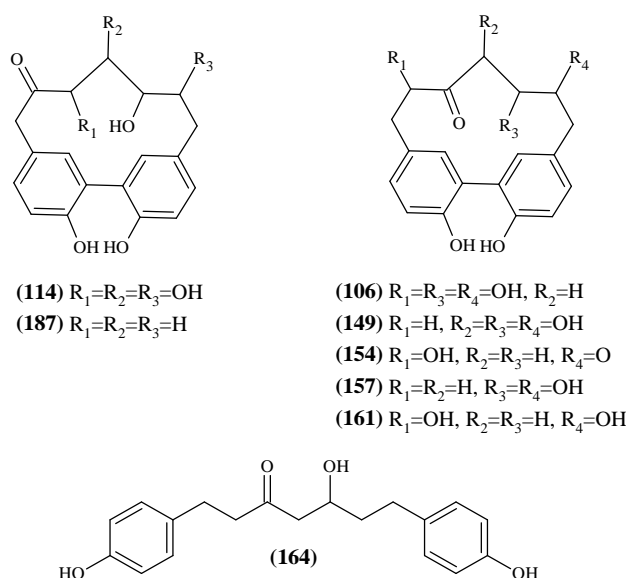


**Figure 15.** The structures of the isolated diarylheptanoids

### V.2.1. Structural Elucidation of the Isolated Diarylheptanoids

The  $^1\text{H}$  and  $^{13}\text{C}$  NMR spectra of **106** and **149** were similar to each other indicating isomeric structures of cyclic diarylheptanoids. Both structures contained one carbonyl, three oxymethine, and three methylene groups in the aliphatic chain. Based on the correlations of the 2D spectra, both **106** and **149** possess the carbonyl group in C-9 position, while the three hydroxyl groups were located at positions C-8, C-10, C-12 or C-10, C-11, C-12, respectively (Table 5). Based on literature data [8], **106** and **149** were identified as carpinontriols A and B, respectively.

In the case of compound **114**, the  $^1\text{H}$  NMR resonances confirmed the macrocyclic diaryl structure. However, the resonance assignment of the aliphatic chain failed in  $\text{CD}_3\text{OD}$  at 295 K, due to the minute amount of the isolated compound. Compared to the literature [74], all the detected  $^1\text{H}$  and  $^{13}\text{C}$  resonances were in good agreement with that of giffonin U.

The  $^1\text{H}$  NMR spectrum of compound **157** indicated the presence of two 1,2,4-trisubstituted aromatic rings. The resonances at  $\delta$  4.47 (dd,  $J = 11.4, 4.0$  Hz, 1H, H-12) and 4.20 (m, 1H, H-11) ppm revealed the presence of two oxymethine groups. In addition, eight more aliphatic resonances recommended the presence of four methylene units. The  $^{13}\text{C}$  NMR spectrum showed one carbonyl resonance at  $\delta$  212.0 ppm. Based on these data, the structure of **157** was established as 11-oxo-3,8,9,17-tetrahydroxy-[7,0]-metacyclophane (giffonin X) [73].

The aromatic resonances in the  $^1\text{H}$  NMR spectrum of **161** indicated a macrocyclic diaryl structure, while the resonances in the aliphatic region suggested the presence of four methylene and two oxymethine groups (at 4.39 and 4.04 ppm, respectively) in the heptane chain. Furthermore, the  $^{13}\text{C}$  spectrum indicated the presence of a carbonyl group ( $\delta$  220.1 ppm). Based on additional 2D correlations, the hydroxyl groups are located at the C-8 and C-12 positions, while the carbonyl group is located at the C-9 position. This structure was previously published in the literature as casuarinondiol [8].

The  $^1\text{H}$  spectrum of compound **154** in  $\text{DMSO}-d_6$  at 295 K showed very broad unresolved resonances, without any coupling patterns, therefore no structural information could be deduced. After the addition of trifluoroacetic acid and recording the spectra at higher temperatures (at 335 K and 370 K), the  $^1\text{H}$  spectrum showed the characteristic pattern of cyclic diarylheptanoid resonances in the aromatic region. However, the

aliphatic resonances could not be assigned due to significantly broad resonances. Nevertheless, comparing the NMR data with those found in the literature [44], the 3,12,17-trihydroxytricyclo[12.3.1.1<sup>2,6</sup>]nonadeca-1(18),2(19),3,5,14,16-hexaene-8,11-dione structure was proposed for compound **154**.

The <sup>1</sup>H NMR spectrum of **187** showed aromatic resonances at  $\delta$  7.05 (dd, <sup>3</sup>J<sub>H,H</sub> = 8.3 Hz, <sup>4</sup>J<sub>H,H</sub> = 2.5 Hz, 1H, H-5), 7.04 (dd, <sup>3</sup>J<sub>H,H</sub> = 8.3 Hz, <sup>4</sup>J<sub>H,H</sub> = 2.5 Hz, 1H, H-15), 6.80 (d, <sup>3</sup>J<sub>H,H</sub> = 8.3 Hz, 1H, H-4), 6.78 (d, <sup>3</sup>J<sub>H,H</sub> = 8.3 Hz, 1H, H-16), 6.79 (d, <sup>4</sup>J<sub>H,H</sub> = 2.5 Hz, 1H, H-18), and 6.60 (d, <sup>4</sup>J<sub>H,H</sub> = 2.5 Hz, 1H, H-19) ppm. These two separated ABX coupling patterns (also confirmed by 2D COSY experiment) indicated the presence of two 1,2,4-trisubstituted aromatic rings. The <sup>1</sup>H resonance at  $\delta$  4.20 (m, 1H, H-11) ppm and its HSQC correlation to <sup>13</sup>C resonance at  $\delta$  67.4 ppm revealed the presence of an oxymethine group. In addition, the aliphatic resonances at 3.19 (m, 1H, H-9a), 3.02 (dd, <sup>2</sup>J<sub>H,H</sub> = 13.2 Hz, <sup>3</sup>J<sub>H,H</sub> = 3.6 Hz, 1H, H-10a), 2.99 (m, 2H, H-7), 2.90 (m, 1H, H-9b), 2.88 (m, 2H, H-13), 2.68 (m, 1H, H-10b), 2.46 (m, 1H, H-12a), and 1.80 (m, 1H, H-12b) ppm along with their HSQC correlations recommended the presence of five methylene units. Four of these -CH<sub>2</sub> units constitute a spin system with that of the oxymethine resonance. The <sup>13</sup>C NMR spectrum revealed a carbonyl resonance at  $\delta$  212.0 ppm, which separates the additional methylene unit from that of the aforementioned spin system confirming a heptane skeleton. Thorough inspection of the HMBC crosspeaks revealed that the carbonyl group is located at the C-8 position while the hydroxyl can be placed at position C-11. Further HMBC correlations between the aromatic rings confirmed the cyclic diarylheptane skeleton, therefore compound **187** could be assigned as 3,11,17-trihydroxytricyclo[12.3.1.1<sup>2,6</sup>]nonadeca-1(18),2(19),3,5,14,16-hexaen-8-one, a newly isolated and identified diarylheptanoid. The structures of the isolated *meta,meta*-cyclophane diarylheptanoids are shown in Figure 15 [131].

The <sup>1</sup>H NMR spectrum of compound **164** indicated the presence of two *para*-substituted aromatic rings. The resonance at  $\delta$  4.00 (m, 1H, H-5) ppm suggested the presence of one oxymethine group. Furthermore, five methylene units were identified. The <sup>13</sup>C NMR spectrum showed a single carbonyl resonance at  $\delta$  211.9 ppm. Based on all these information, a linear diarylheptanoid structure was proposed. The 2D spectra determined the position of the carbonyl group at C-3 and the hydroxyl group at C-5. The <sup>1</sup>H and <sup>13</sup>C resonances were analogous to literature data [143], thus, **164** (Fig. 15) was

identified as 5-hydroxy-1,7-bis-(4'-hydroxyphenyl)-3-heptanone (i.e., 5-hydroxy-3-platyphyllone).

After revealing the exact structures of the cyclic diarylheptanoids, our aim was to study their fragmentation mechanisms by HR-MS and propose possible fragmentation pathways. The proposed mass spectrometric fragmentation pathways of the isolated cyclic diarylheptanoids are shown in Fig. 16 [131].

The mass spectra of compounds **106** and **149** showed a fragmentation pattern similar to that previously described for hazelnut diarylheptanoids [128]. The base peak at  $m/z$  269 was ascribed to a rearrangement of the deprotonated compound and the subsequent opening of the diarylheptanoid cycle, resulting in the neutral loss of a hydroxy-propan-2-one unit. However, the formation of further typical fragment ions has not been reported in the literature. According to our ESI-MS/MS experiments, the presence of the fragment ion at  $m/z$  211 seems to be universal among cyclic diarylheptanoids with a *meta,meta*-cyclophane structure.

Analogously to the above mentioned, after a rearrangement of the pseudomolecular ion and the subsequent cleavages of two C-C bonds (C7-C8 and C12-C13), a neutral loss of a diversely hydroxylated oxopentanal (**106**, **149**, **161**, **157**), and pentenal (**114**, **187**), or oxopentanedial (**154**) molecule occurs which results in the formation of the fragment ion at  $m/z$  211. Similarly, the cleavages of two C-C bonds (C7-C8 and C9-C10) lead to the neutral loss of an ethenol or ethene-diol unit. This results in the formation of the additional characteristic fragment ions at  $m/z$  299 (**114**), 283 (**106**, **149**) or 267 (**157**, **187**).

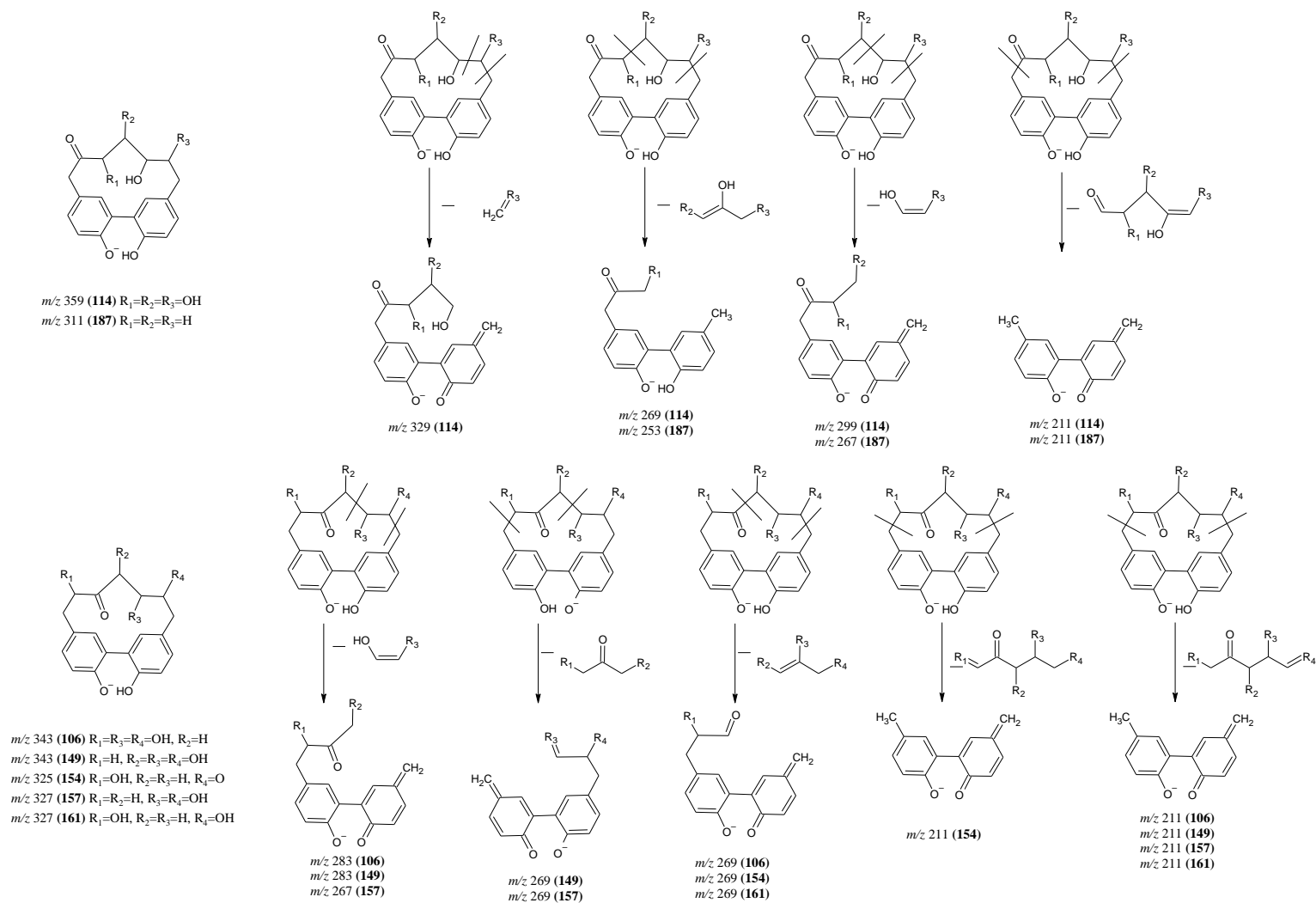


**Figure 16.** Proposed mass spectrometric fragmentation pathways of cyclic diarylheptanoids

### V.2.2. Structural Elucidation of the Isolated Flavonoids

NMR analysis of the isolated **185** confirmed the proposed structure as kaempferol-3-*O*-(4''-*E*-*p*-coumaroyl)-rhamnopyranoside by comparing the NMR spectroscopic data ( $^1\text{H}$  and  $^{13}\text{C}$  resonances) with those found in the literature [144]. The coupling constant of the two olefinic  $^1\text{H}$  resonances suggested *trans* configuration of the double bond. Based on their  $^1\text{H}$  NMR spectra, compounds **191** and **177** were identified as kaempferol-3-*O*-rhamnoside (afzelin) and quercetin-3-*O*-rhamnoside (quercitrin) (Fig. 17), respectively. The  $^1\text{H}$  resonances were similar to those published earlier [145].

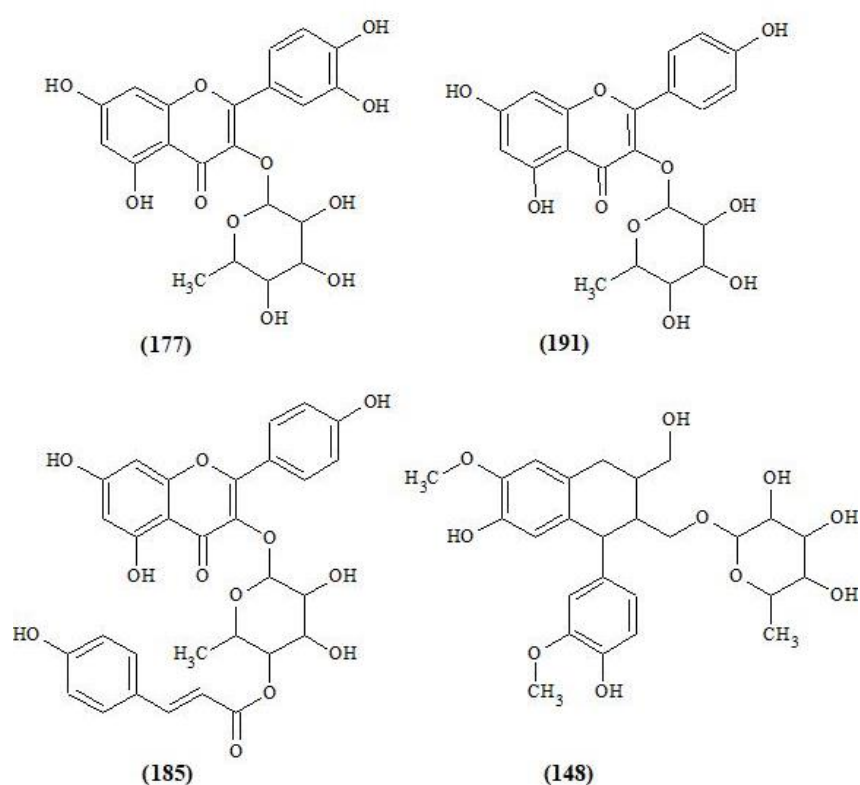


**Figure 17.** The structures of the isolated flavonoid and lignan derivatives

### V.2.2. Structural Elucidation of the Isolated Lignan

Based on the  $^1\text{H}$ ,  $^{13}\text{C}$ , and additional 2D spectra, compound **148** was identified as a lignan glycoside, aviculin (Fig. 17). The NMR spectra were identical to those of a previous report [132]. Presence of lignan-type compounds in *Carpinus* species was established for the first time.

### V.3. Evaluation of the Antioxidant Activity

#### V.3.1. DPPH Assay

Antioxidant activities of hornbeam extracts (bark, leaf, female, and male catkins) prepared with methanol were significantly different ( $p < 0.001$ ) as compared with those of the ethyl acetate extracts (results are shown in Fig. 18), however, a trend in relation to the extraction solvent could not be found. Overall, the leaf methanol extract showed the best antioxidant capacity, while the male catkin methanol extract was also effective. Both samples exhibited radical scavenging activities similar to those of the well-known antioxidant compounds quercetin and trolox. Our results correspond with literature data, where *C. betulus* leaf and bark extracts showed medium to high DPPH neutralizing activity [3, 146].

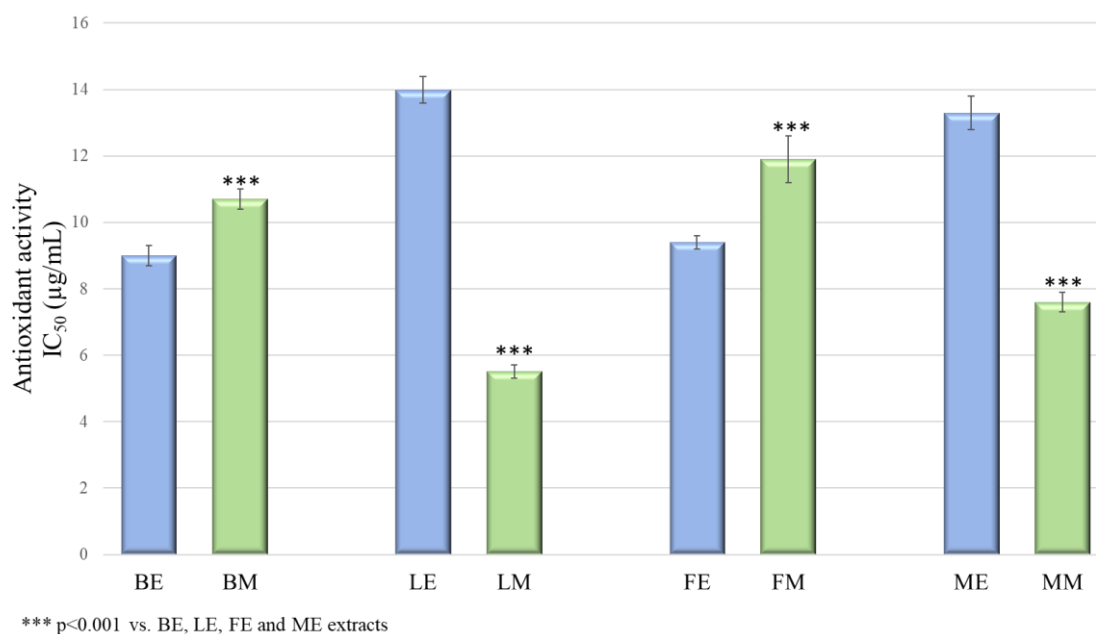


**Figure 18.** DPPH scavenging activity of *C. betulus* extracts prepared with solvents of different polarity. Values are means  $\pm$  SD. \*\*\*  $p < 0.001$  compared with ethyl acetate extracts. Abbreviations: BE: bark ethyl acetate extract, BM: bark methanol extract, LE: leaf ethyl acetate extract, LM: leaf methanol extract, FE: female catkin ethyl acetate extract, FM: female catkin methanol extract, ME: male catkin ethyl acetate extract, MM: male catkin methanol extract

The antioxidant activities of the constituents isolated from *C. betulus* samples were also investigated. In accordance with literature data, the potent antioxidant activity of quercitrin (**177**) was comparable to other quercetin glycosides', like rutin. On the other hand, afzelin (**191**), carpinontriols A (**106**) and B (**149**), casuarinondiols (**161**), and 5-hydroxy-3-

platyphyllone (**164**) showed weak radical scavenging activity [8, 147, 148]. According to literature data, coumaroyl flavonol glycosides show potent free radical scavenging activity [149]. However, kaempferol-3-*O*-(4"-*E-p*-coumaroyl)-rhamnoside (**185**) exhibited no radical scavenging activity at the concentration of 250 µg/mL. Although some of its structural characteristics such as the lack of unsubstituted OH groups (due to the absence of the catechol group in the B ring and the glycosylation at C3-OH) may result in a lower scavenging capacity, these cannot explain the contradiction with the literature. To the best of our knowledge, the DPPH scavenging activity of aviculin (**148**, IC<sub>50</sub> = 23.8 ± 0.9 µg/mL) and giffonin X (**157**, IC<sub>50</sub> = 138 ± 11 µg/mL) was determined for the first time [131].

### V.3.2. DPPH-HPLC-DAD Analysis

The contribution of each antioxidant constituent to the total radical scavenging activity of *C. betulus* extracts (bark, leaf, female, and male catkins) was assessed by a DPPH-HPLC-DAD-MS method. According to the results of our HPLC-MS/MS analyses, the leaf sample was dominated by the presence of gallic acid derivatives and ellagitannins. It was presumed that galloyl hexoses of different polymerization degrees as well as galloyl-HHDP hexose derivatives could contribute significantly to the total antioxidant activity (Table 10), since they are well known for their strong radical scavenging effect [150]. The increasing number of galloyl moieties in the constituents correlated with higher antioxidant capacities. Monogalloyl hexoses (e.g., **4** and **11**) exerted lower reduction in peak intensities as compared to tri-, tetra-, or pentagalloyl hexose isomers (e.g., **85**, **105**, and **138**, respectively). On the other hand, digalloylshikimic acid isomers (**87** and **99**), and digalloylquinic acid (**58**) showed lower reduction in AUC values as compared to their monogalloyl counterparts (e.g., **34** and **16**, respectively). In case of ellagitannins, the galloyl:HHDP rate of the compounds determined the antioxidant capacity. In accordance with literature data [151], galloyl-bis-HHDP hexose isomers (e.g., **40**, **50**, **81**) did not show antioxidant activity as compared to galloyl-HHDP hexoses (e.g., **38**, **43**, **51**, **84**). Flavonol glycosides, and in particular quercetin derivatives, prevailed in *C. betulus* extracts. The aglycone quercetin (**192**) bears all structural criteria of a potent antioxidative compound [150]. However, in case of other flavonol derivatives, the glycosylation of the C3-OH group (e.g., **163** and **177**), the methylation of free hydroxyl groups (e.g., **179** and **188**), or the lack of a catechol moiety in B ring (e.g., **160** and **191**) resulted in lower free radical scavenging activities. Hydroxycinnamic acid derivatives bearing two hydroxyl groups in the *ortho* position (caffeic acid derivatives, **65** and **83**) showed higher radical scavenging ability than those containing only one hydroxyl group (coumaric acid

derivatives, **111**). Methylation of hydroxyl groups in ferulic acid derivatives (**116** and **132**) also leads to the reduction in the radical scavenging activity [150]. In agreement with literature data [8] and our results from the radical scavenging assay of the isolated compounds, diarylheptanoids in the *C. betulus* extracts (**114**, **143**, **149**) exhibited moderate antioxidant effect [131].

#### V.4. Quantitative Analysis of the Main Diarylheptanoids in *Carpinus betulus* Bark

Quantities of the four major diarylheptanoid compounds in hornbeam bark and male catkin methanol and ethyl acetate extracts ranged from 3.55 to 19.13 mg/g dry extract, results are shown in Table 13. Carpinontriol B (**149**) was present in all bark and male catkin extracts, being the most abundant diarylheptanoid of male catkin samples. Carpinontriol A (**106**) was the chief diarylheptanoid in both bark extracts, while in bark ethyl acetate samples, giffonin X (**157**) was present in the second highest concentration.

#### V.5. Stability Studies

The chemical stability of the main *meta,meta*-cyclophanes (**106**, **149**, **154**, and **157**) was also investigated. The effect of the medium, i.e., the pH value, the solvent, and the accompanying compounds in the extracts, as well as the influence of the storage time and temperature was studied.

##### V.5.1. Evaluation of Aqueous Stability at Different pH Values

3,12,17-Trihydroxytricyclo[12.3.1.1<sup>2,6</sup>]nonadeca-1(18),2(19),3,5,14,16-hexaene-8,11-dione (**154**) was stable only at pH 7.4 after 81 h, while in agreement with our recent results [38], carpinontriol B (**149**) remained intact for the whole study at all pH values (Table 14). Therefore, rate constants and half-lives in these cases have not been determined. At pH 6.8, the amount of compound **154** decreased significantly after 81 h (final concentration  $88.9 \pm 2.0\%$ ), while at pH 1.2, its degradation was more significant both after 9 and 81 h (with final concentrations of  $68.5 \pm 4.5\%$  and  $31.0 \pm 7.0\%$ , respectively). Thus, degradation of **154** was remarkably faster at the lower pH values; the half-lives at pH 6.8 and 1.2 differed by one order of magnitude (487.7 h and 54.4 h, respectively) (Table 15).

The concentration of carpinontriol A (**106**) did not show significant changes at pH 1.2 and pH 7.4 after 9 h; however, at the end of the experiment, it displayed significant decomposition ( $p < 0.05$ ; final concentrations were  $70.5 \pm 2.6\%$  and  $71.5 \pm 5.2\%$  at pH 1.2 and

pH 7.4, respectively). At pH 6.8, compound **106** was not only unstable after 81 h, but already after 9 h (with final concentrations of  $75.3 \pm 3.0$  and  $97.4 \pm 1.5\%$ , respectively) (Table 14).

At pH 7.4, giffonin X (**157**) decomposed significantly already after 9 h. On the other hand, its concentration decreased significantly only after 81 h at pH 6.8 and pH 1.2 (with final concentrations of  $93.2 \pm 2.0\%$  and  $83.4 \pm 5.3\%$ , respectively). Interestingly, degradation rate constant of **157** was still by one order of magnitude higher at pH 1.2 than at pH 6.8, the compound was the most stable at a pH value of 6.8 ( $t_{1/2} = 826.8$  h) (Tables 14-15).

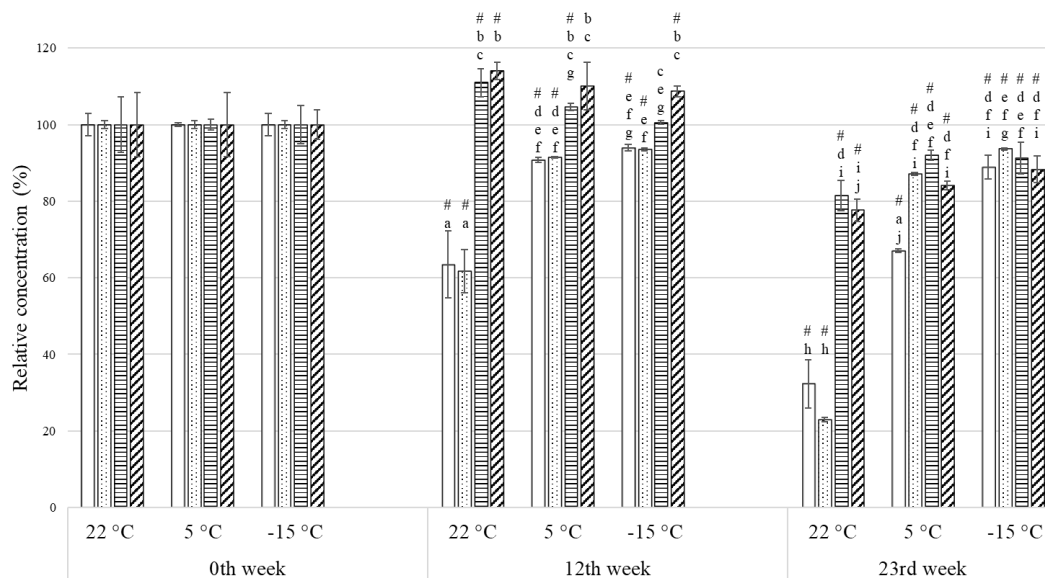
Although compounds **106** and **149** are structural isomers, their stability differs significantly, with **149** staying stable throughout the whole study. The increased stability of compound **149** may be attributed to the electronic stabilization effect of its vicinal triol moiety that may stabilize the compound's structure. On the other hand, both compounds **106** and **157** comprise a vicinal diol group that may make them prone to undergo pinacol rearrangement [152], especially in an acidic medium. On the contrary, according to the literature data, phenolic compounds are more stable at lower pH values [153]. Nevertheless, the pH of the medium did not significantly influence stability of **106** during our investigation, while for compound **157**, the highest pH value influenced the stability negatively. In the case of component **154**, pH 1.2 differed significantly from the other two pH values; pH 7.4 and pH 6.8 provided better stability. However, no generally prevalent correlation could be determined between the pH values of the medium and the degradation kinetic parameters [154].

### ***V.5.2. Evaluation of Storage Stability***

The methanol and aqueous solutions (SM and SA) of the isolated compounds **149** and **154** did not show significant differences when comparing the initial concentration data with values of weeks 12 and 23 (Table 16). Based on this and the lack of degradation products in their chromatograms, **149** and **154** were considered to be stable. The amount of compound **154** increased when being present in methanol and ethyl acetate extracts (EM and EE) that also comprise further accompanying constituents. This elevation can be explained by the degradation of component **106** that was converted into **154** (see Section V.5.3.).

In case of the SM and SA solutions of the isolated compounds **106** and **154**, samples showed statistical differences both in the mid- and long-term studies when compared to the initial concentration values. Therefore, the effects of the temperature and the medium on the stability of these compounds were examined; results are shown in Table 16 and Fig. 19 [154].

a) compound 106



b) compound 157

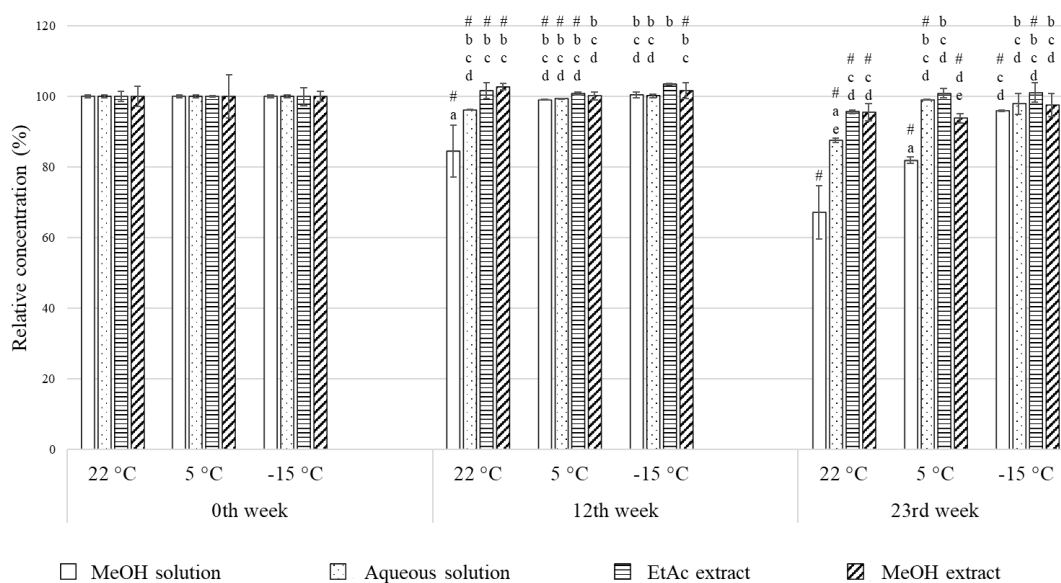


**Figure 19.** Chemical stability of **106** and **157** as a function of time, temperature, and solvent. Concentrations of compounds are relative (%) values compared to the initial value. Values for individual compounds with identical lower case letters (a-j) are not significantly different ( $p < 0.05$ ); #  $p < 0.05$  compared with the initial samples.

Abbreviations: MeOH: methanol; EtAc: ethyl acetate.

After 12 weeks of storage, the concentrations of compound **106** in its methanol and aqueous solutions showed significant differences when stored at 22 °C, as compared to the samples stored at 5 °C. No significant concentration differences were detected for **106** between SA and SM samples stored at temperatures 5 °C and –15 °C. In the case of the methanol extract, the storage temperature did not influence the concentration of compound **106** after 12 weeks.

After 23 weeks of storage, the concentration of **106** decreased significantly in all solutions and extracts at all temperatures, when compared to the initial values. However, lower storage temperatures (both 5 and –15 °C) provided higher stability for the samples. Similarly, when stored for 23 weeks, the concentrations of **157** were statistically lower than the starting concentrations, except for the EE sample stored at 5 °C as well as the SA and EM samples stored at –15 °C.

Moreover, the concentration differences of **106** in the SM and SA solutions were significantly higher at all investigated temperatures than in the ME and EE extracts after 12 weeks of storage. The complex media of the bark extracts provided significantly higher stability in the medium-term at all studied temperatures for **106**. A similar pattern could also be observed at 22 °C after 23 weeks of storage, while both at 5 °C and –15 °C, a concentration decrease of **106** in the aqueous solution was equal to that in the ME and EE extracts.

The matrices of the bark extracts also allowed for appropriate stability for **157** at all storage temperatures after 12 weeks. In the long-term studies (after 23 weeks), the methanol solution (SM) of **157** showed significant concentration differences at higher storage temperatures (22 and 5 °C) when compared to the other media (SA, EM, and EE). The 23-week storage at 22 °C also intensified the degradation of **157** in the aqueous solution when compared to temperatures of 5 and –15 °C.

Analyzing the degradation kinetic parameters of the pure diarylheptanoids **106** and **157**, we can state that the  $k$  value decreases, and the  $t_{1/2}$  value increases as the temperature decreases (Table 17). The thermal degradation of **106** and **157** in aqueous and methanolic solutions follows first-order kinetics, in which the degradation rate depends on the temperature. Our results are in agreement with other studies that found that diarylheptanoids are prone to temperature-dependent degradation [137, 155].

Comparing the effects of the medium,  $k$  values of **106** were lower in the aqueous solution than in the methanolic solution (e.g.,  $4.47 \times 10^{-3}$  vs.  $1.40 \times 10^{-2}$  week<sup>-1</sup> at 5 °C, for SA and SM respectively) (Table 17). Thus, it was concluded that the aqueous medium provided higher stability. This effect was even more pronounced for compound **157**, e.g., calculated half-lives were 1386.29 vs. 97.63 weeks at 5 °C in aqueous and methanolic solution, respectively [154].

### V.5.3. Characterization of the Degradation Products by UHPLC-HR-MS/MS

The degradation products formed in the stability studies were characterized by UHPLC-HR-MS, data are presented in Table 18. In case of carpinontriol A (**106**) and giffonin X (**157**), new compounds **106c** and **157a** appearing in the chromatograms presented molecular ions bearing  $m/z$  values 18 Da less than the pseudomolecular ions of the original compounds (Fig. 20A and 20B.). The deprotonated molecular ions  $[M-H]^-$  of **106c** and **157a** (at  $m/z$  325.1076 and  $m/z$  309.1127, respectively), refer to the elimination of a water molecule from their corresponding parent compounds **106** ( $m/z$  343.1191) and **157** ( $m/z$  327.1240). In Fig. 21, two possible degradation pathways are depicted for both **106** and **157**, highlighting the characteristic structural differences of the hypothetical products.

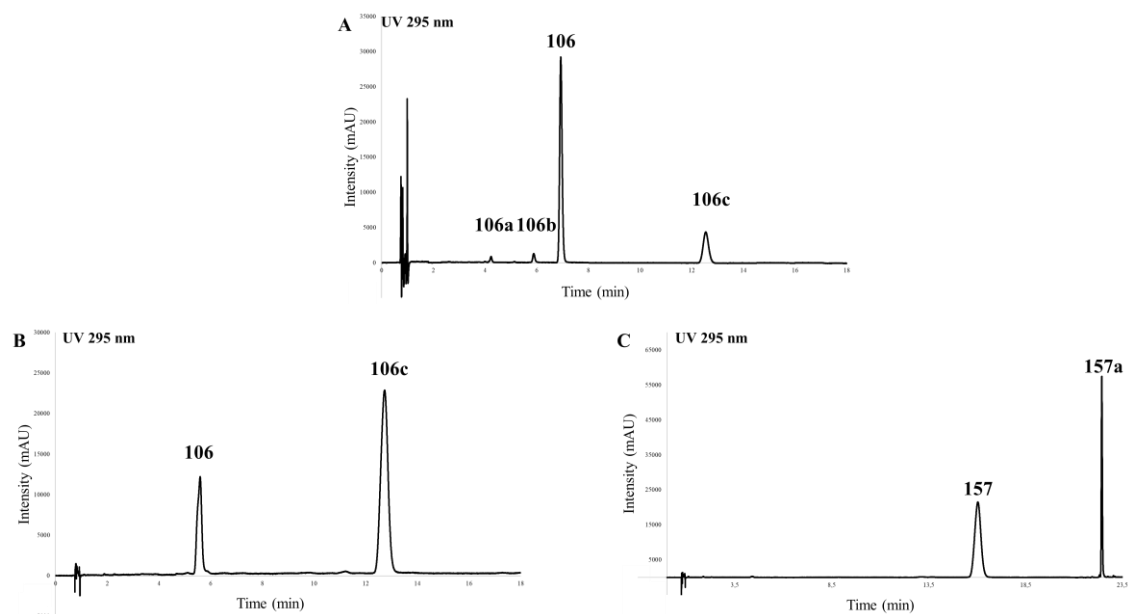
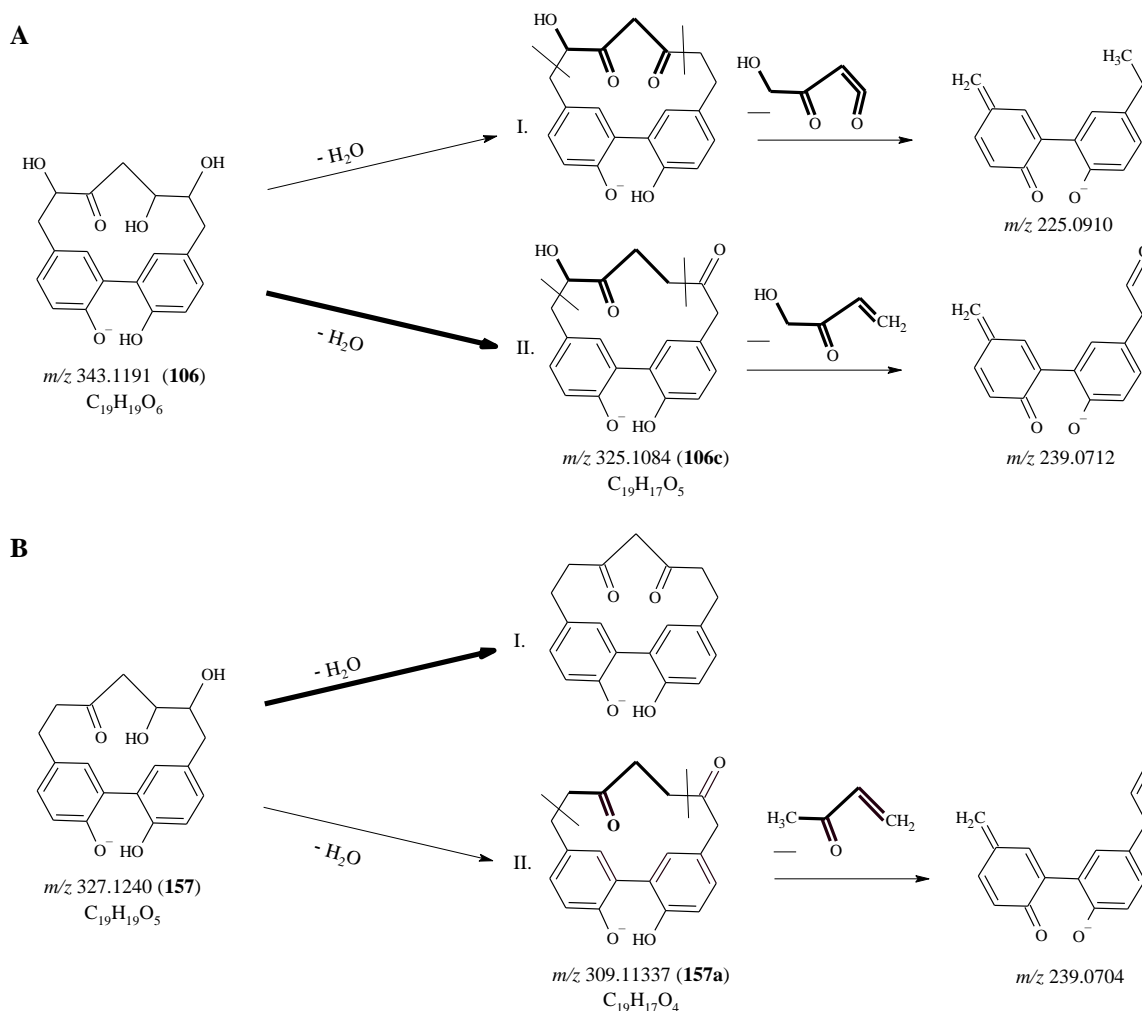


Figure 20. UHPLC-DAD chromatograms of compounds **106** and **157** and their degradation products obtained during the stability studies: (A) carpinontriol A (**106**) after 81 hours at pH 1.2; (B) methanol solution of carpinontriol A (**106**) after 23 weeks at 22 °C; (C) methanol solution of giffonin X (**157**) after 23 weeks at 22 °C. Compound and degradation product numbers refer to Table 18.

As a common structural element, a vicinal diol group is present in the heptane chain of both compounds **106** and **157**, which may be the source of the cleaved water molecule. However, the proposed degradation can undergo through different pathways. The common vicinal diol moiety implies that the pinacol rearrangement is one possible pathway for both **106** and **157**, particularly in an acidic medium [152]. However, when the pH is neutral, there is only

a slight chance for the pinacol rearrangement to occur. At the same time, another possible mechanism is for example the radical oxidative degradation [156]. Nevertheless, there is also a possibility that both degradation pathways (or even other mechanisms) may occur at different pH values [154].



**Figure 21.** (A) The possible degradation pathways of carpinontriol A (**106**) and the proposed mass spectrometric fragmentation of the degradation product **106c**; (B) the possible degradation pathways of giffonin X (**157**) and the proposed mass spectrometric fragmentation of the degradation product **157a**. The more likely degradation pathways are highlighted by bold arrows. Degradation product numbers refer to Table 18.

Position of the cleavage of the water molecule could also be proposed, based on the mass spectrometric fragmentation pathway of cyclic diarylheptanoids [131]. The more likely degradation pathways have been highlighted in Fig. 21 by drawing bold arrows. In case of

compound **106** (Fig. 21A), the putative degradation product generated through pathway I would present a fragment ion at  $m/z$  225.0910, while pathway II would result in the formation of a degradation product showing a fragment ion at  $m/z$  239.0862. Unfortunately, the HR-MS spectrum of the degradation product **106c** presented both fragment ions, though with different intensities. Since the retention time and mass spectrum of compound **106c** corresponds with that of compound **154**, pathway II taking place seems to be more likely. This assumption was further affirmed by the observation that in hornbeam bark extracts the amount of **106** decreased, while that of **154** increased over time during the storage stability assays.

According to mass spectrometric fragmentation patterns of cyclic diarylheptanoids [131], only pathway II would result in the formation of a degradation product for compound **157**, which could present a characteristic fragment ion at  $m/z$  239.0704. However, this ion was not detected in the mass spectrum of the actual degradation product **157a**, thus, it was deduced that only pathway I could take place (Fig. 21B).

Although the common structural element of compounds **106** and **157** (i.e., the vicinal diol group) indicated that the same degradation pathway should take place for both **106** and **157**, our results did not confirm this. A possible explanation is the electronic stabilization effect, which may stabilize a compound's structure or shift the equilibrium toward a degradation product. For example, the stabilizing effect of the vicinal triol moiety may be responsible for the increased stability of carpinontriol B (**149**). Similarly, the additional vicinal diol moiety of compound **106** may alter the mechanism of degradation from that of compound **157**.

Two additional degradation products with the molecular formulas of  $C_{18}H_{17}O_8$  and  $C_{18}H_{17}O_7$  were detected in the chromatogram of **106**, referring to the loss of a carbon-containing moiety and further oxidation mechanisms (Table 18) (Fig. 20C). In case of compound **154**, degradation products were not detected, despite the significant decrease in the initial concentration (the final concentration of **154** at pH 1.2 was  $31.0 \pm 7.0\%$ ) [154].

## V.6. Parallel Artificial Membrane Permeability Assay (PAMPA) Studies

In the PAMPA-BBB experiments, only giffonin X (**157**) was detected in the acceptor phase. It also presented a calculated  $\log P_e$  value greater than  $-6.0$  ( $-5.92 \pm 0.04$ ), which indicates that **157** is capable of crossing the lipid membrane of the blood-brain barrier (Table 19) [157]. However, compound **157** was considered unstable ( $t_{1/2} = 81.6$  h) in the pH 7.4 medium of the PAMPA-BBB model, and its decomposition product could not be detected in the acceptor phase.

In the PAMPA-GI model, compound **154** with one of the lowest  $clog P$  values ( $0.94 \pm 0.46$ ) among the studied diarylheptanoids was not detected in the acceptor phase, suggesting that it is unable to cross the lipid membrane of the gastrointestinal tract. Compounds **106**, **149**, and **157** were detected in the acceptor phase in the PAMPA-GI model, however, none of the diarylheptanoids possessed  $\log P_e$  values greater than the critical  $-5.0$  (Table 19), predicting that neither the compounds are able to pass through the membrane of the gastrointestinal tract [157].

Regarding the polarity of these constituents, none of the compounds have  $clog P$  values higher than 2.5. Compounds **149** and **157** have higher  $clog P$  values than 1.0, while  $clog P$  values of **106** and **154** are lower than 1.0. Compounds **106** and **149** are constitutional isomers, nevertheless, their  $clog P$  values are different ( $clog P$   $0.93 \pm 0.46$  and  $1.92 \pm 0.67$ , respectively). These data suggest poor membrane permeability of the major diarylheptanoid components of the *C. betulus* bark.

A further aspect to consider when assessing the PAMPA results is the decomposition of the constituents in aqueous media at the investigated pH values. Significant changes in compound concentrations occurring in a physiologically relevant time frame might be observed for **157** at pH 7.4 and **154** at pH 1.2. In these cases, the decrease in concentration in the donor and acceptor phases caused by decomposition of the analytes of interest might modify the PAMPA results.

The *in vitro* neuroprotective effect of cyclic diarylheptanoids in HT22 mouse hippocampal neuronal cells [158] and N2a mouse neuroblasts [71] was established. However, based on our results suggesting poor penetration capability, their *in vivo* efficacy is ambiguous [154].

## V.7. Evaluation of the Cytostatic Activity

The isolated diarylheptanoids (**106**, **149**, **154**, **157**) were investigated for their cytotoxic activity on five human cancer cell lines (HT-29, Hep G2, HL-60, U87, A2058) by means of the Alamar Blue assay. We confirmed the concentration-dependent antiproliferative activity of carpinontriol A (**106**) against A2058 human metastatic melanoma cells ( $IC_{50} = 14.9 \pm 2.3 \mu M$ ). In agreement with literature data [94], it was comparable to that of the United States Food and Drug Administration-approved etoposide ( $IC_{50} = 8.9 \pm 0.2 \mu M$ ). The cytostatic activity of **106** in A2058 cells was moderate when compared to the antitumor drug daunomycin ( $IC_{50} = 0.16 \pm 2.3 \mu M$ ) (Table 20). However, it should be noted that in contrast to daunomycin, compound **106** showed a highly selective antiproliferative activity [140]. On the other hand, it should be noted that due to the instability of carpinontriol A (**106**) under the examined storage conditions and

physiological pH values, as well as its minimal ability for passive diffusion through biological membranes, further research is needed to increase its stability and membrane permeability.

No significant *in vitro* activity was observed for the other constituents at a concentration range of 0.16–100  $\mu\text{M}$ . Our results are following previous studies, since  $\text{IC}_{50}$  values exceeding 100  $\mu\text{M}$  were observed for carpinontriol B (**149**) in A549 human lung adenocarcinoma and HeLa human cervical adenocarcinoma cells [128]. Similarly, carpinontriol B was not cytotoxic up to 1000  $\mu\text{M}$  in A375 and SK-Mel-28 human melanoma cell lines [81, 154].

## VI. Conclusions

- We performed the detailed polyphenol profiling of European hornbeam (*Carpinus betulus* L.). Extracts of bark, leaf, male, and female catkin samples were characterized by HPLC-DAD-MS/MS, and 194 compounds were tentatively identified.
- Gallo- and ellagitannins dominated in the methanol extracts, while flavonol glycosides and methoxylated flavones prevailed in the ethyl acetate samples together with diarylheptanoid compounds.
- Six known cyclic diarylheptanoids together with a new derivative were isolated from *Carpinus betulus* for the first time. Moreover, a linear diarylheptanoid and a lignan has also been described in the genus *Carpinus* for the first time, while three known flavonol glycosides were also isolated. A new mass spectrometric fragmentation pathway of cyclic diarylheptanoids with a *meta,meta*-cyclophane structure was proposed.
- The four main cyclic diarylheptanoids were quantified by UHPLC-DAD in *Carpinus betulus* for the first time. Compound **106** prevailed both in bark ethyl acetate and methanol extracts, while **149** was the main diarylheptanoid of male catkin extracts.
- The radical scavenging activity of the extracts and the isolated compounds was assessed by the 2,2-diphenyl-1-picrylhydrazyl (DPPH) assay. Leaf and male catkin methanol extracts showed the highest antioxidant activity. The DPPH scavenging activity of aviculin (**148**) and giffonin X (**157**) was determined for the first time. Potential antioxidant compounds in *C. betulus* extracts contributing to the total radical scavenging activity of the samples were indicated using an off-line DPPH-HPLC method. According to our results, hydrolysable tannins may be responsible for the antioxidant capacity of *Carpinus* extracts.
- We investigated the effects of ambient conditions, including storage time, temperature and medium (pH, solvent and accompanying constituents), on the degradation of the four main cyclic *Carpinus* diarylheptanoids **106**, **149**, **154** and **157**. No significant decrease in the concentration was observed and no degradation products were detected for carpinontriol B (**149**); therefore, it was considered as stable under all investigated conditions. Compound **154** was susceptible of decomposing only at acidic pH values, while the storage time, the temperature and the medium did not affect its concentration. On the other hand, carpinontriol A (**106**) and giffonin X (**157**) showed significant decomposition, their degradation products were formed by the elimination of a water molecule were characterized by UHPLC-HR-MS.

- The membrane penetration ability of the four major diarylheptanoid compounds was also studied by the PAMPA method. Compounds **106**, **149**, and **154** were all detected in the acceptor phase in the PAMPA-GI model; however, their  $\log P_e$  values being lower than  $-5.0$  pointed to a poor membrane permeability. On the other hand, only giffonin X (**157**) was detected in the acceptor phase in the PAMPA-BBB model, and its  $\log P_e$  value ( $-5.92 \pm 0.04$ ) also suggested that it is capable of crossing the lipid membrane via passive diffusion.
- The antiproliferative activity of the compounds was evaluated by the Alamar Blue assay in human HT-29 colon cancer, HepG2 hepatocellular carcinoma, HL-60 leukaemia, U87 glioblastoma and A2058 metastatic melanoma cells. The highly selective cytostatic activity of carpinontriol A (**106**) in human metastatic melanoma cells ( $IC_{50} = 14.9 \pm 2.3 \mu\text{M}$ ) was reported for the first time.

## VII. Summary

Plants are still considered as noteworthy potential sources for new drugs, but the ligneous flora is rarely referred to for the presence of possible medical agents. That is why we performed the comprehensive profiling of phenolic compounds in *C. betulus*. Distinct plant parts were extracted successively with solvents of increasing polarity to obtain an extensive range of extractives. Altogether 194 polyphenols were tentatively characterized by HPLC-DAD-ESI-MS/MS. Seven cyclic diarylheptanoids were isolated from *C. betulus* for the first time, with 3,11,17-trihydroxytricyclo[12.3.1.1<sup>2,6</sup>]nonadeca-1(18),2(19),3,5,14,16-hexaen-8-one (**187**) being a new compound. We also described the occurrence of linear diarylheptanoid and lignan constituents in the genus *Carpinus* for the first time. Additionally, validated UHPLC-DAD methods were developed to determine the quantity of the main diarylheptanoids (**106**, **149**, **154**, and **157**) in *hornbeam* extracts.

The *in vitro* antioxidant properties of the extracts and the isolated compounds were assessed by the DPPH assay. Contribution of the individual constituents to the total radical scavenging activity of the samples was evaluated by an off-line DPPH-HPLC-DAD method. This allowed the identification of gallo- and ellagitannin derivatives being primarily responsible for the antioxidant capacity of the extracts.

Chemical stability of the main diarylheptanoids was evaluated as a function of storage temperature (−15, 5, 22 °C) and time (12 and 23 weeks). The effect of the solvent and the pH (1.2, 6.8, 7.4) on the stability of these compounds was also investigated. Compounds **149** and **154** showed good stability both in solutions at all investigated temperatures, however, only **149** was stable at all three studied biorelevant pH values. Degradation pathways of **106** and **157** were explored and degradation mechanisms involving the cleavage of a water molecule were proposed for them.

In the PAMPA-BBB study only compound **157** possesses a  $\log Pe$  value of  $-5.92 \pm 0.04$ , indicating that it may be able to cross the blood–brain barrier via passive diffusion.

The *in vitro* antiproliferative activity of the compounds was investigated against five human cancer cell lines, confirming that similar activity to the etoposide control ( $IC_{50} = 8.9 \pm 0.2 \mu M$ ) was obtained on the A2058 cell type for compound **106** ( $IC_{50} = 14.9 \pm 2.3 \mu M$ ).

## VIII. Összefoglalás

A növényeket a mai napig potenciális forrásként alkalmazzák a hatóanyag-kutatásban, azonban a fás szárú fajok kevésbé állnak az érdeklődés előterében. Ennek apropóján a közönséges gyertyán (*C. betulus*) fenoloidprofiljának vizsgálatát tűztük ki munkánk céljául. Különböző növényi részeket egymást követő lépésekben növekvő polaritású oldószerekkel vontunk ki a változatos összetétel eléréseért. Összesen 194 polifenolt feltételeztünk HPLC-DAD-ESI-MS/MS módszerrel. Először izoláltunk hét ciklusos diarilheptanoidot a *C. betulus*ból, mely közül a 3,11,17-trihidroxitriciklo[12.3.1.1<sup>2,6</sup>]nonadeka-1(18),2(19),3,5,14,16-hexaén-8-on (**187**) új vegyület. Továbbá először írtuk le lineáris diarilheptanoid és lignán vegyületek jelenlétét a *Carpinus* nemzetségen belül. Ezenkívül validált UHPLC-DAD módszert fejlesztettünk a négy fő diarilheptanoid (**106**, **149**, **154** és **157**) kvantitatív meghatározásához a gyertyán kivonatokban.

A kivonatok és az izolált vegyületek *in vitro* antioxidáns hatását a DPPH-módszerrel vizsgáltuk. Az egyes komponensek hozzájárulását a minták szabadgyök-semlegesítő aktivitásához off-line DPPH-HPLC-DAD módszerrel mértük. Ezek alapján a gallo- és ellagitannin származékok felelősek elsődlegesen a kivonatok szabadgyökfogó kapacitásáért.

A fő diarilheptanoidok kémiai stabilitásának értékelését a tárolási hőmérséklet (–15, 5, 22 °C) és tárolási idő (12 és 23 hét) figyelembevételével végeztük. Továbbá vizsgáltuk az oldószer és a pH (1,2; 6,8; 7,4) hatását a vegyületekre. A **149** és **154** vegyület jó stabilitást mutatott az oldatokban mindhárom hőmérsékleten, habár csak a **149** vegyület volt mindhárom vizsgált bioreleváns pH-értékeken stabil. Valószínűsítettük a **106** és **157** vegyületek degradációs útvonaltát egy olyan bomlási mechanizmus révén, mely során egy vízmolekula lép ki a molekulákból.

A PAMPA-BBB vizsgálatoknál csak a **157** vegyület esetén kaptunk olyan értéket ( $\log Pe = -5.92 \pm 0.04$ ), mely arra utal, hogy a komponens passzív diffúzióval képes áthaladni a vér-agy gáton.

A vegyületek *in vitro* antiproliferatív aktivitását öt human eredetű daganatos sejtvonalon vizsgáltuk, megállapítva, hogy a kontrol etopozidhoz ( $IC_{50} = 8,9 \pm 0,2 \mu M$ ) hasonló aktivitást csak a **106** vegyület ( $IC_{50} = 14,9 \pm 2,3 \mu M$ ) mutatott A2058 sejtvonalon.

## References

1. Grimm GW, Renner SS. Harvesting Betulaceae sequences from GenBank to generate a new chronogram for the family. *Bot J Linn*, 2013;172:465-77.
2. Sikkema R, Caudullo G, de Rigo D. *Carpinus betulus* in Europe: distribution, habitat, usage and threats. In: San-Miguel-Ayanz J, de Rigo D, Caudullo G, Houston Durrant T, Mauri A, editor. *European Atlas of Forest Tree Species*. Luxembourg: Publications Office of the EU; 2016. p. e01d8cf+.
3. Hofmann T, Nebehaj E, Albert L. Antioxidant properties and detailed polyphenol profiling of European hornbeam (*Carpinus betulus* L.) leaves by multiple antioxidant capacity assays and high-performance liquid chromatography/multistage electrospray mass spectrometry. *Ind Crops Prod*, 2016;87:340-9.
4. Bartha D. Magyarország fa- és cserjefajai. Budapest: Mezőgazda Kiadó 1999: 34-5.
5. Dános B. Farmakobotanika, A gyógynövénytan alapjai (Kemotaxonómia). Budapest: Argumentum 2008: 139-48.
6. Netherbárium. 2023 [updated 17 Nov 2023; cited 03 Febr 2024]. Available from: [http://www.netherbarium.hu/index\\_hu.html](http://www.netherbarium.hu/index_hu.html)
7. Project Runeberg. 369. Avenbok, *Carpinus betulus*. L. by N. Hvidbök. 2024 [updated 01 Jan 2024; cited 01 March 2024]. Available from: <https://runeberg.org/nordflor/369.html>
8. Lee JS, Kim HJ, Park H, Lee YS. New diarylheptanoids from the stems of *Carpinus cordata*. *J Nat Prod*, 2002;65:1367-70.
9. Yamada P, Ono T, Shigemori H, Han J, Isoda H. Inhibitory effect of tannins from galls of *Carpinus tschonoskii* on the degranulation of RBL-2H3 Cells. *Cytotechnology*, 2012;64:349-56.
10. Jeon JI, Chang C-S, Chen Z-D, Park TY. Systematic aspects of foliar flavonoids in subsect. *Carpinus* (*Carpinus*, Betulaceae). *Biochem Syst Ecol*, 2007;35:606-13.
11. Tálos-Nebehaj E, Hofmann T, Albert L. Seasonal changes of natural antioxidant content in the leaves of Hungarian forest trees. *Ind Crops Prod*, 2017;98:53-9.
12. Hofmann T, Albert L, Visiné-Rajczi E. Utilization of forestry by-products as a source of natural antioxidants from Hungarian forests. *Chem Eng Trans*, 2023;107:667-72.
13. Zhou Q, Wang J, Zhu Z. Composition of volatiles of the essential oil from the leaves of *Carpinus betulus*. *Chem Nat Compd*, 2022;58:358-60.

14. Ko H, Oh T, Baik J, Hyun C, Kim S, Lee N. Anti-inflammatory activities for the extracts and carpinontriols from branches of *Carpinus turczaninowii*. *Int J Pharmacol*, 2013;9:157-63.
15. Lv H, She G. Naturally occurring diarylheptanoids. *Nat Prod Commun*, 2010;5:1934578X1000501035.
16. Cieckiewicz E, Angenot L, Gras T, Kiss R, Frédérick M. Potential anticancer activity of young *Carpinus betulus* leaves. *Phytomedicine*, 2012;19:278-83.
17. Sheng Q, Fang X, Zhu Z, Xiao W, Wang Z, Ding G, Zhao L, Li Y, Yu P, Ding Z, Sun Q. Seasonal variation of pheophorbide a and flavonoid in different organs of two *Carpinus* species and its correlation with immunosuppressive activity. *In Vitro Cell Dev Biol Anim*, 2016;52:654-61.
18. Frédérick M, Marcowycz A, Cieckiewicz E, Mégalizzi V, Angenot L, Kiss R. *In vitro* anticancer potential of tree extracts from the wallon region forest. *Planta Med*, 2009;75:1634-7.
19. Koo J-E, Hong H-J, Mathema VB, Kang H-K, Hyun J-W, Kim G-Y, Kim Y-R, Maeng Y-H, Hyun C-L, Chang W-Y, Koh Y-S. Inhibitory effects of *Carpinus tschonoskii* leaves extract on CpG-stimulated pro-inflammatory cytokine production in murine bone marrow-derived macrophages and dendritic cells. *In Vitro Cell Dev Biol Anim*, 2012;48:197-202.
20. Zhang R, Kang K-A, Piao M-J, Park J-W, Shin T-Y, Yang Y-T, Hyun J-W. Cytoprotective activity of *Carpinus tschonoskii* against H<sub>2</sub>O<sub>2</sub> induced oxidative stress. *Nat Prod Res*, 2007;13:118-22.
21. Kim M-K, Kim S-C, Kang J-I, Boo H-J, Hyun J-W, Koh Y-S, Park D-B, Yoo E-S, Kang J-H, Kang H-K. Neuroprotective effects of *Carpinus tschonoskii* MAX on 6-hydroxydopamine-induced death of PC12 cells. *Biomol Ther*, 2010;18:454-62.
22. Kang GJ, Kang NJ, Han SC, Koo DH, Kang HK, Yoo BS, Yoo ES. The chloroform fraction of *Carpinus tschonoskii* leaves inhibits the production of inflammatory mediators in HaCaT keratinocytes and RAW264.7 macrophages. *Toxicol Res*, 2012;28:255-62.
23. Song J, Yoon SR, Son YK, Bang WY, Bae C-H, Yeo J-H, Kim H-J, Kim OY. *Carpinus turczaninowii* extract may alleviate high glucose-induced arterial damage and inflammation. *Antioxidants*, 2019;8:172.
24. Alberti Á, Riethmüller E, Béni S. Characterization of diarylheptanoids: An emerging class of bioactive natural products. *J Pharm Biomed Anal*, 2018;147:13-34.

25. Jahng Y, Park JG. Recent studies on cyclic 1,7-diarylheptanoids: Their isolation, structures, biological activities, and chemical synthesis. *Molecules*, 2018;23.
26. Keserü GM, Nógrádi M. The chemistry of natural diarylheptanoids. In: Atta ur R, editor. *Studies in Natural Products Chemistry*. Elsevier; 1995. p. 357-94.
27. Vogel HA, Pelletier PJ. Examen chimique de la racine de Curcuma. *J Pharm Sci Accessoires* 1815;1:289-300.
28. Ganapathy G, Preethi R, Moses JA, Anandharamakrishnan C. Diarylheptanoids as nutraceutical: A review. *Biocatal Agric Biotechnol*, 2019;19:101109.
29. Kunnumakkara AB, Koca C, Dey S, Gehlot P, Yodkeeree S, Danda D, Sung B, Aggarwal BB. Traditional uses of spices: An overview. In: editor. *Molecular Targets and Therapeutic Uses of Spices*. WORLD SCIENTIFIC; 2009. p. 1-24.
30. Claeson P, Tuchinda P, Reutrakul V. Naturally occurring 1,7-diarylheptanoids. *J Indian Chem Soc*, 1994;71:509-21.
31. Claeson P, Claeson UP, Tuchinda P, Reutrakul V. Occurrence, structure and bioactivity of 1,7-diarylheptanoids. In: Atta-ur-Rahman, editor. *Studies in Natural Products Chemistry*. 2002. p. 881-908.
32. Lv H, She G. Naturally occurring diarylheptanoids- A supplementary version. *Rec Nat Prod*, 2012;6:321-33.
33. Vanucci-Bacqué C, Bedos-Belval F. Anti-inflammatory activity of naturally occurring diarylheptanoids – A review. *Bioorg Med Chem*, 2021;31:115971.
34. Yasue M. Studies on the wood extractives of *Ostrya japonica*. On the chemical structures of asadanin and its related compounds. *Bulletin of the Government Forest Experiment Station* 1968:77–168.
35. Yasue M, Miyazaki M, Takahashi T, Imamura H, Honda O. Wood extractives. VIII. Constituents of *Ostrya japonica* wood. *J Japan Wood Res Soc*, 1965;11:111-3.
36. Singldinger B, Dunkel A, Hofmann T. The cyclic diarylheptanoid asadanin as the main contributor to the bitter off-taste in hazelnuts (*Corylus avellana* L.). *J Agric Food Chem*, 2017;65:1677-83.
37. Bottone A, Cerulli A, D’Urso G, Masullo M, Montoro P, Napolitano A, Piacente S. Plant Specialized Metabolites in Hazelnut (*Corylus avellana*) kernel and byproducts: An update on chemistry, biological activity, and analytical aspects. *Planta Med*, 2019;85:840-55.

38. Felegyi-Tóth CA, Tóth Z, Garádi Z, Boldizsár I, Nedves AN, Simon A, Felegyi K, Alberti Á, Riethmüller E. Membrane permeability and aqueous stability study of linear and cyclic diarylheptanoids from *Corylus maxima*. *Pharmaceutics*, 2022;14.
39. Fuchino H, Satoh T, Shimizu M, Tanaka N. Chemical evaluation of *Betula* species in Japan. IV. Constituents of *Betula davurica*. *Chem Pharm Bull*, 1998;46:166-8.
40. Fuchino H, Satoh T, Tanaka N. Chemical evaluation of *Betula* species in Japan. I. Constituents of *Betula ermanii*. *Chem Pharm Bull*, 1995;43:1937-42.
41. Fuchino H, Satoh T, Tanaka N. Chemical evaluation of *Betula* species in Japan. III. Constituents of *Betula maximowicziana*. *Chem Pharm Bull*, 1996;44:1748-53.
42. Fuchino H, Konishi S, Satoh T, Yagi A, Saitsu K, Tatsumi T, Tanaka N. Chemical evaluation of *Betula* species in Japan. II. Constituents of *Betula platyphylla* var. *japonica*. *Chem Pharm Bull*, 1996;44:1033-8.
43. Rastogi S, Pandey MM, Kumar Singh Rawat A. Medicinal plants of the genus *Betula*—Traditional uses and a phytochemical–pharmacological review. *J Ethnopharmacol*, 2015;159:62-83.
44. Tsvetkov DE, Dmitrenok AS, Tsvetkov YE, Tomilov YV, Dokichev VA, Nifantiev NE. Polyphenolic compounds in the extracts of the birch *Betula pendula* knotwood. *Russ Chem Bull*, 2015;64:1413-8.
45. Ponkratova AO, Vedernikov DN, Whaley AK, Kuncova MN, Smirnov SN, Serebryakov EB, Spiridonova DV, Luzhanin VG. New cyclic diarylheptanoids from the false heartwood of *Betula pubescens* Ehrh. *Nat Prod Res*, 2021:1-9.
46. Wu HC, Cheng MJ, Peng CF, Yang SC, Chang HS, Lin CH, Wang CJ, Chen IS. Secondary metabolites from the stems of *Engelhardia roxburghiana* and their antitubercular activities. *Phytochemistry*, 2012;82:118-27.
47. Li G, Xu ML, Choi HG, Lee SH, Jahng YD, Lee CS, Moon DC, Woo MH, Son JK. Four new diarylheptanoids from the roots of *Juglans mandshurica*. *Chem Pharm Bull*, 2003;51:262-4.
48. Tanaka T, Jiang Z-H, Kouno I. Distribution of ellagic acid derivatives and a diarylheptanoid in wood of *Platycarya strobilacea*. *Phytochemistry*, 1998;47:851-4.
49. Jiang Z-H, Tanaka T, Hirata H, Fukuoka R, Kouno I. Three diarylheptanoids from *Rhoiptelea chiliantha*. *Phytochemistry*, 1996;43:1049-54.
50. Liu HB, Cui CB, Gu QQ, Zhang DY, Zhao QC, Guan HS. Pterocarine, a new diarylheptanoid from *Pterocarya tonkinesis*, its cell cycle inhibition at G0/G1 phase and induction of apoptosis in HCT-15 and K562 cells. *Chin Chem Lett*, 2005;16:215-8.

51. Whiting DA, Wood AF. Cyclisation of 1,7-diarylheptanoids through oxidative, reductive, and photochemical radical processes: Total syntheses of the m,m-bridged biaryls myricanone and ( $\pm$ )-myricanol, and a related diaryl ether. *Tetrahedron Lett*, 1978;19:2335-8.
52. Inoue T, Arai Y, Nagai M. Diarylheptanoids in the bark of *Myrica rubra*. *Yakugaku Zasshi*, 1984;104:37-41.
53. Makule E, Schmidt TJ, Heilmann J, Kraus B. Diarylheptanoid glycosides of *Morella salicifolia* bark. *Molecules*, 2017;22.
54. Ibrahim SRM, Fouad MA, Abdel-Lateff A, Okino T, Mohamed GA. Alnuheptanoid A: a new diarylheptanoid derivative from *Alnus japonica*. *Nat Prod Res*, 2014;28:1765-71.
55. Lin WY, Peng Cf Fau - Tsai I-L, Tsai Il Fau - Chen J-J, Chen Jj Fau - Cheng M-J, Cheng Mj Fau - Chen I-S, Chen IS. Antitubercular constituents from the roots of *Engelhardia roxburghiana*. *Planta Med*, 2005;71:171-5.
56. Chen S-D, Gao J-T, Liu J-G, Liu B, Zhao R-Z, Lu C-J. Five new diarylheptanoids from the rhizomes of *Curcuma Kwangsiensis* and their antiproliferative activity. *Fitoterapia*, 2015;102:67-73.
57. Gilli C, Orłowska E, Kaiser D, Steyrer J, Rathgeb A, Lorbeer E, Brecker L, Schinnerl J. Diarylheptanoids, flavonoids and other constituents from two neotropical *Renealmia* species (Zingiberaceae). *Biochem Syst Ecol*, 2014;56:178-84.
58. Cha JM, Subedi L, Khan Z, Kim SY, Lee KR. A new diarylheptanoid from the twigs of *Quercus Acutissima* and their neuroprotective activity. *Chem Nat Compd*, 2020;56:213-6.
59. He J-B, Yan Y-M, Ma X-J, Lu Q, Li X-S, Su J, Li Y, Liu G-M, Cheng Y-X. Sesquiterpenoids and diarylheptanoids from *Nidus Vespae* and their inhibitory effects on nitric oxide production. *Chem Biodiversit*, 2011;8:2270-6.
60. Costantino V, Fattorusso E, Mangoni A, Perinu C, Teta R, Panza E, Ianaro A. Tedarenes A and B: Structural and stereochemical analysis of two new strained cyclic diarylheptanoids from the marine sponge *Tedania ignis*. *J Org Chem Res*, 2012;77:6377-83.
61. Maurent K, Vanucci-Bacqué C, Baltas M, Nègre-Salvayre A, Augé N, Bedos-Belval F. Synthesis and biological evaluation of diarylheptanoids as potential antioxidant and anti-inflammatory agents. *Eur J Med Chem*, 2018;144:289-99.

62. Morikawa T, Tao J, Toguchida I, Matsuda H, Yoshikawa M. Structures of new cyclic diarylheptanoids and inhibitors of nitric oxide production from Japanese folk medicine *Acer nikoense*. *J Nat Prod*, 2003;66:86-91.
63. Morita H, Deguchi J, Motegi Y, Sato S, Aoyama C, Takeo J, Shiro M, Hirasawa Y. Cyclic diarylheptanoids as Na<sup>+</sup>-glucose cotransporter (SGLT) inhibitors from *Acer nikoense*. *Bioorg Med Chem Lett*, 2010;20:1070-4.
64. Masullo M, Lauro G, Cerulli A, Bifulco G, Piacente S. *Corylus avellana*: A source of diarylheptanoids with  $\alpha$ -glucosidase inhibitory activity evaluated by *in vitro* and *in silico* studies. *Front Plant Sci*, 2022;13:805660.
65. Chiba K, Ichizawa H, Kawai S, Nishida T.  $\alpha$ -glucosidase inhibition activity by cyclic diarylheptanoids from *Alnus sieboldiana*. *J Wood Chem Technol*, 2013;33:44-51.
66. Sung SH, Lee M. Anti-adipogenic activity of a new cyclic diarylheptanoid isolated from *Alnus japonica* on 3T3-L1 cells via modulation of PPAR $\gamma$ , C/EBP $\alpha$  and SREBP1c signaling. *Bioorg Med Chem Lett*, 2015;25:4648-51.
67. Yonezawa T, Lee J-W, Akazawa H, Inagaki M, Cha B-Y, Nagai K, Yagasaki K, Akihisa T, Woo J-T. Osteogenic activity of diphenyl ether-type cyclic diarylheptanoids derived from *Acer nikoense*. *Bioorg Med Chem Lett*, 2011;21:3248-51.
68. Akihisa T, Takeda A, Akazawa H, Kikuchi T, Yokokawa S, Ukiya M, Fukatsu M, Watanabe K. Melanogenesis-inhibitory and cytotoxic activities of diarylheptanoids from *Acer nikoense* bark and their derivatives. *Chem Biodiversit*, 2012;9:1475-89.
69. Akazawa H, Fujita Y, Banno N, Watanabe K, Kimura Y, Manosroi A, Manosroi J, Akihisa T. Three new cyclic diarylheptanoids and other phenolic compounds from the bark of *Myrica rubra* and their melanogenesis inhibitory and radical scavenging activities. *J Oleo Sci*, 2010;59:213-21.
70. Yang H, Sung SH, Kim J, Kim YC. Neuroprotective diarylheptanoids from the leaves and twigs of *Juglans sinensis* against glutamate-induced toxicity in HT22 Cells. *Planta Med*, 2011;77:841-5.
71. Chen P, Lin X, Yang C-H, Tang X, Chang Y-W, Zheng W, Luo L, Xu C, Chen Y-H. Study on chemical profile and neuroprotective activity of *Myrica rubra* leaf extract. *Molecules*, 2017;22.
72. Masullo M, Cerulli A, Olas B, Pizza C, Piacente S. Giffonins A–I, antioxidant cyclized diarylheptanoids from the leaves of the hazelnut tree (*Corylus avellana*), source of the Italian PGI product “Nocciola di Giffoni”. *J Nat Prod*, 2015;78:17-25.

73. Masullo M, Lauro G, Cerulli A, Kontek B, Olas B, Bifulco G, Piacente S, Pizza C. Giffonins, antioxidant diarylheptanoids from *Corylus avellana*, and their ability to prevent oxidative changes in human plasma proteins. *J Nat Prod*, 2021;84:646-53.
74. Cerulli A, Lauro G, Masullo M, Cantone V, Olas B, Kontek B, Nazzaro F, Bifulco G, Piacente S. Cyclic diarylheptanoids from *Corylus avellana* green leafy covers: Determination of their absolute configurations and evaluation of their antioxidant and antimicrobial activities. *J Nat Prod*, 2017;80:1703-13.
75. Dai G, Tong Y, Chen X, Ren Z, Yang F. *In vitro* anticancer activity of myricanone in human lung adenocarcinoma A549 cells. *Chemotherapy*, 2014;60:81-7.
76. Paul A, Das S, Das J, Samadder A, Bishayee K, Sadhukhan R, Khuda-Bukhsh AR. Diarylheptanoid–myricanone isolated from ethanolic extract of *Myrica cerifera* shows anticancer effects on HeLa and PC3 cell lines: signalling pathway and drug-DNA interaction. *J Integr Med*, 2013;11:405-15.
77. Liu JX, Di DL, Wei XN, Han Y. Cytotoxic diarylheptanoids from the pericarps of walnuts (*Juglans regia*). *Planta Med*, 2008;74:754-9.
78. Guo H, Li BG, Wu ZJ, Zhang GL. Lupane triterpenoids and a diarylheptanoid from *Clematoclethra actinidioides*. *Planta Med*, 2006;72:180-3.
79. Kontiza I, Vagias C, Jakupovic J, Moreau D, Roussakis C, Roussis V. Cymodienol and cymodiene: new cytotoxic diarylheptanoids from the sea grass *Cymodocea nodosa*. *Tetrahedron Lett*, 2005;46:2845-7.
80. Lee K-S, Li G, Kim SH, Lee C-S, Woo M-H, Lee S-H, Jhang Y-D, Son J-K. Cytotoxic diarylheptanoids from the roots of *Juglans mandshurica*. *J Nat Prod*, 2002;65:1707-8.
81. Esposito T, Sansone F, Franceschelli S, Del Gaudio P, Picerno P, Aquino RP, Mencherini T. Hazelnut (*Corylus avellana* L.) shells extract: Phenolic composition, antioxidant effect and cytotoxic activity on human cancer cell lines. *Int J Mol Sci*, 2017;18.
82. Ishida J, Kozuka M, Wang H, Konoshima T, Tokuda H, Okuda M, Yang Mou X, Nishino H, Sakurai N, Lee KH, Nagai M. Antitumor-promoting effects of cyclic diarylheptanoids on Epstein-Barr virus activation and two-stage mouse skin carcinogenesis. *Cancer letters*, 2000;159:135-40.
83. Dai G, Tong Y, Chen X, Ren Z, Ying X, Yang F, Chai K. Myricanol induces apoptotic cell death and anti-tumor activity in non-small cell lung carcinoma *in vivo*. *Int J Mol Sci*, 2015;16.

84. Ibrahim SRM, Mohamed GA, Khedr AIM, Aljaeid BM. Alnuheptanoid B: A new cyclic diarylheptanoid from *Alnus japonica* stem bark. *Rec Nat Prod*, 2016;362-8.
85. Matsuda H, Yamazaki M, Matsuo K, Asanuma Y, Kubo M. Anti-androgenic activity of Myricae cortex - Isolation of active constituents from bark of *Myrica rubra*. *Biol Pharm Bull*, 2001;24:259-63.
86. Wang Y-Y, Wang C-G, Qi S-N, Liu Z-X, Su G-F, Zheng Y-J. 3,5-Dimethoxy-4-hydroxy myricanol ameliorates photoreceptor cell degeneration in Pde6brd10 mouse model. *Cutan Ocul Toxicol*, 2019;38:36-43.
87. Brand-Williams W, Cuvelier ME, Berset C. Use of a free radical method to evaluate antioxidant activity. *LWT-Food Sci Technol*, 1995;28:25-30.
88. Zhu J, Yi X, Zhang J, Chen S, Wu Y. Chemical profiling and antioxidant evaluation of Yangxinshi Tablet by HPLC–ESI-Q-TOF-MS/MS combined with DPPH assay. *J Chromatogr B*, 2017;1060:262-71.
89. Pacheco-Palencia LA, Hawken P, Talcott ST. Phytochemical, antioxidant and pigment stability of açai (*Euterpe oleracea* Mart.) as affected by clarification, ascorbic acid fortification and storage. *Food Res Int*, 2007;40:620-8.
90. Avdeef A. Permeability—PAMPA. In: Avdeef A, editor. *Absorption and Drug Development*. Hoboken, NJ, USA: John Wiley & Sons; 2012. p. 319-498.
91. Gewirtz D. A critical evaluation of the mechanisms of action proposed for the antitumor effects of the anthracycline antibiotics adriamycin and daunorubicin. *Biochem Pharmacol*, 1999;57:727-41.
92. Lajkó E, Spring S, Hegedüs R, Biri-Kovács B, Ingebrandt S, Mező G, Kőhidai L. Comparative cell biological study of *in vitro* antitumor and antimetastatic activity on melanoma cells of GnRH-III-containing conjugates modified with short-chain fatty acids. *Beilstein J Org Chem*, 2018;14:2495-509.
93. Meresse P, Dechaux E, Monneret C, Bertounesque E. Etoposide: Discovery and medicinal chemistry. *Curr Med Chem*, 2004;11:2443-66.
94. Tóth G, Horváti K, Kraszni M, Ausbüttel T, Pályi B, Kis Z, Mucsi Z, Kovács GM, Bősze S, Boldizsár I. Arylnaphthalene lignans with anti-SARS-CoV-2 and antiproliferative activities from the underground organs of *Linum austriacum* and *Linum perenne*. *J Nat Prod*, 2023;86:672-82.
95. Baranyai Z, Biri-Kovács B, Krátký M, Szeder B, Debreczeni ML, Budai J, Kovács B, Horváth L, Pári E, Németh Z, Cervenak L, Zsila F, Méhes E, Kiss É, Vinšová J, Bősze S. Cellular internalization and inhibition capacity of new anti-glioma peptide

- conjugates: Physicochemical characterization and evaluation on various monolayer- and 3D-spheroid-based *in vitro* platforms. *J Med Chem*, 2021;64:2982-3005.
96. Ben Said R, Hamed AI, Mahalel UA, Al-Ayed AS, Kowalczyk M, Moldoch J, Oleszek W, Stochmal A. Tentative characterization of polyphenolic compounds in the male flowers of *Phoenix dactylifera* by liquid chromatography coupled with mass spectrometry and DFT. *Int J Mol Sci*, 2017;18.
  97. Jaiswal R, Müller H, Müller A, Karar MG, Kuhnert N. Identification and characterization of chlorogenic acids, chlorogenic acid glycosides and flavonoids from *Lonicera henryi* L. (Caprifoliaceae) leaves by LC-MSn. *Phytochemistry*, 2014;108:252-63.
  98. Song X-C, Canellas E, Dreolin N, Nerin C, Goshawk J. Discovery and characterization of phenolic compounds in bearberry (*Arctostaphylos uva-ursi*) leaves using liquid chromatography–ion mobility–high-resolution mass spectrometry. *J Agric Food Chem*, 2021;69:10856-68.
  99. Ambigaipalan P, de Camargo AC, Shahidi F. Phenolic compounds of pomegranate byproducts (outer skin, mesocarp, divider membrane) and their antioxidant activities. *J Agric Food Chem*, 2016;64:6584-604.
  100. Bunse M, Mailänder LK, Lorenz P, Stintzing FC, Kammerer DR. Evaluation of *Geum urbanum* L. Extracts with respect to their antimicrobial potential. *Chem Biodiversit*, 2022;19:e202100850.
  101. Drioiche A, Ailli A, Remok F, Saidi S, Gourich AA, Asbabou A, Kamaly OA, Saleh A, Bouhrim M, Tarik R, Kchibale A, Zair T. Analysis of the chemical composition and evaluation of the antioxidant, antimicrobial, anticoagulant, and antidiabetic properties of *Pistacia lentiscus* from Boulemane as a natural nutraceutical preservative. *Biomedicines*, 2023;11.
  102. Clifford MN, Stoupi S, Kuhnert N. Profiling and characterization by LC-MSn of the galloylquinic acids of green tea, tara tannin, and tannic acid. *J Agric Food Chem*, 2007;55:2797-807.
  103. Singh A, Bajpai V, Kumar S, Sharma KR, Kumar B. Profiling of gallic and ellagic acid derivatives in different plant parts of *Terminalia Arjuna* by HPLC-ESI-QTOF-MS/MS. *Nat Prod Commun*, 2016;11:1934578X1601100227.
  104. Abreu LS, Alves IM, Espírito Santo RFd, Nascimento YMd, Dantas CAG, dos Santos GGL, Le Hyaric M, Guedes MLS, da Silva MS, Villarreal CF, Velozo EdS, Tavares JF.

- Antinociceptive compounds and LC-DAD-ESIMS<sup>n</sup> profile from *Dictyoloma vandellianum* leaves. PLOS ONE, 2019;14:e0224575.
105. Bunse M, Lorenz P, Stintzing FC, Kammerer DR. Insight into the secondary metabolites of *Geum urbanum* L. and *Geum rivale* L. seeds (Rosaceae). Plants 2021;10.
  106. Lachowicz S, Oszmiański J, Rapak A, Ochmian I. Profile and content of phenolic compounds in leaves, flowers, roots, and stalks of *Sanguisorba officinalis* L. determined with the LC-DAD-ESI-QTOF-MS/MS analysis and their *in vitro* antioxidant, antidiabetic, antiproliferative potency. Pharmaceuticals, 2020;13.
  107. Fuchs C, Bakuradze T, Steinke R, Grewal R, Eckert GP, Richling E. Polyphenolic composition of extracts from winery by-products and effects on cellular cytotoxicity and mitochondrial functions in HepG2 cells. J Funct Foods, 2020;70:103988.
  108. Regueiro J, Sánchez-González C, Vallverdú-Queralt A, Simal-Gándara J, Lamuela-Raventós R, Izquierdo-Pulido M. Comprehensive identification of walnut polyphenols by liquid chromatography coupled to linear ion trap–Orbitrap mass spectrometry. Food Chem, 2014;152:340-8.
  109. Justino AB, Franco RR, Silva HCG, Saraiva AL, Sousa RMF, Espindola FS. B procyanidins of *Annona crassiflora* fruit peel inhibited glycation, lipid peroxidation and protein-bound carbonyls, with protective effects on glycated catalase. Sci Rep, 2019;9:19183.
  110. Šuković D, Knežević B, Gašić U, Sredojević M, Ćirić I, Todić S, Mutić J, Tešić Ž. Phenolic profiles of leaves, grapes and wine of grapevine variety vranac (*Vitis vinifera* L.) from Montenegro. Foods, 2020;9.
  111. Hofmann T, Guran R, Zitka O, Visi-Rajczi E, Albert L. Liquid chromatographic/mass spectrometric study on the role of beech (*Fagus sylvatica* L.) wood polyphenols in red heartwood formation. Forests, 2022;13.
  112. Agarwal C, Hofmann T, Vršanská M, Schlosserová N, Visi-Rajczi E, Voběrková S, Pásztor Z. In vitro antioxidant and antibacterial activities with polyphenolic profiling of wild cherry, the European larch and sweet chestnut tree bark. Eur Food Res Technol, 2021;247:2355-70.
  113. Sheng F, Hu B, Jin Q, Wang J, Wu C, Luo Z. The analysis of phenolic compounds in walnut husk and pellicle by UPLC-Q-Orbitrap HRMS and HPLC. Molecules, 2021;26.
  114. El-Shazly MAM, Hamed AA, Kabary HA, Ghareeb MA. LC-MS/MS profiling, antibiofilm, antimicrobial and bacterial growth kinetic studies of *Pluchea dioscoridis* extracts. Acta Chromatogr, 2022;34:338-50.

115. Sun J, Liang F, Bin Y, Li P, Duan C. Screening non-colored phenolics in red wines using liquid chromatography/ultraviolet and mass spectrometry/mass spectrometry libraries. *Molecules*, 2007;12:679-93.
116. Daglia M, Di Lorenzo A, Nabavi SF, Sureda A, Khanjani S, Moghaddam AH, Braidy N, Nabavi SM. Improvement of antioxidant defences and mood status by oral gaba tea administration in a mouse model of post-stroke depression. *Nutrients*, 2017;9:446.
117. Mena P, Calani L, Dall, Asta C, Galaverna G, García-Viguera C, Bruni R, Crozier A, Del Rio D. Rapid and comprehensive evaluation of (poly)phenolic compounds in pomegranate (*Punica granatum* L.) juice by UHPLC-MSn. *Molecules*, 2012;17:14821-40.
118. Alberti Á, Riethmüller E, Béni S, Kéry Á. Evaluation of radical scavenging activity of *Sempervivum tectorum* and *Corylus avellana* extracts with different phenolic composition. *Nat Prod Commun*, 2016;11:1934578X1601100412.
119. Alberti Á, Béni S, Lackó E, Riba P, Al-Khrasani M, Kéry Á. Characterization of phenolic compounds and antinociceptive activity of *Sempervivum tectorum* L. leaf juice. *J Pharm Biomed Anal*, 2012;70:143-50.
120. Jaiswal R, Jayasinghe L, Kuhnert N. Identification and characterization of proanthocyanidins of 16 members of the *Rhododendron* genus (Ericaceae) by tandem LC-MS. *J Mass Spectrom*, 2012;47:502-15.
121. Riethmüller E, Tóth G, Alberti Á, Végh K, Burlini I, Könczöl Á, Balogh GT, Kéry Á. First characterisation of flavonoid- and diarylheptanoid-type antioxidant phenolics in *Corylus maxima* by HPLC-DAD-ESI-MS. *J Pharm Biomed Anal*, 2015;107:159-67.
122. Yang Z-W, Xu F, Liu X, Cao Y, Tang Q, Chen Q-Y, Shang M-Y, Liu G-X, Wang X, Cai S-Q. An untargeted metabolomics approach to determine component differences and variation in their in vivo distribution between Kuqin and Ziqin, two commercial specifications of *Scutellaria Radix*. *RSC Adv*, 2017;7:54682-95.
123. Nurul Islam M, Downey F, Ng CKY. Comprehensive profiling of flavonoids in *Scutellaria incana* L. using LC-Q-TOF-MS. *Acta Chromatogr*, 2013;25:555-69.
124. Alberti A, Blazics B, Kery A. Evaluation of *Sempervivum tectorum* L. flavonoids by LC and LC-MS. *Chromatographia*, 2008;68:107-11.
125. Li C, Seeram NP. Ultra-fast liquid chromatography coupled with electrospray ionization time-of-flight mass spectrometry for the rapid phenolic profiling of red maple (*Acer rubrum*) leaves. *J Sep Sci*, 2018;41:2331-46.

126. Shao SY, Ting Y, Wang J, Sun J, Guo XF. Characterization and identification of the major flavonoids in *Phyllostachys edulis* leaf extract by UPLC–QTOF–MS/MS. *Acta Chromatogr*, 2020;32:228-37.
127. Végh K, Riethmüller E, Hosszú L, Darcsi A, Müller J, Alberti Á, Tóth A, Béni S, Könczöl Á, Balogh GT, Kéry Á. Three newly identified lipophilic flavonoids in *Tanacetum parthenium* supercritical fluid extract penetrating the Blood-Brain Barrier. *J Pharm Biomed Anal*, 2018;149:488-93.
128. Masullo M, Cerulli A, Mari A, de Souza Santos CC, Pizza C, Piacente S. LC-MS profiling highlights hazelnut (Nocciola di Giffoni PGI) shells as a byproduct rich in antioxidant phenolics. *Food Res Int*, 2017;101:180-7.
129. Hofmann T, Visi-Rajczi E, Vaculciakova S, Guran R, Voberkova S, Vrsanska M, Zitka O, Albert L. Direct microwave treatment enhances antioxidant and antibacterial properties of the seed extracts of Kékfrankos grapes. *Heliyon*, 2023;9:e21497.
130. Goel N, Gajbhiye RL, Saha M, Nagendra C, Reddy AM, Ravichandiran V, Das Saha K, Jaisankar P. A comparative assessment of in vitro cytotoxic activity and phytochemical profiling of *Andrographis nallamalayana* J.L.Ellis and *Andrographis paniculata* (Burm. f.) Nees using UPLC-QTOF-MS/MS approach. *RSC Adv*, 2021;11:35918-36.
131. Felegyi-Tóth CA, Garádi Z, Darcsi A, Csernák O, Boldizsár I, Béni S, Alberti Á. Isolation and quantification of diarylheptanoids from European hornbeam (*Carpinus betulus* L.) and HPLC-ESI-MS/MS characterization of its antioxidative phenolics. *J Pharm Biomed Anal*, 2022;210:114554.
132. Lee D, Lee YH, Lee KH, Lee BS, Alishir A, Ko Y-J, Kang KS, Kim KH. Aviculin isolated from *Lespedeza cuneata* induce apoptosis in breast cancer cells through mitochondria-mediated caspase activation pathway. *Molecules*, 2020;25.
133. Aderogba MA, Ndhlala AR, Rengasamy KRR, Van Staden J. Antimicrobial and selected *in vitro* enzyme inhibitory effects of leaf extracts, flavonols and indole alkaloids isolated from *Croton menyharthii*. *Molecules*, 2013;18:12633-44.
134. Fiorini C, David B, Fourasté I, Vercauteren J. Acylated kaempferol glycosides from *Laurus nobilis* leaves. *Phytochemistry*, 1998;47:821-4.
135. Cerulli A, Masullo M, Montoro P, Hošek J, Pizza C, Piacente S. Metabolite profiling of “green” extracts of *Corylus avellana* leaves by 1H NMR spectroscopy and multivariate statistical analysis. *J Pharm Biomed Anal*, 2018;160:168-78.

136. Yamaguchi T, Takamura H, Matoba T, Terao J. HPLC method for evaluation of the free radical-scavenging activity of foods by using 1,1-diphenyl-2-picrylhydrazyl. *Biosci Biotechnol Biochem*, 1998;62:1201-4.
137. Moon KY, Ahn BK, Lee SG, Lee SH, Yeom DW, Choi YW. Enhanced aqueous stability of hirsutenone with antioxidant. *J Pharm Investig*, 2011;41:331-6.
138. Ayanlowo AG, Garádi Z, Boldizsár I, Darcsi A, Nedves AN, Varjas B, Simon A, Alberti Á, Riethmüller E. UHPLC-DPPH method reveals antioxidant tyramine and octopamine derivatives in *Celtis occidentalis*. *J Pharm Biomed Anal*, 2020;191:113612.
139. Simon A, Nghiem KS, Gampe N, Garádi Z, Boldizsár I, Backlund A, Darcsi A, Nedves AN, Riethmüller E. Stability study of *Alpinia galanga* constituents and investigation of their membrane permeability by ChemGPS-NP and the parallel artificial membrane permeability assay. *Pharmaceutics*, 2022;14:1967.
140. Berek-Nagy PJ, Tóth G, Bősze S, Horváth LB, Darcsi A, Csíkos S, Knapp DG, Kovács GM, Boldizsár I. The grass root endophytic fungus *Flavomyces fulophazii*: an abundant source of tetramic acid and chlorinated azaphilone derivatives. *Phytochemistry*, 2021;190:112851.
141. Santos SAO, Freire CSR, Domingues MRM, Silvestre AJD, Neto CP. Characterization of phenolic components in polar extracts of *Eucalyptus globulus* Labill. bark by high-performance liquid chromatography–mass spectrometry. *J Agric Food Chem*, 2011;59:9386-93.
142. Syue P-C, Li K-F, Ku K-L. Revisiting the fragmentation mechanism of catechin isomers. *J Chin Chem Soc*, 2023;70:1901-7.
143. Ryu M, Sung CK, Im YJ, Chun C. Activation of JNK and p38 in MCF-7 cells and the *in vitro* anticancer activity of *Alnus hirsuta* extract. *Molecules*, 2020;25.
144. Yang N-Y, Tao W-W, Duan J-A. Antithrombotic flavonoids from the faeces of *Trogopterus xanthipes*. *Nat Prod Res*, 2010;24:1843-9.
145. Yu K-Y, Wu W, Li S-Z, Dou L-L, Liu L-L, Li P, Liu EH. A new compound, methylbergenin along with eight known compounds with cytotoxicity and anti-inflammatory activity from *Ardisia japonica*. *Nat Prod Res*, 2017;31:2581-6.
146. Agarwal C, Hofmann T, Visi-Rajczi E, Pásztor Z. Low-frequency, green sonoextraction of antioxidants from tree barks of Hungarian woodlands for potential food applications. *Chem Eng Process*, 2021;159:108221.

147. Kim SB, Hwang SH, Suh H-W, Lim SS. Phytochemical analysis of *Agrimonia pilosa* Ledeb, its antioxidant activity and aldose reductase inhibitory potential. *Int J Mol Sci*, 2017;18.
148. Le TT, Yin J, Lee M. Anti-inflammatory and anti-oxidative activities of phenolic compounds from *Alnus sibirica* stems fermented by *Lactobacillus plantarum* subsp. *argentoratensis*. *Molecules*, 2017;22.
149. Tang Y, Lou F, Wang J, Li Y, Zhuang S. Coumaroyl flavonol glycosides from the leaves of *Ginkgo biloba*. *Phytochemistry*, 2001;58:1251-6.
150. Rice-Evans CA, Miller NJ, Paganga G. Structure-antioxidant activity relationships of flavonoids and phenolic acids. *Free Radic Biol Med*, 1996;20:933-56.
151. Badhani B, Sharma N, Kakkar R. Gallic acid: a versatile antioxidant with promising therapeutic and industrial applications. *RSC Adv*, 2015;5:27540-57.
152. Xue Y, Savchenko AI, Agnew-Francis KA, Miles JA, Holt T, Lu H, Chow S, Forster PI, Boyle GM, Ross BP, Fischer K, Kutateladze AG, Williams CM. Seco-pregnane glycosides from australian caustic vine (*Cynanchum viminalis* subsp. *australe*). *J Nat Prod*, 2023;86:490-7.
153. Friedman M, Jürgens HS. Effect of pH on the stability of plant phenolic compounds. *J Agric Food Chem*, 2000;48:2101-10.
154. Felegyi-Tóth CA, Heilmann T, Buda E, Stipsicz B, Simon A, Boldizsár I, Bősze S, Riethmüller E, Alberti Á. Evaluation of the chemical stability, membrane permeability and antiproliferative activity of cyclic diarylheptanoids from European hornbeam (*Carpinus betulus* L.). *Int J Mol Sci*, 2023;24.
155. Lee SG, Shin DJ, Lee ES, Goo YT, Kim CH, Yoon HY, Lee MW, Bang H, Seo SJ, Choi YW. Enhanced chemical stability of hirsutenone incorporated into a nanostructured lipid carrier formulation containing antioxidants. *Bull Korean Chem Soc*, 2018;39:1287-93.
156. Tabboon P, Tuntiyasawasdikul S, Sripanidkulchai B. Quality and stability assessment of commercial products containing phytoestrogen diarylheptanoids from *Curcuma comosa*. *Ind Crops Prod*, 2019;134:216-24.
157. Könczöl Á, Müller J, Földes E, Béni Z, Végh K, Kéry Á, Balogh GT. Applicability of a blood–brain barrier specific artificial membrane permeability assay at the early stage of natural product-based CNS drug discovery. *J Nat Prod*, 2013;76:655-63.
158. Kim NT, Lee DS, Chowdhury A, Lee H, Cha BY, Woo JT, Woo ER, Jang JH. Acerogenin C from *Acer nikoense* exhibits a neuroprotective effect in mouse

hippocampal HT22 cell lines through the upregulation of Nrf-2/HO-1 signaling pathways. *Mol Med Rep*, 2017;16:1537-43.

## List of Publications

Regarding the topic of the thesis:

**Felegyi-Tóth CA**, Garádi Z, Darcsi A, Csernák O, Boldizsár I, Béni S, Alberti Á. Isolation and quantification of diarylheptanoids from European hornbeam (*Carpinus betulus* L.) and HPLC-ESI-MS/MS characterization of its antioxidative phenolics. *J Pharm Biomed Anal*, 2022;210:114554.

**Felegyi-Tóth CA**, Heilmann T, Buda E, Stipsicz B, Simon A, Boldizsár I, Bősze S, Riethmüller E, Alberti Á. Evaluation of the chemical stability, membrane permeability and antiproliferative activity of cyclic diarylheptanoids from European hornbeam (*Carpinus betulus* L.). *Int J Mol Sci*, 2023;24.

Other publications:

Alberti Á, Riethmüller E, **Felegyi-Tóth CA**, Czigle S, Czégényi D, Filep R, Papp N. Phytochemical investigation of polyphenols from the aerial parts of *Tanacetum balsamita* used in Transylvanian ethnobotany and parallel artificial membrane permeability assay. *Plants*. 2024;13(12):1652.

Jakabfi-Csepregi R, Alberti Á, **Felegyi-Tóth CA**, Kőszegi T., Czigle, S, Papp N. A comprehensive study on *Lathyrus tuberosus* L.: Insights into phytochemical composition, antimicrobial activity, antioxidant capacity, cytotoxic, and cell migration effects. *Plants*. 2024;13:232.

**Felegyi-Tóth CA**; Osztie R; Boldizsár I; Alberti Á. Vadgesztenye. *Gyógyszerészet*. 2023;7(12):654-663.

Valiyeva A, **Felegyi-Tóth CA**, Várnai B, Garaev E, Béni S, Kursinszki L. Characterization of alkaloid profile of *Hyoscyamus reticulatus* L. and *Atropa belladonna* subsp. *caucasica* (Kreyer) Avet by LC-MS and NMR. *Nat Prod Res*, 2023;37(19):3357-3362

**Felegyi-Tóth CA**, Tóth Z, Garádi Z, Boldizsár I, Nedves AN, Simon A, Felegyi K, Alberti Á, Riethmüller E. Membrane permeability and aqueous stability study of linear and cyclic diarylheptanoids from *Corylus maxima*. *Pharmaceutics*. 2022;14(6):1250.

Csepregi R, Temesfői V, Das S, Alberti Á, **Tóth CA**, Herczeg R, Papp N, Kőszegi T. Cytotoxic, Antimicrobial, Antioxidant Properties and Effects on Cell Migration of Phenolic Compounds of Selected Transylvanian Medicinal Plants. *Antioxidants*. 2020;9(2):166.

## Acknowledgements

First of all, I wish to express my deep gratitude to my supervisor, **Dr. Ágnes Alberti** director for her guidance and encouragement. I would like to thank the huge amount of time and work she had paid to my professional development. I am especially grateful to her for her confidence in me as she taught me self-reliance and let me accomplish my ideas.

I would like to thank **Dr. Szabolcs Béni** former director of the Department of Pharmacognosy, who has given me the opportunity to take part in the analytical projects of the Department.

I also wish to thank my co-authors, **Zsófia Garádi** and **Dr. András Darcsi** for the NMR investigations, **Dr. Eszter Riethmüller** and **dr. Alexandra Simon** for the PAMPA investigations, **Dr. Imre Boldizsár** for the MS measurements, **Dr. Orsolya Csernák** for her help, and I thank **Dr. Szilvia Bősze** and **Bence Stipsicz** for the bioassays. My thanks also go to the hard-working former students whom I worked together with: **dr. Tímea Heilmann** and **dr. Eszter Buda**. I thank **Béla Dudás** (Egererdő Ltd., Mátrafüred Forestry) for providing the bark samples from Lajosháza.

I am grateful to **Dr. Nóra Gampe** for her tireless efforts in identifying and correcting the mistakes and typos in this thesis.

I thank **Dr. László Kursinszki** for the valuable discussions, **Dr. Anita Zempléni-Tóth**, **dr. Dániel Vesztergombi** and **dr. Petra Malcsiner** for their help and for the opportunity to work together, **Andrea Nagyné Nedves** for the technical help.

Special thanks to the staff of **Laboratory No. 4**, especially **Tamás Czeglédi**, **Dr. Bianka Várnai** and **Dr. Attila Ványolós** for their help, the good times we had in- and outside the laboratory, the scientific and less scientific conversations.

I thank **all my colleagues at the Department of Pharmacognosy**, especially **Dr. Ida Fejős**, **Lenke Tóth**, **Ilona Székely** and **László Kátai** for their help.

I am grateful to my husband, **dr. Kristóf Felegyi**, whom I walked this journey together with. I wish to thank my sons, **Boti** and **Kori** for their patience, my **family's** and **friends'** support, and faith in my work.

## Appendix

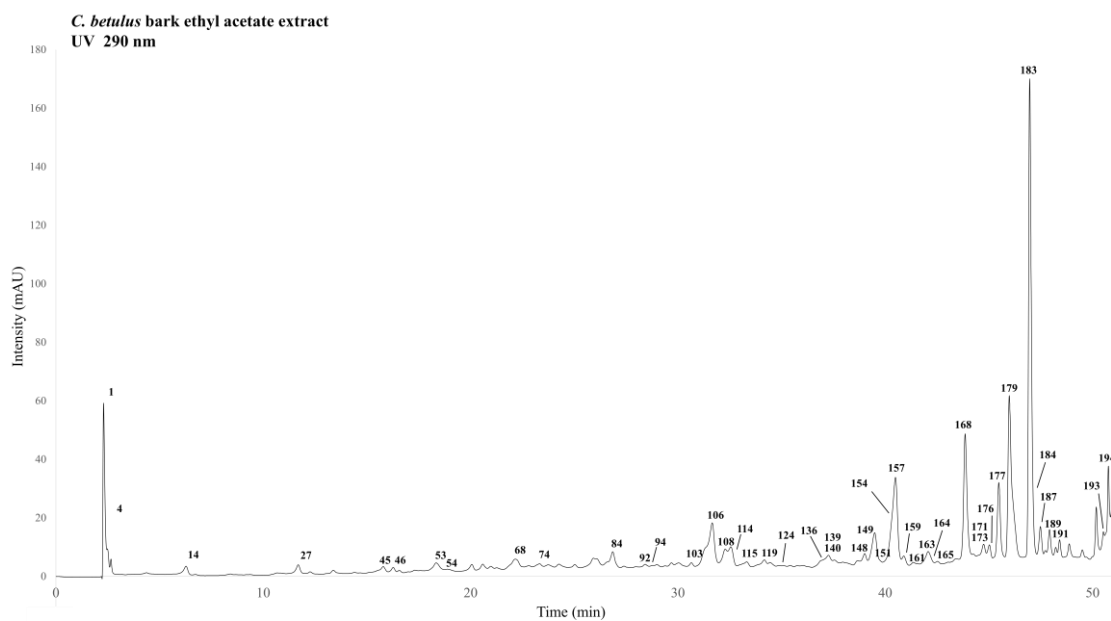


**Figure S1.** UV chromatogram of hornbeam bark extract prepared with ethyl acetate. Detection wavelength: 290 nm. Compound numbers refer to Table 3. For chromatographic conditions see Section III.4.1.

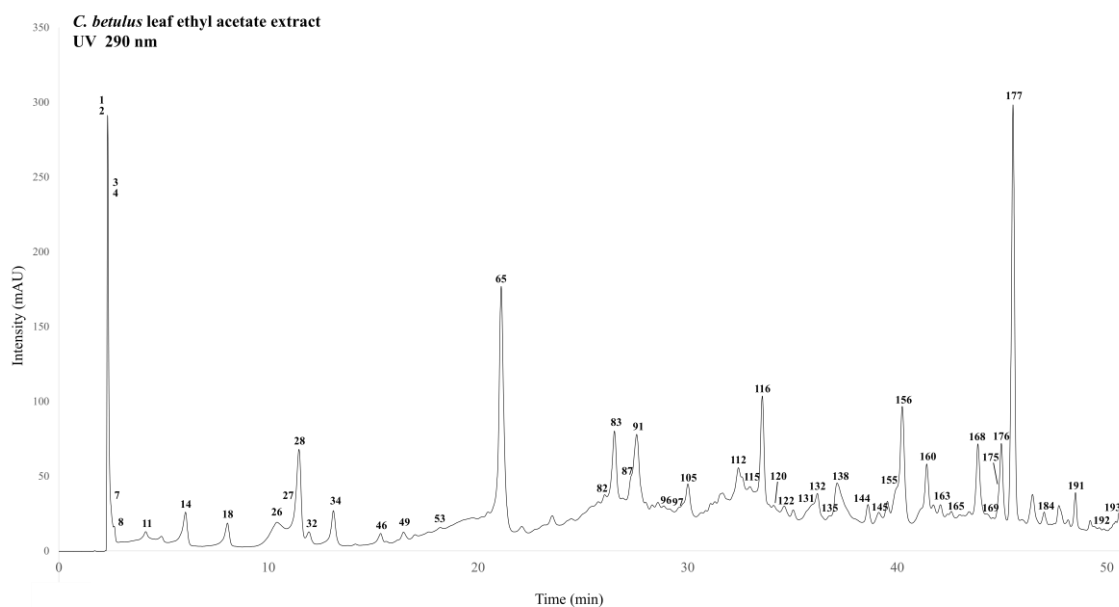


**Figure S2.** UV chromatogram of hornbeam leaf extract prepared with ethyl acetate. Detection wavelength: 290 nm. Compound numbers refer to Table 3. For chromatographic conditions see Section III.4.1.

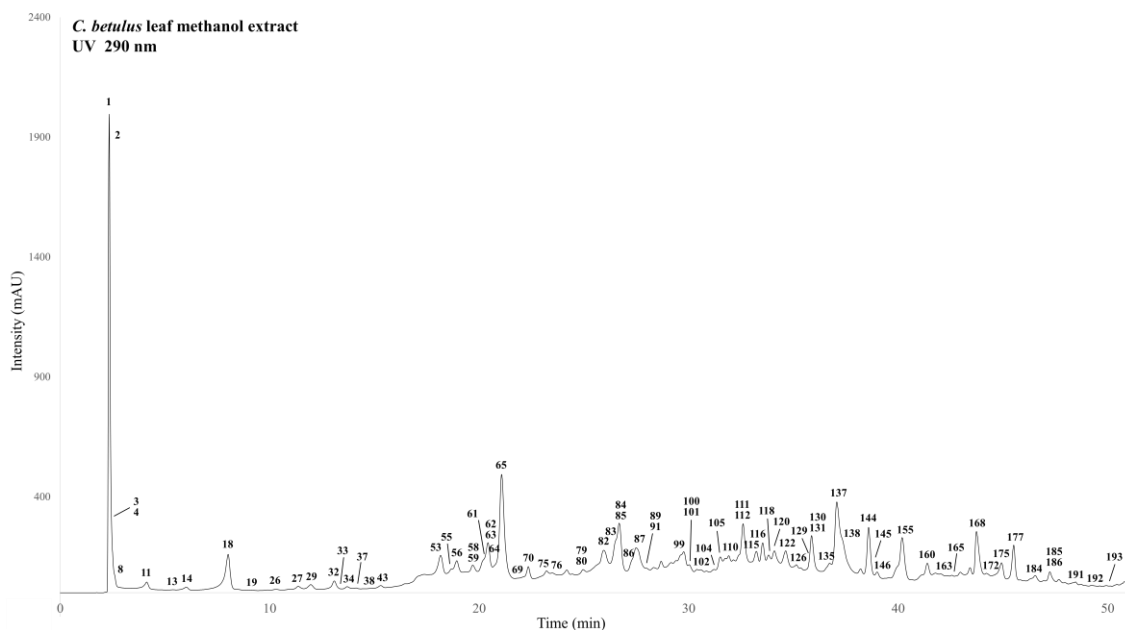


**Figure S3.** UV chromatogram of hornbeam leaf extract prepared with methanol. Detection wavelength: 290 nm. Compound numbers refer to Table 3. For chromatographic conditions see Section III.4.1.

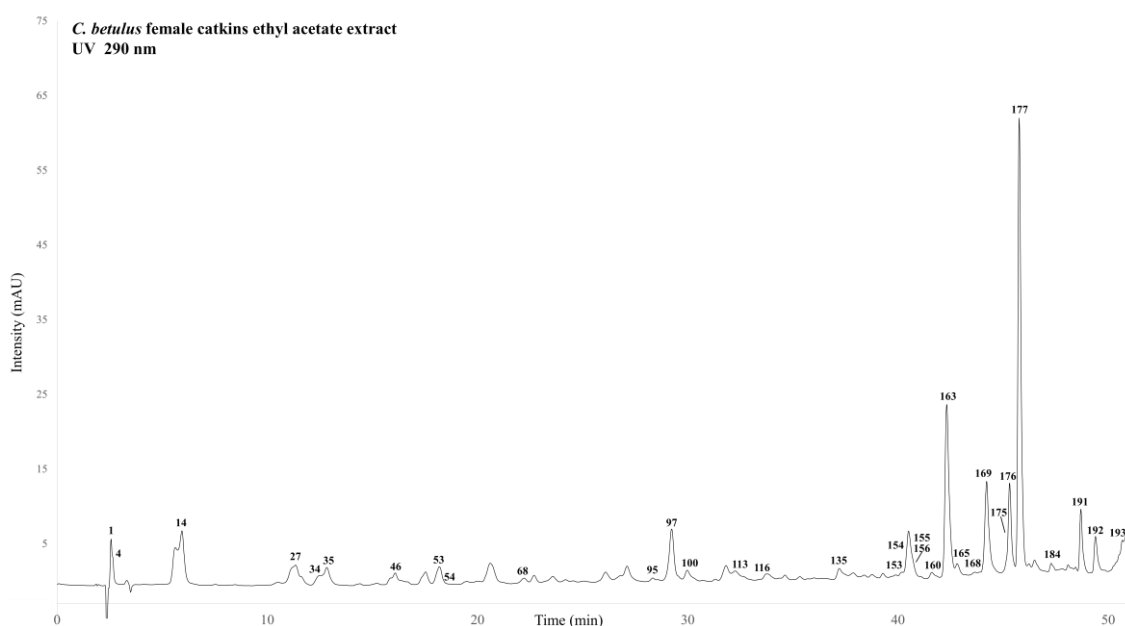


**Figure S4.** UV chromatogram of hornbeam female catkin extract prepared with ethyl acetate. Detection wavelength: 290 nm. Compound numbers refer to Table 3. For chromatographic conditions see Section III.4.1.

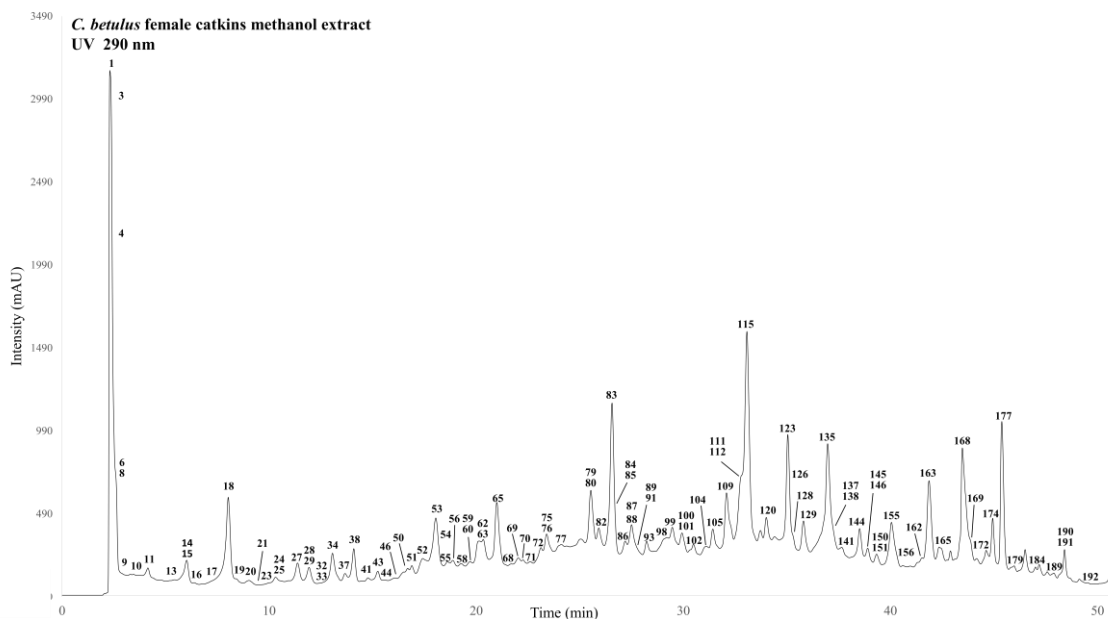


**Figure S5.** UV chromatogram of hornbeam female catkin extract prepared with methanol. Detection wavelength: 290 nm. Compound numbers refer to Table 3. For chromatographic conditions see Section III.4.1.

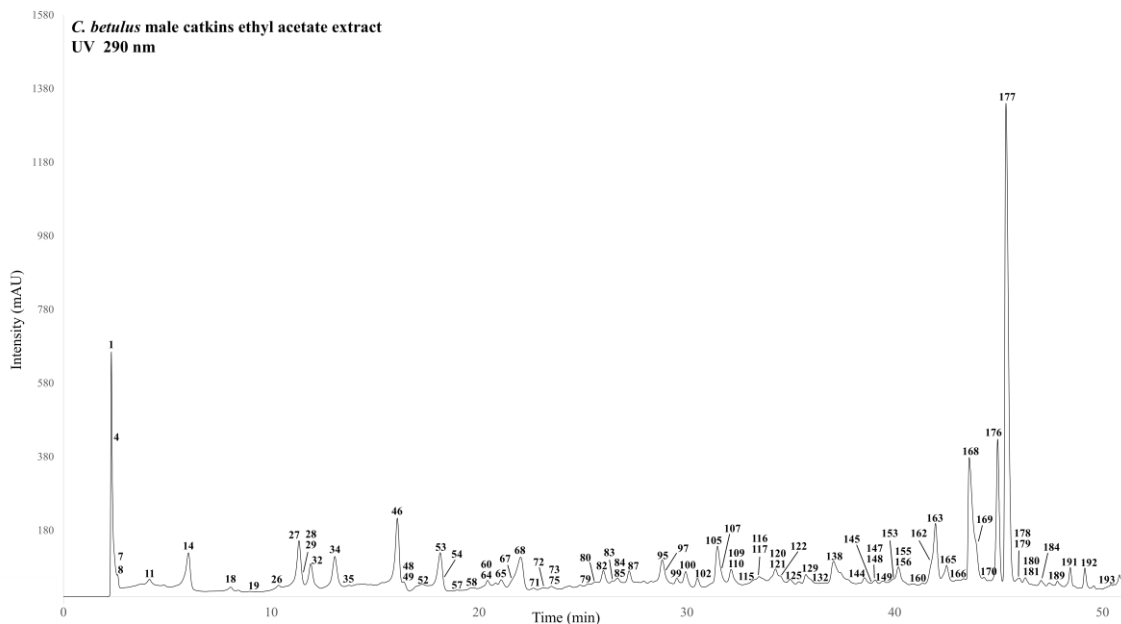


**Figure S6.** UV chromatogram of hornbeam male catkin extract prepared with ethyl acetate. Detection wavelength: 290 nm. Compound numbers refer to Table 3. For chromatographic conditions see Section III.4.1.

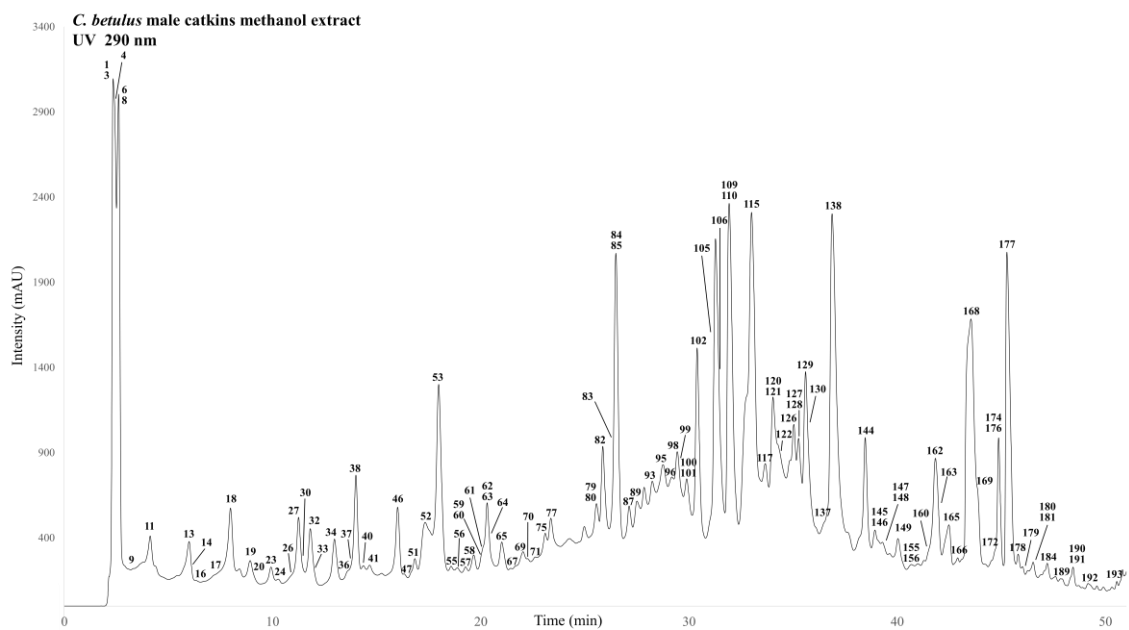


**Figure S7.** UV chromatogram of hornbeam male catkin extract prepared methanol. Detection wavelength: 290 nm. Compound numbers refer to Table 3. For chromatographic conditions see Section III.4.1.

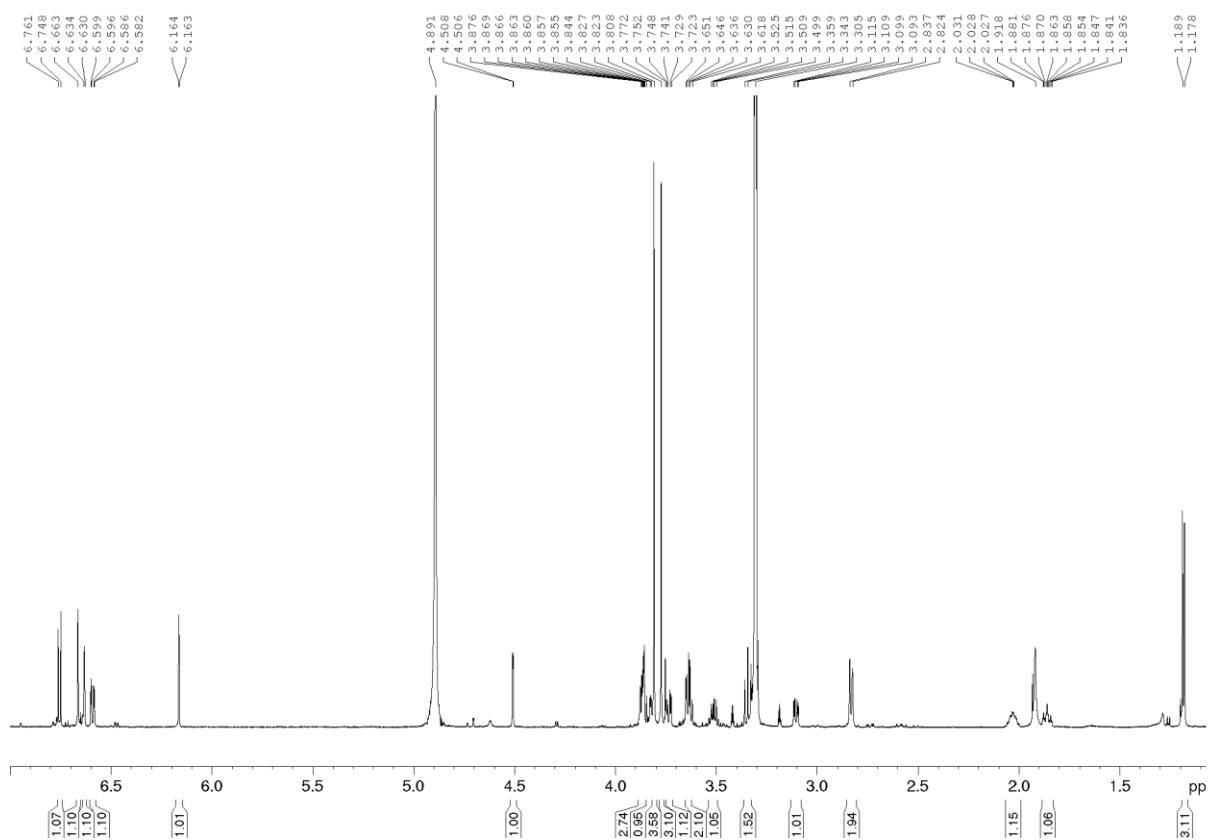


**Figure S8.**  $^1\text{H}$  NMR spectrum of aviculin (148)

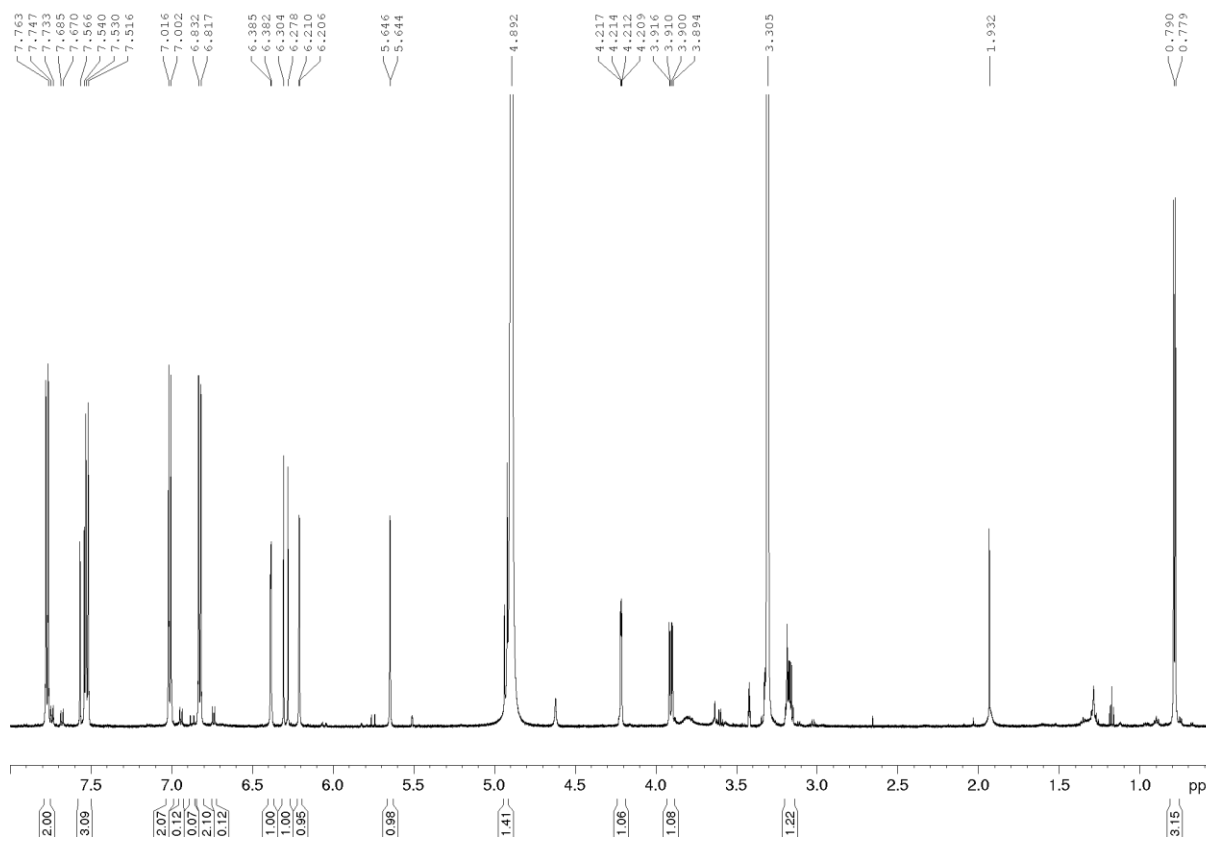


**Figure S9.** <sup>1</sup>H NMR spectrum of kaempferol-3-*O*-(4''-*E*-*p*-coumaroyl)-rhamnopyranoside (**185**)



# Isolation and quantification of diarylheptanoids from European hornbeam (*Carpinus betulus* L.) and HPLC-ESI-MS/MS characterization of its antioxidative phenolics

Csenge Anna Felegyi-Tóth<sup>a</sup>, Zsófia Garádi<sup>a</sup>, András Darcsi<sup>a</sup>, Orsolya Csernák<sup>a</sup>,  
Imre Boldizsár<sup>a,b</sup>, Szabolcs Béni<sup>a</sup>, Ágnes Alberti<sup>a,\*</sup>

<sup>a</sup> Semmelweis University, Department of Pharmacognosy, Üllői út 26, 1085 Budapest, Hungary

<sup>b</sup> Eötvös Loránd University, Department of Plant Anatomy, Institute of Biology, Pázmány Péter sétány 1/C, 1117 Budapest, Hungary

## ARTICLE INFO

### Article history:

Received 5 November 2021

Received in revised form 22 December 2021

Accepted 23 December 2021

Available online 27 December 2021

### Keywords:

European hornbeam

Diarylheptanoid

Isolation

Mass spectrometry

Quantitative analysis

Antioxidant activity

## ABSTRACT

Detailed polyphenol profiling of European hornbeam (*Carpinus betulus* L.) bark, leaf, male and female catkin extracts was performed by high-performance liquid chromatography–diode array detection coupled to tandem mass spectrometry (HPLC-DAD-MS/MS). A total of 194 compounds were characterized and tentatively identified. Gallo- and ellagitannins dominated in the methanol extracts, while flavonol glycosides and methoxylated flavones prevailed in the ethyl acetate samples. In the quest for diarylheptanoids, twelve compounds were isolated by the combination of subsequent reversed-phase flash chromatographic and high-performance liquid chromatographic methods. The structural elucidation of the isolated components was performed by ultrahigh-performance liquid chromatography–Orbitrap mass spectrometry (UHPLC-Orbitrap-MS) as well as 1D and 2D nuclear magnetic resonance (NMR) spectroscopy. Six known cyclic diarylheptanoids, together with a new compound were described in *Carpinus betulus* for the first time. The occurrence of a linear diarylheptanoid and a lignan has also been unprecedented in the genus *Carpinus*. Moreover, three known flavonol glycosides were isolated. Based on the identification of characteristic fragment ions, a new mass spectrometric fragmentation pathway for *meta,meta*-cyclophane-type diarylheptanoids was proposed. Quantities of the four major cyclic diarylheptanoids in European hornbeam were determined by a validated UHPLC-DAD method for the first time. The antioxidant properties of the extracts and the isolated compounds were assessed by the 2,2-diphenyl-1-picrylhydrazyl (DPPH) assay. Contribution of the individual constituents to the total radical scavenging activity of the samples was evaluated by an off-line DPPH-HPLC-DAD method. This allowed the identification of gallo- and ellagitannin derivatives as the constituents being primarily responsible for the antioxidant capacity of the extracts.

© 2021 The Author(s). Published by Elsevier B.V.

CC\_BY\_NC\_ND\_4.0

## 1. Introduction

Plants are still considered as noteworthy potential sources for new drugs, but the ligneous flora is rarely referred to for the presence of possible medical agents. The genus *Carpinus* (Betulaceae) comprises approximately 35 woody species spread in Europe, Eastern Asia, North, and Central America, with the highest number of species being native to China. European hornbeam (*Carpinus betulus* L.) is a common forest tree species widespread throughout Europe [1]. It is an important raw material for the wood industry: its valuable wood is used for tools, building constructions, flooring, to

prepare wooden parts of musical instruments (e.g. piano mechanisms), and as fuel wood and charcoal. Occurrence of bioactive constituents such as flavonol and flavone mono- and diglycosides were reported for *C. betulus* [2]. Hofmann and coworkers [3] characterized phenolic compounds by HPLC-MS/MS in *C. betulus* leaves, however, other parts of the plant were not analyzed. The authors investigated the seasonal changes in the antioxidant capacity of European hornbeam leaf extracts throughout the vegetation period, too. In a recent study, DPPH scavenging activity of European hornbeam bark extracts was assessed [4].

Although no specific applications of the waste (i.e. bark, leaves, etc.) resulting from processing of hornbeam wood have yet been identified, results of several studies and experiments support that *Carpinus* species could become easily affordable sources of new bioactive ingredients. The ethyl acetate and methanol extracts of *C.*

\* Corresponding author.

E-mail address: [alberti.agnes@pharma.semmelweis-univ.hu](mailto:alberti.agnes@pharma.semmelweis-univ.hu) (Á. Alberti).

*betulus* bark and leaf demonstrated in vitro growth inhibitory activity against various human cancer cell lines [5], while extracts of the cultivar *C. betulus* 'Fastigiata' presented immunosuppressive effects [6]. Although, diarylheptanoids have not yet been identified in *C. betulus*, other hornbeam species contain these compounds, e.g. the known cyclic diarylheptanoids, carpinontriols A and B as well as casuarinondiols were isolated from *Carpinus cordata* [7]. Diarylheptanoids attract interest in natural product research, due to their notable biological activities such as their cytotoxic, anti-inflammatory, anti-microbial, and antioxidant effects [8].

The aim of this study was a detailed and extensive phytochemical characterization of European hornbeam by HPLC-DAD-MS/MS. Distinct plant parts: leaf, bark, female, and male catkin samples were collected to compare their phenolic composition. *C. betulus* extracts were prepared with solvents of different polarity, in order to obtain diverse compositions of phenolics. We aimed to screen the phenolic profile of hornbeam samples with special regard to cyclic diarylheptanoids. Thus, our further aim was to confirm their plausible presence in *C. betulus* samples, reveal their structures by NMR experiments, and assess their quantities. To determine the in vitro antioxidant activity of the extracts and the isolated compounds, the DPPH assay was employed. An off-line DPPH-HPLC-DAD-MS method was applied to assess the contribution of individual constituents to the total radical scavenging activity of each extract.

## 2. Materials and methods

### 2.1. Chemicals and reagents

Chloroform, ethyl acetate, methanol, and *n*-hexane of reagent grade as well as HPLC grade methanol and acetonitrile were purchased from Molar Chemicals Kft. (Halásztelek, Hungary). Acetic acid 100% for HPLC LiChropur™, DPPH (2,2-diphenyl-1-picrylhydrazyl), rutin, trolox (6-hydroxy-2,5,7,8-tetramethylchromane-2-carboxylic acid), trifluoroacetic acid, methanol-*d*<sub>4</sub>, and DMSO-*d*<sub>6</sub> for NMR measurements were acquired from Sigma-Aldrich (Steinheim, Germany). High-purity water was gained by a Millipore Direct Q5 Water Purification System (Billerica, MA, USA).

### 2.2. Plant material and sample preparation

For the qualitative HPLC-MS analyses, the UHPLC-DAD quantitation, and the DPPH assays, bark, leaf, female, and male catkin samples of *C. betulus* were collected in Hungary, in the Buda Hills (Budai-hegység, April 2015), Mátraháza (May 2016) and Visegrád Mountains (Visegrádi-hegység, July 2018). Authenticated samples and herbarium specimens are deposited at the Herbarium of the Department of Pharmacognosy, Semmelweis University, Budapest, Hungary. Dried and milled samples (3.0 g each) were extracted by Soxhlet extraction (6 h) with ethyl acetate and methanol (250 mL each). The extracts were distilled to dryness under reduced pressure with a rotary evaporator (Büchi Rotavapor R-200, Flawil, Switzerland) at 50 °C. The samples were redissolved in 4.0 mL methanol of HPLC gradient grade and filtered through Minisart RC 15 0.2 µm syringe filters (Sartorius AG, Goettingen, Germany). Prior to analysis, the purified samples were evaporated to dryness at 50 °C under reduced pressure and redissolved in 1.0 mL 70% (v/v) HPLC grade methanol.

### 2.3. Isolation procedures

For the isolation of the constituents, bark samples of *C. betulus* were collected in Hungary, in Mátraháza (May 2017) and Lajosháza (May 2019). The combined and dried samples (500 g) were ground and extracted at room temperature in ultrasonic bath with chloroform (3 × 2 L, 2 h each). In the following, the residue was extracted

consecutively with solvents of increasing polarity: ethyl-acetate and then methanol (3 × 2 L for both solvents, 2 h each). The ethyl acetate extract was distilled to dryness under reduced pressure with a rotary evaporator at 50 °C. The residue was suspended in 70% (v/v) methanol (to get a concentration of 500 mg in 4 mL) and fractionated using a CombiFlash NextGen 300+ (Teledyne Isco, Lincoln, NE, USA) flash chromatograph, applying a RediSep Rf Gold C18 column (100 g, Teledyne Isco) as stationary phase. Eluent A was 0.3% acetic acid in water, eluent B was methanol, and the following gradient elution was applied at a flow rate of 60 mL/min: 30% B (0–3 min), 30–100% B (3–33 min), 100% B (33–38 min). 144 fractions (of 16 mL each) were collected. Fractions 56–60 yielded compound **177** (23.5 mg). Chromatographic separations of additional fractions were performed by semi-preparative HPLC on a Waters 2690 HPLC system equipped with a Waters 996 diode array detector (Waters Corporation, Milford, MA, USA). As stationary phase, a Luna C18 100 A (150 × 10 mm i.d., 5 µm; Phenomenex Inc; Torrance, CA, USA) column or a Kinetex C18 100 A (150 × 10 mm i.d., 5 µm; Phenomenex Inc) column was used (Fig. S1). Different gradient elution methods consisting of 0.3% acetic acid in water (eluent A) and methanol (eluent B) were applied at a flow rate of 1 mL/min. Fractions 38–41 were separated to obtain **106** (3.5 mg, *t*<sub>R</sub> = 22.3 min), **114** (1.3 mg, *t*<sub>R</sub> = 24.1 min), and **154** (1.5 mg, *t*<sub>R</sub> = 30.0 min), using the gradient as follows: 33% B (0–20 min), 33–100% B (20–25 min), 100% B (25–33 min). Fractions 68–71 were chromatographed using the gradient 50% B (0–20 min), 50–100% B (20–23 min), 100% B (23–33 min), to yield compound **191** (2.2 mg, *t*<sub>R</sub> = 24.1 min). For the chromatographic separation of fractions 61–67 to purify **164** (0.7 mg, *t*<sub>R</sub> = 13.6 min) and **187** (0.5 mg, *t*<sub>R</sub> = 14.4 min), we applied a different gradient elution system consisting of 0.3% acetic acid in water (eluent A) and acetonitrile (eluent B) at a flow rate of 1 mL/min: 40–64% B (0–16 min), 64–100% B (16–17 min).

The methanol extract of the bark sample was distilled to dryness under reduced pressure with a rotary evaporator at 50 °C. The residue was redissolved in 70% (v/v) methanol (to get a concentration of 1000 mg in 4 mL) and separated by flash chromatography as described for the ethyl acetate extract. Fractions were further separated by semi-preparative HPLC (using the same instrumentation and stationary phase as detailed above). Different gradient elutions were employed at a flow rate of 1 mL/min. Fractions 50–55 were purified with the gradient as follows (eluent A: 0.3% acetic acid in water, eluent B: methanol): 50% B (0–20 min), 50–100% B (20–22 min), 100% B (22–32 min), 6 fractions were collected. Fraction 2 (*t*<sub>R</sub> = 12 min) was further chromatographed applying the following gradient elution (eluent A: 0.3% acetic acid in water, eluent B: acetonitrile): 22–24% B (0–22 min), to yield **148** (1.2 mg, *t*<sub>R</sub> = 19.2 min). Fractions 56–61 from flash chromatography were separated to collect 8 fractions, with the gradient (eluent A: 0.3% acetic acid in water, eluent B: methanol): 45–50% B (0–20 min), 50–100% B (20–22 min), 100% B (22–32 min). Fraction 8 (*t*<sub>R</sub> = 23 min) was chromatographed with the gradient elution (eluent A: 0.3% acetic acid in water, eluent B: acetonitrile) 35% B (0–16 min), 35–100% B (16–17 min), to yield **149** (1.7 mg, *t*<sub>R</sub> = 13.7 min), **157** (2.0 mg, *t*<sub>R</sub> = 14.7 min), and **161** (0.7 mg, *t*<sub>R</sub> = 12.5 min). Fractions 73–75 from flash chromatography were separated to yield **185** (3.3 mg, *t*<sub>R</sub> = 17.1 min), using the following gradient elution (eluent A: 0.3% acetic acid in water, eluent B: acetonitrile): 40–60% B (0–25 min). The isolation procedure is depicted in Fig. S1. Purity of the isolated substances was surveyed by HPLC-DAD-MS/MS.

### 2.4. HPLC-DAD-ESI-MS/MS analyses

Qualitative phytochemical screening of *Carpinus* extracts was performed with an Agilent 6410B triple quadrupole equipped with an electrospray ionization source (ESI) coupled to an Agilent 1100 HPLC system (G1379A degasser, G1312A binary gradient pump,

G1329A autosampler, G1316A column thermostat and G1315C diode array detector) (Agilent Technologies, Santa Clara, CA, USA and Waldbronn, Germany). The separation of *Carpinus* extracts was carried out on a Zorbax SB-C18 column (150 × 3.0 mm i.d., 3.5 μm; Agilent Technologies). Eluent A was 0.3% acetic acid in water and eluent B was methanol. A gradient elution was performed at a flow rate of 0.3 mL/min as follows: 10–40% B (0–35 min), 40–60% B (35–45 min), 60–100% B (45–47 min), 100% (47–50 min), 100–10% B (50–51 min), the column temperature was set to 25 °C. The injection volume was 10 μL. Nitrogen was applied as drying gas (350 °C, 9 L/min), the nebulizer pressure was 45 psi. The fragmentor voltage was set to 120 V, the capillary voltage was 3500 V. High purity nitrogen was used as collision gas, the collision energy varied between 10 and 40 eV. Full scan mass spectra were recorded in negative ionization mode in the range of *m/z* 100–1000. The MassHunter B.01.03 software was used for data acquisition and qualitative analyses.

## 2.5. UHPLC-ESI-Orbitrap-MS/MS conditions

High-resolution mass spectra of the isolated compounds were obtained using a Dionex Ultimate 3000 UHPLC system (3000RS diode array detector, TCC-3000RS column thermostat, HPG-3400RS pump, SRD-3400 solvent rack degasser, WPS-3000TRS autosampler), hyphenated with an Orbitrap Q Exactive Focus Mass Spectrometer equipped with electrospray ionization source (Thermo Fischer Scientific, Waltham, MA, USA). An Acquity UPLC BEH C18 column (30 × 2.1 mm i.d., 1.7 μm; Waters Corporation) was used (column temperature: 25 °C), and the mobile phase consisted of 0.1% formic acid in water (eluent A) and a mixture of 0.1% formic acid in water and acetonitrile (20:80, v/v) (eluent B). The following gradient elution was applied at a flow rate of 0.3 mL/min: 10–60% B (0.0–3.5 min), 60–100% B (3.5–4.0 min), 100% B (4.0–4.5 min), 100–10% B (4.5–7.0 min). The injection volume was 1 μL. The ESI source was operated in negative ionization mode and operation parameters were optimized automatically using the built-in software. The working parameters were as follows: spray voltage 2500 V; capillary temperature 320 °C; sheath gas (N<sub>2</sub>), 47.5 °C; auxiliary gas (N<sub>2</sub>) 11.25 arbitrary units, and spare gas (N<sub>2</sub>) 2.25 arbitrary units. The resolution of the full scan was of 70000, and the scanning range was between *m/z* 100–500 units. The most intense ions detected in full scan spectrum were selected for data-dependent MS/MS scan at a resolving power of 35000, in the range of *m/z* 50–500. Parent ions were fragmented with normalized collision energy of 10%, 30%, and 45%.

## 2.6. Quantitative UHPLC-DAD conditions

Quantities of the isolated diarylheptanoids carpinontriols A (**106**) and B (**149**), 3,12,17-trihydroxytricyclo[12.3.1.1<sup>2,6</sup>]nonadecan-1(18),2(19),3,5,14,16-hexaene-8,11-dione (**154**), and giffonin X (**157**) were determined by UHPLC-DAD. The *Carpinus* extracts were analyzed by an ACQUITY UPLC H-Class PLUS System equipped with a quaternary solvent delivery pump (QSM), an auto-sampler manager (FTN), a column compartment (CM), and a photodiode array (PDA) detector (Waters Corporation). An Acquity BEH C18 column (100 × 2.1 mm i.d., 1.7 μm; Waters Corporation) maintained at 30 °C was used as stationary phase. Eluent A was 0.3% acetic acid in water and eluent B was acetonitrile, the following gradient elution was applied (flow rate: 0.3 mL/min): 12.0–13.5% B (0.0–19.0 min), 13.5–75.0% B (19.0–25.5 min), 75.0–100.0% B (25.5–26.0 min), 100.0% B (26.0–28.0 min), 100.0–12.0% B (28.0–28.5 min). The injection volume was 2 μL. Chromatograms were recorded at 295 nm.

## 2.7. Validation of the quantitative method

### 2.7.1. Preparation of standard solutions, linearity, and selectivity

Quantitation was performed by the external standard method. Stock solutions containing 1 mg/mL of the isolated **106**, **149**, **154**, and **157** in HPLC grade methanol were prepared. For the preparation of the calibration curve, stock solutions were diluted with methanol of HPLC grade, to yield solutions with concentrations of 1, 2.5, 5, 25, 50, 100, and 250 μg/mL. Each standard solution was prepared in triplicate and injected once. Standard solutions were stored at 4 °C before injection. Linearity curves were constructed by plotting peak areas against corresponding concentrations. Slope, intercept, and correlation coefficient were determined by least squares polynomial regression analysis. Limits of detection (LOD) and quantitation (LOQ) were determined at signal-to-noise (S/N) ratios 3 and 10, respectively. The selectivity of the method was evaluated by analyzing blank samples (extracts obtained by extraction with *n*-hexane), and spiked samples (extracts fortified with standard solutions of the analytes).

### 2.7.2. Precision, accuracy, and repeatability

Quality control samples were prepared at 5, 50, and 250 μg/mL nominal concentrations. All samples were prepared in triplicate and injected once on the same day (intra-day precision and accuracy) or on three consecutive days (inter-day precision and accuracy). Retention time repeatability was assessed by injecting the standard solutions in six successive parallels.

### 2.7.3. Recovery

Extraction recovery for giffonin X (**157**) was tested in a concentration range to match with that of the target analyte in the plant sample. 1.0–1.0 g dried *C. betulus* bark samples were spiked with 0.25 mL aliquots of a solution of **157** (1.0 mg/mL) and extracted at room temperature in ultrasonic bath with ethyl acetate and methanol (3 × 10.0 mL, 30 min each), respectively. Samples were prepared in three parallels. Further sample preparation steps were the same as described in Section 2.2. Recovery (R) was calculated as  $R = 100 \times (C_{\text{found}} - C_{\text{initial}}) / C_{\text{added}}$ , where  $C_{\text{found}}$  = measured concentration in the fortified sample,  $C_{\text{initial}}$  = initial concentration in the sample,  $C_{\text{added}}$  = concentration in the standard solution used.

## 2.8. NMR conditions

NMR spectra of the isolated compounds were recorded in methanol-*d*<sub>4</sub> on a Varian DDR 600 (600/150 MHz) instrument equipped with a 5-mm inverse-detection gradient (IDPFG) probehead at 298 K or on a BRUKER AVANCE III HD 600 (600/150 MHz) instrument equipped with Prodigy cryo-probehead at 295 K. High temperature NMR experiments were conducted on a Bruker Avance III 400 (400/100 MHz) equipped with a PA BBO 400W1 BBF-H-D-05 Z (Billerica, MA, USA) probehead at 370 K in DMSO-*d*<sub>6</sub>. The pulse programs were taken from the vendor's software library (TopSpin 3.5 or Vnmrj 3.2). <sup>13</sup>C and <sup>1</sup>H chemical shifts (δ) are given in ppm relative to the NMR solvent or relative to tetramethylsilane (TMS), while coupling constants (*J*) are given in ppm and in Hz, respectively. The complete <sup>1</sup>H and <sup>13</sup>C resonance assignments were achieved using 1D <sup>1</sup>H NMR, <sup>13</sup>C NMR, DeptQ, and homo- and heteronuclear 2D <sup>1</sup>H-<sup>1</sup>H COSY, <sup>1</sup>H-<sup>13</sup>C edHSQC, <sup>1</sup>H-<sup>13</sup>C HMBC, <sup>1</sup>H-<sup>1</sup>H NOESY or <sup>1</sup>H-<sup>1</sup>H ROESY, and <sup>1</sup>H-<sup>1</sup>H TOCSY experiments.

## 2.9. Evaluation of the antioxidant activity

### 2.9.1. DPPH assay

Antioxidant activities of *C. betulus* extracts and the isolated compounds were determined by spectrophotometry in an in vitro decolorization assay using DPPH as free radical. For comparison, solutions of trolox and rutin were also studied. The following method was applied: 10 mg of DPPH was dissolved in 25.0 mL HPLC grade methanol, stock solutions were diluted with HPLC methanol just before measuring, so that the absorbance of the diluted free radical solution was approximately 0.90. Detection was carried out at 515 nm wavelength which is the characteristic absorption maximum of the DPPH radical. Hornbeam extracts of 5 different concentrations were added to the free radical solutions (2.5 mL), in triplicate. After incubation for 6 min at room temperature in the dark, the decrease in absorbance was measured with a HITACHI U-2000 spectrophotometer (Hitachi Ltd., Tokyo, Japan). Half maximal inhibitory concentration value ( $IC_{50}$ ,  $\mu\text{g/mL}$ ) was determined for each sample [9]. Comparison between hornbeam extracts prepared with ethyl acetate and methanol was performed by oneway analysis of variance (ANOVA), followed by Tukey's post hoc HSD test.

### 2.9.2. DPPH-HPLC-DAD analysis

An off-line DPPH-HPLC-DAD method was applied to compare the contribution of each compound to the total antioxidant effect against DPPH [10]. Hornbeam samples (0.5 mg/mL) were mixed with a DPPH solution (1.5 mg DPPH / 1 mL HPLC methanol, prepared right before the assays) at the ratio of 1:1 (v:v). The mixtures were incubated at room temperature for 30 min, while protected from light. The control samples were made by adding methanol instead of the DPPH solution to the samples in the same ratio. The DPPH-treated samples and control samples were evaluated in 3 parallels by HPLC-DAD-MS using the same method as detailed in Section 2.4. Phenolics with antioxidant activities decompose while reacting with the DPPH radicals, thus their AUC (area under the curve) values in HPLC-DAD-MS chromatograms decrease, as compared to control samples. We calculated the changes in AUC values using the following formula:  $(\%) = (1 - AUC_{DPPH} / AUC_{control}) \times 100$ .

## 3. Results and discussion

### 3.1. HPLC-DAD-MS screening of *Carpinus betulus* polyphenols

HPLC-DAD-ESI-MS/MS in negative ionization mode was used to evaluate the phenolic profile of the extracts. In this study, 194 compounds were tentatively characterized by comparing their retention times, UV spectra, and mass spectrometric fragmentation patterns with data from the literature. Occurrence of the detected compounds, their chromatographic and mass spectrometric properties are listed in [Supplementary Table S1](#). UV chromatograms of the extracts detected at 290 nm are shown in [Supplementary Figs. S2-S9](#).

In line with literature data, gallotannins and ellagitannins prevailed in hornbeam extracts [3]. Gallic acid derivatives eluting at low retention times were characterized by their typical fragment ions at  $m/z$  169 which is the deprotonated molecular ion of gallic acid, and  $m/z$  125 which is created by the cleavage of the carboxyl group from gallic acid [11,12]. Compounds **8**, **16**, and **18**, characterized as galloylquinic acid isomers, could also be distinguished from the relative intensities of their fragment ions [13]. In case of 5-*O*-galloylquinic acid (**16**), the fragment ion at  $m/z$  191 is dominating, while the relative intensity of the fragment ion at  $m/z$  173 indicates the 4-*O*-galloylquinic acid structure for compound **18**. 3-*O*-galloylquinic acid (**8**) which showed the lowest retention time, yielded comparatively intense fragment ions both at  $m/z$  169 and 191.

Gallotannins (**G**, [Table S1](#)) were found typically in methanol extracts of leaf, female, and male flower samples. The compounds contain a hexose core (mainly glucose) with its hydroxyl groups partly or completely substituted with a varying number of galloyl moieties via ester linkage. These components exhibited the representative fragment ions of gallic acid at  $m/z$  169 and  $m/z$  125 as well as neutral losses of 170 Da (gallic acid), 152 Da (galloyl moiety), and 134 Da (galloyl moiety losing a water molecule) [11]. Eight tri-galloyl hexose isomers (**41**, **52**, **60**, **75**, **82**, **85**, **88**, **102**) were detected displaying the  $[M-H]^-$  ion at  $m/z$  635. The fragment ions  $[M-H-170]^-$  at  $m/z$  465 and  $[M-H-170-152]^-$  at  $m/z$  313 were generated by the cleavage of a gallic acid and a galloyl moiety, respectively. Compounds **96**, **105**, **110**, and **120** presenting  $[M-H]^-$  ions at  $m/z$  787 were characterized as tetragalloyl hexose isomers. Pentagalloyl hexose isomers (**118**, **123**, **128**, **138**) exhibited their  $[M-H]^-$  ion at  $m/z$  939.

Ellagitannins (**E**, [Table S1](#)) contain hexahydroxydiphenol (HHDP) groups attached via ester linkage to a polyol core (e.g. glucose). These compounds were identified by the presence of the ellagic acid fragment ion at  $m/z$  301, the monogalloyl hexose fragment ion at  $m/z$  331, and the ellagic acid hexoside fragment ion at  $m/z$  463 [11,12,14]. Compounds **6**, **20**, **23**, **30**, **38**, **43**, **51**, and **84**, with  $[M-H]^-$  ions at  $m/z$  633, identified as galloyl-HHDP hexose isomers, and galloyl-bis-HHDP hexoses with  $[M-H]^-$  ions at  $m/z$  935 (**40**, **50**, **66**, **77**, **81**, **90**) were found in the methanolic extracts of bark and flower samples. Three digalloyl-HHDP hexoses (**37**, **61**, **134**) presenting the  $[M-H]^-$  ion at  $m/z$  785, and five trigalloyl-HHDP hexose isomers (**89**, **109**, **127**, **129**, **144**) with the  $[M-H]^-$  ion at  $m/z$  937 were identified.

Glycosylated and methoxy-substituted hydroxybenzoic acid derivatives (**B**, [Table S1](#)) were present primarily in the methanolic extract of the bark sample. Their typical fragment ions included the dihydroxybenzoic acid moiety at  $m/z$  153 and its fragment ion at  $m/z$  109, yielded by the cleavage of the  $CO_2$  group [11,14]. In contrast to hydroxybenzoic acids, hydroxycinnamic acid derivatives (**C**, [Table S1](#)) were representative of leaf, female, and male catkin samples. Similarly to the galloylquinic acids, the relative intensities of fragment ions in the mass spectra of the cinnamoylquinic acid isomers could facilitate their differentiation. Thus, an abundant fragment ion at  $m/z$  191 indicated the identification of **65** as 5-*O*-caffeoylquinic acid, **91** as 5-*p*-*O*-coumaroylquinic acid, and **116** as 5-*O*-feruloylquinic acid [15]. The minor components **83**, **111**, and **132** displayed identical fragmentation patterns. According to the results of Jaiswal et al. [15], these compounds eluting at higher retention times were assumed as the more hydrophobic *cis* isomers of the corresponding 5-*O*-caffeoyl-, 5-*O*-coumaroyl-, and 5-*O*-feruloylquinic acids, respectively.

In accordance with previous studies [2,3], flavonol and flavone derivatives occurred in the flower and leaf extracts (**F**, [Table S1](#)) mainly in their glycosidic form. Cleavage of a hexose, a deoxyhexose or a pentose sugar moiety during the collision-induced dissociation (CID) of flavonoid glycosides resulted in neutral losses of 162, 146, and 132 Da, respectively [16]. The glycosylation site of flavonol glycosides could also be deduced. Flavonol-3-*O*-glycosides favour the homolytic cleavage of the saccharide moiety during their CID in negative ionization mode. Thus, the relative abundance of the radical aglycone ion  $[Y_0-H]^-$  (deriving from a homolytic cleavage) was higher in their mass spectra than that of the aglycone anion  $[Y_0]^-$  [17]. Peak **155** presenting the  $[M-H]^-$  ion at  $m/z$  463 was identified as myricetin-3-*O*-deoxyhexoside, based on the relative abundance of its  $[M-H-147]^-$  ion at  $m/z$  316. Analogously, **135** and **153** displayed their  $[M-H]^-$  ions at  $m/z$  479 and 449, respectively, and the  $[M-H-163]^-$  and  $[M-H-133]^-$  ions at  $m/z$  316. Therefore, **135** and **153** were identified as myricetin-3-*O*-hexoside and myricetin-3-*O*-pentoside, respectively. Quercetin- and kaempferol-3-*O*-monoglycoside derivatives (**160**, **163**, **169**, **176**, **177**, **191**) were characterized similarly [16-19].

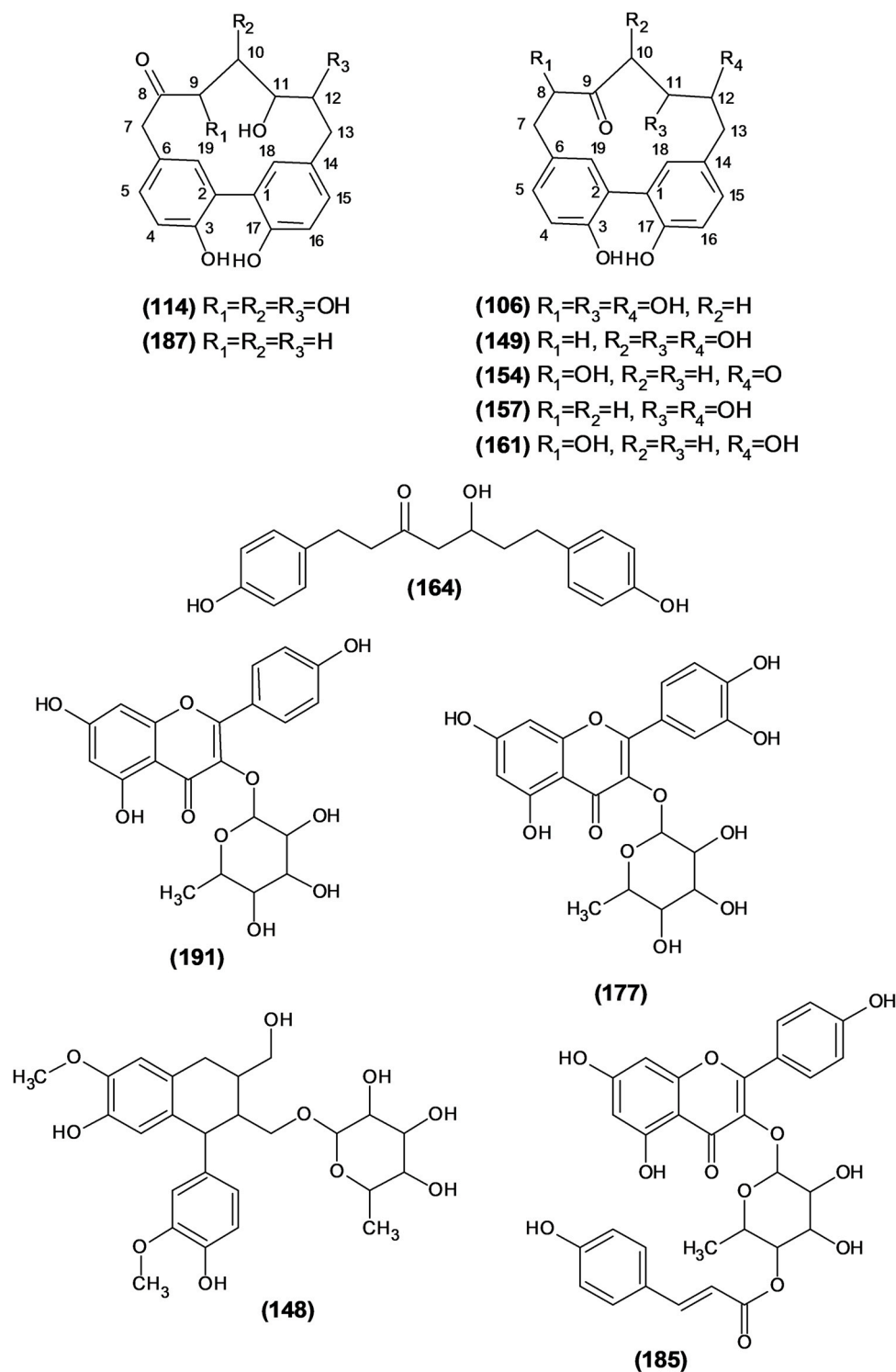


Fig. 1. Compounds isolated from *C. betulus* bark.

Compounds **185** and **186** showed complex UV spectra with absorption maxima at 267, 317, and 345 nm. In their mass spectra, two successive losses of 146 Da and the aglycone anion at  $m/z$  285 could be observed, thus the constituents were supposed to be kaempferol-dideoxyhexoside isomers. However, as a result of a more rigorous analysis, one of the 146 Da losses was later characterized as a coumaroyl moiety (coumaric acid- $H_2O$ ). This presumption was confirmed by the presence of the fragment ion at  $m/z$  163, which could be assigned to the  $[M-H]^-$  ion of coumaric acid. Thus, **185** and **186**

were established as kaempferol-deoxyhexoside coumaroyl ester isomers [20]. NMR analysis of the isolated **185** confirmed the proposed structure (see Section 3.2.).

Methoxylated flavones as well as their glycosylated and sulfated derivatives were detected in bark samples. Neutral losses of 15 Da referred to the cleavage of methyl radicals ( $-CH_3^{\cdot}$ ) indicating the presence of methoxy groups in the molecule [21]. Accordingly, compound **179** exhibiting fragment ions at  $m/z$  315 and 300 was assumed as a methoxyflavone derivative. Constituents **159**, **181**, and

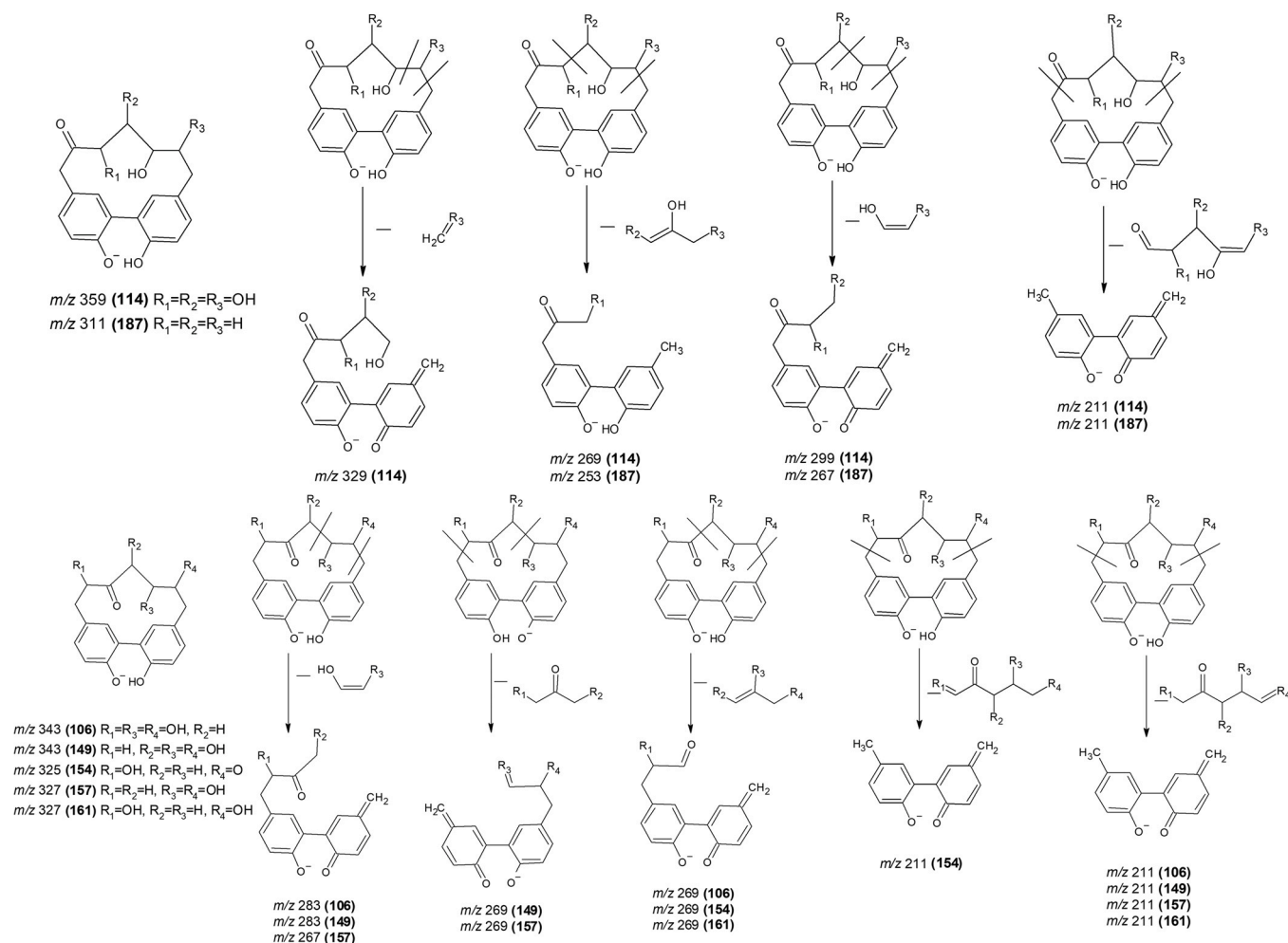


Fig. 2. Proposed mass spectrometric fragmentation pathways of cyclic diarylheptanoids isolated from *C. betulus* bark.

**183** presented fragment ions at  $m/z$  328, 313, and 298 which denoted the cleavage of two methyl radicals, thus, these compounds were characterized as dimethoxyflavone derivatives. Similarly, compounds **188** and **190** with  $[M-H]^-$  ions at  $m/z$  343 and fragment ions at  $m/z$  328, 313, 298 were identified as trimethoxyflavones. Both **174** and **158** displayed a neutral loss of 80 Da which indicated the cleavage of a  $SO_3$  moiety [22], therefore, they were recorded as trihydroxy-dimethoxyflavone-*O*-sulfate and its pentoside, respectively.

Constituents **48** and **54** exhibiting  $[M-H]^-$  ions at  $m/z$  289 were identified as flavan-3-ol derivatives catechin or epicatechin, due to their typical fragment ion  $[M-H-CO_2]^-$  at  $m/z$  245, deriving from the decarboxylation of catechin or epicatechin [11]. Compound **115** with its pseudomolecular ion at  $m/z$  305 and  $[M-H-OH-CO_2]^-$  ion at  $m/z$  245 was referred to as gallocatechin or epigallocatechin. Peaks **107** and **152** presenting their  $[M-H]^-$  ions at  $m/z$  441 and fragment ions at  $m/z$  289, 245, 169, and 125 were tentatively characterized as catechin gallate or epicatechin gallate [11].

The UV spectra of several constituents (**D**, Table S1) were similar to those of gallic acid derivatives ( $\lambda_{max} = 280\text{--}290$  nm), however, their mass spectra did not display the characteristic fragment ions at  $m/z$  169 and 125. Although cyclic diarylheptanoids, also exhibiting intense UV absorption in this range, have not yet been detected in *C. betulus*, we hypothesized their presence due to their occurrence in other *Carpinus* species [7]. Compounds **106** and **149** were presumed as carpinontriols A and B, respectively, since their mass spectra showed a fragmentation pattern similar to that previously described for hazelnut diarylheptanoids [20]. The base peak at  $m/z$  269 was

ascribed to a rearrangement of the deprotonated compound and the subsequent opening of the diarylheptanoid cycle, resulting in the neutral loss of a hydroxy-propan-2-one unit. However, the formation of further typical fragment ions has not been reported in the literature. According to our ESI-MS/MS experiments, the presence of the fragment ion at  $m/z$  211 seems to be universal among cyclic diarylheptanoids with a *meta,meta*-cyclophane structure. Analogously to the above mentioned, after a rearrangement of the pseudomolecular ion and the subsequent cleavages of two C-C bonds (C7-C8 and C12-C13), a neutral loss of a diversely hydroxylated oxopentanal (**106**, **149**, **161**, **157**), and pentenal (**114**, **187**), or oxopentenedial (**154**) molecule occurs which results in the formation of the fragment ion at  $m/z$  211. Similarly, the cleavages of two C-C bonds (C7-C8 and C9-C10) lead to the neutral loss of an ethenol or ethene-diol unit. This results in the formation of the additional characteristic fragment ions at  $m/z$  299 (**114**), 283 (**106**, **149**) or 267 (**157**, **187**). Our NMR results later confirmed the presumed structures of the isolated cyclic diarylheptanoids (see Section 3.2.). Their structures and proposed mass spectrometric fragmentation pathways are shown in Figs. 1 and 2, respectively. In parallel to the isolated diarylheptanoids, compounds **94**, **103**, **108**, **119**, **124**, **136**, **140**, **143**, **171**, and **173** also exhibited typical fragment ions at  $m/z$  269 and 211, thus we assumed their structures as cyclic diarylheptanoids, too.

Furthermore, **74**, **139**, **145**, and **164** were characterized as linear diarylheptanoids, previously unprecedented in *Carpinus* species. The deprotonated molecular ion  $[M-H]^-$  of **164** was detected at  $m/z$  313 and its typical fragment ions at  $m/z$  207, 163, 149 (Fig. 3), thus the

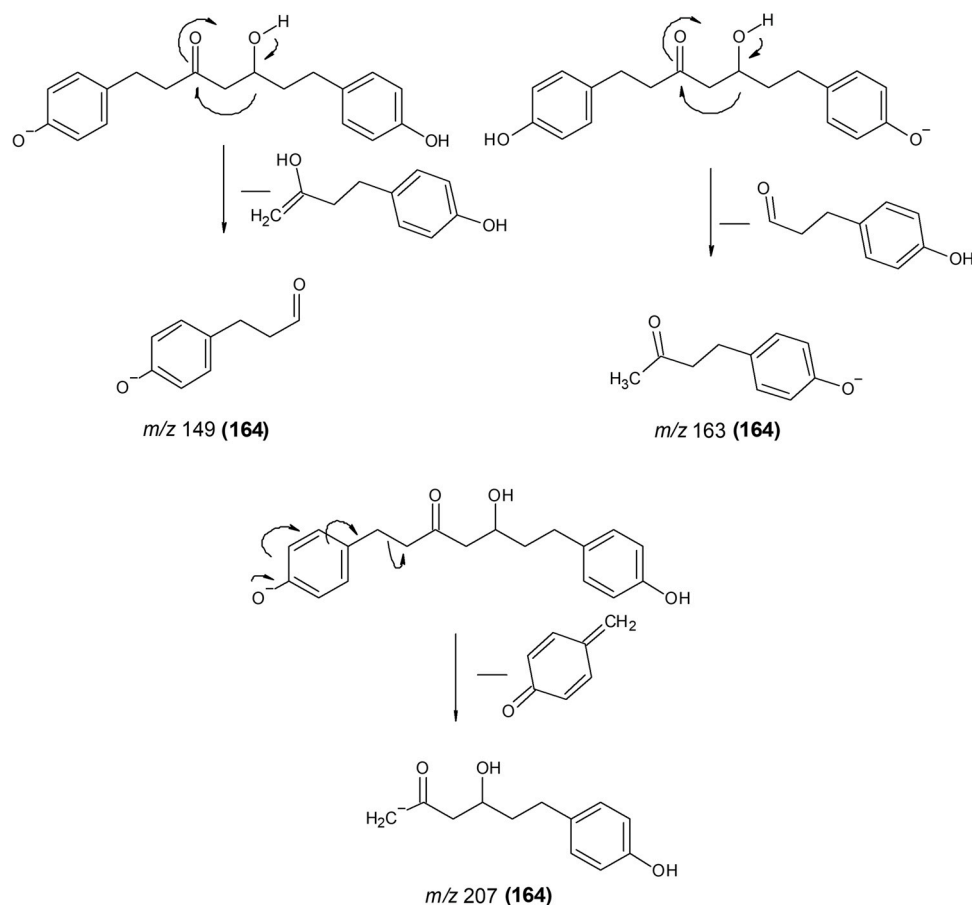


**Fig. 3.** Proposed mass spectrometric fragmentation pathway of the linear diarylheptanoid 5-hydroxy-3-platyphyllone isolated from *C. betulus* bark.

component was indicated as 5-hydroxy-1,7-bis-(4'-hydroxyphenyl)-3-heptanone (5-hydroxy-3-platyphyllone) [23]. Compound **145** presented a neutral loss of 150 Da, while peaks **74** and **139** showed a neutral loss of 180 Da, indicating the cleavage of a pentose and a hexose moiety from the hydroxyl group on the linear C<sub>7</sub> chain, respectively [23]. Based on these data, **145** was tentatively characterized as oregonin, while compounds **74** and **139** were denoted as linear diarylheptanoid hexosides.

Finally, the UV spectrum of **148** was similar to those of diarylheptanoids or gallic acid derivatives, however, their characteristic fragment ions at *m/z* 211 or 169 were not presented in the mass spectrum of **148**. According to the neutral losses observed during the CID of **148**, the presence of a deoxyhexose moiety [M-H-146]<sup>-</sup>, a hydroxyl group connected to a saturated chain [M-H-146-18]<sup>-</sup>, and two methoxy groups [M-H-146-18-15-15]<sup>-</sup> could be deduced. However, further conclusions could not be drawn, therefore, NMR analysis was necessary to determine the structure of **148** (see Section 3.2.).

### 3.2. Structural elucidation of the isolated compounds

In order to unambiguously identify their structures, eight diarylheptanoids (**106**, **114**, **149**, **154**, **157**, **161**, **164**, **187**), one lignan (**148**), and three flavonoids (**177**, **185**, **191**) were isolated by C<sub>18</sub> flash chromatography followed by multiple successive C<sub>18</sub> semi-preparative HPLC separations. Their structures were established by 1D and 2D NMR experiments as well as HR-ESI-MS (Orbitrap) analyses. Fig. 1 presents the structures of the isolated constituents, Table 1 summarizes the high-resolution mass spectrometric data of the diarylheptanoid-type compounds, while their <sup>1</sup>H NMR and <sup>13</sup>C NMR data are shown in Tables S2 and S3.

The <sup>1</sup>H and <sup>13</sup>C NMR spectra of **106** and **149** were similar to each other indicating isomeric structures of cyclic diarylheptanoids. Both structures contained one carbonyl, three oxymethine, and three methylene groups in the aliphatic chain. Based on the correlations of the 2D spectra, both **106** and **149** possess the carbonyl group in C-9 position, while the three hydroxyl groups were located at positions C-8, C-10, C-12 or C-10, C-11, C-12, respectively. Based on literature data [7], **106** and **149** were identified as carpinontriols A and B, respectively.

In the case of compound **114**, the <sup>1</sup>H NMR resonances confirmed the macrocyclic diaryl structure. However, the resonance assignment of the aliphatic chain failed in CD<sub>3</sub>OD at 295 K, due to the minute amount of the isolated compound. Compared to the literature [24], all the detected <sup>1</sup>H and <sup>13</sup>C resonances were in good agreement with that of giffonin U.

The <sup>1</sup>H NMR spectrum of compound **157** indicated the presence of two 1,2,4-trisubstituted aromatic rings. The resonances at δ 4.47 (dd, *J*=11.4, 4.0 Hz, 1H, H-12) and δ 4.20 (m, 1H, H-11) ppm revealed the presence of two oxymethine groups. In addition, eight more aliphatic resonances recommended the presence of four methylene units. The <sup>13</sup>C NMR spectrum showed one carbonyl resonance at δ 212.0 ppm. The characteristic multiplicities and splitting patterns suggested the cyclic diarylheptanoid structure. The correlations of the 2D spectra revealed that the carbonyl group was in C-9 position and the hydroxyl groups were in C-11 and C-12 positions. Based on these data, the structure of **157** was established as 11-oxo-3,8,9,17-tetrahydroxy-[7,0]-metacyclophane (giffonin X) [25].

The aromatic resonances in the <sup>1</sup>H NMR spectrum of **161** indicated a macrocyclic diaryl structure, while the resonances in the aliphatic region suggested the presence of four methylene and two oxymethine groups (at 4.39 and 4.04 ppm, respectively) in the

**Table 1**  
HR-MS data of the isolated diarylheptanoid compounds <sup>a</sup>.

No.	[M-H] <sup>+</sup> (m/z) experimental	[M-H] <sup>+</sup> (m/z) calculated	Error (ppm)	Fragment ions (m/z)	Molecular formula	Structure
<b>106</b>	343.1184	343.1187	2.23	283, 269, 257, 239, 225, 211, 197, 193, 183	C <sub>19</sub> H <sub>20</sub> O <sub>6</sub>	carpinontriol A
<b>114</b>	359.1134	359.1136	2.42	329, 299, 269, 257, 239, 211, 197, 193	C <sub>19</sub> H <sub>20</sub> O <sub>7</sub>	giffonin U
<b>149</b>	343.1186	343.1187	2.84	284, 283, 270, 269, 239, 211, 197, 193	C <sub>19</sub> H <sub>20</sub> O <sub>6</sub>	carpinontriol B
<b>154</b>	325.1079	325.1081	2.46	307, 269, 239, 211, 209, 197, 193, 183, 113	C <sub>19</sub> H <sub>18</sub> O <sub>5</sub>	3,12,17-trihydroxytricyclo[12.3.1.1 <sup>2,6</sup> ]nonadeca-1(18),2(19),3,5,14,16-hexaene-8,11-dione
<b>157</b>	327.1238	327.1238	3.48	300, 269, 268, 267, 241, 239, 211, 197, 193, 183	C <sub>19</sub> H <sub>20</sub> O <sub>5</sub>	giffonin X
<b>161</b>	327.1235	327.1238	- 0.9	283, 269, 267, 253, 239, 225, 211, 197, 193	C <sub>19</sub> H <sub>20</sub> O <sub>5</sub>	casuarinontriol
<b>164</b>	313.1437	313.3682	0.78	254, 251, 241, 239, 227, 211, 210, 207, 189, 163, 149	C <sub>19</sub> H <sub>22</sub> O <sub>4</sub>	5-hydroxy-1,7-bis-(4'-hydroxyphenyl)-3-heptanone
<b>187</b>	311.1287	311.1289	3.00	286, 267, 253, 241, 211, 197	C <sub>19</sub> H <sub>20</sub> O <sub>4</sub>	3,11,17-trihydroxytricyclo[12.3.1.1 <sup>2,6</sup> ]nonadeca-1(18),2(19),3,5,14,16-hexaen-8-one

<sup>a</sup> For NMR spectral data and structural elucidation of compounds see Section 3.2. Operating conditions for Orbitrap MS can be found in Section 2.5.

heptane chain. Furthermore, the <sup>13</sup>C spectrum indicated the presence of a carbonyl group ( $\delta$  220.1 ppm). Based on additional 2D correlations, the hydroxyl groups are located at the C-8 and C-12 positions, while the carbonyl group is located at the C-9 position. This structure was previously published in the literature as casuarinontriol [7].

The <sup>1</sup>H spectrum of compound **154** in DMSO-*d*<sub>6</sub> at 295 K showed very broad unresolved resonances, without any coupling patterns, therefore no structural information could be deduced. After the addition of trifluoroacetic acid and recording the spectra at higher temperatures (at 335 K and 370 K), the <sup>1</sup>H spectrum showed the characteristic pattern of cyclic diarylheptanoid resonances in the aromatic region. However, the aliphatic resonances could not be assigned due to significantly broad resonances. Nevertheless, comparing the NMR data with those found in the literature [26], the 3,12,17-trihydroxytricyclo[12.3.1.1<sup>2,6</sup>]nonadeca-1(18),2(19),3,5,14,16-hexaene-8,11-dione structure was proposed for compound **154**.

The <sup>1</sup>H NMR spectrum of **187** showed aromatic resonances at  $\delta$  7.05 (dd, <sup>3</sup>J<sub>H,H</sub>=8.3 Hz, <sup>4</sup>J<sub>H,H</sub>=2.5 Hz, 1H, H-5), 7.04 (dd, <sup>3</sup>J<sub>H,H</sub>=8.3 Hz, <sup>4</sup>J<sub>H,H</sub>=2.5 Hz, 1H, H-15), 6.80 (d, <sup>3</sup>J<sub>H,H</sub>=8.3 Hz, 1H, H-4), 6.78 (d, <sup>3</sup>J<sub>H,H</sub>=8.3 Hz, 1H, H-16), 6.79 (d, <sup>4</sup>J<sub>H,H</sub>=2.5 Hz, 1H, H-18) and 6.60 (d, <sup>4</sup>J<sub>H,H</sub>=2.5 Hz, 1H, H-19) ppm. These two separated ABX coupling patterns (also confirmed by 2D COSY experiment) indicated the presence of two 1,2,4-trisubstituted aromatic rings. The <sup>1</sup>H resonance at  $\delta$  4.20 (m, 1H, H-11) ppm and its HSQC correlation to <sup>13</sup>C resonance at  $\delta$  67.4 ppm revealed the presence of an oxymethine group. In addition, the aliphatic resonances at 3.19 (m, 1H, H-9a), 3.02 (dd, <sup>2</sup>J<sub>H,H</sub>=13.2 Hz, <sup>3</sup>J<sub>H,H</sub>=3.6 Hz, 1H, H-10a), 2.99 (m, 2H, H-7), 2.90 (m, 1H, H-9b), 2.88 (m, 2H, H-13), 2.68 (m, 1H, H-10b), 2.46 (m, 1H, H-12a), and 1.80 (m, 1H, H-12b) ppm along with their HSQC correlations recommended the presence of five methylene units. Four of these -CH<sub>2</sub>- units constitute a spin system with that of the oxymethine resonance. The <sup>13</sup>C NMR spectrum revealed a carbonyl resonance at  $\delta$  212.0 ppm, which separates the additional methylene unit from that of the aforementioned spin system confirming a heptane skeleton. Thorough inspection of the HMBC crosspeaks revealed that the carbonyl group is located at the C-8 position while the hydroxyl can be placed at position C-11. Further HMBC correlations between the aromatic rings confirmed the cyclic diarylheptane skeleton, therefore compound **187** could be assigned as 3,11,17-trihydroxytricyclo[12.3.1.1<sup>2,6</sup>]nonadeca-1(18),2(19),3,5,14,16-hexaen-8-one, a newly isolated and identified diarylheptanoid.

The <sup>1</sup>H NMR spectrum of compound **164** indicated the presence of two *para*-substituted aromatic rings. The resonance at  $\delta$  4.00 (m, 1H, H-5) ppm suggested the presence of one oxymethine group. Furthermore, five methylene units were identified. The <sup>13</sup>C NMR spectrum showed a single carbonyl resonance at  $\delta$  211.9 ppm. Based on all these informations, a linear diarylheptanoid structure was proposed. The 2D spectra determined the position of the carbonyl group at C-3 and the hydroxyl group at C-5. The <sup>1</sup>H and <sup>13</sup>C resonances were analogous to literature data [27], thus, **164** was identified as 5-hydroxy-1,7-bis-(4'-hydroxyphenyl)-3-heptanone (5-hydroxy-3-platyphyllone).

Based on the <sup>1</sup>H, <sup>13</sup>C, and additional 2D spectra, compound **148** was identified as a lignan glycoside, aviculin. The NMR spectra was identical to that of a previous report [28]. Presence of lignan-type compounds in *Carpinus* species was established for the first time. The compound **185** was confirmed as kaempferol-3-O-(4"-*E*-*p*-coumaroyl)-rhamnopyranoside by comparing the NMR spectroscopic data (<sup>1</sup>H and <sup>13</sup>C resonances) with those found in the literature [29]. The coupling constant of the two olefinic <sup>1</sup>H resonances suggested *trans* configuration of the double bond. Based on their <sup>1</sup>H NMR spectra, compounds **191** and **177** were identified as kaempferol-3-O-rhamnoside (afzelin) and quercetin-3-O-rhamnoside (quercitrin), respectively. The <sup>1</sup>H resonances were similar to those published earlier [30].

**Table 2**Quantitative determination of the main diarylheptanoids in *Carpinus betulus* extracts (data are expressed as mg/g dry extract).

Compound	Quantity $\pm$ SD (mg/g dry extract)			
	BE	BM	ME	MM
Carpinontriol A ( <b>106</b> )	19.13 $\pm$ 0.10	13.94 $\pm$ 0.26	n.d.	3.55 $\pm$ 0.05
Carpinontriol B ( <b>149</b> )	6.44 $\pm$ 0.18	4.16 $\pm$ 0.15	7.60 $\pm$ 0.12	16.25 $\pm$ 0.19
3,12,17-Trihydroxytricyclo [12.3.1.1 <sup>2,6</sup> ]nonadeca-1(18),2(19),3,5,14,16-hexaene-8,11-dione ( <b>154</b> )	16.04 $\pm$ 0.12	11.05 $\pm$ 0.02	n.d.	n.d.
Giffonin X ( <b>157</b> )	18.07 $\pm$ 0.03	9.97 $\pm$ 0.10	n.d.	n.d.

Abbreviations: BE: bark ethyl acetate extract, BM: bark methanol extract, ME: male catkin ethyl acetate extract, MM: male catkin methanol extract, n.d.: not detected.

**Table 3**

Method validation: regression, LOQ and LOD of the quantitative method.

Compound	Regression equation	r <sup>2</sup>	Regression range ( $\mu$ g/mL)	LOD ( $\mu$ g/mL)	LOQ ( $\mu$ g/mL)
Carpinontriol A ( <b>106</b> )	y = 88.99x + 177.77	0.9997	1–250	0.15	0.5
Carpinontriol B ( <b>149</b> )	y = 95.80x + 228.73	0.9995	1–250	0.1	0.3
3,12,17-Trihydroxytricyclo[12.3.1.1 <sup>2,6</sup> ]nonadeca-1(18),2(19),3,5,14,16-hexaene-8,11-dione ( <b>154</b> )	y = 43.17x - 16.79	0.9999	1–250	0.2	0.6
Giffonin X ( <b>157</b> )	y = 86.71x + 177.24	0.9996	1–250	0.15	0.5

### 3.3. Quantitative analysis and method validation

There are currently no literature data regarding the quantitative analysis of diarylheptanoids in *C. betulus*. Thus, additional aim of this study was to determine the quantities of the major diarylheptanoid constituents in hornbeam extracts: carpinontriols A (**106**) and B (**149**), 3,12,17-trihydroxytricyclo[12.3.1.1<sup>2,6</sup>]nonadeca-1(18),2(19),3,5,14,16-hexaene-8,11-dione (**154**), and giffonin X (**157**) by an UHPLC-DAD method.

Ethyl acetate and methanol extracts of all samples (bark, leaf, female, and male catkins) were analyzed. In accordance with the results of the qualitative screening, the evaluated diarylheptanoids were not detected in leaf and female flower extracts. Quantities of the studied compounds in hornbeam bark and male catkin methanol and ethyl acetate extracts ranged from 3.55 to 19.13 mg/g dry extract, results are shown in Table 2. Compound **149** was present in all bark and male catkin extracts, being the most abundant diarylheptanoid of male catkin samples. Compound **106** was the chief diarylheptanoid in both bark extracts, while in bark ethyl acetate samples, **157** was present in the second highest concentration.

The linearity regression equations, correlation coefficients (r<sup>2</sup>), linearity ranges, LOD and LOQ values of the method are shown in Table 3. Excellent linearity was achieved (r<sup>2</sup>  $\geq$  0.9995) in the range of 1–250  $\mu$ g/mL for all analytes. The LOD and LOQ values were within the ranges of 0.1–0.2  $\mu$ g/mL and 0.3–0.6  $\mu$ g/mL, respectively. Intra-day and inter-day precision evaluated at low, mid, and high concentration ranges was also acceptable (0.16–3.33 RSD%), while intra- and inter-day accuracy results varied from 80.31% to 107.06% (Table 4). The extraction recovery rate of **157** was 96.29%  $\pm$  1.36% for the ethyl acetate extract, and 114.91%  $\pm$  2.19% in case of the methanol extract. These results indicate that the method was reliable and repeatable. Retention time repeatability was suitable for all four compounds, relative standard deviation ranged from 0.18% to 0.58% (n = 6). In order to evaluate the selectivity of the method, blank samples (hexane extracts which do not contain the analytes of interest) were compared to extracts spiked with **106**, **149**, **154**, and **157**. No co-elution was observed at the retention times of the analytes of interest, indicating that this method provides good selectivity.

### 3.4. DPPH scavenging activity

Antioxidant capacities of hornbeam bark, leaf, male, and female catkin extracts prepared with methanol and ethyl acetate were compared. Table 5 summarizes the results of the DPPH scavenging assay, data are expressed as means  $\pm$  SD. Antioxidant activities of hornbeam extracts prepared with methanol were significantly

different ( $p < 0.001$ ) as compared with those of the ethyl acetate extracts (results are shown in Fig. 4), however, a trend in relation to the extraction solvent could not be found. Overall, the leaf methanol extract showed the best antioxidant capacity, while male catkin methanol extract was also effective in the test. Both samples exhibited radical scavenging activities similar to those of the well-known antioxidant compounds quercetin and trolox. Our results correspond with literature data, where *C. betulus* leaf and bark extracts showed medium to high DPPH neutralizing activity [3,4].

We also investigated the antioxidant activities of the constituents isolated from *C. betulus* samples. For comparison, reference compounds with known radical scavenging activity were also studied, results are shown in Table 5. In accordance with literature data, the potent antioxidant activity of quercitrin (**177**) was comparable to other quercetin glycosides, like rutin. On the other hand, afzelin (**191**), carpinontriols A (**106**) and B (**149**), casuarinondiol (**161**), and 5-hydroxy-3-platyphyllone (**164**) showed weak radical scavenging activity [7,31,32]. According to literature data, coumaroyl flavonol glycosides show potent free radical scavenging activity [33]. However, kaempferol-3-O-(4'-E-p-coumaroyl)-rhamnoside (**185**) exhibited no radical scavenging activity at the concentration of 250  $\mu$ g/mL. Although some of its structural characteristics such as the lack of unsubstituted OH groups (due to the absence of the catechol group

**Table 4**

Method validation: Precision and accuracy of the quantitative method.

Nominal conc ( $\mu$ g/mL)	Precision (RSD%)		Accuracy (%)	
	Intra-day	Inter-day	Intra-day	Inter-day
<b>Carpinontriol A (106)</b>				
5	0.53	0.75	80.95	81.69
50	1.81	1.48	105.22	106.54
250	0.16	0.24	99.62	99.63
<b>Carpinontriol B (149)</b>				
5	0.96	1.65	80.31	81.34
50	0.73	0.88	104.92	105.02
250	0.59	0.80	99.43	99.61
<b>3,12,17-Trihydroxytricyclo [12.3.1.1<sup>2,6</sup>]nonadeca-1(18),2(19),3,5,14,16-hexaene-8,11-dione (154)</b>				
5	0.76	2.38	107.68	107.38
50	1.37	2.06	97.27	98.43
250	0.43	3.33	100.14	103.74
<b>Giffonin X (157)</b>				
5	2.84	1.69	81.10	81.81
50	0.72	1.81	105.54	107.06
250	1.56	1.44	99.48	100.29

**Table 5**DPPH scavenging activity of *C. betulus* extracts, constituents isolated from the bark, and reference compounds (Data are expressed as means  $\pm$  SD).

Extracts	IC <sub>50</sub> $\pm$ SD ( $\mu$ g/mL)
Bark ethyl acetate extract (BE)	9.0 $\pm$ 0.3
Bark methanol extract (BM)	10.7 $\pm$ 0.3
Leaf ethyl acetate extract (LE)	14.0 $\pm$ 0.4
Leaf methanol extract (LM)	5.5 $\pm$ 0.2
Female catkin ethyl acetate extract (FE)	9.4 $\pm$ 0.2
Female catkin methanol extract (FM)	11.9 $\pm$ 0.7
Male catkin ethyl acetate extract (ME)	13.3 $\pm$ 0.5
Male catkin methanol extract (MM)	7.6 $\pm$ 0.3
<b>Isolated constituents</b>	
Carpinotriol A ( <b>106</b> )	77.2 $\pm$ 4.5
Carpinotriol B ( <b>149</b> )	123 $\pm$ 10
Giffonin X ( <b>157</b> )	138 $\pm$ 11
Casuarinondiol ( <b>161</b> )	> 250
5-Hydroxy-3-platyphyllone ( <b>164</b> )	121 $\pm$ 9
Aviculin ( <b>148</b> )	23.8 $\pm$ 0.9
Quercitrin ( <b>177</b> )	6.9 $\pm$ 0.5
Afzelin ( <b>191</b> )	> 250
Kaempferol-3-O-(4'- <i>E-p</i> -coumaroyl) rhamnopyranoside ( <b>185</b> )	> 250
<b>Reference compounds</b>	
Trolox	5.3 $\pm$ 0.2
Rutin	7.3 $\pm$ 0.3

in the B ring and the glycosylation at C3-OH) may result in a lower scavenging capacity, these can not explain the contradiction with the literature. To the best of our knowledge, the DPPH scavenging activity of aviculin (**148**, IC<sub>50</sub> 23.8  $\pm$  0.9  $\mu$ g/mL) and giffonin X (**157**, IC<sub>50</sub> 138  $\pm$  11  $\mu$ g/mL) was determined for the first time.

In order to assess the contribution of the individual antioxidant constituents to the total antioxidant activity of *C. betulus* extracts, an off-line DPPH-HPLC-DAD-MS method was applied. Upon reaction with DPPH, phenolics which can neutralize DPPH<sup>•</sup> by providing hydrogen atoms or by electron donation, will be oxidized to form free radicals, and subsequently stable quinoidal structures. As a consequence of this structural change, peak areas (peak intensities) of these antioxidants will decrease in the HPLC chromatogram [10]. Chromatograms of hornbeam samples were compared before and after reacting with DPPH. The antioxidant effect was characterized by the decrease of the intensity (area under the curve, AUC) values in

percentage. The compounds which reduced the peak intensity by more than 20% were considered as potential antioxidants [10]. Values are means of intensity reductions determined for each extract containing the specific compound. Results are presented in [Supplementary Table S4](#). Representative HPLC-UV chromatograms demonstrating untreated and DPPH-treated bark methanolic samples are shown in [Fig. 5](#). According to the results of our HPLC-MS/MS analyses, the leaf sample was dominated by the presence of gallic acid derivatives and ellagitannins. It was presumed that galloyl hexoses of different polymerization degrees as well as galloyl-HHDP hexose derivatives could contribute significantly to the total antioxidant activity, since they are well known for their strong radical scavenging effect [34]. The increasing number of galloyl moieties in the constituents correlated with higher antioxidant capacities. Monogalloyl hexoses (e.g. **4** and **11**) exerted lower reduction in peak intensities as compared to tri-, tetra-, or pentagalloyl hexose isomers (e.g. **85**, **105**, and **138**, respectively). On the other hand, digalloyl-shikimic acid isomers (**87** and **99**), and digalloylquinic acid (**58**) showed lower reduction in AUC values as compared to their monogalloyl counterparts (e.g. **34** and **16**, respectively). In case of ellagitannins, the galloyl:HHDP rate of the compounds determines the antioxidant capacity. In accordance with literature data [35], galloyl-bis-HHDP hexose isomers (e.g. **40**, **50**, **81**) did not show antioxidant activity as compared to galloyl-HHDP hexoses (e.g. **38**, **43**, **51**, **84**). Flavonol glycosides, and in particular quercetin derivatives, prevailed in *C. betulus* extracts. The aglycone quercetin (**192**) bears all structural criteria of a potent antioxidative compound [34]. However, in case of other flavonol derivatives, the glycosidation of the C3-OH group (e.g. **163** and **177**), the methylation of free hydroxyl groups (e.g. **179** and **188**), or the lack of a catechol moiety in B ring (e.g. **160** and **191**) resulted in lower free radical scavenging activities. Hydroxycinnamic acid derivatives bearing two hydroxyl groups in the *ortho* position (caffeic acid derivatives, **65** and **83**) showed higher radical scavenging ability than those containing only one hydroxyl group (coumaric acid derivatives, **111**). Methylation of hydroxyl groups in ferulic acid derivatives (**116** and **132**) also leads to the reduction in the radical scavenging activity [34]. In agreement with literature data [7] and our results from the radical scavenging assay of the isolated compounds, diarylheptanoids in the *C. betulus* extracts (**114**, **143**, **149**) exhibited moderate antioxidant effect.

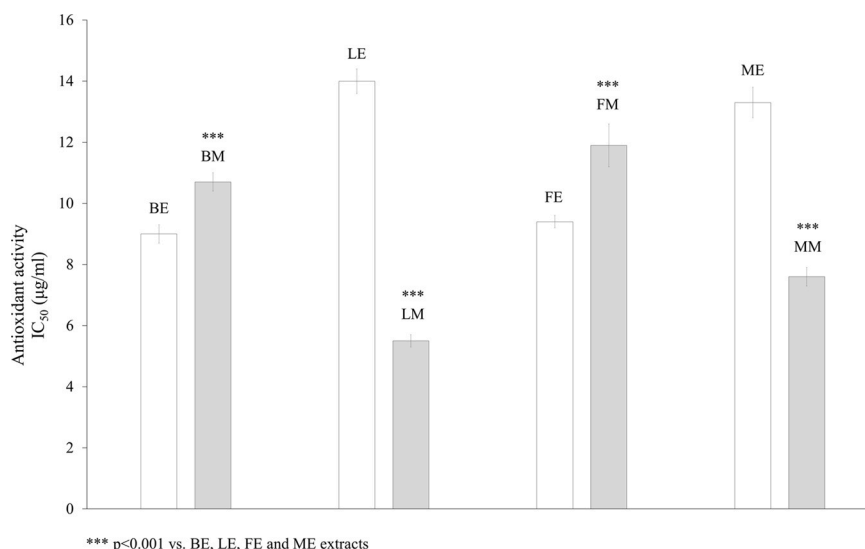


**Fig. 4.** DPPH scavenging activity of *C. betulus* extracts prepared with solvents of different polarity. Values are means  $\pm$  SD. \*\*\*  $p < 0.001$  compared with ethyl acetate extracts. Abbreviations: BE: bark ethyl acetate extract, BM: bark methanol extract, LE: leaf ethyl acetate extract, LM: leaf methanol extract, FE: female catkin ethyl acetate extract, FM: female catkin methanol extract, ME: male catkin ethyl acetate extract, MM: male catkin methanol extract.

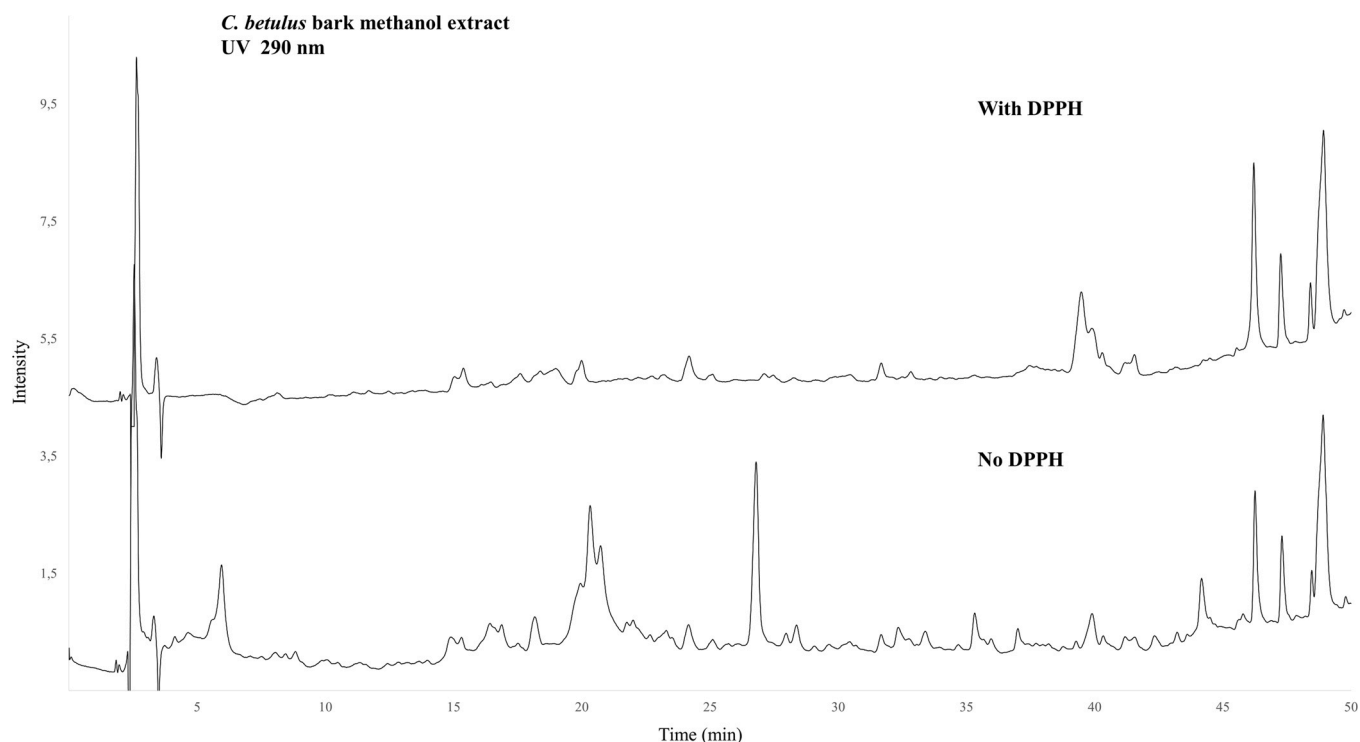


Fig. 5. Chromatograms of untreated and DPPH-treated *C. betulus* bark methanolic extract samples.

#### 4. Conclusions

In the present study, a comprehensive profiling of phenolic compounds in *C. betulus* was performed. Distinct plant parts (bark, leaf, female, and male catkin samples) were extracted successively with solvents of increasing polarity (ethyl acetate and methanol) to obtain as extensive a range of extractives as possible. Altogether 194 polyphenols were tentatively characterized by HPLC-DAD-ESI-MS/MS. Gallo- and ellagitannins dominated in the methanol extracts, while flavonol glycosides and methoxylated flavones prevailed in the ethyl acetate samples. Seven cyclic diarylheptanoids (**106**, **114**, **149**, **154**, **157**, **161**, **187**) were isolated from *C. betulus* for the first time, with 3,11,17-trihydroxytricyclo[12.3.1.1<sup>2,6</sup>]nonadeca-1(18),2(19),3,5,14,16-hexaen-8-one (**187**) being a new compound. We also described the occurrence of linear diarylheptanoid (**164**) and lignan (**148**) constituents in the genus *Carpinus* for the first time. Three known flavonol glycosides (**177**, **185**, **191**) were also isolated. A new mass spectrometric fragmentation pathway of cyclic diarylheptanoids with a *meta,meta*-cyclophane structure was proposed. Additionally, this is the first report of quantitative data regarding the main diarylheptanoids in *C. betulus* extracts. A selective, reliable, and repeatable UHPLC-DAD method was developed and validated to determine the contents of **106**, **149**, **154**, and **157**. Compound **106** prevailed both in bark ethyl acetate and methanol extracts, while **149** was the main diarylheptanoid of male catkin extracts. The antioxidant properties of the extracts and the isolated compounds were assessed by the DPPH assay. Leaf and male catkin methanol extracts showed the highest antioxidant activity. The DPPH scavenging activity of aviculin (**148**) and giffonin X (**157**) was determined for the first time. Potential antioxidant compounds in *C. betulus* extracts contributing to the total radical scavenging activity of the samples were indicated using an off-line DPPH-HPLC method. According to our results, hydrolyzable tannins may be responsible for the antioxidant capacity of *Carpinus* extracts.

#### CRediT authorship contribution statement

**Csenge Anna Felegyi-Tóth**: Investigation, Data curation, Writing – original draft, Visualization. **Zsófia Garádi**: Investigation, Data curation, Writing – original draft. **András Darcsi**: Investigation. **Orsolya Csernák**: Writing – original draft, Validation. **Imre Boldizsár**: Investigation, Data curation. **Szabolcs Béni**: Writing – review & editing. **Ágnes Alberti**: Conceptualization, Writing – review & editing, Supervision.

#### Declaration of Competing Interest

The authors declare that they have no known competing financial interests or personal relationships that could have appeared to influence the work reported in this paper.

#### Acknowledgements

We thank Béla Dudás (Egererdő Ltd., Mátrafüred Forestry) for providing the bark samples from Lajosháza. We thank Dr. László Kursinszki for the valuable discussions, Tamás Czeglédi and Andrea Nagyné Nedves for the technical help. This work was supported by grants from the National Research, Development and Innovation Office, Hungary, NKFIH, grant ID K 120342 and K 135712. Prepared with the professional support of the Doctoral Student Scholarship Program of the Co-operative Doctoral Program of the Ministry of Innovation and Technology, financed by the National Research, Development and Innovation Fund, Hungary (grant ID: KDP-1007075, Z.G.). S.B. thanks the financial support from the János Bolyai Research Scholarship of the Hungarian Academy of Sciences and from the Bolyai+New National Excellence Program (ÚNKP-20-5-SE-31) of the Ministry of Human Capacities, Hungary.

## Appendix A. Supporting information

Supplementary data associated with this article can be found in the online version at [doi:10.1016/j.jpba.2021.114554](https://doi.org/10.1016/j.jpba.2021.114554).

## References

- [1] R. Sikkema, G. Caudullo, D. de Rigo, *Carpinus betulus* in Europe: distribution, habitat, usage and threats, in: J. San-Miguel Ayanz, D. de Rigo, G. Caudullo, T. Houston Durrant, A. Mauri (Eds.), European Atlas of Forest Tree Species, Publication Office of the European Union, Luxembourg, 2016, pp. 74–75.
- [2] J.I. Jeon, C.S. Chang, Z.D. Chen, T.Y. Park, Systematic aspects of foliar flavonoids in subsect. *Carpinus* (*Carpinus*, Betulaceae), *Biochem. Syst. Ecol.* 35 (2007) 606–613, <https://doi.org/10.1016/j.bse.2007.04.004>
- [3] T. Hofmann, E. Nebehaj, L. Albert, Antioxidant properties and detailed polyphenol profiling of European hornbeam (*Carpinus betulus* L.) leaves by multiple antioxidant capacity assays and high-performance liquid chromatography/multistage electrospray mass spectrometry, *Ind. Crops Prod.* 87 (2016) 340–349, <https://doi.org/10.1016/j.indcrop.2016.04.037>
- [4] C. Agarwal, T. Hofmann, E. Visi-Rajczi, Z. Pásztor, Low-frequency, green sonoextraction of antioxidants from tree barks of Hungarian woodlands for potential food applications, *Chem. Eng. Process.* 159 (2021) 108221, <https://doi.org/10.1016/j.cep.2020.108221>
- [5] E. Ciekiewicz, L. Angenot, T. Gras, R. Kiss, M. Frédérick, Potential anticancer activity of young *Carpinus betulus* leaves, *Phytomedicine* 19 (2012) 278–283, <https://doi.org/10.1016/j.phymed.2011.09.072>
- [6] Q. Sheng, X. Fang, Z. Zhu, W. Xiao, Z. Wang, G. Ding, L. Zhao, Y. Li, P. Yu, Z. Ding, Q. Sun, Seasonal variation of pheophorbide a and flavonoid in different organs of two *Carpinus* species and its correlation with immunosuppressive activity, *Vitr. Cell. Dev. Biol. Anim.* 52 (2016) 654–661, <https://doi.org/10.1007/s11626-016-0041-1>
- [7] J.S. Lee, H.J. Kim, H. Park, Y.S. Lee, New diarylheptanoids from the stems of *Carpinus cordata*, *J. Nat. Prod.* 65 (2002) 1367–1370, <https://doi.org/10.1021/np020048l>
- [8] Y. Jahng, J.G. Park, Recent Studies on Cyclic 1,7-Diarlylheptanoids: Their Isolation, Structures, Biological Activities, and Chemical Synthesis, *Molecules* 23 (2018) 3107, <https://doi.org/10.3390/molecules23123107>
- [9] W. Brand-Williams, M.E. Cuvelier, C. Berset, Use of a free radical method to evaluate antioxidant activity, *LWT – Food Sci. Technol.* 28 (1995) 25–30, [https://doi.org/10.1016/S0023-6438\(95\)80008-5](https://doi.org/10.1016/S0023-6438(95)80008-5)
- [10] J. Zhu, X. Yi, J. Zhang, S. Chen, Y. Wu, Chemical profiling and antioxidant evaluation of Yangxinshi Tablet by HPLC–ESI–Q–TOF–MS/MS combined with DPPH assay, *J. Chromatogr. B.* 1060 (2017) 262–271, <https://doi.org/10.1016/j.jchromb.2017.06.022>
- [11] P. Ambigaipalan, A.C. de Camargo, F. Shahidi, Phenolic Compounds of Pomegranate Byproducts (Outer Skin, Mesocarp, Divider Membrane) and Their Antioxidant Activities, *J. Agric. Food Chem.* 64 (2016) 6584–6604, <https://doi.org/10.1021/acs.jafc.6b02950>
- [12] A. Singh, V. Bajpai, S. Kumar, K.R. Sharma, B. Kumar, Profiling of Gallic and Ellagic Acid Derivatives in Different Plant Parts of *Terminalia Arjuna* by HPLC–ESI–QTOF–MS/MS, *Nat. Prod. Commun.* 11 (2016) 239–244, <https://doi.org/10.1177/1934578x1601100227>
- [13] M.N. Clifford, S. Stoupi, N. Kuhnert, Profiling and Characterization by LC–MS<sup>n</sup> of the Galloylquinic Acids of Green Tea, Tara Tannin, and Tannic Acid, *J. Agric. Food Chem.* 55 (2007) 2797–2807, <https://doi.org/10.1021/jf063533i>
- [14] F. Sheng, B. Hu, Q. Jin, J. Wang, C. Wu, Z. Luo, The Analysis of Phenolic Compounds in Walnut Husk and Pellicle by UPLC–Q–Orbitrap HRMS and HPLC, *Molecules* 26 (2021) 3013, <https://doi.org/10.3390/molecules26103013>
- [15] R. Jaiswal, H. Müller, A. Müller, M. Gamaleldin, E. Karar, N. Kuhnert, Identification and characterization of chlorogenic acids, chlorogenic acid glycosides and flavonoids from *Lonicera henryi* L. (Caprifoliaceae) leaves by LC–MS<sup>n</sup>, *Phytochemistry* 108 (2014) 252–263, <https://doi.org/10.1016/j.phytochem.2014.08.023>
- [16] Á. Alberti, S. Béni, E. Lackó, P. Riba, M. Al-Khrasani, Á. Kéry, Characterization of phenolic compounds and antinociceptive activity of *Sempervivum tectorum* L. leaf juice, *J. Pharm. Biomed. Anal.* 70 (2012) 143–150, <https://doi.org/10.1016/j.jpba.2012.06.017>
- [17] Á. Alberti, B. Blazics, Á. Kéry, Evaluation of *Sempervivum tectorum* L. Flavonoids by LC and LC–MS, *Chromatographia* 58 (2008) 107–111, <https://doi.org/10.1365/s10337-008-0750-z>
- [18] Á. Alberti, E. Riethmüller, S. Béni, Á. Kéry, Evaluation of Radical Scavenging Activity of *Sempervivum tectorum* and *Corylus avellana* Extracts with Different Phenolic Composition, *Nat. Prod. Commun.* 11 (2016) 431–568, <https://doi.org/10.1177/1934578x1601100412>
- [19] E. Riethmüller, G. Tóth, Á. Alberti, K. Végh, I. Burlini, Á. Könczöl, G.T. Balogh, Á. Kéry, First characterisation of flavonoid- and diarylheptanoid-type antioxidant phenolics in *Corylus maxima* by HPLC–DAD–ESI–MS, *J. Pharm. Biomed. Anal.* 107 (2015) 159–167, <https://doi.org/10.1016/j.jpba.2014.12.016>
- [20] M. Masullo, A. Cerulli, A. Mari, C.C. de Souza Santos, C. Pizza, S. Piacente, LC–MS profiling highlights hazelnut (*Nocciola di Giffoni* PGI) shells as a byproduct rich in antioxidant phenolics, *Food Res. Int.* 101 (2017) 180–187, <https://doi.org/10.1016/j.foodres.2017.08.063>
- [21] K. Végh, E. Riethmüller, L. Hosszú, A. Darcsi, J. Müller, Á. Alberti, A. Tóth, S. Béni, Á. Könczöl, G.T. Balogh, Á. Kéry, Three newly identified lipophilic flavonoids in *Tanacetum parthenium* supercritical fluid extract penetrating the Blood–Brain Barrier, *J. Pharm. Biomed. Anal.* 149 (2018) 488–493, <https://doi.org/10.1016/j.jpba.2017.11.029>
- [22] Z.W. Yang, F. Xu, X. Liu, Y. Cao, Q. Tang, Q.Y. Chen, M.Y. Shang, G.X. Liu, X. Wang, S.Q. Cai, An untargeted metabolomics approach to determine component differences and variation in their in vivo distribution between Kuqin and Ziqin, two commercial specifications of *Scutellaria Radix*, *RSC Adv.* 7 (2017) 54682, <https://doi.org/10.1039/c7ra10705f>
- [23] Á. Alberti, E. Riethmüller, S. Béni, Characterization of diarylheptanoids: An emerging class of bioactive natural products, *J. Pharm. Biomed. Anal.* 147 (2018) 13–34, <https://doi.org/10.1016/j.jpba.2017.08.051>
- [24] A. Cerulli, G. Lauro, M. Masullo, V. Cantone, B. Olas, B. Kontek, F. Nazzaro, G. Bifulco, S. Piacente, Cyclic Diarylheptanoids from *Corylus avellana* Green Leafy Covers: Determination of Their Absolute Configurations and Evaluation of Their Antioxidant and Antimicrobial Activities, *J. Nat. Prod.* 80 (2017) 1703–1713, <https://doi.org/10.1021/acs.jnatprod.6b00703>
- [25] M. Masullo, G. Lauro, A. Cerulli, B. Kontek, B. Olas, G. Bifulco, S. Piacente, C. Pizza, Giffonins, Antioxidant Diarylheptanoids from *Corylus avellana*, and Their Ability to Prevent Oxidative Changes in Human Plasma Proteins, *J. Nat. Prod.* 84 (2021) 646–653, <https://doi.org/10.1021/acs.jnatprod.0c01251>
- [26] D.E. Tsvetkov, A.S. Dmitrenok, Y.E. Tsvetkov, Y.V. Tomilov, V.A. Dokichev, N.E. Nifantiev, Polyphenolic compounds in the extracts of the birch *Betula pendula* knotwood, *Russ. Chem. Bull.* 64 (2015) 1413–1418, <https://doi.org/10.1007/s11172-015-1025-0>
- [27] M. Ryu, C.K. Sung, Y.J. Im, C. Chun, Activation of JNK and p38 in MCF-7 Cells and the In Vitro Anticancer Activity of *Alnus hirsuta* Extract, *Molecules* 25 (2020) 1073, <https://doi.org/10.3390/molecules25051073>
- [28] D. Lee, Y.H. Lee, K.H. Lee, B.S. Lee, A. Alishir, Y.J. Ko, K.S. Kang, K.H. Kim, Aviculin Isolated from *Lespedeza cuneata* Induce Apoptosis in Breast Cancer Cells through Mitochondria-Mediated Caspase Activation Pathway, *Molecules* 25 (2020) 1708, <https://doi.org/10.3390/molecules25071708>
- [29] N.Y. Yang, W.W. Tao, J.A. Duan, Antithrombotic flavonoids from the faeces of *Trogopterus xanthipes*, *Nat. Prod. Res.* 24 (2010) 1843–1849, <https://doi.org/10.1080/14786419.2010.482057>
- [30] K.Y. Yu, W. Wu, S.Z. Li, L.L. Dou, L.L. Liu, P. Li, E.H. Liu, A new compound, methylbergenin along with eight known compounds with cytotoxicity and anti-inflammatory activity from *Ardisia japonica*, *Nat. Prod. Res.* 31 (2017) 2581–2586, <https://doi.org/10.1080/14786419.2017.1283495>
- [31] S.B. Kim, S.H. Hwang, H.W. Suh, S.S. Lim, Phytochemical Analysis of *Agrimonia pilosa* Ledeb, Its Antioxidant Activity and Aldose Reductase Inhibitory Potential, *Int. J. Mol. Sci.* 18 (2017) 379, <https://doi.org/10.3390/ijms18020379>
- [32] T.T. Le, J. Yin, M.W. Lee, Anti-Inflammatory and Anti-Oxidative Activities of Phenolic Compounds from *Alnus sibirica* Stems Fermented by *Lactobacillus plantarum* subsp. *argentoratensis*, *Molecules* 22 (2017) 1566, <https://doi.org/10.3390/molecules22091566>
- [33] Y. Tang, F. Lou, J. Wang, Y. Li, S. Zhuang, Coumaroyl flavonol glycosides from the leaves of *Ginkgo biloba*, *Phytochemistry* 58 (2001) 1251–1256, [https://doi.org/10.1016/S0031-9422\(01\)00320-X](https://doi.org/10.1016/S0031-9422(01)00320-X)
- [34] C.A. Rice-Evans, N.J. Miller, G. Paganga, Structure–antioxidant activity relationships of flavonoids and phenolic acids, *Free Rad. Biol. Med.* 20 (1996) 933–956, [https://doi.org/10.1016/0891-5849\(95\)02227-9](https://doi.org/10.1016/0891-5849(95)02227-9)
- [35] B. Badhani, N. Sharma, R. Kakkar, Gallic acid: A versatile antioxidant with promising therapeutic and industrial applications, *RSC Adv.* 5 (2015) 27540–27557, <https://doi.org/10.1039/C5RA01911G>



Article

# Evaluation of the Chemical Stability, Membrane Permeability and Antiproliferative Activity of Cyclic Diarylheptanoids from European Hornbeam (*Carpinus betulus* L.)

Csenge Anna Felegyi-Tóth <sup>1</sup>, Tímea Heilmann <sup>1</sup>, Eszter Buda <sup>1</sup>, Bence Stipsicz <sup>2,3</sup>, Alexandra Simon <sup>1</sup>, Imre Boldizsár <sup>1,4</sup>, Szilvia Bősze <sup>3,5</sup>, Eszter Riethmüller <sup>1</sup> and Ágnes Alberti <sup>1,\*</sup>

<sup>1</sup> Department of Pharmacognosy, Semmelweis University, Üllői út 26, 1085 Budapest, Hungary; felegyi\_toth.csenge\_anna@pharma.semmelweis-univ.hu (C.A.F.-T.); heilmann.timea@stud.semmelweis.hu (T.H.); buda.eszter@stud.semmelweis.hu (E.B.); simon.alexandra@pharma.semmelweis-univ.hu (A.S.); boldizsar.imre@semmelweis.hu (I.B.); riethmuller.eszter@pharma.semmelweis-univ.hu (E.R.)

<sup>2</sup> Institute of Biology, Doctoral School of Biology, Eötvös Loránd University, Pázmány Péter sétány 1/C, H-1117 Budapest, Hungary; stipsicz@student.elte.hu

<sup>3</sup> ELKH-ELTE Research Group of Peptide Chemistry, Eötvös Loránd Research Network, Eötvös Loránd University, Pázmány Péter sétány 1/A, H-1117 Budapest, Hungary; szilvia.bosze@ttk.elte.hu

<sup>4</sup> Department of Plant Anatomy, Institute of Biology, Eötvös Loránd University, Pázmány Péter sétány 1/C, 1117 Budapest, Hungary

<sup>5</sup> National Public Health Center, Albert Flórián út 2-6, 1097 Budapest, Hungary

\* Correspondence: alberti.agnes@semmelweis.hu

**Abstract:** Four cyclic diarylheptanoids—carpinontriols A (1) and B (2), giffonin X (3) and 3,12,17-trihydroxytricyclo [12.3.1.1<sup>2,6</sup>]nonadeca-1(18),2(19),3,5,14,16-hexaene-8,11-dione (4)—were isolated from *Carpinus betulus* (Betulaceae). Chemical stability of the isolated diarylheptanoids was evaluated as a function of storage temperature (−15, 5, 22 °C) and time (12 and 23 weeks). The effect of the solvent and the pH (1.2, 6.8, 7.4) on the stability of these diarylheptanoids was also investigated. Compounds 2 and 4 showed good stability both in aqueous and methanolic solutions at all investigated temperatures. Only 2 was stable at all three studied biorelevant pH values. Degradation products of 1 and 3 were formed by the elimination of a water molecule from the parent compounds, as confirmed by ultrahigh-performance liquid chromatography–high-resolution tandem mass spectrometry (UHPLC-HR-MS). The permeability of the compounds across biological membranes was evaluated by the parallel artificial membrane permeability assay (PAMPA). Compound 3 possesses a log $P_e$  value of  $-5.92 \pm 0.04$  in the blood–brain barrier-specific PAMPA-BBB study, indicating that it may be able to cross the blood–brain barrier via passive diffusion. The in vitro antiproliferative activity of the compounds was investigated against five human cancer cell lines, confirming that 1 inhibits cell proliferation in A2058 human metastatic melanoma cells.

**Keywords:** diarylheptanoid; chemical stability; degradation products; mass spectrometry; PAMPA; antiproliferative activity



**Citation:** Felegyi-Tóth, C.A.; Heilmann, T.; Buda, E.; Stipsicz, B.; Simon, A.; Boldizsár, I.; Bősze, S.; Riethmüller, E.; Alberti, Á. Evaluation of the Chemical Stability, Membrane Permeability and Antiproliferative Activity of Cyclic Diarylheptanoids from European Hornbeam (*Carpinus betulus* L.). *Int. J. Mol. Sci.* **2023**, *24*, 13489. <https://doi.org/10.3390/ijms241713489>

Academic Editor: Bernhard Biersack

Received: 28 July 2023

Revised: 26 August 2023

Accepted: 28 August 2023

Published: 30 August 2023



**Copyright:** © 2023 by the authors. Licensee MDPI, Basel, Switzerland. This article is an open access article distributed under the terms and conditions of the Creative Commons Attribution (CC BY) license (<https://creativecommons.org/licenses/by/4.0/>).

## 1. Introduction

Herbs have been used for medicinal purposes since ancient times, and to this day, plants are also potential sources of new drugs. Among plant-derived natural products, diarylheptanoids have gained interest due to their bioactivity, including anticancer [1], neurogenic [2], anti-inflammatory [3], anti-adipogenic [4] and antimicrobial [5] effects. Diarylheptanoids are characterized by a 1,7-diphenylheptane skeleton and can be classified into linear and cyclic forms (Figure 1). The latter can be further divided in two groups: *meta,meta*-cyclophanes and *meta,para*-cyclophanes, according to the connection of the two phenyl rings [6]. Linear diarylheptanoids are distributed in plants belonging to the

families Zingiberaceae and Betulaceae, while cyclic representatives occur in Myricaceae, Aceraceae, Betulaceae and Juglandaceae species [5–7]. The number of newly identified compounds is increasing steadily. In their review in 2012, Lv and She summarized more than 400 diarylheptanoids that have been identified in natural sources, among which were 112 cyclic derivatives [7]. In contrast, the paper of Jahng et al. covered nearly 150 cyclic diarylheptanoids [5].

Curcumin (Figure 1B), the yellow pigment of turmeric (*Curcuma longa* L., Zingiberaceae), is one of the most well-known linear diarylheptanoids. Its biological activities have been investigated in numerous in vitro, in vivo and clinical studies [8]; however, its applications are limited because of its poor pharmacokinetic features, high instability and low solubility in aqueous media. Curcumin is degraded quickly through solvolysis and oxidative degradation at ambient temperature, with a half-life of less than an hour, and this process is further promoted by the elevation of the temperature or an alkaline medium [9]. Hirsutenone (Figure 1B), another linear diarylheptanoid aglycone, which is abundant in several species belonging to the Betulaceae family, also lacks chemical stability. The half-life of this compound is less than seven days at room temperature, and it is rapidly hydrolysed in an aqueous solution [10]. Degradation of hirsutenone is further facilitated by the elevation of the temperature: the half-life of hirsutenone in aqueous solution is reduced from 5.78 days at 25 °C to 1.59 days at 50 °C [11].

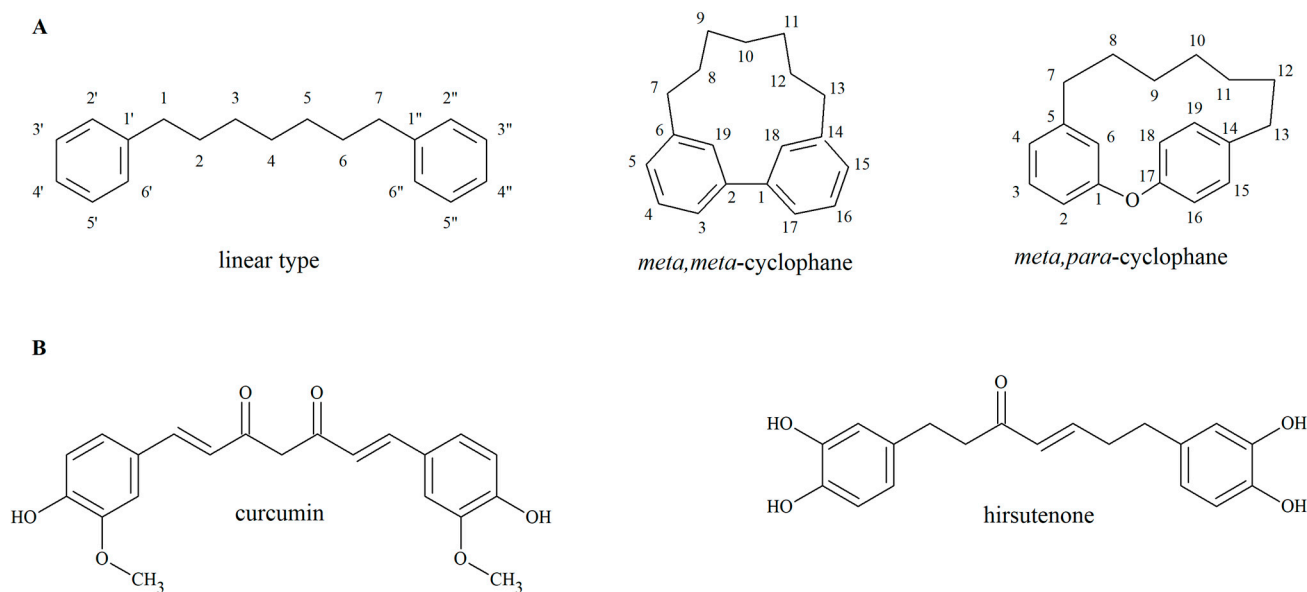


**Figure 1.** The structures of linear, *meta,meta*-cyclophane-type and *meta,para*-cyclophane-type diarylheptanoids (A); structures of curcumin and hirsutenone (B).

Although there are several stability testing studies regarding linear diarylheptanoids, the chemical stability of the cyclic derivatives is underexplored [12]. Cyclic-type diarylheptanoids are characteristic of species belonging to the genera *Carpinus* [13] or *Corylus* [14,15] in the Betulaceae family. In our previous work, we identified the characteristic *meta,meta*-cyclophane-type cyclic diarylheptanoids carpinontriols A (1) and B (2), giffonin X (3) and 3,12,17-trihydroxytricyclo [12.3.1.1<sup>2,6</sup>]nonadeca-1(18),2(19),3,5,14,16-hexaene-8,11-dione (4) (Figure 2) in European hornbeam (*Carpinus betulus* L., Betulaceae) for the first time [16].

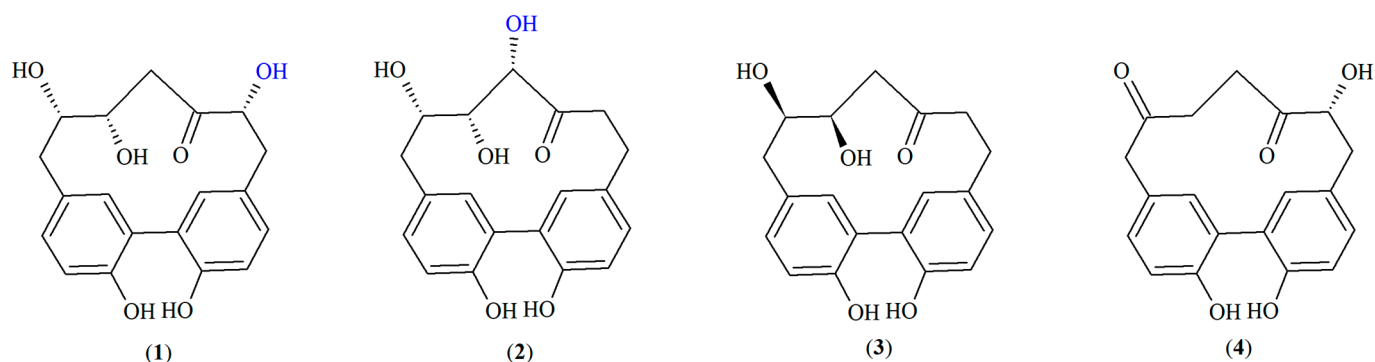


**Figure 2.** Structures of the investigated cyclic diarylheptanoids: (1) carpinontriol A, (2) carpinontriol B, (3) giffonin X, (4) 3,12,17-trihydroxytricyclo [12.3.1.1<sup>2,6</sup>]nonadeca-1(18),2(19),3,5,14,16-hexaene-8,11-dione.

Although 1–4 are known compounds, data on their physical–chemical properties or bioactivities are deficient or completely missing. Lee et al. found that 1 and 2 showed only weak antioxidant activity [13]. In another study, 2 inhibited lipid peroxidation induced by H<sub>2</sub>O<sub>2</sub> in human plasma [17]. In vitro and in vivo antitumor activities of other *meta,meta*-cyclophane-type diarylheptanoids isolated from the pericarp of *Juglans nigra* L. [18] or the bark of *Myrica rubra* (Lour) Siebold & Zucc. Ref. [19] have been reported. According to this, the cyclic diarylheptanoids of *C. betulus* may be potential new sources of antitumor agents. Therefore, it is worth exploring their cytotoxic activity and revealing their physical–chemical properties that may restrict their prospective therapeutic use.

Correspondingly, our aim was to determine the aqueous and storage stability of the cyclic diarylheptanoid compounds 1–4. In the storage stability test, effects of the temperature and storage time have been investigated. The influence of the medium, i.e., that of the solvent and the presence of accompanying substances, was also examined. Additionally, the aqueous stability was studied at different physiologically relevant pH values. Our further aim was to determine the ability of the compounds to permeate membranes by passive diffusion, the parallel artificial membrane permeability assays for the gastrointestinal tract (PAMPA-GI) and the blood–brain barrier (PAMPA-BBB) have been used. To further enhance our understanding of the pharmacological properties of cyclic diarylheptanoids, we also aimed to investigate the in vitro antiproliferative activity of the isolated constituents in various human cancer cell lines.

## 2. Results and Discussion

### 2.1. Evaluation of Aqueous Stability at Different pH Values

The stability of the isolated diarylheptanoids (Figure 2) was evaluated in aqueous medium at 37 °C at three biorelevant pH values (pH 1.2 modelling the gastric fluid, pH 6.8 simulating the intestinal fluid, pH 7.4 mimicking the blood and the tissues). Table 1 summarizes the results; compound concentrations are expressed as % values compared to the initial values. To calculate the kinetic parameters [degradation rate constant (*k*) and half-life (*t*<sub>1/2</sub>)], a linear regression model was used, which followed first-order kinetics in line with previous data for diarylheptanoids (Table 2) [11].

Compound 4 was stable only at pH 7.4 after 81 h, while in agreement with our recent results [12], compound 2 remained intact for the whole study at all pH values. Therefore, rate constants and half-lives in these cases have not been determined. At pH 6.8, the amount of compound 4 decreased significantly after 81 h (final concentration 88.9 ± 2.0%), while at pH 1.2, its degradation was more significant both after 9 and 81 h (with final concentrations of 68.5 ± 4.5% and 31.0 ± 7.0%, respectively). Thus, degradation of 4 was remarkably faster at the lower pH values; the half-lives at pH 6.8 and 1.2 differed by one order of magnitude (487.7 h and 54.4 h, respectively).

**Table 1.** Aqueous stability of the isolated diarylheptanoid compounds <sup>a,b</sup>.

Incubation Time	pH	Compound			
		1	2	3	4
9 h	pH 7.4	96.9 ± 1.2 <sup>a</sup>	102.0 ± 0.9 <sup>a</sup>	82.6 ± 7.7 <sup>#b</sup>	102.0 ± 3.7 <sup>a</sup>
	pH 6.8	97.4 ± 1.5 <sup>#a</sup>	105.2 ± 3.9 <sup>a</sup>	98.9 ± 0.8 <sup>a</sup>	105.8 ± 2.6 <sup>a</sup>
	pH 1.2	97.1 ± 8.9 <sup>a</sup>	101.7 ± 4.2 <sup>a</sup>	100.6 ± 6.9 <sup>a</sup>	68.5 ± 4.5 <sup>#</sup>
81 h	pH 7.4	71.5 ± 5.2 <sup>#b</sup>	101.5 ± 1.1 <sup>a</sup>	46.7 ± 4.7 <sup>#</sup>	103.1 ± 2.2 <sup>a</sup>
	pH 6.8	75.3 ± 3.0 <sup>#b</sup>	101.9 ± 6.4 <sup>a</sup>	93.2 ± 2.0 <sup>#ab</sup>	88.9 ± 2.0 <sup>#</sup>
	pH 1.2	70.5 ± 2.6 <sup>#b</sup>	100.7 ± 5.1 <sup>a</sup>	83.4 ± 5.3 <sup>#b</sup>	31.0 ± 7.0 <sup>#</sup>

<sup>a</sup> Data are expressed as relative concentrations (%) after 9 and 81 h compared to the initial value. <sup>b</sup> Data are expressed as mean values ± SD ( $n = 3$ ). Values with identical lower-case letters (a–b) in the same column are not significantly different (Tukey test,  $p < 0.05$ ); #  $p < 0.05$  compared with the initial concentration.

**Table 2.** Kinetic parameters of the investigated *Carpinus* diarylheptanoids following storage at 37 °C at different pH values.

Compound	pH 7.4		pH 6.8		pH 1.2	
	$k$ (h <sup>-1</sup> )	$t_{1/2}$ (h)	$k$ (h <sup>-1</sup> )	$t_{1/2}$ (h)	$k$ (h <sup>-1</sup> )	$t_{1/2}$ (h)
1	$4.19 \times 10^{-3}$	165.6	$3.65 \times 10^{-3}$	189.6	$4.15 \times 10^{-3}$	167.1
2	-	-	-	-	-	-
3	$8.49 \times 10^{-3}$	81.6	$8.38 \times 10^{-4}$	826.8	$2.32 \times 10^{-3}$	298.4
4	-	-	$1.42 \times 10^{-3}$	487.7	$1.27 \times 10^{-2}$	54.4

The concentration of compound **1** did not show significant changes at pH 1.2 and pH 7.4 after 9 h; however, at the end of the experiment, it displayed significant decomposition ( $p < 0.05$ ; final concentrations were  $70.5 \pm 2.6\%$  and  $71.5 \pm 5.2\%$  at pH 1.2 and pH 7.4, respectively). At pH 6.8, compound **1** was not only unstable after 81 h, but already after 9 h (with final concentrations of  $75.3 \pm 3.0$  and  $97.4 \pm 1.5\%$ , respectively).

At pH 7.4, compound **3** decomposed significantly already after 9 h. On the other hand, its concentration decreased significantly only after 81 h at pH 6.8 and pH 1.2 (with final concentrations of  $93.2 \pm 2.0\%$  and  $83.4 \pm 5.3\%$ , respectively). Interestingly, degradation rate constant of **3** was still by one order of magnitude higher at pH 1.2 than at pH 6.8, the compound was the most stable at a pH value of 6.8 ( $t_{1/2} = 826.8$  h).

Although compounds **1** and **2** are structural isomers, their stability differs significantly, with **2** staying stable throughout the whole study. The increased stability of compound **2** may be attributed to the electronic stabilization effect of its vicinal triol moiety that may stabilize the compound's structure. On the other hand, both compounds **1** and **3** comprise a vicinal diol group that may make them prone to undergo pinacol rearrangement [20], especially in an acidic medium. On the contrary, according to the literature data, phenolic compounds are more stable at lower pH values [21]. Nevertheless, the pH of the medium did not significantly influence stability of **1** during our investigation, while for compound **3**, the highest pH value influenced the stability negatively. In the case of component **4**, pH 1.2 differed significantly from the other two pH values; pH 7.4 and pH 6.8 provided better stability. However, no generally prevalent correlation could be determined between the pH values of the medium and the degradation kinetic parameters.

## 2.2. Evaluation of Storage Stability

A further aim of our work was to determine the mid-term (12 weeks) and long-term (23 weeks) stability of the four major diarylheptanoids by evaluating the effects of storage time and temperature. Influence of the medium, i.e., that of the solvent (in aqueous and methanol solutions) as well as that of other accompanying compounds (being present in methanol and ethyl acetate extracts of the hornbeam bark) was also investigated. Aqueous and methanol solutions of the isolated compounds together with hornbeam bark extracts

prepared with ethyl acetate and methanol were stored at 22, 5 and  $-15$  °C. The storage temperatures were chosen to represent common storage conditions such storage at ambient temperature, in a refrigerator or in a freezer, respectively.

The methanol and aqueous solutions (SM and SA) of the isolated compounds **2** and **4** did not show significant differences when comparing the initial concentration data with values of weeks 12 and 23 (Table 3). Based on this and the lack of degradation products in their chromatograms, **2** and **4** were considered to be stable. The amount of compound **4** increased when being present in methanol and ethyl acetate extracts (EM and EE) that also comprise further accompanying constituents. This elevation can be explained by the degradation of component **1** that was converted into **4** (see Section 2.3).

In case of the SM and SA solutions of the isolated compounds **1** and **3**, samples showed statistical differences both in the mid- and long-term studies when compared to the initial concentration values. Therefore, the effects of the temperature and the medium on the stability of these compounds were examined; results are shown in Table 3 and Supplementary Figure S1.

After 12 weeks of storage, the concentrations of compound **1** in its methanol and aqueous solutions showed significant differences when stored at 22 °C, as compared to the samples stored at 5 °C. No significant concentration differences were detected for **1** between SA and SM samples stored at temperatures 5 °C and  $-15$  °C. In the case of the methanol extract, the storage temperature did not influence the concentration of compound **1** after 12 weeks.

**Table 3.** Chemical stability of *Carpinus* diarylheptanoids: Effects of storage time, temperature and medium on the concentrations of compounds **1–4** as compared to the initial value (%) <sup>a</sup>.

Storage Time (Week)	Storage Temperature (°C)	Medium	Compound			
			1	2	3	4
12	22	SM	63.5 ± 8.7 <sup>#a</sup>	99.7 ± 0.4 <sup>a</sup>	84.5 ± 7.4 <sup>#a</sup>	100.1 ± 0.5 <sup>ab</sup>
		SA	61.7 ± 5.7 <sup>#a</sup>	100.4 ± 1.1 <sup>a</sup>	96.2 ± 0.1 <sup>#bcd</sup>	100.8 ± 1.1 <sup>a</sup>
		EE	110.9 ± 3.6 <sup>#bc</sup>	100.2 ± 0.7 <sup>a</sup>	101.6 ± 2.2 <sup>#bc</sup>	106.3 ± 2.6 <sup>#</sup>
		EM	114.0 ± 2.2 <sup>#b</sup>	101.1 ± 1.1 <sup>a</sup>	102.7 ± 0.9 <sup>#bc</sup>	120.9 ± 2.6 <sup>#</sup>
	5	SM	90.8 ± 2.3 <sup>#def</sup>	99.4 ± 0.6 <sup>a</sup>	99.0 ± 0.1 <sup>#bcd</sup>	100.1 ± 0.6 <sup>ab</sup>
		SA	91.4 ± 0.2 <sup>#def</sup>	99.9 ± 0.4 <sup>a</sup>	99.3 ± 0.1 <sup>#bcd</sup>	100.5 ± 0.7 <sup>ab</sup>
		EE	104.6 ± 1.0 <sup>#bcg</sup>	99.5 ± 0.4 <sup>#a</sup>	100.8 ± 0.5 <sup>#bcd</sup>	102.0 ± 1.7
		EM	110.1 ± 6.2 <sup>bc</sup>	99.9 ± 0.8 <sup>a</sup>	100.2 ± 1.1 <sup>bcd</sup>	105.5 ± 2.5
	−15	SM	94.0 ± 0.8 <sup>#efg</sup>	99.1 ± 1.3 <sup>a</sup>	100.4 ± 1.2 <sup>bcd</sup>	99.1 ± 0.7 <sup>ab</sup>
		SA	93.5 ± 0.4 <sup>#ef</sup>	99.1 ± 1.3 <sup>a</sup>	100.1 ± 0.6 <sup>bcd</sup>	98.6 ± 1.3 <sup>b</sup>
		EE	100.5 ± 0.5 <sup>ceg</sup>	100.1 ± 0.7 <sup>a</sup>	103.5 ± 0.2 <sup>b</sup>	103.5 ± 0.8
		EM	108.7 ± 1.5 <sup>#bc</sup>	99.8 ± 0.7 <sup>a</sup>	101.6 ± 3.1 <sup>#bc</sup>	102.8 ± 3.3 <sup>#</sup>
23	22	SM	32.3 ± 6.3 <sup>#h</sup>	99.9 ± 0.6 <sup>a</sup>	67.1 ± 7.5 <sup>#</sup>	100.2 ± 0.5 <sup>ab</sup>
		SA	23.0 ± 0.5 <sup>#h</sup>	99.8 ± 0.9 <sup>a</sup>	87.6 ± 0.7 <sup>#ae</sup>	100.3 ± 0.6 <sup>ab</sup>
		EE	81.5 ± 3.9 <sup>#di</sup>	99.7 ± 0.5 <sup>a</sup>	95.7 ± 0.5 <sup>#cd</sup>	108.5 ± 2.7 <sup>#</sup>
		EM	77.7 ± 2.9 <sup>#ij</sup>	99.7 ± 0.3 <sup>#a</sup>	95.6 ± 2.4 <sup>#cd</sup>	135.7 ± 9.7 <sup>#</sup>
	5	SM	67.1 ± 7.5 <sup>#aj</sup>	99.2 ± 0.5 <sup>a</sup>	81.9 ± 1.0 <sup>#a</sup>	100.3 ± 0.5 <sup>ab</sup>
		SA	87.2 ± 0.4 <sup>#dfi</sup>	99.9 ± 0.5 <sup>a</sup>	99.1 ± 0.1 <sup>#bcd</sup>	100.0 ± 0.5 <sup>ab</sup>
		EE	92.1 ± 1.3 <sup>#def</sup>	100.1 ± 0.4 <sup>a</sup>	100.9 ± 1.3 <sup>bcd</sup>	107.8 ± 2.6 <sup>#</sup>
		EM	84.1 ± 1.1 <sup>#dfi</sup>	99.2 ± 1.2 <sup>a</sup>	93.8 ± 1.3 <sup>#de</sup>	107.0 ± 4.1
	−15	SM	88.9 ± 3.1 <sup>#dfi</sup>	99.1 ± 1.2 <sup>a</sup>	95.8 ± 0.1 <sup>#cd</sup>	99.8 ± 1.2 <sup>ab</sup>
		SA	93.7 ± 0.3 <sup>#efg</sup>	99.1 ± 1.2 <sup>a</sup>	97.9 ± 2.9 <sup>bcd</sup>	99.9 ± 1.2 <sup>ab</sup>
		EE	91.3 ± 4.2 <sup>#def</sup>	99.8 ± 0.4 <sup>a</sup>	101.1 ± 2.7 <sup>#bcd</sup>	108.0 ± 2.2 <sup>#</sup>
		EM	88.3 ± 3.4 <sup>#dfi</sup>	99.6 ± 0.7 <sup>a</sup>	97.6 ± 3.2 <sup>bcd</sup>	103.6 ± 3.5

<sup>a</sup> Results are expressed as mean values ± SD ( $n = 3$ ). Values with identical lower-case letters (a–j) in the same column are not significantly different (Tukey test,  $p < 0.05$ ); <sup>#</sup>  $p < 0.05$  compared with the initial samples. Abbreviations: SM: methanol solution; SA: aqueous solution; EE: ethyl acetate extract; EM: methanol extract.

After 23 weeks of storage, the concentration of **1** decreased significantly in all solutions and extracts at all temperatures, when compared to the initial values. However, lower storage temperatures (both 5 and  $-15\text{ }^{\circ}\text{C}$ ) provided higher stability for the samples. Similarly, when stored for 23 weeks, the concentrations of **3** were statistically lower than the starting concentrations, except for the EE sample stored at  $5\text{ }^{\circ}\text{C}$  as well as the SA and EM samples stored at  $-15\text{ }^{\circ}\text{C}$ .

Moreover, the concentration differences of **1** in the SM and SA solutions were significantly higher at all investigated temperatures than in the ME and EE extracts after 12 weeks of storage. The complex media of the bark extracts provided significantly higher stability in the medium-term at all studied temperatures for **1**. A similar pattern could also be observed at  $22\text{ }^{\circ}\text{C}$  after 23 weeks of storage, while both at  $5\text{ }^{\circ}\text{C}$  and  $-15\text{ }^{\circ}\text{C}$ , a concentration decrease of **1** in the aqueous solution was equal to that in the ME and EE extracts.

The matrices of the bark extracts also allowed for appropriate stability for **3** at all storage temperatures after 12 weeks. In the long-term studies (after 23 weeks), the methanol solution of **3** showed significant concentration differences at higher storage temperatures ( $22$  and  $5\text{ }^{\circ}\text{C}$ ) when compared to the other media (SA, EM and EE). The 23-week storage at  $22\text{ }^{\circ}\text{C}$  also intensified the degradation of **3** in the aqueous solution when compared to temperatures of  $5$  and  $-15\text{ }^{\circ}\text{C}$ .

Analysing the degradation kinetic parameters of the pure diarylheptanoids **1** and **3**, we can state that the  $k$  value decreases, and the  $t_{1/2}$  value increases as the temperature decreases (Table 4). The thermal degradation of **1** and **3** in aqueous and methanolic solutions follows first-order kinetics, in which the degradation rate depends on the temperature. Our results are in agreement with other studies that found that diarylheptanoids are prone to temperature-dependent degradation [10,11].

**Table 4.** Kinetic parameters of carpinontriol A (**1**) and giffonin X (**3**) in aqueous and methanolic solutions following storage at  $22\text{ }^{\circ}\text{C}$ ,  $5\text{ }^{\circ}\text{C}$  and  $-15\text{ }^{\circ}\text{C}$  for 23 weeks.

Temperature ( $^{\circ}\text{C}$ )	Medium	Carpinontriol A ( <b>1</b> )		Giffonin X ( <b>3</b> )	
		$k$ ( $\text{Week}^{-1}$ )	$t_{1/2}$ (Week)	$k$ ( $\text{Week}^{-1}$ )	$t_{1/2}$ (Week)
22	SA	$5.97 \times 10^{-2}$	11.61	$5.90 \times 10^{-3}$	117.48
	SM	$4.53 \times 10^{-2}$	15.30	$1.85 \times 10^{-2}$	37.47
5	SA	$4.47 \times 10^{-3}$	147.48	$5.0 \times 10^{-4}$	1386.29
	SM	$1.40 \times 10^{-2}$	50.23	$7.10 \times 10^{-3}$	97.63
-15	SA	$1.70 \times 10^{-3}$	407.73	-	-
	SM	$3.60 \times 10^{-3}$	192.54	$1.60 \times 10^{-3}$	433.22

Abbreviations: SA: aqueous solution; SM: methanol solution.

Comparing the effects of the medium,  $k$  values of **1** were lower in the aqueous solution than in the methanolic solution (e.g.,  $4.47 \times 10^{-3}$  vs.  $1.40 \times 10^{-2}\text{ week}^{-1}$  at  $5\text{ }^{\circ}\text{C}$ , for SA and SM respectively) (Table 4). Thus, it was concluded that the aqueous medium provided higher stability. This effect was even more pronounced for compound **3**, e.g., calculated half-lives were 1386.29 vs. 97.63 weeks at  $5\text{ }^{\circ}\text{C}$  in aqueous and methanolic solution, respectively.

### 2.3. Characterization of the Degradation Products by UHPLC-HR-MS/MS

The structural analysis of the degradation products formed in the storage and pH stability studies was performed by ultrahigh-performance liquid chromatography–high-resolution tandem mass spectrometry (UHPLC-HR-MS/MS) measurements. The chromatographic and mass spectrometric data of the original constituents and the degradation products are presented in Table 5. The high-resolution electrospray ionization mass spectrometry (HR-ESI-MS) and HR-MS/MS spectra of the isolated compounds and their degradation products are shown in the Supplementary Material (Supplementary Figures S2–S13).

In case of **1** and **3**, new compounds **1c** and **3a** appearing in the chromatograms presented molecular ions bearing  $m/z$  values 18 Da less than the molecular ions of the original compounds. The deprotonated molecular ions of **1c** and **3a** (at  $m/z$  325.1076  $[M - H]^-$  and  $m/z$  309.1127  $[M - H]^-$ , respectively), refer to the elimination of a water molecule from their corresponding parent compounds **1** ( $m/z$  343.1191) and **3** ( $m/z$  327.1240). In Scheme 1, two possible degradation pathways are depicted for both **1** and **3**, highlighting the characteristic structural differences of the hypothetical products.

As a common structural element, a vicinal diol group is present in the heptane chain of both compounds **1** and **3**, which may be the source of the cleaved water molecule. However, the proposed degradation can undergo through different pathways. The common vicinal diol moiety implies that the pinacol rearrangement is one possible pathway for both **1** and **3**, particularly in an acidic medium [20]. However, when the pH is neutral, there is only a slight chance for the pinacol rearrangement to occur. At the same time, another possible mechanism is for example the radical oxidative degradation [22]. Nevertheless, there is also a possibility that both degradation pathways (or even other mechanisms) may occur at different pH values.

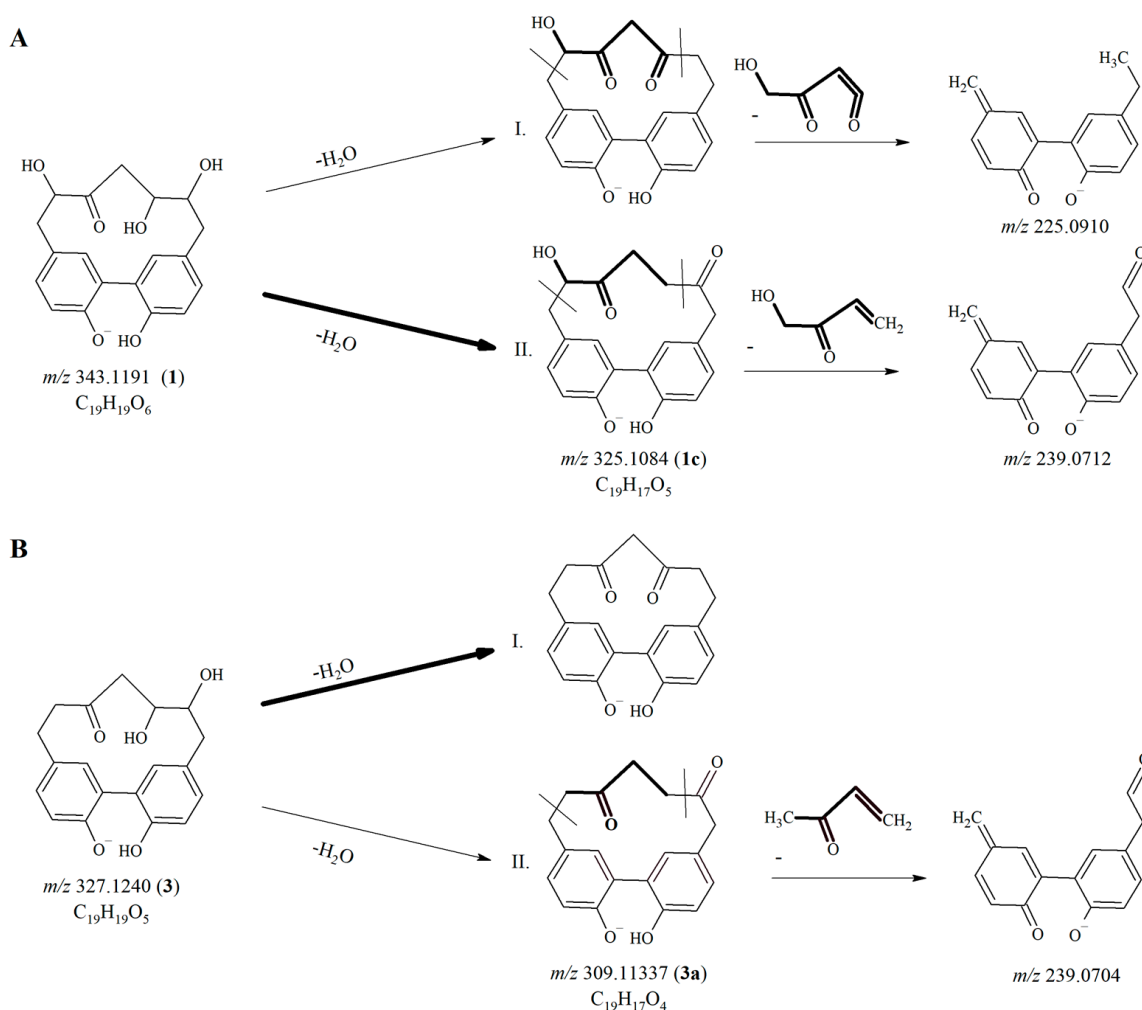
**Table 5.** HR-MS data of the diarylheptanoids **1** and **3** and their degradation products.

No.	$[M - H]^-$ ( $m/z$ ) Experimental	$[M - H]^-$ ( $m/z$ ) Calculated	Error (ppm)	Molecular Formula	Fragment Ions ( $m/z$ )
<b>1</b>	343.1199	343.1182	3.75	$C_{19}H_{19}O_6$	283.0976 ( $C_{17}H_{15}O_4$ ), 271.0977 ( $C_{16}H_{15}O_4$ ), 269.0820 ( $C_{16}H_{13}O_4$ ), 241.0869 ( $C_{15}H_{13}O_3$ ), 211.0758 ( $C_{14}H_{11}O_2$ )
<b>1a</b>	361.0927	361.0923	2.37	$C_{18}H_{17}O_8$	343.0812 ( $C_{18}H_{15}O_7$ ), 285.0769 ( $C_{16}H_{13}O_5$ ), 258.0534 ( $C_{14}H_{10}O_5$ ), 327.0872 ( $C_{18}H_{15}O_6$ ), 309.0764 ( $C_{18}H_{13}O_5$ ),
<b>1b</b>	345.0977	345.0974	2.25	$C_{18}H_{17}O_7$	285.0767 ( $C_{16}H_{13}O_5$ ), 258.0531 ( $C_{14}H_{10}O_5$ ), 225.0549 ( $C_{14}H_9O_3$ ) 269.0820 ( $C_{16}H_{13}O_4$ ), 253.0862 ( $C_{16}H_{13}O_3$ ),
<b>1c</b>	325.1084	325.1076	4.06	$C_{19}H_{17}O_5$	241.0865 ( $C_{15}H_{13}O_3$ ), 239.0862 ( $C_{15}H_{11}O_3$ ), 225.0910 ( $C_{15}H_{13}O_2$ ), 211.0759 ( $C_{14}H_{11}O_2$ ) 269.0821 ( $C_{16}H_{13}O_4$ ), 267.1028 ( $C_{17}H_{15}O_3$ ),
<b>3</b>	327.1240	327.1233	4.05	$C_{19}H_{19}O_5$	253.0866 ( $C_{16}H_{13}O_3$ ), 239.0716 ( $C_{15}H_{11}O_3$ ), 211.0758 ( $C_{14}H_{11}O_2$ ) 267.1020 ( $C_{17}H_{15}O_3$ ),
<b>3a</b>	309.1134	309.1127	4.10	$C_{19}H_{17}O_4$	253.0876 ( $C_{16}H_{13}O_3$ ), 225.09131 ( $C_{15}H_{13}O_2$ ), 211.0758 ( $C_{14}H_{11}O_2$ )

Position of the cleavage of the water molecule could also be proposed, based on the mass spectrometric fragmentation pathway of cyclic diarylheptanoids [16]. The more likely degradation pathways have been highlighted in Scheme 1 by drawing bold arrows. In case of compound **1** (Scheme 1A), the putative degradation product generated through pathway I would present a fragment ion at  $m/z$  225.0910, while pathway II would result in the formation of a degradation product showing a fragment ion at  $m/z$  239.0862. Unfortunately, the HR-MS spectrum of the degradation product **1c** presented both fragment ions, though with different intensities. Since the retention time and mass spectrum of

compound **1c** corresponds with that of compound **4**, pathway II taking place seems to be more likely. This assumption was further affirmed by the observation that in hornbeam bark extracts the amount of **1** decreased, while that of **4** increased over time during the storage stability assays.

According to mass spectrometric fragmentation patterns of cyclic diarylheptanoids [16], only pathway II would result in the formation of a degradation product for compound **3**, which could present a characteristic fragment ion at  $m/z$  239.0704. However, this ion was not detected in the mass spectrum of the actual degradation product **3a**; thus, it was deduced that only pathway I could take place (Scheme 1B).



**Scheme 1.** The possible degradation pathways of compound **1** and the proposed mass spectrometric fragmentation of the degradation product **1c** (A); the possible degradation pathways of compound **3** and the proposed mass spectrometric fragmentation of the degradation product **3a** (B). Degradation product numbers refer to Table 5.

Although the common structural element of compounds **1** and **3** (i.e., the vicinal diol group) indicated that the same degradation pathway should take place for both **1** and **3**, our results did not confirm this. A possible explanation is the electronic stabilization effect, which may stabilize a compound's structure or shift the equilibrium toward a degradation product. For example, the stabilizing effect of the vicinal triol moiety may be responsible for the increased stability of compound **2**. Similarly, the additional vicinal carboxylic acid moiety of compound **1** may alter the mechanism of degradation from that of compound **3**.

Two additional degradation products with the molecular formulas of  $C_{18}H_{17}O_8$  and  $C_{18}H_{17}O_7$  were detected in the chromatogram of **1**, referring to the loss of a carbon-

containing moiety and further oxidation mechanisms. In case of compound **4**, degradation products were not detected, despite the significant decrease in the initial concentration (the final concentration of **4** at pH 1.2 was  $31.0 \pm 7.0\%$ ).

#### 2.4. Parallel Artificial Membrane Permeability Assay (PAMPA) Studies

The ability of the isolated cyclic diarylheptanoid compounds to cross biological membranes of the gastrointestinal tract and the blood–brain barrier by passive diffusion was investigated by the PAMPA model [23].

In the PAMPA-BBB experiments, only giffonin X (**3**) was detected in the acceptor phase. It also presented a calculated  $\log P_e$  value greater than  $-6.0$  ( $-5.92 \pm 0.04$ ), which indicates that **3** is capable of crossing the lipid membrane of the blood–brain barrier (Table 6) [24]. However, compound **3** was considered unstable ( $t_{1/2} = 81.6$  h) in the pH 7.4 medium of the PAMPA-BBB model and its decomposition product could not be detected in the acceptor phase.

In the PAMPA-GI model, compound **4** with one of the lowest  $\text{clog} P$  values ( $0.94 \pm 0.46$ ) among the studied diarylheptanoids was not detected in the acceptor phase, suggesting that it is unable to cross the lipid membrane of the gastrointestinal tract. Compounds **1–3** were detected in the acceptor phase in the PAMPA-GI model; however, none of the diarylheptanoids possessed  $\log P_e$  values greater than the critical  $-5.0$  (Table 6), predicting that neither the compounds are able to pass through the membrane of the gastrointestinal tract [24].

**Table 6.** Results of the PAMPA experiments:  $\log P_e$  values ( $n = 9$ ) and the calculated  $\text{clog} P$  values (Chemsketch Freeware).

Compound	$\log P_e$ PAMPA-BBB ( $n = 9$ )	$\log P_e$ PAMPA-GI ( $n = 9$ )	$\text{clog} P$
<b>1</b>	n.d.	$-6.25 \pm 0.04$	$0.93 \pm 0.46$
<b>2</b>	n.d.	$-5.46 \pm 0.06$	$1.92 \pm 0.67$
<b>3</b>	$-5.92 \pm 0.04$	$-5.22 \pm 0.07$	$1.77 \pm 0.41$
<b>4</b>	n.d.	n.d.	$0.94 \pm 0.46$

Abbreviations: n.d.: not detected in the acceptor phase; PAMPA-GI: parallel artificial membrane permeability assay for the gastrointestinal tract; PAMPA-BBB: parallel artificial membrane permeability assay for the blood–brain barrier.

Regarding the polarity of these constituents, none of the compounds have  $\text{clog} P$  values higher than 2.5. Compounds **2** and **3** have higher  $\text{clog} P$  values than 1.0, while  $\text{clog} P$  values of **1** and **4** are lower than 1.0. Compounds **1** and **2** are constitutional isomers; nevertheless, their  $\text{clog} p$  values are different ( $\text{clog} P$   $0.93 \pm 0.46$  and  $1.92 \pm 0.67$ , respectively). These data suggest poor membrane permeability of the major diarylheptanoid components of the *C. betulus* bark.

A further aspect to consider when assessing the PAMPA results is the decomposition of the constituents in aqueous media at the investigated pH values. Significant changes in compound concentrations occurring in a physiologically relevant time frame might be observed for **3** at pH 7.4 and **4** at pH 1.2. In these cases, the decrease in concentration in the donor and acceptor phases caused by decomposition of the analytes of interest might modify the PAMPA results.

The in vitro neuroprotective effect of cyclic diarylheptanoids in mouse hippocampal HT22 cells [25] and N2a cells [26] was established. However, based on our results suggesting poor penetration capability, their in vivo efficacy is ambiguous.

#### 2.5. Evaluation of the Cytostatic Activity

The in vitro antiproliferative activities of the isolated *Carpinus* diarylheptanoids were studied by the Alamar Blue assay in HT-29 (colorectal carcinoma), HepG2 (hepatocellular carcinoma), HL-60 (acute promyelocytic leukaemia), U87 (glioblastoma) and A2058

(melanoma, derived from metastatic site: lymph node) human cancer cell lines for the first time (Supplementary Table S1). We confirmed the concentration-dependent antiproliferative activity of carpinontriol A (**1**) against A2058 human metastatic melanoma cells ( $IC_{50} = 14.9 \pm 2.3 \mu\text{M}$ ). It was comparable to that of the United States Food and Drug Administration (FDA)-approved etoposide ( $IC_{50} = 8.9 \pm 0.2 \mu\text{M}$ ). The cytostatic activity of **1** in A2058 cells was moderate when compared to the antitumor drug daunomycin ( $IC_{50} = 0.16 \pm 2.3 \mu\text{M}$ ). However, it should be noted that in contrast to daunomycin, compound **1** showed a highly selective antiproliferative activity.

No significant in vitro activity was observed for the other constituents at a concentration range of 0.16–100  $\mu\text{M}$ . Our results are the following previous studies, since  $IC_{50}$  values exceeding 100  $\mu\text{M}$  were observed for carpinontriol B (**2**) in A549 human lung adenocarcinoma and HeLa human cervical adenocarcinoma cells [17,27]. Similarly, carpinontriol B was not cytotoxic up to 1000  $\mu\text{M}$  in A375 and SK-Mel-28 human melanoma cell lines [28].

### 3. Materials and Methods

#### 3.1. Solvents and Chemicals

Chloroform, ethyl acetate and methanol of reagent grade as well as HPLC-grade methanol and acetonitrile were purchased from Molar Chemicals Kft. (Halásztelek, Hungary). Dimethyl sulfoxide (DMSO), *n*-dodecane, sodium chloride (NaCl), hydrochloric acid (HCl), disodium hydrogen phosphate heptahydrate ( $\text{Na}_2\text{HPO}_4 \cdot 7\text{H}_2\text{O}$ ) and sodium dihydrogen phosphate monohydrate ( $\text{NaH}_2\text{PO}_4 \cdot \text{H}_2\text{O}$ ) were obtained from Reanal-Ker (Budapest, Hungary), while phosphatidylcholine, cholesterol and the porcine polar brain lipid extract were purchased from Merck (Darmstadt, Germany). Acetic acid 100% for HPLC LiChropur<sup>TM</sup>, pyruvate and PBS tablet (Phosphate Buffered Saline, pH 7.4) were acquired from Sigma-Aldrich (Steinheim, Germany). Roswell Park Memorial Institute 1640 medium (RPMI-1640) and Dulbecco's Modified Eagle's Medium (DMEM) were supplied by Lonza (Basel, Switzerland). Fetal bovine serum (FBS) was purchased from Biosera (Nuaille, France). Non-essential amino acids, penicillin/streptomycin (10,000 units penicillin and 10 mg streptomycin/mL) and trypsin were obtained from Gibco (Thermo Fisher Scientific, Waltham, MA, USA). High-purity water was gained by a Millipore Direct Q5 Water Purification System (Billerica, MA, USA).

#### 3.2. Plant Material and Sample Preparation

Bark samples of *C. betulus* were collected in Hungary, in the Visegrád Hills (Visegrádi-hegység, July 2018) to prepare the samples for the stability studies. Authenticated samples and herbarium specimens are deposited at the Herbarium of the Department of Pharmacognosy, Semmelweis University, Budapest, Hungary. Dried and milled samples (12 g) were extracted in an ultrasonic bath (Bandelin Sonorex Digitec DT 1028, Berlin, Germany) with chloroform, ethyl acetate and methanol consecutively ( $3 \times 120 \text{ mL}$  for all solvents, 2 h each) at room temperature. The extracts were distilled to dryness with a rotary evaporator (Büchi Rotavapor R-200, Flawil, Switzerland) at 45 °C. The samples were suspended in 70% methanol of HPLC-gradient grade and filtered through Minisart RC 15 0.2  $\mu\text{m}$  syringe filters (Sartorius AG, Goettingen, Germany).

#### 3.3. Isolation of Diarylheptanoids

For the isolation of the most dominant diarylheptanoids, *C. betulus* bark was collected in Mátraháza (Hungary; May 2016). Similarly to the analytical samples (Section 2.2), dried and milled bark (500 g) was extracted in an ultrasonic bath successively with chloroform, ethyl-acetate and methanol ( $3 \times 2 \text{ L}$  for all solvents, 2 h each). The methanol extract was evaporated to dryness under reduced pressure at 50 °C and suspended in 70% methanol (final concentration: 0.5 mg/mL). The extract was then fractionated by flash chromatography (CombiFlash NextGen 300+, Teledyne Isco, Lincoln, NE, USA), using a RediSep Rf Gold C18 column (100 g, Teledyne Isco) as stationary phase. Eluent A was 0.3% acetic acid in water; eluent B was methanol (gradient elution: 0 min 30% B, 4 min 62.5% B, 19 min

100% B, 29 min 100% B; flow rate: 60 mL/min). Fractions of 16 mL each were collected and further fractionated by (semi)preparative HPLC.

The combined fractions 31–34 were separated by semipreparative HPLC (Waters 2690 HPLC system equipped with Waters 996 diode array detector) (Waters Corporation, Milford, MA, USA). The Luna C18 100 A (150 × 10 mm i.d., 5 µm; Phenomenex Inc., Torrance, CA, USA) column as stationary phase, and 0.3% acetic acid in water (as eluent A) and methanol (as eluent B) were used. The following gradient elution was applied to obtain **1** ( $t_R = 22.3$  min) and **4** ( $t_R = 30.0$  min): 0 min 33% B, 20 min 33% B, 25 min 100% B, 33 min 100% B (flow rate: 1 mL/min).

Fractions 42–52 were combined and further chromatographed by preparative HPLC (Hanbon Sci.&Tech. Newstyle, Huaian, China) using a Gemini NX-C18 (150 × 21.2 mm, 5 µm; Phenomenex Inc.) column as stationary phase to collect 7 subfractions. The following gradient elution (flow rate: 5 mL/min) was used (eluent A: 0.3% acetic acid in water; eluent B: methanol): 0 min 40% B, 25 min 60% B, 26 min 100% B, 37 min 100% B. Subfraction 4 ( $t_R = 19$  min) was separated using the same Waters 2690 HPLC instrument and Luna C18 100 A (150 × 10 mm i.d., 5 µm; Phenomenex Inc.) column as stationary phase. Eluent A was 0.3% acetic acid in water, eluent B was acetonitrile, flow rate of the mobile phase was 1 mL/min. The utilized gradient elution (0 min 35% B, 16 min 35% B, 17 min 100% B) yielded **2** ( $t_R = 14.0$  min) and **3** ( $t_R = 14.8$  min).

The quantity and purity of the isolated substances was as follows: carpinontriol A (**1**) (1.3 mg, >97%), carpinontriol B (**2**) (1.2 mg, >99%), giffonin X (**3**) (2.0 mg, >99%), 3,12,17-trihydroxytricyclo [12.3.1.1<sup>2,6</sup>]nonadeca-1(18),2(19),3,5,14,16-hexaene-8,11-dione (**4**) (1.0 mg, >98%). The purity of subfractions containing the isolated compounds collected during the final isolation step was evaluated by UHPLC-DAD (Supplementary Figures S14–S17).

### 3.4. UHPLC-DAD and UHPLC-DAD-HR-MS/MS Analyses

For the analysis of the samples from the chemical stability as well as the PAMPA studies, sample concentrations were determined using our previously developed ultrahigh-performance liquid chromatography–diode array detection (UHPLC-DAD) method validated for linearity, precision and accuracy [16]. Briefly, an ACQUITY UPLC H-Class PLUS System hyphenated with a quaternary solvent delivery pump (QSM), an auto-sampler manager (FTN), a column compartment (CM) and a photodiode array (PDA) detector (Waters Corporation) was employed. Stationary phase: Acquity BEH C18 column (100 × 2.1 mm i.d., 1.7 µm; Waters Corporation), column temperature: 30 °C. The mobile phase consisted of 0.3% acetic acid in water (eluent A) and acetonitrile (eluent B). The following gradient elution was applied at a flow rate of 0.3 mL/min: 0 min 12.0% B, 19.0 min 13.5% B, 25.5 min 75.0% B, 26.0 min 100.0% B, 28.0 min 100.0% B, 28.5 min 12.0% B.

High-resolution mass spectra of the degradation products formed during the stability studies were obtained using a Dionex Ultimate 3000 UHPLC system (3000RS diode array detector, TCC-3000RS column thermostat, HPG-3400RS pump, SRD-3400 solvent rack degasser, WPS-3000TRS autosampler), hyphenated with an Orbitrap<sup>®</sup> Q Exactive Focus Mass Spectrometer equipped with an electrospray ionization source (Thermo Fischer Scientific, Waltham, MA, USA). For the chromatographic separation of the constituents, the same Acquity UPLC BEH C18 (30 × 2.1 mm i.d., 1.7 µm; Waters Corporation) column as stationary phase (maintained at 25 °C) was used. Mobile phase: 0.1% formic acid in water (eluent A) and a mixture of 0.1% formic acid in water and acetonitrile (20:80, *v/v*) (eluent B). Gradient elution was as follows: 10–60% B (0.0–3.5 min), 60–100% B (3.5–4.0 min), 100% B (4.0–4.5 min), 100–10% B (4.5–7.0 min), flow rate: 0.3 mL/min. The ESI source was operated in negative ionization mode and operation parameters were optimized automatically using the built-in software. The working parameters were as follows: spray voltage 2500 V; capillary temperature 320 °C; sheath gas (N<sub>2</sub>), 47.5 °C; auxiliary gas (N<sub>2</sub>) 11.25 arbitrary units, spare gas (N<sub>2</sub>) 2.25 arbitrary units. The resolution of the full scan was of 70,000, the scanning range was between *m/z* 100–500 units. The most intense ions detected in full scan spectrum were selected for data-dependent MS/MS scan at a resolving power of 35,000, in

the range of  $m/z$  50–500. Parent ions were fragmented with normalized collision energy of 10%, 30% and 45%.

### 3.5. Stability Studies

In the present work, we studied the effects of different conditions, including storage time, storage temperature and solvent, on the stability of the cyclic diarylheptanoids 1–4. Their chemical stability at different pH values was also investigated. Additionally, degradation kinetics of the compounds were examined, while degradation pathways and mechanisms were also explored.

#### 3.5.1. Evaluation of Aqueous Stability at Different pH Values

The buffers modelling the gastric fluid (pH 1.2), the intestinal fluid (pH 6.8) and the blood and the tissues (pH 7.4) were prepared as follows. Buffer pH = 1.2: 1.0 g NaCl and 3.5 mL HCl dissolved in distilled water, final volume: 500.0 mL. Buffer pH = 6.8: 20.2 g  $\text{Na}_2\text{HPO}_4 \cdot 7\text{H}_2\text{O}$  and 3.4 g  $\text{NaH}_2\text{PO}_4 \cdot \text{H}_2\text{O}$  dissolved in distilled water, final volume: 1000.0 mL, pH adjustment with 0.5 M NaOH or 0.5 M HCl. Buffer pH = 7.4: one PBS tablet dissolved in 200.0 mL distilled water. The stock solutions of compounds 1–4 were prepared with dimethyl sulfoxide (DMSO) at a concentration of 10.0 mM. The stock solutions were diluted 100-fold with each buffer separately to obtain the working solutions (297.0  $\mu\text{L}$  buffer + 3.0  $\mu\text{L}$  stock solution). All working solutions were filtered through Phenex-RC 15 mm, 0.2  $\mu\text{m}$  syringe filters (Gen-Lab Ltd., Budapest, Hungary). The samples were incubated for 81 h at 37 °C; aliquots were taken for analysis every 9 h in accordance with the time required to quantify the analytes of interest in one set of samples. The total incubation time of 81 h was applied to obtain data for ten measurement points. The previously described UHPLC-DAD method was used to examine the changes in compound concentrations (see Section 3.4).

For the determination of pH stability, the initial AUC values were compared with the data after 9 and 81 h using paired-sample  $t$  test; significant difference was reported at  $p < 0.05$ . The effects of the pH were analysed through one-way analysis of variance (ANOVA) followed by Tukey's post hoc HSD test ( $p < 0.05$ ). All experiments were performed in triplicates ( $n = 3$ ).

We used the following equations to calculate the first-order reaction rate constant ( $k$ ) and the half-life ( $t_{1/2}$ ) indicating the time required to reduce the concentration of diarylheptanoids by 50% [29]:

$$\ln(c_t/c_0) = -k \times t \quad (1)$$

$$t_{1/2} = -\ln 0.5 \times k^{-1} \quad (2)$$

where  $c_t$  is the concentration of the diarylheptanoids at time  $t$ ,  $c_0$  is the initial concentration,  $k$  is the reaction rate constant,  $t$  is the treatment time.

#### 3.5.2. Evaluation of Storage Stability

The chemical stability of the isolated compounds in solutions was examined at a concentration of 50  $\mu\text{g}/\text{mL}$  in methanol and water (in the latter case using methanol as co-solvent, final composition: water-methanol 90:10,  $v/v$ ). Furthermore, the methanol and ethyl acetate extracts of *C. betulus* bark (concentration 4  $\text{mg}/\text{mL}$ ) were also studied in order to assess the effects of the accompanying substances. The storage stability studies were performed at a neutral pH value. All solutions were filtered through Phenex-RC 15 mm, 0.2  $\mu\text{m}$  syringe filters (Gen-Lab Ltd., Budapest, Hungary). The samples were prepared in triplicate and stored protected from light at  $22 \pm 2.0$  °C,  $5 \pm 1.5$  °C and  $-15 \pm 2.0$  °C for 23 weeks. Quantities of the analytes of interest were quantified at weeks 12 and 23 using the abovementioned UHPLC-DAD method (see Section 3.4).

For the determination of the stability, the initial AUC values were compared with the data of weeks 12 and 23 using paired-sample T test; significance was reported at  $p < 0.05$ .

The effects of the temperature and the medium (i.e., solvent and accompanying substances) were analysed through one-way analysis of variance (ANOVA) followed by Tukey's post hoc HSD test ( $p < 0.05$ ). To establish the kinetic parameters  $t_{1/2}$  and  $k$ , Equations (1) and (2) were applied, respectively.

### 3.6. Parallel Artificial Membrane Permeability Assay (PAMPA) Studies

A parallel artificial membrane permeability assay (PAMPA) was used to determine the effective permeability ( $P_e$ ) for the *Carpinus* diarylheptanoids. Stock solutions of the isolated compounds (10 mM in DMSO) were diluted with the defined buffer (pH 7.4 for the PAMPA-BBB and pH 6.8 for the PAMPA-GI assays) to obtain the donor solutions (composition: 297.0  $\mu$ L buffer + 3.0  $\mu$ L stock solution). Donor solutions were filtered through Phenex-RC 15 mm, 0.2  $\mu$ m syringe filters (Gen-Lab Ltd., Budapest, Hungary).

For the PAMPA-BBB test, 5  $\mu$ L of porcine polar brain lipid extract (PBLE) solution (16.0 mg PBLE + 8.0 mg cholesterol dissolved in 600.0  $\mu$ L *n*-dodecane) was applied for each well of the 96-well polycarbonate-based filter donor plates (top plate) (Multiscreen™-IP, MAIPN4510, pore size 0.45  $\mu$ m; Merck). For the PAMPA-GI assay, the wells of the top plate were coated with 5  $\mu$ L of the mixture of 8.0 mg phosphatidylcholine + 4.0 mg cholesterol dissolved in 300.0  $\mu$ L *n*-dodecane. The 150.0  $\mu$ L aliquots of the filtrated donor solutions were placed on the membrane. The 96-well PTFE acceptor plates (bottom plates) (Multiscreen Acceptor Plate, MSSACCEPTOR; Merck), were filled with 300.0  $\mu$ L buffer solution (0.01 M PBS buffer, pH 7.4). The donor plate was placed upon the acceptor plate, and both plates were incubated together at 37 °C for 4 h in a Heidolph Titramax 1000 Vibrating platform shaker (Heidolph, Schwabach, Germany).

After the incubation, the plates were separated and the compound concentrations in the donor ( $C_D(t)$ ) and acceptor ( $C_A(t)$ ) solutions were determined using the aforementioned UHPLC-DAD method (see Section 3.4). In advance, concentrations of the analytes of interest in the donor solutions at zero time point ( $C_D(0)$ ) were also established by UHPLC-DAD. The effective permeability and the membrane retention in the PAMPA-BBB and the PAMPA GI experiments were calculated by Equations (3) and (4), respectively [30]:

$$P_e = \frac{-2.303}{A(t - \tau_{SS})} \cdot \left( \frac{V_A \cdot V_D}{V_A + V_D} \right) \cdot \lg \left[ 1 - \left( \frac{V_A + V_D}{(1 - MR) \cdot V_D} \right) \times \left( \frac{C_A(t)}{C_D(0)} \right) \right] \quad (3)$$

$$P_e = \frac{-2.303}{A(t - \tau_{SS})} \cdot \left( \frac{1}{1 + r_a} \right) \cdot \lg \left[ -r_a + \left( \frac{1 + r_a}{1 - MR} \right) \times \left( \frac{C_D(t)}{C_D(0)} \right) \right] \quad (4)$$

where  $P_e$  is the effective permeability coefficient (cm/s),  $A$  is the filter area (0.24 cm<sup>2</sup>),  $V_D$  and  $V_A$  are the volumes in the donor (0.15 cm<sup>3</sup>) and acceptor phases (0.30 cm<sup>3</sup>),  $t$  is the incubation time (s),  $\tau_{SS}$  is the time (s) to reach steady state (240 s),  $C_D(t)$  is the concentration (mol/cm<sup>3</sup>) of the compound in the donor phase at time  $t$ ,  $C_D(0)$  is the concentration (mol/cm<sup>3</sup>) of the compound in the donor phase at time 0, MR is the estimated membrane retention factor (the estimated mole fraction of solute lost to the membrane) and  $r_a$  is the sink asymmetry ratio (gradient-pH-induced), defined as:

$$r_a = \frac{V_D}{V_A} \times \frac{P_e^{(A \rightarrow D)}}{P_e^{(D \rightarrow A)}} \quad (5)$$

$$MR = 1 - \frac{C_D(t)}{C_D(0)} - \frac{V_A}{V_D} \frac{C_A(t)}{C_D(0)} \quad (6)$$

All experiments were performed in three replicates on three consecutive days ( $n = 9$ ); caffeine standard was used as positive, while rutin was used as negative control. Clog  $P$  values were calculated using ACD/ChemSketch (Freeware) 2 January 2020 (Advanced Chemistry Development, Inc., Toronto, ON, Canada).

### 3.7. Evaluation of the In Vitro Activity of the Isolated Diarylheptanoids

#### 3.7.1. Cell Culturing and Media

For the experiments, the following human cell lines were used: A2058 (melanoma, derived from metastatic site: lymph node), HepG2 (hepatocellular carcinoma), U87 (glioblastoma), HT-29 (colorectal carcinoma) and HL-60 (acute promyelocytic leukaemia). Cell lines were generous gifts from Dr. József Tóvári (Department of Experimental Pharmacology, National Institute of Oncology, Budapest, Hungary).

For maintaining the U87 cell culture, DMEM supplemented with 10% FBS, 2 mM L-glutamine, 100 µg/mL penicillin/streptomycin, 1 mM pyruvate and 1% non-essential amino acids (CM DMEM) were used. A2058, HT-29, HepG2 and HL-60 cells were cultured in RPMI-1640 medium supplemented with 10% FBS, 2 mM L-glutamine and a penicillin-streptomycin antibiotics mixture (50 IU/mL and 50 µg/mL, respectively). The cultures were maintained at 37 °C in a humidified atmosphere with 5% CO<sub>2</sub>.

#### 3.7.2. Determination of the In Vitro Antiproliferative Activity

The cells were grown to confluency and then divided into 96-well tissue culture plates (Sarstedt, Nümbrecht, Germany) with an initial cell number of 5000 cells/well. Cells were incubated at 37 °C in a 5% CO<sub>2</sub> humidified atmosphere overnight. Before the assay, 50 µL of the supernatant was removed and replaced with a 50 µL serum-free medium (SFM). The stock solutions of the compounds (*c* = 20 mM) were serially diluted with SFM and added to the cells in 100 µL volume. The final concentration of each compound in the cells was 0.16 µM, 0.8 µM, 4 µM, 20 µM and 100 µM (each concentration has four parallels). The cells were treated for 24 h with the compounds and negative control cells (no compound control) were treated with SFM only (incubated at 37 °C). As a positive control, we employed daunomycin (DAU) [31,32] and etoposide [33] as FDA-approved clinically used drugs as well as compound Sal (5-chloro-2-hydroxy-*N*-[4-(trifluoromethyl)phenyl]benzamide) as a cytostatic drug candidate [34]. After 24 h of incubation, cells were washed 3 times with SFM, and then the cells were further cultured in 10% FBS-containing complete medium (CM). After three days, a 22 µL Alamar Blue (resazurin sodium salt, Merck) solution (0.15 mg/mL in PBS) was added to each well, and after 4 h of incubation, the fluorescence was measured at λ<sub>Ex</sub> = 530/30 and λ<sub>Em</sub> = 610/10 nm using a Synergy H4 multi-mode microplate reader (BioTek, Bad Friedrichshall, Germany). The percentage of cytostasis was calculated with the following equation:

$$\text{Cytostatic effect (\%)} = [1 - (\text{OD}_{\text{treated}} / \text{OD}_{\text{control}})] \times 100 \quad (7)$$

where the values OD<sub>treated</sub> and OD<sub>control</sub> correspond to the optical densities of the treated and the control wells, respectively.

Cytostasis (%) was plotted as a function of concentration, fitted to a dose–response curve and the 50% inhibitory concentration (IC<sub>50</sub>) value was determined from these curves. Data were evaluated with Excel (version: 365; Microsoft, Redmond, WA, USA) and the curves were defined using Microcal OriginPro (version: 2018; OriginLab, Northampton, MA, USA) software.

In each case, two independent experiments were carried out with four parallel measurements and the mean IC<sub>50</sub> values together with ±SD were represented. The Excel (version: 365) (Microsoft, Redmond, WA, USA) and Microcal OriginPro (version: 2018) (OriginLab, Northampton, MA, USA) softwares were used for data evaluation.

## 4. Conclusions

In the present work, we isolated the most characteristic *meta,meta*-cyclophane-type diarylheptanoids from the bark of the European hornbeam: carpinontriols A (1) and B (2), giffonin X (3) and 3,12,17-trihydroxytricyclo [12.3.1.1<sup>2,6</sup>]nonadeca-1(18),2(19),3,5,14,16-hexaene-8,11-dione (4).

Stability testing is essential in the development of new pharmaceuticals. Therefore, we investigated the effects of ambient conditions, including storage time, temperature and medium (pH, solvent and accompanying constituents), on the degradation of *Carpinus* diarylheptanoids 1–4. Degradation kinetics of the cyclic diarylheptanoid compounds were also examined. No significant decrease in the concentration was observed and no degradation products were detected for carpinontriol B (2); therefore, it was considered as stable under all investigated conditions. Compound 4 was susceptible of decomposing only at acidic pH values, while the storage time, the temperature and the medium did not affect its concentration. On the other hand, carpinontriol A (1) and giffonin X (3) showed significant decomposition, and degradation products were also detected in their UHPLC-HR-MS chromatograms. Degradation pathways of 1 and 3 were explored and degradation mechanisms involving the cleavage of a water molecule were proposed for them.

The membrane penetration ability of the isolated compounds was also studied by the PAMPA method. Compounds 1–3 were all detected in the acceptor phase in the PAMPA-GI model; however, their  $\log P_e$  values being lower than  $-5.0$  pointed to a poor membrane permeability. On the other hand, only giffonin X (3) was detected in the acceptor phase in the PAMPA-BBB model, and its  $\log P_e$  value ( $-5.92 \pm 0.04$ ) also suggested that it is capable of crossing the lipid membrane. Nonetheless, calculated  $\text{clog } P$  values of all compounds were lower than 2.5, indicating that they are indeed not able to cross biological membranes by passive diffusion.

The antiproliferative activity of the compounds was evaluated by the Alamar Blue assay in human HT-29 colon cancer, HepG2 hepatocellular carcinoma, HL-60 leukaemia, U87 glioblastoma and A2058 metastatic melanoma cells to obtain a dose–response for the new compounds. The highly selective cytostatic activity of carpinontriol A (1) in human metastatic melanoma cells was reported for the first time ( $\text{IC}_{50} = 14.9 \pm 2.3 \mu\text{M}$ ). Furthermore, similar activity to the etoposide control ( $\text{IC}_{50} = 8.9 \pm 0.2 \mu\text{M}$ ) was obtained on the A2058 cell type for compound 1.

**Supplementary Materials:** The following supporting information can be downloaded at: <https://www.mdpi.com/article/10.3390/ijms241713489/s1>.

**Author Contributions:** Conceptualization and methodology, C.A.F.-T., S.B., E.R. and Á.A.; Investigation, C.A.F.-T., T.H., E.B., B.S., A.S. and I.B.; data curation, C.A.F.-T.; writing—original draft preparation, C.A.F.-T., T.H., E.B., B.S. and A.S.; writing—review and editing, I.B., S.B., E.R. and Á.A.; visualization, C.A.F.-T.; supervision, Á.A.; funding acquisition, B.S., I.B., S.B., E.R. and Á.A. All authors have read and agreed to the published version of the manuscript.

**Funding:** This research was funded by grants from the National Research, Development and Innovation Office: NKFIH, K 120342 (PI: Á.A.), FK 125302 (PI: E.R.), K 135712 (PI: I.B.), K-142904 (PI: S.B.); EFOP-1.8.0-VEKOP-17-2017-0000 (B.S. and S.B.); VEKOP-2.3.3-15-2017-00020. This work was supported by the ELTE Thematic Excellence Programme 2020 Supported by National Research, Development and Innovation Office TKP2020-IKA-05. (B.S. and S.B.). S.B. is grateful for the ELTE 2018-1.2.1-NKP-2018-00005 project (under the 2018-1.2.1-NKP funding scheme).

**Institutional Review Board Statement:** Not applicable.

**Informed Consent Statement:** Not applicable.

**Data Availability Statement:** Not applicable.

**Conflicts of Interest:** The authors declare that they have no known competing financial interests or personal relationships that could have appeared to influence the work reported in this paper.

## References

1. Dai, G.; Tong, Y.; Chen, X.; Ren, Z.; Ying, X.; Yang, F.; Chai, K. Myricanol Induces Apoptotic Cell Death and Anti-Tumor Activity in Non-Small Cell Lung Carcinoma in Vivo. *Int. J. Mol. Sci.* **2015**, *16*, 2717–2731. [[CrossRef](#)] [[PubMed](#)]
2. Tang, G.; Dong, X.; Huang, X.; Huang, X.J.; Liu, H.; Wang, Y.; Ye, W.C.; Shi, L. A Natural Diarylheptanoid Promotes Neuronal Differentiation via Activating ERK and PI3K-Akt Dependent Pathways. *Neurosci.* **2015**, *303*, 389–401. [[CrossRef](#)] [[PubMed](#)]

3. Vanucci-Bacqué, C.; Bedos-Belval, F. Anti-Inflammatory Activity of Naturally Occurring Diarylheptanoids – A Review. *Bioorg. Med. Chem.* **2021**, *31*, 115971. [[CrossRef](#)]
4. Shen, S.; Liao, Q.; Feng, Y.; Liu, J.; Pan, R.; Lee, S.M.-Y.; Lin, L. Myricanol Mitigates Lipid Accumulation in 3T3-L1 Adipocytes and High Fat Diet-Fed Zebrafish via Activating AMP-Activated Protein Kinase. *Food Chem.* **2019**, *270*, 305–314. [[CrossRef](#)]
5. Jahng, Y.; Park, J.G. Recent Studies on Cyclic 1,7-Diarylheptanoids: Their Isolation, Structures, Biological Activities, and Chemical Synthesis. *Molecules* **2018**, *23*, 3107. [[CrossRef](#)] [[PubMed](#)]
6. Alberti, Á.; Riethmüller, E.; Béni, S. Characterization of Diarylheptanoids: An Emerging Class of Bioactive Natural Products. *J. Pharm. Biomed. Anal.* **2018**, *147*, 13–34. [[CrossRef](#)] [[PubMed](#)]
7. Lv, H.; She, G. Naturally Occurring Diarylheptanoids—A Supplementary Version. *Rec. Nat. Prod.* **2012**, *6*, 321–333.
8. Doello, K.; Ortiz, R.; Alvarez, P.J.; Melguizo, C.; Cabeza, L.; Prados, J. Latest in Vitro and in Vivo Assay, Clinical Trials and Patents in Cancer Treatment using Curcumin: A Literature Review. *Nutr. Cancer* **2018**, *70*, 569–578. [[CrossRef](#)]
9. Nelson, K.M.; Dahlin, J.L.; Bisson, J.; Graham, J.; Pauli, G.F.; Walters, M.A. The Essential Medicinal Chemistry of Curcumin. *J. Med. Chem.* **2017**, *60*, 1620–1637. [[CrossRef](#)]
10. Lee, S.G.; Shin, D.J.; Lee, E.S.; Goo, Y.T.; Kim, C.H.; Yoon, H.Y.; Lee, M.W.; Bang, H.; Seo, S.J.; Choi, Y.W. Enhanced Chemical Stability of Hirsutenone Incorporated into a Nanostructured Lipid Carrier Formulation Containing Antioxidants. *Bull. Korean Chem. Soc.* **2018**, *39*, 1287–1293. [[CrossRef](#)]
11. Moon, K.Y.; Ahn, B.K.; Lee, S.G.; Lee, S.H.; Yeom, D.W.; Choi, Y.W. Enhanced Aqueous Stability of Hirsutenone with Antioxidant. *J. Pharm. Investig.* **2011**, *41*, 331–336. [[CrossRef](#)]
12. Felegyi-Tóth, C.A.; Tóth, Z.; Garádi, Z.; Boldizsár, I.; Nedves, A.N.; Simon, A.; Felegyi, K.; Alberti, Á.; Riethmüller, E. Membrane Permeability and Aqueous Stability Study of Linear and Cyclic Diarylheptanoids from *Corylus maxima*. *Pharmaceutics* **2022**, *14*, 1250. [[CrossRef](#)] [[PubMed](#)]
13. Lee, J.S.; Kim, H.J.; Park, H.; Lee, Y.S. New Diarylheptanoids from the Stems of *Carpinus cordata*. *J. Nat. Prod.* **2002**, *65*, 1367–1370. [[CrossRef](#)] [[PubMed](#)]
14. Masullo, M.; Lauro, G.; Cerulli, A.; Bifulco, G.; Piacente, S. *Corylus avellana*: A Source of Diarylheptanoids With  $\alpha$ -Glucosidase Inhibitory Activity Evaluated by in vitro and in silico Studies. *Front. Plant Sci.* **2022**, *13*, 805660. [[CrossRef](#)]
15. Masullo, M.; Lauro, G.; Cerulli, A.; Kontek, B.; Olas, B.; Bifulco, G.; Piacente, S.; Pizza, C. Giffonins, Antioxidant Diarylheptanoids from *Corylus avellana*, and Their Ability to Prevent Oxidative Changes in Human Plasma Proteins. *J. Nat. Prod.* **2021**, *84*, 646–653. [[CrossRef](#)]
16. Felegyi-Tóth, C.A.; Garádi, Z.; Darcsi, A.; Csernák, O.; Boldizsár, I.; Béni, S.; Alberti, Á. Isolation and Quantification of Diarylheptanoids from European Hornbeam (*Carpinus betulus* L.) and HPLC-ESI-MS/MS Characterization of Its Antioxidative Phenolics. *J. Pharm. Biomed. Anal.* **2022**, *210*, 114554. [[CrossRef](#)]
17. Cerulli, A.; Lauro, G.; Masullo, M.; Cantone, V.; Olas, B.; Kontek, B.; Nazzaro, F.; Bifulco, G.; Piacente, S. Cyclic Diarylheptanoids from *Corylus avellana* Green Leafy Covers: Determination of Their Absolute Configurations and Evaluation of Their Antioxidant and Antimicrobial Activities. *J. Nat. Prod.* **2017**, *80*, 1703–1713. [[CrossRef](#)]
18. Liu, J.-X.; Di, D.-L.; Wei, X.-N.; Han, Y. Cytotoxic Diarylheptanoids from the Pericarps of Walnuts (*Juglans regia*). *Planta Med.* **2008**, *74*, 754–759. [[CrossRef](#)]
19. Dai, G.; Tong, Y.; Chen, X.; Ren, Z.; Yang, F. In vitro Anticancer Activity of Myricanone in Human Lung Adenocarcinoma A549 Cells. *Chemotherapy* **2015**, *60*, 81–87. [[CrossRef](#)]
20. Xue, Y.; Savchenko, A.I.; Agnew-Francis, K.A.; Miles, J.A.; Holt, T.; Lu, H.; Chow, S.; Forster, P.I.; Boyle, G.M.; Ross, B.P.; et al. seco-Pregnane Glycosides from Australian Caustic Vine (*Cynanchum viminalis* subsp. *australe*). *J. Nat. Prod.* **2023**, *86*, 490–497. [[CrossRef](#)]
21. Friedman, M.; Jürgens, H.S. Effect of pH on the Stability of Plant Phenolic Compounds. *J. Agric. Food Chem.* **2000**, *48*, 2101–2110. [[CrossRef](#)]
22. Tabboon, P.; Tuntiyasawasdikul, S.; Sripanidkulchai, B. Quality and Stability Assessment of Commercial Products Containing Phytoestrogen Diaryheptanoids from *Curcuma comosa*. *Ind. Crops Prod.* **2019**, *134*, 216–224. [[CrossRef](#)]
23. Ayanlowo, A.G.; Garádi, Z.; Boldizsár, I.; Darcsi, A.; Nedves, A.N.; Varjas, B.; Simon, A.; Alberti, Á.; Riethmüller, E. UHPLC-DPPH Method Reveals Antioxidant Tyramine and Octopamine Derivatives in *Celtis occidentalis*. *J. Pharm. Biomed. Anal.* **2020**, *191*, 113612. [[CrossRef](#)]
24. Könczöl, Á.; Müller, J.; Földes, E.; Béni, Z.; Végh, K.; Kéry, Á.; Balogh, G.T. Applicability of a Blood–Brain Barrier Specific Artificial Membrane Permeability Assay at the Early Stage of Natural Product-Based CNS Drug Discovery. *J. Nat. Prod.* **2013**, *76*, 655–663. [[CrossRef](#)] [[PubMed](#)]
25. Kim, N.T.; Lee, D.S.; Chowdhury, A.; Lee, H.; Cha, B.Y.; Woo, J.T.; Woo, E.R.; Jang, J.H. Acerogenin C from *Acer nikoense* exhibits a neuroprotective effect in mouse hippocampal HT22 cell lines through the upregulation of Nrf-2/HO-1 signaling pathways. *Mol. Med. Rep.* **2017**, *16*, 1537–1543. [[CrossRef](#)]
26. Chen, P.; Lin, X.; Yang, C.-H.; Tang, X.; Chang, Y.-W.; Zheng, W.; Luo, L.; Xu, C.; Chen, Y.-H. Study on Chemical Profile and Neuroprotective Activity of *Myrica rubra* Leaf Extract. *Molecules* **2017**, *22*, 1226. [[CrossRef](#)]
27. Masullo, M.; Cerulli, A.; Mari, A.; de Souza Santos, C.C.; Pizza, C.; Piacente, S. LC-MS Profiling Highlights Hazelnut (*Nocciola di Giffoni* PGI) Shells as a Byproduct Rich in Antioxidant Phenolics. *Food Res. Int.* **2017**, *101*, 180–187. [[CrossRef](#)] [[PubMed](#)]

28. Esposito, T.; Sansone, F.; Franceschelli, S.; Del Gaudio, P.; Picerno, P.; Aquino, R.P.; Mencherini, T. Hazelnut (*Corylus avellana* L.) Shells Extract: Phenolic Composition, Antioxidant Effect and Cytotoxic Activity on Human Cancer Cell Lines. *Int. J. Mol. Sci.* **2017**, *18*, 392. [[CrossRef](#)]
29. Pacheco-Palencia, L.A.; Hawken, P.; Talcott, S.T. Phytochemical, Antioxidant and Pigment Stability of Açai (*Euterpe oleracea* Mart.) as Affected by Clarification, Ascorbic Acid Fortification and Storage. *Food Res. Int.* **2007**, *40*, 620–628. [[CrossRef](#)]
30. Avdeef, A. Permeability—PAMPA. In *Absorption and Drug Development*, 2nd ed.; John Wiley & Sons: Hoboken, NJ, USA, 2012; pp. 319–498.
31. Gewirtz, D. A Critical Evaluation of the Mechanisms of Action Proposed for the Antitumor Effects of the Anthracycline Antibiotics Adriamycin and Daunorubicin. *Biochem. Pharmacol.* **1999**, *57*, 727–741. [[CrossRef](#)]
32. Lajkó, E.; Spring, S.; Hegedüs, R.; Biri-Kovács, B.; Ingebrandt, S.; Mező, G.; Kőhidai, L. Comparative Cell Biological Study of in vitro Antitumor and Antimetastatic Activity on Melanoma Cells of GnRH-III-containing Conjugates Modified with Short-chain Fatty Acids. *Beilstein J. Org. Chem.* **2018**, *14*, 2495–2509. [[CrossRef](#)] [[PubMed](#)]
33. Meresse, P.; Dechaux, E.; Monneret, C.; Bertounesque, E. Etoposide: Discovery and Medicinal Chemistry. *Curr. Med. Chem.* **2004**, *11*, 2443–2466. [[CrossRef](#)] [[PubMed](#)]
34. Baranyai, Z.; Biri-Kovács, B.; Krátký, M.; Szeder, B.; Debreczeni, M.L.; Budai, J.; Kovács, B.; Horváth, L.; Pári, E.; Németh, Z.; et al. Cellular Internalization and Inhibition Capacity of New Anti-Glioma Peptide Conjugates: Physicochemical Characterization and Evaluation on Various Monolayer- and 3D-Spheroid-Based in Vitro Platforms. *J. Med. Chem.* **2021**, *64*, 2982–3005. [[CrossRef](#)] [[PubMed](#)]

**Disclaimer/Publisher’s Note:** The statements, opinions and data contained in all publications are solely those of the individual author(s) and contributor(s) and not of MDPI and/or the editor(s). MDPI and/or the editor(s) disclaim responsibility for any injury to people or property resulting from any ideas, methods, instructions or products referred to in the content.